

Birla Central Library

PILANI (Rajasthan)

Class No :- 665.7

Book No :- 49554

Accession No - 41789

GAS PRODUCERS
and BLAST FURNACES

GAS PRODUCERS and BLAST FURNACES

THEORY AND METHODS OF CALCULATION

Wilhelm Gumz, D.Eng.

Consultant, Battelle Memorial Institute
Columbus, Ohio

**John Wiley & Sons, Inc., New York
Chapman & Hall, Limited, London**

663.7
G935 G

41789

COPYRIGHT, 1950

BY

JOHN WILEY & SONS, INC.

All Rights Reserved

*This book or any part thereof must not
be reproduced in any form without
the written permission of the publisher.*

PRINTED IN THE UNITED STATES OF AMERICA

PREFACE

Gasification and kindred problems, the most important and common of which are concerned with pig iron production in the blast furnace, may be designated as applied physical chemistry. Their industrial importance, which needs no emphasis, is rapidly increasing owing to the development of the synthetic fuel industry and the advances that are expected in metallurgy.

Developed so far mostly along merely empirical lines—even overlooking the close relationship of gas producers and blast furnaces—gas technology as well as furnace design need a better evaluation of their accumulated facts and empirical knowledge, a better understanding of the reactions going on in the shaft of gas producers and furnaces—in other words, a straightforward calculation. A process is completely mastered only if it can be calculated. Calculation not only makes the process clearly understandable, it also reveals ways of improvement or even new process techniques, it discloses the relationship to similar processes, the practical influence of different charges or operating conditions, etc. Experiments, especially on a large scale, which require considerable time, materials, and man hours, might be unnecessary or they might be directed to a better success. Calculation is more rapid and decisive than experiment as it is free of uncontrolled operational variables. In spite of the fact that many people are repelled by even the word “theory” as something unrealistic, the merits of calculation are numbered in the hundreds, and the theory, as far as it is close to facts, is a true presentation of all complex and sometimes confusing observations and experimental facts of “practical” operation. Results of practice and perfect theory *coincide*. Conversely, practical experience is limited to the operation conditions under which it is acquired; generalizations are possible only by theory.

Gas formation is a complex process. A great number of constituents are formed, and a number of reactions take place simultaneously. Iron ore reduction is a process still more complex; the number of possible reactions is increased. Without true knowledge

of the reactions going on and the physical and chemical factors influencing them, it is difficult even to interpret experimental results. Such common statements as "equilibria cannot be reached in gas producers and blast furnaces," which are the themes of many books and papers, would remove the major basis of theoretical calculation—if they were true.

No doubt such statements as well as the urgent problems of present-day industrial development make a revision of our approach to these problems obligatory. Fortunately, considerable progress has been made in this field, and by means of correlation of processes like gas production in rotating grate gas producers, in slagging ash producers, cupola and blast furnaces, a generally applicable theory can be presented.

In this book several solutions are offered for the mathematical treatment of the problems. Quite a number of practical cases are chosen and presented numerically not only to prove the generally close agreement of calculation and measurement but also to display the general applicability of the methods discussed and to cover the whole field of gas producer and blast furnace practice as far as it can be subjected to calculation. It may be left to the reader to increase the number of examples after he has received the necessary tools and directions.

ACKNOWLEDGMENTS

I wish to acknowledge my indebtedness to the work of Sergei Traustel, former member of the Institute of Fuel Utilization (Professor Dr. Rudolf Drawe, director) of Berlin Engineering University. I also gratefully acknowledge the encouragement and help received from Dr. Manson Benedict. My thanks are also due the management of Hydrocarbon Research, Inc., New York, for permission to write this book while I was associated with that organization. For help in preparing the manuscript I am grateful to Bertha Halberstadt and James A. Finneran of Hydrocarbon Research.

Columbus, Ohio
June 1950

W. GUMZ

CONTENTS

SYMBOLS AND ABBREVIATIONS	ix
-------------------------------------	----

PART ONE. GAS PRODUCERS

1. GASIFICATION REACTIONS.	3
Fundamental Equations	3
The Equilibrium Constants	20
The Gasification Mechanism	25
2. GAS COMPOSITION AT EQUILIBRIUM	32
Basis of Calculation	32
General Case	41
The Triangle Method of Traustel	50
The Newtonian Approximation Method Developed by Traustel	58
The Degree of Reduction, a Semigraphical Method	63
The Heat Balance	68
3. GAS COMPOSITION AT INCOMPLETE EQUILIBRIUM	76
Calculation Scheme and Sample Calculations	86
Triangle Method	86
General Calculation Rules	91
Newton's Approximation Method	92
4. OTHER CALCULATION METHODS	96
Calculations Based on the Gas Analysis	96
Other Solutions Proposed	102
5. APPLICATIONS OF THE SEMIGRAPHICAL METHOD FOR ASSOCIATED PROBLEMS	105
Methanization	105
Reforming of Methane	107
6. MATHEMATICAL TREATMENT OF GAS-PRODUCER PERFORMANCE . .	109
Influence of the Moisture Content of the Gasifying Agent	109
Effect of Preheating the Blast	118
Recycling Off-Gas	120
Effect of External Heat Losses	121
Concurrent and Down-Draft Gasification	123
Gasification in Suspension	124
Down-Draft Gasification of Wood	129
Slagging-Ash Gas Producers	136
Gasification with Oxygen and Oxygen-Enriched Air	145

Gasification of Anthracite with Oxygen-Steam Mixture, Compared with Experimental Results	149
The Thyssen-Gálocsy Process	151
Water-Gas Production	154
Effect of Pressure on Gasification	160
Water Gas at High Pressure	160
Water Gas at Pressures below 1 Atm	162
Producer Gas under Pressure	163
Pressure Gasification with Oxygen-Steam Mixtures	167

PART TWO. BLAST FURNACES

7. COMPOSITION OF GAS IN BLAST FURNACES	173
Reactions in the Blast Furnace	173
Mechanism of Furnace Reactions	189
Shaft Reactions and Their Localization in the Blast Furnace	192
The Hearth Reactions	207
Yield	219
8. METHOD OF COMPUTATION	225
9. EXAMPLE OF COMPUTATION	236
Charcoal Blast Furnace Sandviken No. 3 (M. Wiberg)	236
The Blast-Furnace Curve	246
Blast Furnace under Pressure	250
Blast Furnace with Oxygen-Enriched Blast	253
Water-Gas High-Pressure Low-Shaft Blast Furnace	261
Cupola Furnace	263
Hot-Blast Cupola Furnace	267
A New Type of Hot-Blast Cupola Furnace	268
Influence of Weather Conditions	270

PART THREE. REACTION KINETICS

10. REACTION KINETICS	275
---------------------------------	-----

APPENDIX

Table I. Properties of Gases	297
Table II. Properties of Steam-Air or Gas Mixtures	298
Table III. Enthalpy of Gases (kcal/SCM)	302
Table IV. Enthalpy of Formation (kcal/kmol)	303
Table V. Equilibrium Constants (Heterogeneous Reactions)	304
Table VI. Equilibrium Constants (Homogeneous Reactions)	305
Table VII. Enthalpy of Carbon (Coke), Blast-Furnace Slag (Burdén) and Pig Iron (kcal/kg)	306
Table VIII. Conversion Table—Metric to English System	307
NAME INDEX	309
SUBJECT INDEX	313

SYMBOLS AND ABBREVIATIONS

A	carbon consumption 10^3 g/cm ² sec (see p. 278)
at	(technical) atmosphere = 10,000 kg/m ²
Atm	(physical) atmosphere = 10,332.3 kg/m ² = 760 mm Hg
c, C	carbon content (weight %) of a fuel
c	$\frac{n}{v}$ molar concentration (moles per unit volume)
c'	(additional) carbon content originating from the burden
C_F	total carbon carrier in the fuel
C_G	total carbon carrier in the product gas
c_h	carbon content (weight %) of the hypothetical fuel
C_M	total carbon carrier in the gasifying agent
c_p	specific heat at constant pressure
C_{pig}	carbon content of the pig iron
d, D	diameter [m]
d_F	apparent density of the fuel bed (bulk weight)
E	enthalpy
ΔF	maximum work (constant temperature and pressure)
F	fuel gasified per SCM of product gas [kg/SCM]
F^*	fuel including carbon in the pig iron (carburizing carbon)
F_h	hypothetical fuel per SCM of product gas [kg/SCM]
G	product gas per kg of fuel gasified [SCM/kg], as a subscript referring to product gas
h, H_2	hydrogen content of the fuel [weight %]
h	heat transmission coefficient
H	enthalpy (with subscripts)
H_C	enthalpy of the coke (fuel, carbon) [kcal/kg]
H_F	total hydrogen carrier in the fuel
ΔH_f	enthalpy of formation
H_G	total hydrogen carrier in the product gas
H_G	enthalpy of the product gas [kcal/SCM]

h_h	hydrogen content of the hypothetical fuel
H_i	net heating value [kcal/kg or kcal/SCM]
H'_i	net heating value (of a fuel) after deduction of external heat losses (%)
$H_{i,C}$	net heating value (identical with gross heating value) of the carbon [kcal/kg]
$H_{i,F}$	net heating of the fuel [kcal/kg]
$H_{i,G}$	net heating value of the product gas [kcal/SCM]
$H_{i,M}$	net heating value of the blast (if any) [kcal/SCM]
H_M	total hydrogen carrier in the blast
H_M	enthalpy of the gasifying medium (blast) [kcal/SCM]
$H'_{M_xO_y}$	heat of reaction for reducing the metal oxide M_xO_y by means of CO
$H''_{M_xO_y}$	heat of reaction for reducing the metal oxide M_xO_y by means of H_2 or CO, H_2 mixtures
H_g	gross heating value or calorific value [kcal/kg or kcal/SCM]
H_{prod}	heat content (enthalpy) of the manufactured product including heat of fusion if product is a molten metal (e.g., pig iron) [kcal/kg]
H_{sl}	heat content (enthalpy) of the slag including the heat of fusion [kcal/kg]
H_μ	heat content (enthalpy) of the burden [kcal/kg burden]
$H^*_{w_f}$	heat content of the moisture in the fuel reduced to the fuel quantity F^*
$H^*_{w_\mu}$	heat content of the moisture in the burden reduced to the fuel quantity F^*
k, k', K	constant factor
k	thermal conductivity [kcal/m hr °C]
K_{27}	equilibrium constant of the reaction indicated by the number of its equation (e.g., equation 27)
K_c	equilibrium constant, expressed by a quotient of molar concentrations (c)
kcal	kilocalorie
kmol	kilomole
K_p	equilibrium constant, expressed by a quotient of partial pressures of the gas constituents

K_{pB}	equilibrium constant of the Boudouard reaction $= \frac{(p_{CO})^2}{p_{CO_2}}$
K'_{pB}	reciprocal of $K_{pB} = \frac{p_{CO_2}}{(p_{CO})^2}$
K_{pW}	equilibrium constant of the heterogeneous water-gas reaction $= \frac{p_{H_2} p_{CO}}{p_{H_2O}}$
K'_{pW}	reciprocal of $K_{pW} = \frac{p_{H_2O}}{p_{H_2} p_{CO}}$
K_W	equilibrium constant of the water-gas shift reaction $= \frac{p_{CO} p_{H_2O}}{p_{CO_2} p_{H_2}}$
K'_W	reciprocal of $K_W = \frac{p_{CO_2} p_{H_2}}{p_{CO} p_{H_2O}}$
K_x	equilibrium constant expressed by a quotient of mole fractions (x)
m	molecular weight [kg]
M	gasifying medium or agent (blast) [SCM/SCM], as a subscript referring to the blast
$n, n_A, n_B \dots$	number, number of moles of substance A, B, \dots
n, N_2	nitrogen content of the fuel [weight %]
N_F	total nitrogen carrier in the fuel
N_G	total nitrogen carrier in the gas
n_h	nitrogen content of the hypothetical fuel
N_M	total nitrogen carrier in the gasifying agent
o, O_2	oxygen content of the fuel [weight %]
o'	(additional) oxygen content originating from the burden
O_F	total oxygen carrier in the fuel
O_G	total oxygen carrier in the product gas
o_h	oxygen content of the hypothetical fuel
O_M	total oxygen carrier in the gasifying agent
p	partial pressure
P	total pressure [Atm]
p_{sl}	slag ratio (acids/bases)
R	gas constant
Re	Reynolds number

Q	heat quantity [kcal, or kcal/kg, kcal/kmol, kcal/SCM]
Q_{el}	heat input by electrical heating
Q_{ext}	external heat losses by radiation and convection
Q_{hearth}	heat requirement of the hearth reactions (of a blast furnace) [kcal/kg burden]
Q_{hydr}	heat of hydration [kcal/kg]
Q_{preh}	heat requirement in the preheating (or pre-reaction) zone of a blast furnace [kcal/kg burden]
Q_{red}	heat of reduction [kcal/kg]
Q_{shaft}	heat requirement of the shaft reactions [kcal/kg burden]
Q_{sl}	heat requirement of slag formation [kcal/kg burden]
Q_Z	sum of the heat requirements of the shaft reactions, the hearth reactions, and of slag formation [kcal/kg burden]
S'	entropy (at constant pressure)
SCM	standard cubic meter (at 0°C, 760 mm Hg)
t	temperature [degree centigrade]
T	absolute temperature [degree Kelvin] = $273 + t^{\circ}\text{C}$
v	volume, molecular volume [m^3 , SCM]
vel	velocity [m/sec]
w, W	moisture of the fuel [weight %]

Greek Letters

α	thermal diffusivity
$\alpha_1, \alpha_2, \dots$	conversion factors
γ	coke/iron ratio (cupola furnace)
ϵ	ratio of gas constituents
ϵ	yield
ϵ'	product yield (pig iron yield)
ϵ''	slag yield
η	efficiency [%]
η_c	combustion efficiency ratio = $\frac{\text{CO}_2}{\text{CO}_2 + \text{CO}} 100 \text{ [%]}$
η_g	gasification efficiency = $\frac{H_{i,G}}{FH_{i,F}} 100 \text{ [%]}$
η_{therm}	thermal efficiency [%]
μ	(micron) = 0.001 mm

μ	burden/fuel ratio
μ_p	burden/fuel ratio (pressurized furnace)
μ_r	burden/fuel ratio after prereduction of the burden
ν	kinematic viscosity [m^2/sec]
ξ	degree of steam decomposition
Π	quotient of mass action
Σ	sum of . . .
ρ	density [kg/m^3] of a gas
ρ_0	density at 0°C [kg/m^3]
ρ_s	density of a solid
φ, ψ, χ	functions
φ', ψ', χ'	first derivatives
$\varphi'_x, \psi'_x, \chi'_x$	partial derivatives of φ, ψ, χ with respect to x

P A R T O N E

Gas Producers

1

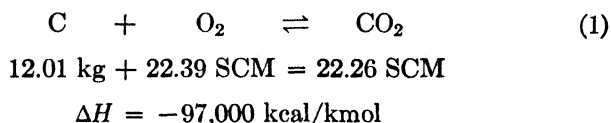
GASIFICATION REACTIONS

Fundamental equations

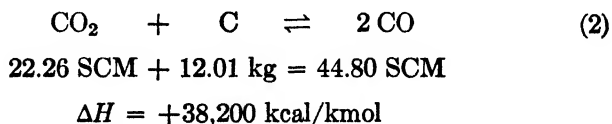
Gasification is a reaction between solid carbon and an oxygen-carrying gasifying agent, the blast, e.g., air, steam, carbon dioxide, or mixtures thereof, which yields combustible gases (CO , H_2 , CH_4). Contrary to the process of combustion which takes place with excess oxygen or at least with the theoretical oxygen requirement (stoichiometric or air-saturated combustion), gasification takes place with excess carbon, especially considering the usual process of gasifying lump fuel in a countercurrent process. A concurrent gasification which could take place with the theoretical carbon requirement will be dealt with in a later chapter. In this case, the time of gasification would become infinite. The gasification process, therefore, should by no means be considered as some kind of incomplete combustion; rather it includes oxidation as well as reduction processes, which for physical reasons are associated with certain bed levels or reaction spaces.

The gasification process can be described by the following basic chemical reactions between carbon and the oxygen carriers or the gases formed from them.

- (1) Combustion of carbon in the oxidation zone:



- (2) The proper reaction of gasification in the reducing zone, the reduction of CO_2 to CO and H_2O to H_2 and CO :



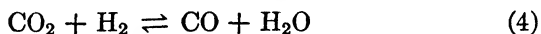
GASIFICATION REACTIONS



$$22.4 \text{ SCM} + 12.01 \text{ kg} = 22.43 \text{ SCM} + 22.40 \text{ SCM}$$

$$\Delta H = +28,200 \text{ kcal/kmol}$$

Equations 2 and 3 are related by the water-gas shift equation



$$\Delta H = +10,000 \text{ kcal/kmol}$$

(3) In addition, methane formation in the reduction zone must be considered, on the basis of the simple overall equation:



$$12.01 \text{ kg} + 44.86 \text{ SCM} = 22.38 \text{ SCM}$$

$$\Delta H = -21,100 \text{ kcal/kmol}$$

The metric system is used in these equations. The unit of matter is the mole, properly called the kilogram-mole (abbreviated kmol). The molecular weights are based on the International Atomic Weights Table of 1941. The molal volumes are derived from the molecular weight and the experimentally observed density (see Appendix, Table I), $v = m/\rho$, which explains the deviation from the unit molal volume of 22.414 SCM/kmol for ideal gases.* In all thermochemical data the new convention for signs is used, whereby energy (work or heat) added to a closed system from the surroundings is considered positive, and all energy given up or to be given up to the surroundings is considered negative. The enthalpy change (ΔH) accompanying a heat-producing (exothermic) reaction, such as equation 1, has a negative sign, since the enthalpy of carbon dioxide formation must be removed from the system in order to maintain thermal equilibrium, i.e., to carry out the reaction isothermally.

This way of writing

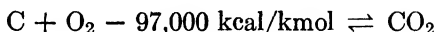


is in contrast to the one to which many engineers are accustomed:



* The standard conditions for temperature and pressure are 0°C, 760 mm Hg.

The import of the latter statement is that the products of the reaction are CO_2 and 97,000 kcal of heat. However, it can easily be seen that this equation is no equation from a thermal point of view. A more satisfactory way of writing it is, as proposed,



This equation states that in the reaction of carbon with oxygen, 97,000 kcal/kmol have to be removed from a closed system in order to form CO_2 and to attain thermal equilibrium.

The thermochemical data given in scientific and technical literature differ considerably from each other. Not only are the results expressed in different units (kcal/kmol, kcal/gmol), but the numerical values show discrepancies. One reason for the discrepancies is the nature of carbon, which exists in two modifications, as diamond and as graphite. If diamond has an enthalpy of formation $\Delta H = 0$, then for graphite as α -graphite, $\Delta H = +490$ kcal/kmol, and as β -graphite, $\Delta H = +220$ kcal/kmol. Neither of the two modifications, however, is technically used. The carbon of coke consists of crystallites, crystal fragments of different size with more or less well-formed or distorted crystal lattice. In spite of a certain (but small) degree of graphitization of commercial coke, it is a very long step toward pure crystalline graphite, as can be seen particularly from such physical properties as pore volume, specific weight, thermal and electrical conductivity. In physics and thermochemistry β -graphite is used preferably as a basis, since it is a well-defined body material, unlike coke or other kinds of carbon. However, the use of these values in calculations of technical gasification processes for coke or coal is not justified. As a good average value for the heat of formation of carbon in coke or coal, the value of

$$-\Delta H = 97,000 \text{ kcal/kmol} = 8080 \text{ kcal/kg C}$$

is adopted in all the following calculations, in accordance with the value given in DIN 1872 (German Industry Standards). Because of the uncertainty of thermochemical measurements, the last two figures are rounded off; the same has been done with the enthalpy of formation of steam, in order to indicate the warranted precision. P. Dolch,¹ who points out the importance of

¹ P. Dolch, Die Wärmetönungen der Vergasungsreaktionen von Kohlenstoff, *Feuerungstechn.*, Vol. 27 (1939), No. 4, pp. 109–112.

uniform units in thermochemical calculations, suggests the following values for carbon from coke made from bituminous coal,

$$-\Delta H_f = 96,000 \text{ kcal/kmol} = 8000 \text{ kcal/kg}$$

and for carbon from brown coal (lignite) coke,

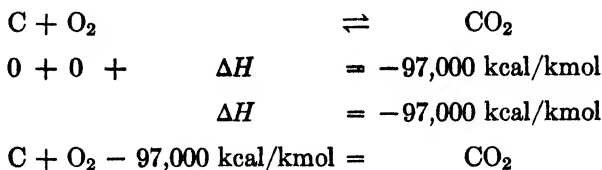
$$-\Delta H_f = 97,800 \text{ kcal/kmol} = 8150 \text{ kcal/kg}$$

The deviations of the individual kinds of coal are not well enough established, however, and the variation in measurement is too great to justify such suggestions. Besides, it would be necessary not only to differentiate according to the kind and rank of coal, but also according to the conditions of preparation of cokes. In view of the limits of error of such determinations, it seems to be perfectly justifiable to use in calculations the above-mentioned standard value for carbon in coal or coke of $-\Delta H_f = 97,000 \text{ kcal/kmol}$. Table 1 gives a compilation of enthalpies of formation.

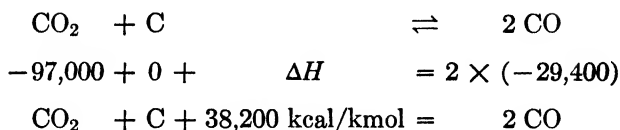
TABLE 1
ENTHALPY OF FORMATION

$\Delta H_f \text{ kcal/kmol}$			
Substance	State of Aggregation	ΔH_f	Remarks
C	Solid	0	Referring to coke carbon
CO	Gaseous	-29,400	
CO ₂	Gaseous	-97,000	
CH ₄	Gaseous	-21,100	
H ₂	Gaseous	0	
H ₂ O	Gaseous	-57,600	
O ₂	Gaseous	0	

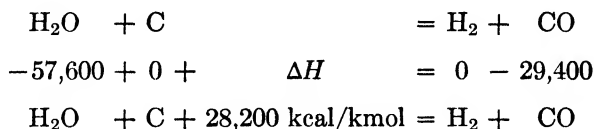
To determine the amount of heat to be added or removed in any reaction, it is necessary merely to add the respective enthalpies of formation of the individual substances (and to balance the energy amounts on both sides of the equation). For instance, equation 1,



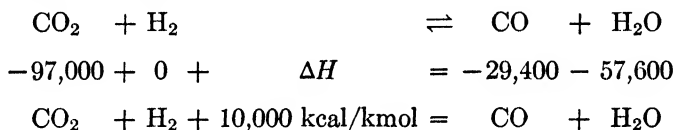
The other equations may be treated in the same way. Equation 2,



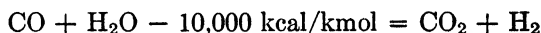
Equation 3,



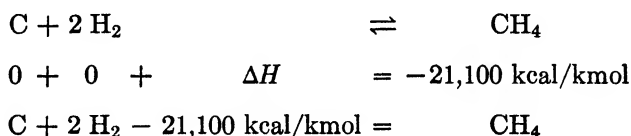
Equation 4, as written above,



or the reverse reaction (CO shift reaction),

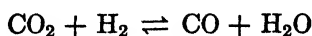


Equation 5,



Equations 1 to 5 are chemical overall reactions which show the starting material and the final result. They tell nothing, however, of the real path of the reactions. Consequently, conclusions as to the reaction velocity cannot be drawn from them. The equations serve only to obtain material and heat balances and the equilibrium constants for the overall reactions.

The gasification reactions, equations 2 to 5, can proceed from left to right or from right to left as indicated by the arrows. To explain the law of mass action which regulates the course of chemical reactions, let us consider the homogeneous water-gas reaction as an example. Equation 4,



Chemical reaction takes place as a consequence of collisions between the molecules of the various reactants; hence the velocity with which the reactants are consumed is proportional to their concentration. However, only that small fraction of collisions leads to a reaction which occurs with more than average energy, and, in turn, does not depend on concentration but on temperature. It should be expressed by the proportionality factor k (< 1). The velocity of the reaction from left to right is:

$$vel = k[CO_2][H_2] \quad (6)$$

and of the reaction from right to left,

$$vel' = k'[CO][H_2O] \quad (7)$$

At equilibrium * both velocities are equal

$$vel = vel' \quad (8)$$

and

$$k[CO_2][H_2] = k'[CO][H_2O] \quad (8a)$$

If K_c is called the equilibrium constant (dependent only upon the temperature), we get it from equation 8a,

$$K_c = \frac{k}{k'} = \frac{[CO][H_2O]}{[CO_2][H_2]} \quad (9)$$

The expressions in brackets mean molar concentrations, $c = n/v$ (moles per unit volume). Concentration also can be expressed in more customary units, e.g., in partial pressures p , in volume % of the gases involved, or in mole fractions ($x = n/\Sigma n$). If change is made from the molar concentration n/v to partial pressures, from the general equation of state

$$p = n \frac{RT}{v} \quad (10)$$

$$c = \frac{n}{v} = \frac{p}{RT} \quad p = cRT \quad (11)$$

is obtained or, in terms of mole fractions,

* Equilibrium may be defined as a boundary state toward which the reactions proceed at a more or less rapid rate. A reaction beyond the equilibrium is impossible. The term *equilibrium* does not imply an oscillation about an equilibrium state, but an approaching to a final state.

$$x = \frac{p}{P} = c \frac{RT}{P} \quad (12)$$

By using these relations, the general equation becomes

$$K_c = K_p(RT)^{\Sigma\nu} = K_x \frac{(RT)^{\Sigma\nu}}{P} \quad (13)$$

where ν is the sum of the molal quantities on the right and left sides of the equation, the ones on the right side being positive, the ones on the left side being negative.

In the equation under consideration (equation 4), the algebraic sum of molal quantities on the right and left sides is

$$\Sigma\nu = 0$$

Consequently,

$$(RT)^{\Sigma\nu} = 1$$

and

$$K_c = K_p = K_x \quad (14)$$

By changing to partial pressures

$$K_p = \frac{p_{\text{CO}} p_{\text{H}_2\text{O}}}{p_{\text{CO}_2} p_{\text{H}_2}} \quad (15)$$

In the producer-gas reaction or so-called Boudouard reaction according to equation 2,



the reaction velocity becomes

$$vel = k[\text{CO}_2][\text{C}] \quad (16)$$

and

$$vel' = k'[\text{CO}][\text{CO}] = k'[\text{CO}]^2 \quad (17)$$

The concentration of the solid phase $[\text{C}]$, the vapor pressure of the solid carbon to be inserted here, is constant at any one temperature, hence does not affect the equilibrium. For calculating the equilibrium constants of systems including solids (and liquids), the solids are assumed to have activities of unity. Only the gas molal quantities are considered. The equilibrium constant resulting from equations 16 and 17 is then

$$K_c = \frac{k}{k'} = \frac{[\text{CO}]^2}{[\text{CO}_2]} \quad (18)$$

and the sum of the molal quantities, right and left, is

$$\Sigma \nu = 2 - 1 = 1$$

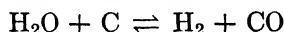
This means that this reaction is not independent of pressure. According to equation 13,

$$K_c = K_p RT \quad (19)$$

$$K_p = \frac{p_{\text{CO}}^2}{p_{\text{CO}_2}} = \frac{(v_{\text{CO}})^2 P^2}{(v_{\text{CO}_2}) P} = \frac{(v_{\text{CO}})^2 P}{v_{\text{CO}_2}} \quad (20)$$

If volume % is used, the equilibrium constant is directly proportional to the pressure. From now on the constant of the Boudouard reaction (equation 20) will be designated as K_{pB} and its reciprocal as K'_{pB} . In a system with a total pressure of P atmospheres* we have to use the constants $P^{-1}K_{pB}$ or PK'_{pB} if the gas constituents are expressed as volume %.

The heterogeneous water-gas reaction according to equation 3,



results in

$$vel = k[\text{H}_2\text{O}][\text{C}] \quad (21)$$

$$vel' = k'[\text{H}_2][\text{CO}] \quad (22)$$

$$K_c = \frac{k}{k'} = \frac{[\text{H}_2][\text{CO}]}{[\text{H}_2\text{O}]} \quad (23)$$

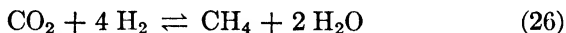
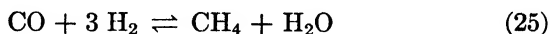
The sum of the molal quantities on the right and left sides of equation 3 is $2 - 1 = 1$; consequently, the equilibrium constant of the pressure dependent reaction is

$$K_p = \frac{p_{\text{H}_2} p_{\text{CO}}}{p_{\text{H}_2\text{O}}} = \frac{v_{\text{H}_2} v_{\text{CO}}}{v_{\text{H}_2\text{O}}} P \quad (24)$$

In the following discussion, this K_p value will be called K_{pw} and its reciprocal K'_{pw} . The arbitrary way of writing equations of reaction (interchange of right and left sides) makes it necessary to watch the definition when numerical values of the equilibrium constants are used.

* As all calculations are based on the standard pressure of 760 mm Hg, all pressures have to be expressed in "physical atmospheres": 1 physical Atm = 10,332.3 kg/m² = 14.69604 lb/sq in.; 1 lb/sq in. (abs) = 0.068046 physical Atm.

Finally, the reaction of methane formation will be considered, equation 5, as well as other possibilities of homogeneous methane formation reactions, such as



According to equation 5,



$$vel = k[\text{C}][\text{H}_2][\text{H}_2] \quad (28)$$

$$vel' = k'[\text{CH}_4] \quad (29)$$

$$K_c = \frac{k}{k'} \frac{[\text{CH}_4]}{[\text{H}_2]^2} \quad (30)$$

The sum of the molal quantities $\nu = 1 - 2 = -1$.

$$K_c = K_p(RT)^{-1} \quad (31)$$

$$K_p = \frac{p_{\text{CH}_4}}{p_{\text{H}_2}^2} = (RT)K_c = \frac{v_{\text{CH}_4}}{(v_{\text{H}_2})^2} P^{-1} \quad (32)$$

This reaction, too, is dependent on pressure, though in an opposite sense from the two reactions (equations 2 and 3) treated before. We shall designate this equilibrium constant K_{pM} in the following discussion.

For the reaction according to equation 25,

$$vel = k[\text{CO}][\text{H}_2][\text{H}_2][\text{H}_2] \quad (33)$$

$$vel' = k'[\text{CH}_4][\text{H}_2\text{O}] \quad (34)$$

$$K_c = \frac{k}{k'} = \frac{[\text{CH}_4][\text{H}_2\text{O}]}{[\text{CO}][\text{H}_2]^3} \quad (35)$$

As the sum of the molal quantities is $\Sigma\nu = 2 - 4 = -2$,

$$K_p = \frac{p_{\text{CH}_4} p_{\text{H}_2\text{O}}}{p_{\text{CO}} p_{\text{H}_2}^3} = \frac{(v_{\text{CH}_4})(v_{\text{H}_2\text{O}})}{(v_{\text{CO}})(v_{\text{H}_2})^3} P^{-2} = (RT)^2 K_c \quad (36)$$

Furthermore, for the reaction according to equation 26,

$$K_p = \frac{p_{\text{CH}_4} p_{\text{H}_2\text{O}}^2}{p_{\text{CO}_2} p_{\text{H}_2}^4} = \frac{(v_{\text{CH}_4})(v_{\text{H}_2\text{O}})^2}{(v_{\text{CO}_2})(v_{\text{H}_2})^4} P^{-2} = (RT)^2 K_c \quad (37)$$

and, for the reaction according to equation 27,

$$K_p = \frac{p_{\text{CH}_4} p_{\text{CO}_2}}{p_{\text{CO}}^2 p_{\text{H}_2}} = \frac{(v_{\text{CH}_4})(v_{\text{CO}_2})}{(v_{\text{CO}})^2 (v_{\text{H}_2})^2} P^{-2} = (RT)^2 K_c \quad (38)$$

For numerical calculations it is important that the equilibrium constants of interdependent reactions are obtainable from each other. Thus, as already stated, the Boudouard reaction according to equation 2 and the heterogeneous water-gas reaction according to equation 3 are related by the homogeneous water-gas shift reaction. Consequently, if the equilibria of two of these reactions are known, the third constant follows. According to equations 20 and 24,

$$K_{pB} = \frac{p_{\text{CO}}^2}{p_{\text{CO}_2}} \quad K_{pW} = \frac{p_{\text{H}_2} p_{\text{CO}}}{p_{\text{H}_2\text{O}}}$$

$$\frac{K_{pB}}{K_{pW}} = \frac{p_{\text{CO}}^2}{p_{\text{CO}_2}} \frac{p_{\text{H}_2\text{O}}}{p_{\text{H}_2} p_{\text{CO}}} = \frac{p_{\text{CO}} p_{\text{H}_2\text{O}}}{p_{\text{CO}_2} p_{\text{H}_2}} = K_W \quad (39)$$

$$K_W = \frac{K_{pB}}{K_{pW}} = K_{pB} K'_{pW} \quad (39a)$$

For equations 5 and 25 to 27, designating the K_p values by the number of their equation,

$$K_{p25} = \frac{p_{\text{CH}_4} p_{\text{H}_2\text{O}}}{p_{\text{CO}} p_{\text{H}_2}^3} = \frac{p_{\text{CH}_4}}{p_{\text{H}_2}^2} \frac{p_{\text{H}_2\text{O}}}{p_{\text{H}_2} p_{\text{CO}}} = K_{pM} K'_{pW} \quad (40)$$

which is identical with equation 36,

$$\begin{aligned} K_{p26} &= \frac{p_{\text{CH}_4} p_{\text{H}_2\text{O}}^2}{p_{\text{CO}_2} p_{\text{H}_2}^4} = \frac{p_{\text{CH}_4} p_{\text{H}_2\text{O}}}{p_{\text{CO}} p_{\text{H}_2}^3} \frac{p_{\text{CO}} p_{\text{H}_2\text{O}}}{p_{\text{CO}_2} p_{\text{H}_2}} \\ &= K_{p25} K_W = K_{pM} K'_{pW} K_W \quad (41) \end{aligned}$$

which is identical with equation 37, and

$$K_{p_{27}} = \frac{p_{\text{CH}_4} p_{\text{CO}_2}}{p_{\text{H}_2}^2 p_{\text{CO}}^2} = K_{p_M} K'_{p_B} \quad (42)$$

which is identical with equation 38.

Accordingly, all reactions could be based on only three fundamental reactions, the Boudouard reaction (equation 2), the heterogeneous water-gas reaction (equation 3), and the reaction of

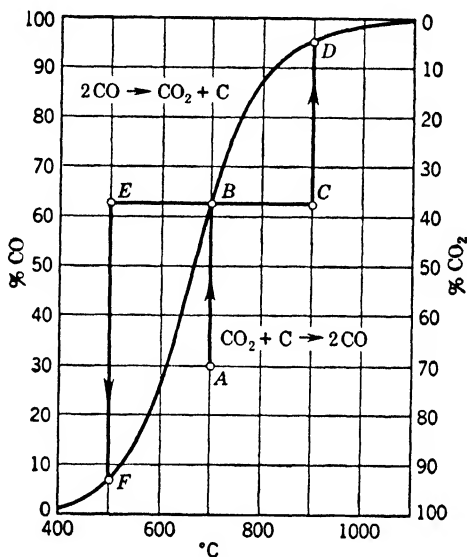
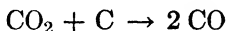


FIG. 1. Equilibrium of Boudouard's reaction ($P = 1$ Atm).

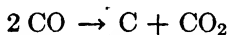
methane formation (equation 5). All their equilibrium constants could be obtained from these three reactions, and they are sufficient for the calculatory treatment of all gasification reactions so far considered. The equilibrium constants are tabulated in Tables V and VI on pages 304 and 305 of the appendix.

When considering any reaction equation, the question that arises first is in which direction does the reaction proceed? What are the effects of increasing temperature and pressure? Every chemical system attempts to establish and to maintain equilibrium. Thus the equilibrium constant is the most important consideration in determining whether a system is in equilibrium or in what direction the reaction has to proceed in order to attain equilibrium. Figure 1 illustrates the Boudouard reaction according to equa-

tion 2. By means of the equilibrium constants the gas composition has been calculated (see method of calculation on page 32) and plotted as a function of temperature. At 1 Atm a gas composition of 63.0% CO and 37.0% CO₂ corresponds to a temperature of 700°C. If a gas mixture of 30% CO and 70% CO₂ is considered at the same temperature (point *A* of Figure 1), it must tend towards an increase of the CO content. The reaction

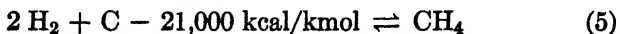
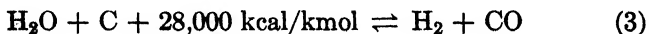
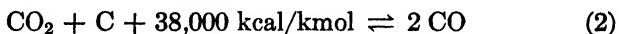


therefore must take place. This happens in a producer when the combustion gases high in temperature and rich in CO₂ reach the reducing zone. If the temperature of a gas mixture in equilibrium (point *B* of Figure 1) is increased to 900° (point *C*), the system is no longer in equilibrium and the reaction proceeds as above, increasing CO formation until point *D* (95.11%) is reached and equilibrium at the higher temperature is re-established. If, however, the temperature is lowered to 500°C, starting from point *E* (Figure 1), the reaction must follow the equation



until a CO content of only 6.53% or a CO₂ content of 93.47% is reached (point *F*). A heavy deposition of carbon would occur (soot formation). Cooling of this kind takes place in the pre-heating and distillation zone of a producer—outside the *reaction zone*—but soot formation is never as pronounced as might be expected from the above considerations (occasional soot formation may be due to the decomposition of heavy hydrocarbons). The explanation is that the gases, in cooling below a certain temperature range, do not maintain chemical equilibrium, inasmuch as the rates of the reactions at the lower temperatures are so low that the reactions practically “freeze” and stop altogether. This is an important supposition for gas production calculations.

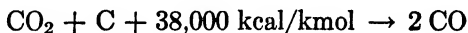
Considering the three main reactions more closely,



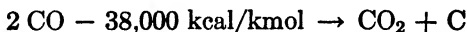
we may ask what else, aside from stoichiometric data, can we read in them? Equations 2 and 3 are endothermic (heat-consuming) reactions; heat must be added if the temperature is to be kept constant. As the amount of heat values show, the Boudouard reaction (equation 2) is somewhat more endothermic than the heterogeneous water-gas reaction (equation 3). Methane formation, according to equation 5, is weakly exothermic; it produces heat which must be removed if the temperature is to remain constant.

A general answer to our question is provided by Le Châtelier-Braun's *principle of least resistance*. Accordingly, a system in equilibrium tends to counteract any change of external conditions. An increase of pressure causes a shift in the direction of lower pressure which is the side of the equation of fewer molal quantities. Increase in temperature causes a shift toward the side of heat absorption in order to reduce the temperature. In other words, the system tries to follow the universal natural principle, the path of least resistance, and to adjust itself to the change of conditions.

In equation 2, the number of gas moles on the left-hand side is one (CO_2), on the right-hand side, two (2 CO). Increasing pressure indicates, according to the principle of least resistance, a shift towards CO_2 ; and decreasing pressure, a shift towards CO formation. Increasing temperature, according to Le Châtelier-Braun's principle, as seen in Figure 1, results in a shift in the endothermic reaction,



towards CO formation. Decreasing the temperature, conversely, leads to the exothermic formation of CO_2 and carbon deposition according to the equation



A *positive* sign of the heat means that the reaction is favored by temperature *increase*, a *negative* sign that it is favored by temperature *decrease*. In Figure 1 ($P = 1 \text{ Atm}$) the S-shaped curve separates the area into two fields in such a way that, in the upper left field, equation 2 proceeds from right to left and, in the lower right field, the reaction proceeds from left to right.

A second example is the exothermic methane formation reaction (Figure 2). A gas mixture containing 30% CH_4 and 70% H_2 at 700°C (point A, Figure 2) tends towards equilibrium at 10.58% CH_4 and 89.42% H_2 according to the equation for methane decomposition:



If point B (Figure 2) of the state of equilibrium is raised to 900°C (point C), the system favors a further methane decomposition.

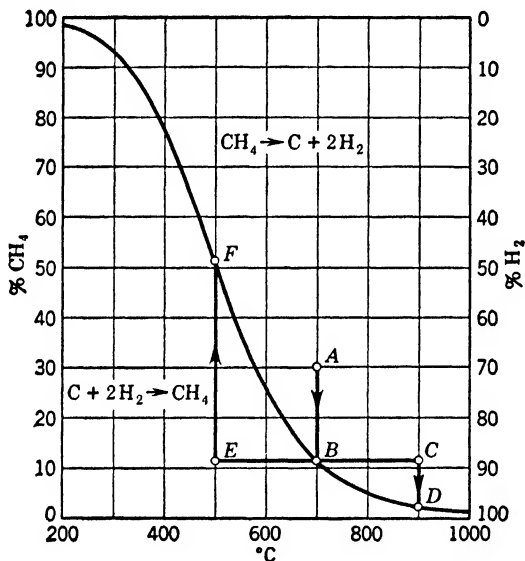
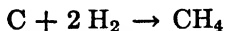


FIG. 2. Equilibrium of methane formation ($P = 1 \text{ Atm}$).

If, however, the temperature is lowered to 500°C (point E), the reaction favors methane formation:



Therefore, the conditions are the reverse of those in the previous example and show the difference between exothermic and endothermic reactions.

That the effect of pressure and temperature is not confined to general, qualitative statements, as by Le Châtelier-Braun's principle, is indicated by Figures 3 to 5, which present quantitative

results for the main reactions (equations 2, 3, and 5). Figure 3, at the left, presents the isobars (lines of constant pressure) and, at the right, isotherms (lines of constant temperatures) for the Boudouard reaction over wide pressure and temperature ranges, whereby the effects of pressure and temperature in the range presented are well illustrated. With changing pressures, the character of the isotherms is the same. Because of the distortion of the

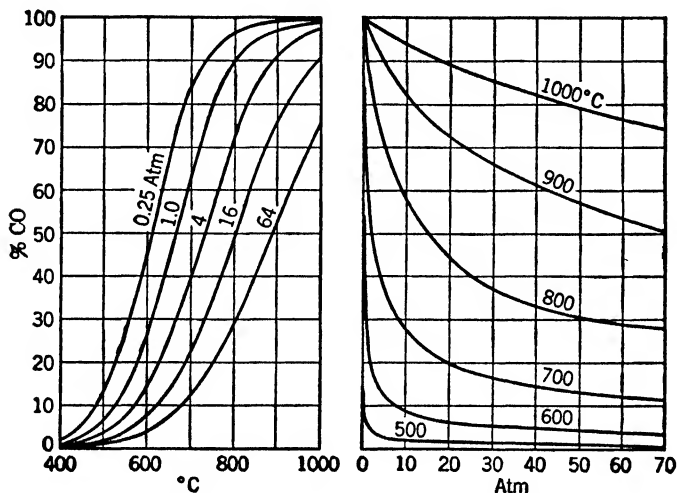


FIG. 3. Isobars and isotherms of the Boudouard reaction.

curves at constant temperature, however, entirely different parts of the curve are reached and different effects are found in practice. At 650°C, for instance, and 1 Atm, in the straight center region of the curve a moderate increase in temperature causes a large increase in CO content. At 64 Atm, however, with the more gradual curvature, a moderate increase in temperature effects only a slight increase in CO content. The effect of pressure can best be seen from the right-hand side of the diagram. Increasing pressure in the low and medium temperature ranges effects an initially rapid, then slower, increase in CO₂ (lowering of heating value) and, at very high temperatures, the curve becomes almost a straight line.

Figure 4 is a similar illustration of the heterogeneous water-gas reaction. The (CO + H₂) content is plotted upward, the H₂O downward as the ordinate. The CO and H₂ contents are each

half of the sum. The character of the curves is similar as in the CO_2 reduction, but the position of the equilibrium is different, as can best be seen from a superimposition of the two diagrams on each other (see Figure 6).

Figure 5 is a diagram, according to equation 5, of the methane formation in the same pressure and temperature range. The band of isobars is more dispersed so that their similarity cannot

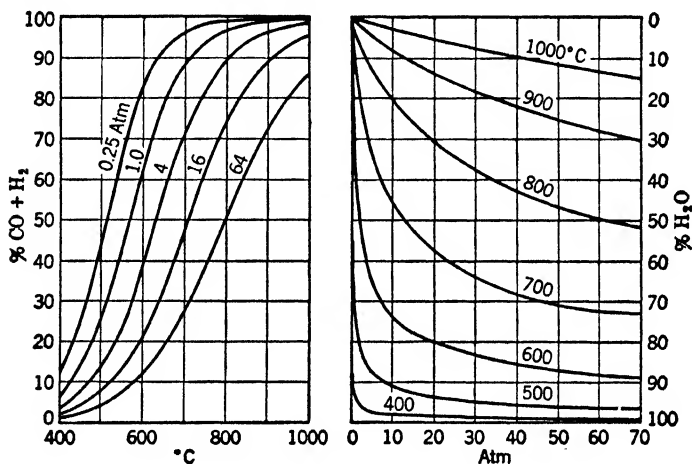


FIG. 4. Isobars and isotherms of the heterogeneous water-gas reaction.

be seen easily. This similarity would be more apparent if the curves were extended farther to the right and left into the regions of lower and higher temperatures. Since methane formation contributes appreciably to the heating value of gas, the value of pressure increase can be seen from this figure. Since, according to Figures 3 and 4, the CO_2 and H_2O contents increase with increase in pressure, an extremely large increase in heating value can be brought about in pressure gasification by washing these gases out, although at the expense of gas yield. The higher the pressure and the lower the temperature, the larger the methane formation; a cold, pressure gas producer, one with high steam content in the blast, will therefore produce a gas with a maximum heating value. The lower the temperature, the lower the pressures required; however, the slowing up of reaction rates as the temperature decreases imposes certain limits. From Figures 3, 4, and 6 it

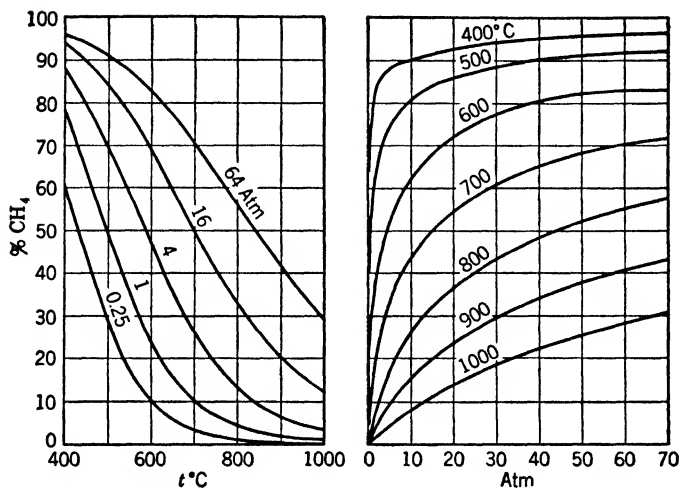


FIG. 5. Isobars and isotherms of the reaction of methane formation.

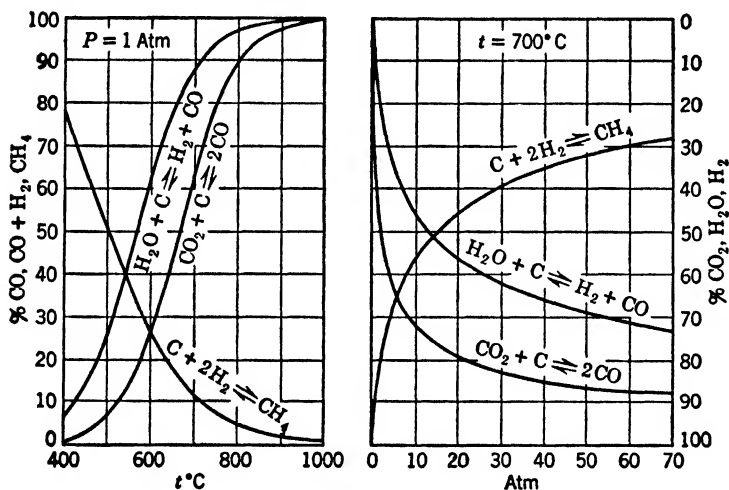


FIG. 6. Comparison of the three main reactions of gasification.

can also be seen that the increase in CO_2 and steam is considerable in the low pressure range, and that CO_2 and steam removal is therefore very effective in enriching the gas.

Figure 6 shows a comparison of the three reactions considered; in order not to confuse the picture, at only one pressure ($P = 1$

Atm) and one temperature ($t = 700^{\circ}\text{C}$). As can be seen, the heterogeneous water-gas reaction yields, at equilibrium, more combustible gas than does the Boudouard reaction at identical conditions. This means in practice that steam reduction has advanced farther than CO_2 reduction and that, with increasing temperature, the CO increase is more pronounced than the increase of H_2 . In the temperature range of 700 to 750°C , frequently occurring in the reduction zone of usual gas producers, the hydrogen shift is only very slight; in the higher temperature range of slagging ash gas producers, the hydrogen content is practically constant, and therefore an accurate measure for the steam content of the blast.

Of course Figures 3 to 6, which were supposed to illustrate the reactions according to equations 2 to 5, cannot be used to determine the composition of a producer gas. The three equations in the gas producer must be considered to proceed simultaneously and influence each other (simultaneous reactions).

The equilibrium constants

The preliminary condition for every gasification calculation is the exact knowledge of the equilibrium constants. The direct measurement of the equilibrium by determining the gas composition at constant temperature and known initial gas composition is very difficult, for the reason that the necessary simultaneous temperature measurement is difficult. "Static" and "dynamic" methods can be used. The dynamic method has the disadvantage that the decision whether or not the reaction has attained equilibrium is difficult to make. In the static method the reactant gas is left in contact with the solid phase (if necessary, by recycling) until the gas composition does not change, often requiring hours. The reason for these difficulties is that, although the reactions absorb or give off heat, a constant temperature must be maintained. The entering and issuing gases are also supposed to be at the same temperature. The addition (or removal) of heat, however, does not proceed without a temperature gradient. If the temperature gradient were made very large, considerable temperature differences would be found within the cross-section; if it were made small, the time required for heat exchange, and consequently the time to reach desired final state, would be very long. In addition, it is not the temperature of the gas phase that should be measured by introducing the thermoelement into the reaction tube which is

decisive in heterogeneous reactions, but the temperature at the phase boundary. As this cannot be measured directly, it is easy to understand why agreement of these methods has usually not been achieved and why the basis for gasification calculations has therefore not been very exact.*

The equilibrium constants can also be determined by thermodynamic methods, and to this method we owe the present accurate knowledge of these values. The derivation of the thermodynamic relations can be found in the textbooks and handbooks on thermodynamics.

A measure for the driving force of chemical reactions is the work of reaction, called *maximum work*, because it is the maximum amount of work that can be obtained from the reaction. This *principle of maximum work* is a version of the second law of thermodynamics, well suited for chemical reactions. This maximum work is at constant pressure and constant temperature †

$$\Delta F = \Delta H - T \Delta S' \quad (43)$$

where H is the enthalpy and S' is the entropy at constant pressure (reaction entropy).

The thermodynamic derivation of the law of mass action results in

$$\Delta F = -RT \ln K_p \quad (44)$$

Both equations provide a relationship between the equilibrium constant, K_p , and the enthalpy and entropy of the participating substances. An exact knowledge of these values (on an absolute scale) is, therefore, sufficient to determine K_p from c_p measurements and entropy values. Since specific heat data are no longer limited exclusively to calorimetric measurements, but can be determined by spectroscopic methods with uniform accuracy for the whole temperature range, we have at our disposal quite reliable and accurate values of equilibrium constants. Examples for

* It should be mentioned that the slowness in attaining the equilibrium state in the laboratory has led many workers to false conceptions of the processes taking place in gas producers and the possibility of approaching the equilibrium in gas producers of commercial size. These differences between laboratory equipment and large-scale dimensions will be discussed further on page 292.

† Isothermal reactions are usually considered at a definite, therefore constant, temperature.

calculating equilibrium constants from specific heat and entropy data are repeatedly reported in the literature.²

The numerical values of the equilibrium constants used below are taken from *Research Paper* RP 1634 of the National Bureau of Standards³ and expressed by equations in order to get smooth values for any intermediate temperatures. The equilibrium constant of the Boudouard reaction (equation 2) may be expressed by

$$\log K_{pB} = 3.26730 - \frac{8820.690}{T} - 0.001208714T \\ + 0.153734 \times 10^{-6}T^2 + 2.295483 \times \log T \quad (45)$$

In the temperature range between 700 and 1500°K, within which gasification processes may occur, the maximum deviation of the numerical values given by equation 45 is -0.0007 for $\log K_{pB}$, corresponding to -0.16% of the K value itself. Even extrapolation beyond this range is possible, as shown by Table 2.

The equilibrium constant of the heterogeneous water-gas reaction is given by the following equation:

$$\log K_{pW} = -33.45778 - \frac{4825.986}{T} - 0.005671122T \\ + 0.8255484 \times 10^{-6}T^2 + 14.515760 \times \log T \quad (46)$$

The agreement between the results of this equation and the Bureau of Standards values is shown in Table 3. Within the range of

² Barnett F. Dodge, *Chemical Engineering Thermodynamics*, New York and London, 1944, pp. 497-528. Olaf A. Hougen and Kenneth M. Watson, *Chemical Process Principles*, Part 2, New York, 1947. A. Eucken and M. Jakob, *Der Chemie-Ingenieur*, Vol. III, Part 1, Leipzig, 1937. H. Ulich, *Kurzes Lehrbuch der physikalischen Chemie*, Dresden and Leipzig, 1938. H. Ulich, Näherungsformeln zur Berechnung von Reaktionsarbeiten und Gleichgewichten aus thermochemischen Daten, *Z. Elektrochem.*, Vol. 45 (1937), No. 7, pp. 521-533. O. Fuchs and K. Rinn, Die Berechnung von Gleichgewichten in der Gasphase aus thermischen Daten, *Angew. Chem.*, Vol. 50 (1937), No. 34, pp. 708-712. Carl Schwarz, Die spezifischen Wärmen der Gase als Hilfswerte zur Berechnung von Gleichgewichten, *Arch. Eisenhüttenwes.*, Vol. 9 (1936), No. 8, pp. 389-396.

³ Donald D. Wagman, John E. Kilpatrick, William J. Taylor, Kenneth S. Pitzer, and Frederick D. Rossini, Heats, free energies, and equilibrium constants of some reactions involving O₂, H₂, H₂O, C, CO, CO₂, and CH₄, *J. Research Bur. Standards*, Vol. 34 (1945), pp. 143-161.

TABLE 2

COMPARISON OF EQUILIBRIUM CONSTANT ACCORDING TO EQUATION 45 AND
BUREAU OF STANDARDS VALUE

T °K	$\log K_{pB}$ (Equation 45)	$\log K_{pB}$ (Bureau of Standards)
300	-20.79759	-20.81089
400	-13.27034	-13.28281
500	-8.74457	-8.75242
600	-5.72654	-5.72851
700	-3.57358	-3.57358
800	-1.96315	-1.96284
900	-0.71568	-0.71538
1000	+0.27808	+0.27865
1100	+1.08638	+1.08638
1200	+1.75585	+1.75658
1300	+2.31863	+2.31863
1400	+2.79782	+2.79835
1500	+3.21033	+3.21033

TABLE 3

COMPARISON OF THE EQUILIBRIUM CONSTANT ACCORDING TO EQUATION 46 AND
BUREAU OF STANDARDS VALUE

T °K	$\log K_{pW}$ (Equation 46)	$\log K_{pW}$ (Bureau of Standards)
300	-15.21416	-15.85786
400	-9.88823	-10.11277
500	-6.56132	-6.65217
600	-4.27960	-4.29593
700	-2.61853	-2.61852
800	-1.35825	-1.35664
900	-0.37227	-0.37226
1000	+0.41694	+0.41665
1100	+1.06373	+1.06373
1200	+1.60064	+1.59959
1300	+2.05385	+2.05385
1400	+2.44206	+2.44243
1500	+2.77903	+2.77906

validity (700 to 1500°K), the maximum deviation is 0.019% of $\log K_{pw}$ values or 0.37% of K_{pw} value.

According to equation 39a, an equation for the equilibrium constant of the homogeneous water-gas reaction will be obtained by equations 45 and 46 from

$$\log K_W = \log K_{pB} - \log K_{pw} \quad (47)$$

or

$$\log K_W = 36.72508 - \frac{3994.704}{T} + 0.004462408T \\ - 0.671814 \times 10^{-6}T^2 - 12.220277 \times \log T \quad (47a)$$

The reaction of methane formation according to equation 5 has the following constant of equilibrium:

$$\log K_{pM} = -13.06361 + \frac{4662.80}{T} - 2.09594 \times 10^{-3}T \\ + 0.38620 \times 10^{-6}T^2 + 3.034338 \times \log T \quad (48)$$

A comparison with Bureau of Standards data is shown in Table 4. Within range of its proper validity, 700 to 1500°K, the equation gives deviations of 0.005 or less.

TABLE 4

COMPARISON OF THE EQUILIBRIUM CONSTANT ACCORDING TO EQUATION 48
AND BUREAU OF STANDARDS VALUE

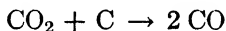
T °K	$\log K_{pM}$ (Equation 48)	$\log K_{pM}$ (Bureau of Standards)
300	+9.40146	+8.8177
400	+5.71233	+5.4899
500	+3.50016	+3.4268
600	+2.01734	+2.0001
700	+0.95261	+0.9526
800	+0.14392	+0.1494 *
900	-0.49209	-0.4881 *
1000	-1.00754	-1.0075
1100	-1.43432	-1.4345
1200	-1.79367	-1.7936
1300	-2.10013	-2.1006
1400	-2.36399	-2.3638
1500	-2.59271	-2.5927

* Probably error or misprint in the original report. No conformity between given logarithm and antilogarithm.

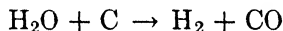
The numerical values of the equilibrium constants K_{pW} , K'_{pW} , K_{pM} , K'_{pM} , and K_{pM} are summarized in Table V of the appendix, page 304; the numerical values of some derived equilibrium constants as K_W and its reciprocals K'_W , K_{p25} , K_{p26} , K_{p27} in Table VI of the appendix, page 305.

The gasification mechanism

This mechanism can be pictured roughly as follows. The oxygen carrier (e.g., the air) introduced into the fuel bed first burns part of the carbon until practically all free oxygen is exhausted. The mechanism of this combustion process in the oxidation zone of a gas producer in the stationary state is characterized by gas combustion, e.g., combustion of the primary products of combustion, which may be carbon monoxide or dioxide or simultaneously formed CO and CO₂, depending on the temperature. From a present-day point of view, the favored reaction at the surface of the coke is



If the oxidizing atmosphere also contains water vapor, the following reaction also occurs:



Free oxygen, however, penetrates to the surface of the coke to only a small extent, if at all, and is already burned at the boundary layer with the formed gases, CO and H₂ going to CO₂ and H₂O. Quantitative gas analyses in the phase boundary and directly on the surface of the coke are impossible as are exact local temperature measurements, so that the course of combustion under commercial conditions cannot be followed directly. The strongest support for this view is the slagging behavior of the fuels. If the oxygen of the air of combustion penetrated to the surface of the coke and burned to CO₂ as the primary reaction, the interior of the coke bed, which is protected from any appreciable external heat loss, would show temperatures of about 2000°C (dissociation taken into consideration). At these temperatures, the ashes of all known fuels would melt together to a thin slag and cover the reacting surfaces to a large extent. Since most cokes have ash-melting temperatures of about 1200 to 1500°C even an extensive humidification of the combustion air would not be sufficient to

prevent slag formation, as can be seen in Figure 7. This idea does not coincide with experience and observation. If it is assumed, however, that the reactions $\text{CO}_2 + \text{C} \rightarrow 2 \text{CO}$ and $\text{H}_2\text{O} + \text{C} \rightarrow \text{H}_2 + \text{CO}$ take place at the surface of the coke, reaction temperatures according to the lower part of the curve (Figure 7) result, in accordance with the fact that slag formation

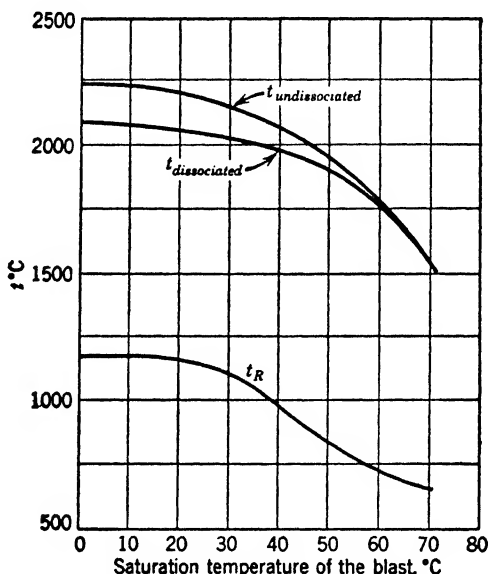


FIG. 7. Combustion and reaction temperatures of carbon at different saturation temperatures of the blast.

can be controlled completely by saturating air with steam to a wet-bulb temperature of 50 to 55°C for slag-melting temperatures of approximately 1200°C. In Figure 7 the radiant energy transfer between the gas combustion zone and the coke surface is not considered, and consequently the calculated temperature of the coke surface is shifted somewhat above the reported values.

A further indirect proof of the correctness and suitability of this presentation of the combustion mechanism is given by Traustel's⁴ statement that a direct reaction $\text{C} + \text{O}_2 \rightarrow \text{CO}_2$ in the combustion of powdered coal or coke (in suspension) would lead,

⁴Sergei Traustel, *Verbrennung in der Schwebe*, *Feuerungstechn.*, Vol. 29 (1941), No. 1/3, pp. 1-6, 25-31, 49-60.

according to Nusselt,⁵ to an infinite time, $z = \infty$, whereas experience shows that combustion of powdered coal is achieved with nearly the theoretical amount of air and nearly complete combustion, therefore within very finite combustion time. The combustion mechanism by way of gasification occurring at the fuel surface results in a finite time of combustion and in good agreement between theory and practice.

The oxidation zone of the gas producer is followed by the reduction zone where the reactions according to equations 2 to 5 take place. The secondary gasification reaction of CO_2 is, according to several research workers,⁶ approximately one hundred times slower than the combustion with oxygen. This fact does not influence the commercial process of combustion appreciably for reasons given below, though it has been assumed that in the commercial process the gasification reaction is an intermediate link of the combustion reaction.* Since reduction is a strongly endothermic reaction, the reactions in the fuel bed shift more and more into the low-temperature range, whereby they become increasingly slower. The rate of reaction becomes so small that it influences the total time of reaction considerably; externally, it can be seen by the expansion of the reduction zone.

Gasification reactions are heterogeneous, i.e., they take place at the phase boundary, therefore at the surface of the coke. The temperature prevailing there is decisive in fixing the composition of the gas formed. In accord with the surface temperature concept, a somewhat better gas is formed at the beginning of the reduction zone; with increasing height and decreasing surface temperature the quality of the gas deteriorates slightly (increasing CO_2 content). The gas thus formed in the boundary layer is mixed by diffusion and convection with the gas of combustion leaving the oxidation zone. Consequently, in spite of higher temperature in the beginning of the reduction zone, a still very poor, however rapidly improving, total gas exists in the gas phase. In the same manner, as material exchange takes place at the coke

⁵ W. Nusselt, *Der Verbrennungs-Vorgang in der Kohlenstaubfeuerung*, Z. VDI, Vol. 68 (1924), No. 6, pp. 124-128, and Vol. 70 (1926), No. 27, p. 914.

⁶ Arnold Eucken, *Lehrbuch der chemischen Physik*, Vol. II, Part 2, 2nd ed., Leipzig, 1944, pp. 1478-79.

* In high vacuum technique where the influences of convection and diffusion are eliminated, the reaction proceeds somewhat differently.

surface between the gas of combustion and the formed combustible gas, heat transfer between the gas phase and coke occurs where endothermic gasification reactions convert heat. The reactions finally come to a standstill (1) when the CO_2 concentration of the gas phase is equal to that of the phase boundary so that there can be no material exchange because a difference of concentration is lacking or too small, and (2) when the temperature differences are evened out and no more heat transfer can take place. Solid

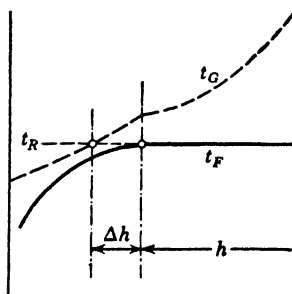


FIG. 8. Gas (t_G) and coke temperature (t_F) at the end of the reduction zone. (Definition of the reaction temperature.)

and gaseous phases are in equilibrium with regard to temperature as well as to material. This temperature, which can be determined accurately from the heat balances of the reaction zones (oxidation and reduction zone), is called the *reaction temperature*. It is that temperature at which or up to which the reactions proceed and which determines the gas composition, hence its importance for the gasification calculations. Although the reaction temperature in a gas producer could be localized, namely, as the surface temperature of the coke at the end of the

reduction zone, such a localization in practice is of lesser importance, since we can obtain the exact value from heat balance better than by measurement.* The surface temperature at an arbitrary point of the reduction zone will be slightly, but not appreciably, higher than this temperature, since a better gas and therefore a higher heat consumption and a livelier reaction rate always correspond to a higher temperature, so that some kind of self-adjustment of the process takes place (see Figure 8).

Naturally, the temperature in the gas phase is entirely different from the reaction temperature. The innumerable false conceptions of the gasification process and of the attainment of equilibria in gas producers are caused by the false attribution of measured temperatures and simultaneous gas analyses. The mineral matter of the fuel when the carbon in their direct surroundings is ex-

* The approximate localization of heat losses has some importance because of the necessary distribution of the total external heat loss of the gas producer to the different zones of the producer.

hausted behaves differently again. Thereby the automatic temperature control is eliminated, and the temperatures can increase further and cause sintering and melting of the slag. There will still be an exchange of material between the gas phase and the fuel surface located below, i.e., the surface of the remaining combustible matter, through the ash-and-slag skeleton. Slag formation, consequently, does not lead necessarily to the prevention of the combustion or gasification process, although a certain slowing down may occur because of the impediment of the physical exchange of material.

Figure 9 shows in simplest and highly schematic form the change in gas composition if a perfect cross-sectional mixture were formed in every layer. Merely a gasification of carbon with (dry) air is presented. In the oxidation zone, the oxygen content decreases from 21 to 0%; the CO_2 content increases proportionately. When reduction starts, the CO content increases at the expense of CO_2

until the exchange is complete from the material and heat balance point of view. In reality, the cross-sectional mixture is already imperfect in the oxidation zone, so that a temporary coexistence of CO and oxygen is possible; the CO_2 peak is thereby flattened out. The flattening out is intensified by the fact that the gas volume in the gas producer fuel bed is formed by the complicated void space (intergranular) so that differences in grain size, particle size distribution, and differences in density, pressure, and temperature blot out the line between oxidation and reduction zones still further. Moreover, the velocity of the processes is far from constant; the increase and decrease will therefore not be in straight lines. Both combustion and gasification, since we are dealing with equalizing processes, will take place rapidly at first, owing to the high concentration difference (O_2 , CO_2), and slowly fade out, so that at the border of oxidation and reduction zones the slow combustion process will be concealed by the vigorous initial reduction. The change in oxygen, CO_2 , and CO content

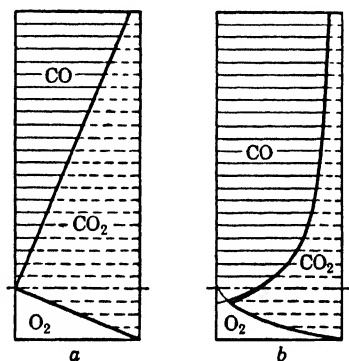


FIG. 9. Diagrammatic sketches of the change in gas composition.

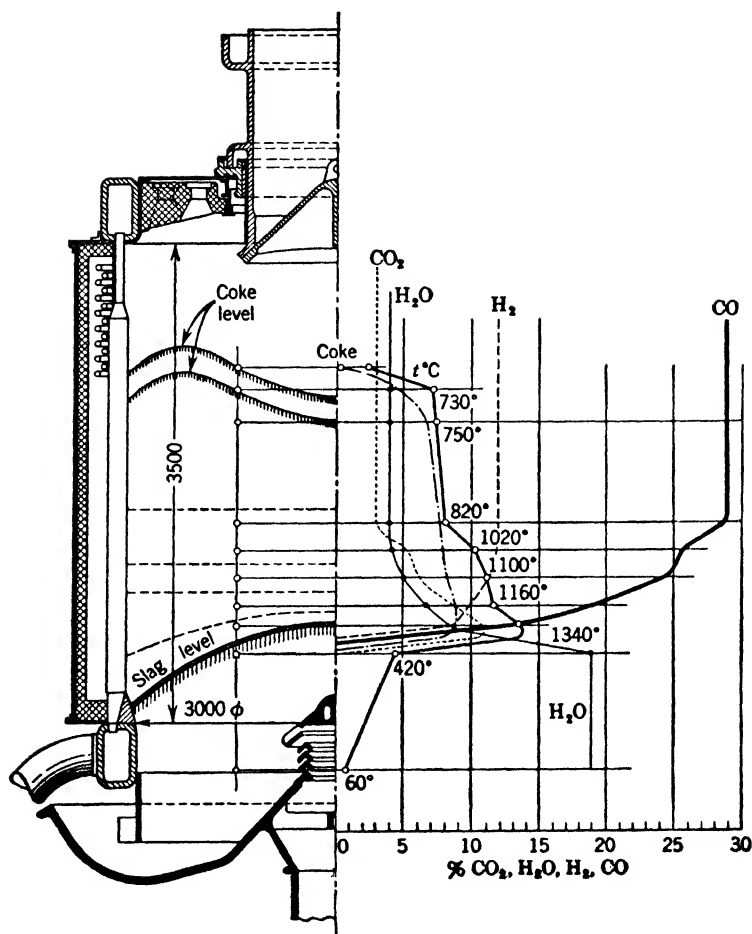


FIG. 10. Gas composition and temperatures in a commercial size gas producer (3 m inside diameter), according to W. Horak.

takes, therefore, the shape seen in Figure 9b. It is qualitatively well confirmed by Horak's ⁷ measurements of a gas producer of 3-meter shaft diameter (Figure 10).

From this representation of processes taking place in gas producers, it is clear that the overall reaction is a combination of a

⁷ Wilhelm Horak, Untersuchungen an einem Gaserzeuger mit Dampfmantel, *Z. Oester Ver. Gas- u. Wasserfachm.*, Vol. 74 (1933), No. 11-12, pp. 170-180, 194-203.

physical and a chemical partial reaction. To bring about a reaction, the reactant (i.e., oxygen of the air, steam, CO_2) has to be brought to the surface of the solid. This is a purely physical process which takes place by transfer of matter (convection) in large aggregates or by diffusion (molecular transfer of matter) in smaller dimensions, and correspondingly slower. Only then the chemical reaction can take place. In general, the rate of chemical reactions is so fast in the high-temperature range (above 900°C) that it can be neglected in view of the relatively slow processes of physical transfer of matter and energy. Between approximately 700 and 900°C the rate of chemical reaction becomes noticeable, and it plays a dominating part in the range between 500 and 600°C or below, which is of practical interest for ignition processes only. The phenomena in the oxidation zone are governed exclusively by physical influences, owing to the high temperatures. The height of the zone as a measure of oxidation velocity is therefore determined only by physical factors (particle size or particle size characteristic). With particle sizes used in most large-scale gas producers, the oxidation zone usually is approximately 100 to 150 mm (4 to 6 in.) high, and is not appreciably influenced by the gas velocity or by the nature of the fuel. The slight effect of the gas velocity is explained by the fact that the shorter time of contact at high air velocity is completely counterbalanced by the more vigorous exchange of matter and the stronger turbulence.

The reduction zone of a gas producer has the same cross-section and the same cross-sectional gas charge as the oxidation zone. It is, however, considerably longer because of the lower temperatures and the increasing effect of the rate of chemical reaction, especially noticeable in the last part of this zone, causing the very slow decline of reaction. The reduction zone is about 800 mm (32 in.) high. A reduction of this zone is of little consequence for the gas composition. The total height of the bed of a gas producer for smaller nut sizes is, therefore, approximately 1 meter, including an ash zone of 50 to 100 mm. No gasification reactions take place in the preheating, distillation, and drying zones; only heat transfer which is essential for the heat balance.

2

GAS COMPOSITION AT EQUILIBRIUM

Basis of calculation

To calculate the equilibrium gas analysis at a known temperature and pressure, the equilibrium constants and, as further equations of condition, the material balances are utilized. First a simple problem, the Boudouard reaction according to equation 2, will be discussed.

The product gas consists of only two constituents, the unconverted CO_2 and the produced CO , so that

$$v_{\text{CO}} + v_{\text{CO}_2} = 1 \quad (49)$$

and by definition (equation 20),

$$K_{pB}P^{-1} = \frac{(v_{\text{CO}})^2}{v_{\text{CO}_2}}$$

The unknown v_{CO} is found as follows:

$$K_{pB}P^{-1} = \frac{(v_{\text{CO}})^2}{1 - v_{\text{CO}}} \quad (50)$$

$$(v_{\text{CO}})^2 + K_{pB}P^{-1}v_{\text{CO}} - K_{pB}P^{-1} = 0 \quad (51)$$

$$v_{\text{CO}} = -\frac{K_{pB}P^{-1}}{2} \pm \sqrt{\left(\frac{K_{pB}P^{-1}}{2}\right)^2 + K_{pB}P^{-1}} \quad (52)$$

The positive square root of this equation is used; furthermore, from equation 49,

$$v_{\text{CO}_2} = 1 - v_{\text{CO}} \quad (53)$$

Table 5 and Figure 3 show the result of this calculation.

As a second example, the heterogeneous water-gas reaction according to equation 3 will be considered. As equations of condition we use

$$v_{H_2} + v_{CO} + v_{H_2O} = 1 \quad (54)$$

and

$$K_{pw}P^{-1} = \frac{v_{H_2}v_{CO}}{v_{H_2O}} \quad (24)$$

As a third equation of condition, the following relationship is used:

$$v_{H_2} = v_{CO} \quad (55)$$

It is based on the fact that equal molal quantities of hydrogen and carbon monoxide are produced as well as equal volumes, if the

TABLE 5
GASIFICATION OF CARBON WITH OXYGEN
(v_{CO} %, °C, pressure in physical atmospheres)

$P =$	0.25	1	4	16	64 Atm
$t = 400^\circ\text{C}, v_{CO} \% =$	1.78	0.89	0.45	0.22	0.11
500	13.29	6.53	3.26	1.64	0.83
600	45.45	26.43	10.44	7.53	3.77
700	83.67	63.00	53.52	22.89	12.12
800	96.89	89.51	72.50	49.24	29.10
900	99.35	97.51	92.31	76.04	53.18
1000	99.83	99.64	97.46	91.13	75.59

very slight differences between the true molal volume of hydrogen (22.43 SCM/kmol) and of carbon monoxide (22.41 SCM/kmol) are disregarded * in equations 54 and 55.

$$v_{H_2O} = 1 - 2v_{H_2} \quad (56)$$

And from equation 24,

$$K_{pw}P^{-1} = \frac{(v_{H_2})^2}{1 - 2v_{H_2}} \quad (57)$$

$$(v_{H_2})^2 + 2K_{pw}P^{-1} - K_{pw}P^{-1} = 0 \quad (58)$$

$$v_{H_2} = -K_{pw}P^{-1} \pm \sqrt{(K_{pw}P^{-1})^2 + K_{pw}P^{-1}} \quad (59)$$

* It is not difficult to allow for this difference. At $p = 1$ Atm, $t = 700^\circ\text{C}$ the deviation of H_2 and CO is $+0.02$ and -0.03% , respectively. This difference is negligible.

The result of the calculation is given in Table 6. See also Figure 4.

TABLE 6
GASIFICATION OF CARBON WITH STEAM
(v_{CO} , v_{H_2} %, °C, pressures in physical atmospheres)

$P =$	0.25	1	4	16	64 Atm
$t = 400^\circ\text{C}, v_{\text{CO}}, v_{\text{H}_2} \% =$	5.81	2.99	1.51	0.77	0.39
500	21.97	12.67	6.82	3.53	1.61
600	41.21	30.61	19.28	10.87	5.78
700	48.24	44.14	35.14	23.47	13.73
800	49.61	48.52	44.93	36.57	24.97
900	49.80	49.58	48.59	44.55	35.88
1000	49.96	49.85	49.41	47.89	43.42

As a third example, the reaction of methane formation according to equation 5 will be considered:

$$v_{\text{H}_2} + v_{\text{CH}_4} = 1 \quad (60)$$

$$PK_{PM} = \frac{v_{\text{CH}_4}}{(v_{\text{H}_2})^2} \quad (32)$$

$$PK_{PM} = \frac{v_{\text{CH}_4}}{(1 - v_{\text{CH}_4})^2} = \frac{v_{\text{CH}_4}}{1 - 2v_{\text{CH}_4} + (v_{\text{CH}_4})^2} \quad (61)$$

TABLE 7
METHANE FORMATION FROM HYDROGEN AND CARBON
(v_{CH_4} %, °C, pressures in physical atmospheres)

$P =$	0.25	1	4	16	64 Atm
$t = 400^\circ\text{C}, v_{\text{CH}_4} \% =$	61.30	78.16	88.39	94.01	96.06
500	29.73	51.60	71.51	84.51	91.92
600	10.49	25.51	48.73	69.41	83.25
700	3.11	10.58	27.68	50.95	71.04
800	1.16	4.32	14.01	33.43	56.67
900	0.50	1.91	6.88	20.21	42.29
1000	0.13	0.94	3.54	11.83	29.90

$$(v_{\text{CH}_4})^2 - \left(2 + \frac{1}{PK_{pM}}\right)v_{\text{CH}_4} + 1 = 0 \quad (62)$$

$$v_{\text{CH}_4} = 1 + \frac{1}{2PK_{pM}} \pm \sqrt{\left[1 + \frac{1}{2PK_{pM}}\right]^2 - 1} \quad (63)$$

In this third example the negative square root is used. The result of the calculation is given in Table 7 and Figure 5.

Another way to present such calculations is the method of the *degree of dissociation*.

If it is assumed that in the reaction (equation 2)



n molecules of CO_2 are present, of which nx are reduced to CO on the solid carbon. Then $2nx$ molecules of CO are formed, and $n(1 - x)$ molecules of CO_2 are left. The sum of these, therefore, the sum of the molecules in the reacting system, is

$$2nx + n(1 - x) = n(1 + x) \quad (64)$$

The partial pressure of CO_2 is

$$\frac{p_{\text{CO}_2}}{P} = \frac{1 - x}{1 + x} \quad (65)$$

The partial pressure of CO is

$$\frac{p_{\text{CO}}}{P} = \frac{2x}{1 + x} \quad (66)$$

and the relation between x and K_{pB} is

$$K_{pB} = \frac{p_{\text{CO}}^2}{p_{\text{CO}_2}} = \frac{4x^2P}{1 - x^2} \quad (67)$$

From this equation the degree of dissociation, α_B , in % is

$$x = \frac{\alpha_B}{100} = \sqrt{\frac{K_{pB}}{K_{pB} + 4P}} = \frac{1}{\sqrt{1 + (4P/K_{pB})}} \quad (68)$$

or

$$\alpha_B = \frac{100}{\sqrt{1 + 4PK'_{pB}}} \quad (69)$$

Sample Calculation. $P = 1 \text{ Atm}$, $t = 700^\circ\text{C}$, $K'_{pB} = 0.93226$.

$$\alpha_B = \frac{100}{\sqrt{1 + 4 \times 1 \times 0.93226}} = \frac{100}{\sqrt{4.72904}} = \frac{100}{2.1746} = 45.99\%$$

Let the initial quantity of CO_2 be v'_{CO_2} , and $x = \frac{\alpha_B}{100}$ then is, according to equations 66 and 65,

$$v_{\text{CO}} = \frac{(2\alpha_B/100)v'_{\text{CO}_2}}{1 + \alpha_B v'_{\text{CO}_2}} \quad (70)$$

$$v_{\text{CO}_2} = \frac{v'_{\text{CO}_2} - \alpha_B v'_{\text{CO}_2}}{1 + \alpha_B v'_{\text{CO}_2}} \quad (71)$$

In this sample calculation, $v'_{\text{CO}_2} = 1$; therefore

$$v_{\text{CO}} = \frac{2 \times 0.4599}{1.4599} = 0.6300$$

$$v_{\text{CO}_2} = \frac{1 - 0.4599}{1.4599} = 0.3700$$

These values are in accord with the previous calculation (see Table 5, value for 700°C , 1 Atm).

Considering the heterogeneous water-gas reaction, let n molecules of steam enter the system of which nx molecules are decomposed; nx molecules of hydrogen and nx molecules of carbon monoxide are formed, and $n(1 - x)$ molecules of steam remain. The sum of the reactants is

$$2nx + n(1 - x) = n(1 + x) \quad (72)$$

Furthermore,

$$\frac{p_{\text{CO}}}{P} = \frac{x}{1 + x} \quad (73)$$

$$\frac{p_{\text{H}_2}}{P} = \frac{x}{1 + x} \quad (74)$$

$$\frac{p_{\text{H}_2\text{O}}}{P} = \frac{1 - x}{1 + x} \quad (75)$$

$$K_{pW} = \frac{p_{\text{H}_2} p_{\text{CO}}}{p_{\text{H}_2\text{O}}} = \frac{x^2 P}{1 - x^2} \quad (76)$$

$$x = \frac{\alpha_W}{100} = \sqrt{\frac{K_{pW}}{K_{pW} + P}} = \frac{1}{\sqrt{1 + (P/K_{pW})}} \quad (77)$$

$$\alpha_W = \frac{100}{\sqrt{1 + PK'_{pW}}} \quad (78)$$

$$v_{H_2} = v_{CO} = \frac{(\alpha_W/100)v'_{H_2O}}{1 + \alpha_W v'_{H_2O}} \quad (79)$$

$$v_{H_2O} = \frac{v'_{H_2O} - (\alpha_W/100)v'_{H_2O}}{1 + \alpha_W v'_{H_2O}} \quad (80)$$

Sample Calculation. $P = 16$ Atm, $t = 700^\circ\text{C}$.

$$\alpha_W = \frac{100}{\sqrt{1 + 16 \times 0.60176}} = \frac{100}{\sqrt{10.62816}}$$

$$\alpha_W = \frac{100}{3.260} = 30.67\%$$

With $v'_{H_2O} = 1$,

$$v_{H_2} = v_{CO} = \frac{0.3067}{1.3067} = 0.2347$$

(Compare Table 6.)

Methane formation, according to equation 5, starts with $2n$ molecules of hydrogen, of which $2nx$ molecules are used for the formation of nx molecules of methane, and $2n(1 - x)$ molecules of hydrogen remain. The sum of the reactants is therefore

$$2n(1 - x) + nx = n(2 - x) \quad (81)$$

$$\frac{p_{CH_4}}{P} = \frac{x}{2 - x} \quad (82)$$

$$\frac{p_{H_2}}{P} = \frac{2(1 - x)}{2 - x} \quad (83)$$

$$K_{pM} = \frac{p_{CH_4}}{p_{H_2}^2} = \frac{x(2 - x)}{4(1 - x)^2 P} \quad (84)$$

From this equation,

$$x^2 - 2x + \frac{4PK_{pM}}{4PK_{pM} + 1} = 0 \quad (85)$$

$$x = \frac{\alpha_M}{100} = 1 \pm \sqrt{1 - \frac{4PK_{pM}}{4PK_{pM} + 1}} = 1 - \frac{1}{\sqrt{1 + 4PK_{pM}}} \quad (86)$$

Sample Calculation. $P = 64 \text{ Atm}$, $t = 700^\circ\text{C}$, $v'_{\text{H}_2} = 1$.

$$\alpha_M = 100 - \frac{100}{\sqrt{1 + 4 \times 64 \times 0.13237}} = 100 - \frac{100}{5.9065} = 83.07\%$$

$$v_{\text{CH}_4} = \frac{(\alpha_M/200)v'_{\text{H}_2}}{1 - (\alpha_M/200)v'_{\text{H}_2}} = \frac{0.41535}{0.58465} = 71.04\%$$

$$v_{\text{H}_2} = \frac{v'_{\text{H}_2} - (\alpha_M/100)v'_{\text{H}_2}}{1 - (\alpha_M/200)v'_{\text{H}_2}} = \frac{0.16930}{0.58465} = 28.96\%$$

Considering next the simple case of an inert gas added to the gasifying agent, e.g., nitrogen of the air, we find that the pressure of the reacting system is reduced when carbon is gasified with dry air to produce a so-called air gas.

The composition of the gasifying agent is

$$v'_{\text{O}_2} = 0.21; \quad v'_{\text{N}_2} = 0.79$$

Two equations provide the following simple relationships:

$$K_{pB}P^{-1} = \frac{(v_{\text{CO}})^2}{v_{\text{CO}_2}} \quad (20)$$

and

$$v_{\text{CO}} + v_{\text{CO}_2} + v_{\text{N}_2} = 1 \quad (87)$$

To eliminate the third unknown, the ratio of oxygen to nitrogen in the blast and in the product gas is used. The following equation results when both sides of the oxygen and nitrogen balances are divided:

$$\frac{0.21}{0.79} = \frac{0.5v_{\text{CO}} + v_{\text{CO}_2}}{v_{\text{N}_2}} \quad (88)$$

From these equations,

$$v_{\text{CO}_2} = 1 - v_{\text{CO}} - \frac{0.79}{0.21} 0.5v_{\text{CO}} - \frac{0.79}{0.21} v_{\text{CO}_2} \quad (89)$$

$$v_{\text{CO}_2} = \frac{1 - v_{\text{CO}} - (0.79/0.21)0.5v_{\text{CO}}}{1 + (0.79/0.21)} \quad (90)$$

$$(v_{\text{CO}})^2 = \frac{1 - v_{\text{CO}}[1 + (0.79/0.21)0.5]}{1 + (0.79/0.21)} K_{pB}P^{-1} \quad (91)$$

$$\begin{aligned}
 (v_{\text{CO}})^2 &= \frac{K_{p_B} P^{-1}}{1 + (0.79/0.21)} - v_{\text{CO}} K_{p_B} P^{-1} \frac{1 + (0.79/0.21)0.5}{1 + (0.79/0.21)} \\
 &= 0.21 K_{p_B} P^{-1} - 0.605 v_{\text{CO}} K_{p_B} P^{-1} \quad (92)
 \end{aligned}$$

$$(v_{\text{CO}})^2 + 0.605 K_{p_B} P^{-1} v_{\text{CO}} - 0.21 K_{p_B} P^{-1} = 0$$

$$v_{\text{CO}} = -0.3025 K_{p_B} P^{-1}$$

$$\pm \sqrt{(0.3025 K_{p_B} P^{-1})^2 + 0.21 K_{p_B} P^{-1}} \quad (93)$$

From equation 90,

$$v_{\text{CO}_2} = 0.21 - 0.605 v_{\text{CO}} \quad (90a)$$

and from equation 87,

$$v_{\text{N}_2} = 1 - (v_{\text{CO}} + v_{\text{CO}_2}) \quad (87a)$$

The results of this calculation at $P = 1$ Atm are given in Table 8 and Figure 11.

TABLE 8

THEORETICAL ANALYSIS OF AIR GAS PRODUCED BY GASIFYING CARBON WITH DRY AIR

($p = 1$ Atm)

$t^\circ\text{C}$	CO%	CO ₂ %	N ₂ %	$\frac{\text{CO}}{\text{CO} + \text{CO}_2}$	$\frac{\text{CO}}{\text{CO}_2}$
350	0.12	20.93	78.95	0.00	0.00
400	0.41	20.75	78.84	0.02	0.02
450	1.18	20.39	78.43	0.05	0.06
500	2.90	19.24	77.86	0.13	0.15
550	6.21	17.24	76.55	0.27	0.36
600	11.52	14.03	74.45	0.45	0.82
650	18.34	9.91	71.75	0.65	1.85
700	25.05	5.84	69.11	0.81	4.28
750	29.82	2.96	67.22	0.90	10.07
800	32.00	1.64	66.36	0.95	19.51
850	33.66	0.64	65.70	0.98	52.59
900	34.21	0.30	65.49	0.99	114.03
1000	34.58	0.08	65.34	0.998	432.25
1100	34.66	0.03	65.31	0.999	1155.33
1500	34.71	0.000	65.29	1.000	∞

The same problem is solved below by the method of degree of conversion or dissociation.

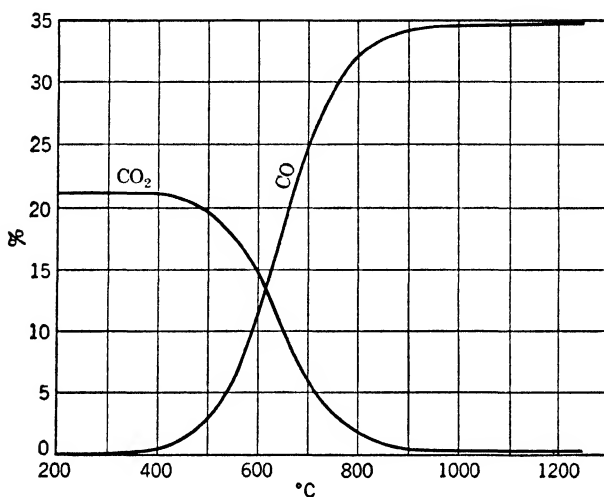


FIG. 11. Air-gas composition (carbon gasified by dry air at 1 Atm).

The theoretical combustion of carbon to the complete exhaustion of the available oxygen results in the following gas of combustion:

$$v'_{\text{CO}_2} = 0.21 \quad v'_{\text{N}_2} = 0.79$$

which, in its turn, serves as the gasifying agent in the reduction zone of the producer. From

$$K_{pB}P^{-1} = \frac{(v_{\text{CO}})^2}{v_{\text{CO}_2}} \quad (20)$$

$$v_{\text{CO}} = \frac{(2\alpha_B/100)v'_{\text{CO}_2}}{1 + (\alpha_B/100)v'_{\text{CO}_2}} \quad (94)$$

$$v_{\text{CO}_2} = \frac{v'_{\text{CO}_2}[1 - (\alpha_B/100)]}{1 + (\alpha_B/100)v'_{\text{CO}_2}} \quad (95)$$

is obtained

$$K_{pB}P^{-1} = \frac{4(\alpha_B/100)^2 v'_{\text{CO}_2}}{v'_{\text{CO}_2}[1 - (\alpha_B/100)][1 + (\alpha_B/100)v'_{\text{CO}_2}]} \quad (96)$$

Consequently by solving for α_B ,

$$\frac{\alpha_B}{100} = \frac{1 - v'_{\text{CO}_2}}{2v'_{\text{CO}_2}[(4P/K_{pB}) + 1]} \pm \sqrt{\left[\frac{1 - v'_{\text{CO}_2}}{2v'_{\text{CO}_2}[(4P/K_{pB}) + 1]} \right]^2 + \frac{1}{v'_{\text{CO}_2}[(4P/K_{pB}) + 1]}} \quad (97)$$

Sample Calculation. At $P = 1$ Atm, $t = 700^\circ\text{C}$,

$$K_{pB} = 1.07266 \quad v'_{\text{CO}_2} = 0.21$$

$$\frac{\alpha_B}{100} = 0.68192 \quad (\text{from equation 97})$$

and, according to equations 94 and 95,

$$v_{\text{CO}} = \frac{2 \times 0.68192 \times 0.21}{1 + 0.68192 \times 0.21} = \frac{0.28641}{1.14320} = 0.25053$$

$$v_{\text{CO}_2} = \frac{0.21 - 0.14320}{1.14320} = \frac{0.6680}{1.14320} = 0.05843$$

in accord with the numerical results of Table 8.

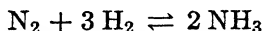
General case

The above examples are of only little practical interest, since they are not sufficient to explain the whole process of gas production. They were discussed as an introduction to conditions of gasification because of their mathematical simplicity. For instance, the air used in gasification is never completely dry, and, even when furnaces are operated with predried air, the emphasis is on maintaining a constant (usually small) amount of moisture. Some steam is always present, also a small amount of hydrogen is formed in practice in the air-gas process and in blast furnaces. From our knowledge of reaction kinetics between carbon and oxygen and carbon monoxide and oxygen it can be assumed that traces of steam are indispensable as catalysts for these reactions without which the reaction would take place very slowly. For the heterogeneous water-gas reaction according to equation 3, it has been assumed that only carbon monoxide and hydrogen are formed. We know, however, that carbon dioxide and small amounts of methane are also formed when steam reacts with incandescent carbon. Consequently, equation 3 is not sufficient to describe actual conditions, for the CO produced reacts with

excess steam according to equation 4 (homogeneous water-gas reaction) to form CO_2 and H_2 , and methane is formed from hydrogen and carbon monoxide or dioxide and/or steam according to equations 25 to 27.

All these reactions occur simultaneously and should be considered as such in the calculations. It has already been mentioned that the number of possible reactions can be reduced to the three basic equations. Whichever reaction is written, it can always be derived from these three equations, and therefore, from a mathematical point of view, leads to no new, independent equation of condition. In any case the equilibrium constant can be obtained from the three basic equilibrium constants K_{pB} , K_{pW} , and K_{pM} .*

Some limitations in the following derivations may be mentioned which are of little consequence for the practical result (with the exception of a few special problems). Let the fuel consist of only the basic constituents C, O_2 , H_2 , and N_2 , neglecting sulfur and other materials.† In most cases it may even be assumed that only carbon enters the reaction zone of a gas producer. In counter-current (upflow) producers, the other constituents are driven off completely as volatile matter; in concurrent (downflow or equal flow) producers, these other constituents are completely burned to steam and carbon dioxide in the oxidation zone. By neglecting the sulfur content of the fuel, the formation of sulfurous acid, hydrogen sulfide, and organic sulfur compounds and the slight formation of ammonia according to the reaction



are eliminated.

Finally, the calculations will be made using rounded-off molal volumes and ideal gas conditions in the calculation of the equilibrium constants. The application of Dalton's law ($\Sigma p = P$) is assumed.

The basic equations on which the calculation process is built are the definitions of the equilibrium constants of the Boudouard reaction K_{pB} (equation 20), of the heterogeneous water-gas reaction K_{pW} (equation 24), and of the reaction of methane formation K_{pM} (equation 32), Dalton's law (sum of partial pressures equals total pressure or sum of partial volumes equals 1), and the four

* As an example, see equations 25 and 27 and 40 and 42.

† On the effect of ash constituents on the gas composition, see page 137.

material balances—carbon, hydrogen, oxygen, and nitrogen balances. Thus eight equations with the following eight unknowns are available: v_{CO} , v_{CO_2} , v_{H_2} , $v_{\text{H}_2\text{O}}$, v_{CH_4} , and v_{N_2} , the amount of gasifying agent or medium (M) necessary in SCM per SCM of product gas, and the amount of gasified fuel (F) in kilograms per SCM of product gas. The temperature of reaction is an additional unknown, the heat balance being a further equation for its determination. The problem is to find the gas composition for a specific (known) temperature.

The material balances indicate that the material input into the reaction zone of the gas producer consisting of fuel and gasifying agent must be equal to the material output of product gas. The calculation refers to the amount of carbon (or fuel) actually gasified, and does not consider the material fractions in the residues and fly-dust losses. These losses do not affect the composition of the gas; they are to be considered only in the determination of the actual yield based on the amount of carbon charged to the producer.

Since the materials dealt with are partly solid, partly gaseous, a uniform unit, the mole, must be used to arrive at dimensionally correct equations. By *carbon balance*:

$$FC_F + MC_M = C_G \quad (98)$$

C_F = carbon carriers in the fuel, in a solid fuel $C_F = c$ (= carbon content of the fuel) or $c = 1$ if pure carbon is considered. In a gaseous fuel $C_F = \text{CO} + \text{CO}_2 + \text{C}_n\text{H}_m$ (if CO, etc., mean the volume % of carbon monoxide, etc.). $C_M = v'_{\text{CO}} + v'_{\text{CO}_2} + v'_{\text{CH}_4} + nv'_{\text{C}_n\text{H}_m}$ are the carbon carriers of the gasification medium. In most cases, $C_M = 0$, as the partial volumes of the gasifying agent (denoted as v) in air (disregarding the slight CO_2 content of the air of 0.03 volume % or $v_{\text{CO}_2} = 0.00030$ in dry air). Only if product gas is recycled or combustion gases are added, do carbon carriers appear in the gasifying agent. $C_G = v_{\text{CO}} + v_{\text{CO}_2} + v_{\text{CH}_4}$ are the carbon carriers in the product gas, v_{CO} , etc., being the partial volume of carbon monoxide, etc.*

* Since synthesis of higher hydrocarbons than methane does not take place to any considerable extent under the operating conditions of a gas producer, the consideration of these three carbon carriers is sufficient. It should, however, be noted that only the gas issuing from the reaction zone is being dealt with. In countercurrent (upflow) gasification of coal the products of distillation are admixed so that, in the finished product gas, higher hydrocarbons, gaseous and vaporous (tars, oils), may be present.

To change equation 98 into molal units, the definition of the mole is used. Accordingly, m kg of a material (m = molecular weight) is equal to 1 mole; or, if the material is gaseous, v_m SCM (v_m = mole volume = 22.416 SCM in round figures) is equal to 1 mole. Since 12.01 kg of carbon corresponds to 1 mole, FC_F kg of carbon is equal to $FC_F/12.01$ moles, and 1 SCM of product gas or M SCM of gasifying agent is equal to $1/22.416$ or $M/22.416$ moles, respectively.

Expressed in kilomoles, the carbon balance is

$$\frac{FC_F}{12.01} + \frac{MC_M}{22.416} = \frac{C_G}{22.416} \quad (99)$$

and per SCM of product gas

$$\frac{22.416}{12.01} FC_F + MC_M = C_G \quad (100)$$

This equation is used preferably for the determination of fuel or carbon consumption per SCM product gas or of the reciprocal, the gas yield in SCM per kilogram of fuel.

$$FC_F = 0.5358(v_{CO} - Mv'_{CO} + v_{CO_2} - Mv'_{CO_2} + v_{CH_4} - Mv'_{CH_4} - Mnv'_{C_{nH_m}}) \quad (101)$$

and with $C_F = 1$ (pure carbon) and $C_M = 0$ (no carbon carrier in the gasifying agent),

$$F = 0.5358(v_{CO} + v_{CO_2} + v_{CH_4}) \quad (102)$$

By *hydrogen balance*,

$$FH_F + MH_M = H_G \quad (103)$$

where $H_F = h + w$ are the hydrogen carriers of the fuel, h is the hydrogen content found by the ultimate analysis, and w is the water content.* In upflow gasification, these constituents are usually missing, particularly the water content, since only fixed carbon is gasified. Naturally, only those fuel constituents should be considered which as the "actual gasification fuel" enter the reaction zones of a producer. In a down-draft producer all

* Although somewhat unusual, lower-case letters are chosen as weight % of the solid fuel constituents in order to avoid more elaborate expressions or confusion with other symbols.

fuel constituents are actual gasification fuel, including water content. $H_M = v'_{H_2} + v'_{H_2O} + 2v'_{CH_4} + \frac{m}{2} v'_{C_nH_m}$ are the hydrogen carriers of the gasifying medium, v' is again the partial volume of the gases in that medium. In most cases, only one constituent, the steam content (moisture of the air, saturation of the blast, or gasification with pure steam as in the water-gas process), is present, since other hydrogen carriers occur only if product gas is recycled or if outside gas is added (e.g., gasification with simultaneous methane decomposition of methane-containing gases in a gas producer). $H_G = v_{H_2} + v_{H_2O} + 2v_{CH_4}$ are the hydrogen carriers of the product gas. Expressed in moles, the hydrogen balance becomes

$$\frac{Fh}{2.016} + \frac{Fw}{18.016} + \frac{MH_M}{22.416} = \frac{H_G}{22.416} \quad (104)$$

and per SCM of product gas

$$\begin{aligned} \frac{22.416}{2.016} Fh + \frac{22.416}{18.016} Fw + M(v'_{H_2} + v'_{H_2O} + 2v'_{CH_4} \\ + \frac{m}{2} v'_{C_nH_m}) = v_{H_2} + v_{H_2O} + 2v_{CH_4} \end{aligned} \quad (105)$$

If $h = 0$; $w = 0$; $v'_{H_2} = v'_{CH_4} = v'_{C_nH_m} = 0$,

$$Mv'_{H_2O} = v_{H_2} + v_{H_2O} + 2v_{CH_4} \quad (106)$$

This equation can be used for calculation of the amount of gasifying agent, preferably in water-gas production.

By *oxygen balance*,

$$FO_F + MO_M = O_G \quad (107)$$

where $O_F = o + 0.5w$ are the oxygen carriers of the fuel, o = oxygen content, w = water content of the fuel. The notes with reference to H_F apply here also. $O_M = v'_{O_2} + v'_{CO_2} + 0.5v'_{H_2O} + 0.5v'_{CO}$ are the oxygen carriers of gasifying medium, v' the partial volumes of the gases in this gasifying agent. $O_G = 0.5v_{CO} + v_{CO_2} + 0.5v_{H_2O}$ are the oxygen carriers of the product gas.

Expressed in moles, the oxygen balance becomes

$$\frac{F_{\text{O}}}{32.0} + \frac{F \times 0.5 w}{18.016} + \frac{M O_M}{22.416} = \frac{O_G}{22.416} \quad (108)$$

and per SCM product gas,

$$\begin{aligned} \frac{22.416}{32.0} F_{\text{O}} + \frac{22.416}{36.032} F_W + M(v'_{\text{O}_2} + v'_{\text{CO}_2} + 0.5v'_{\text{H}_2\text{O}} + 0.5v'_{\text{CO}}) \\ = 0.5v_{\text{CO}} + v_{\text{CO}} + 0.5v_{\text{H}_2\text{O}} \end{aligned} \quad (109)$$

By *nitrogen balance*,

$$F N_F + M N_M = N_G \quad (110)$$

where $N_F = n$ are the nitrogen carriers of the fuel, n is the nitrogen content of the fuel. Usually this amount is neglected because gasification of pure carbon is assumed. $N_M = v'_{\text{N}_2}$ are the nitrogen carriers of the gasifying agent, v'_{N_2} is its nitrogen content, $N_G = v_{\text{N}_2}$, the nitrogen carriers in the product gas, v_{N_2} the nitrogen content in the product gas in partial volumes. Expressed in moles, the nitrogen balance becomes

$$\frac{F n}{28.016} + \frac{M N_M}{22.416} = \frac{N_G}{22.416} \quad (111)$$

and per SCM of product gas:

$$\frac{22.416}{28.016} F n + M v'_{\text{N}_2} = v_{\text{N}_2} \quad (112)$$

This equation, if $n = 0$ (no nitrogen in the fuel), yields an especially simple relationship for the calculation of the amount of gasifying agent:

$$M = \frac{v_{\text{N}_2}}{v'_{\text{N}_2}} \quad (113)$$

This equation fails only with water gas, and then it is necessary to refer to the hydrogen balance (equation 105).

If the gasifying agent, M , is determined by three different methods, by the nitrogen balance, $M_{(\text{N}_2)}$, the oxygen balance, $M_{(\text{O}_2)}$, or the hydrogen balance, $M_{(\text{H}_2)}$, the same result should be obtained as a proof of the correctness of the numerical calculation. To utilize this and similar possibilities of control, all gasifica-

tion calculation for the gas composition is carried out to two places after the decimal point. This care is not an exaggerated accuracy and has nothing to do with the possible accuracy and reliability of a gas analysis; it is, rather, a requirement of calculation technique. Since gasification calculation is usually carried out on a calculating machine, to take it at least three figures after the decimal point is not difficult.

In the previous example of an air gas at 700°C and 1 Atm, the amount of blast is found by the nitrogen balance to be

$$M_{(N_2)} = \frac{69.11}{79.00} = 0.8748$$

and by the oxygen balance to be

$$M_{(O_2)} = \frac{12.53 + 5.84}{21} = 0.8748$$

Another example, a gas produced from carbon and a rather wet gasifying agent of the following characteristics,

$$v'_{O_2} = 0.1260, \quad v'_{N_2} = 0.04740, \quad v'_{H_2O} = 0.4000$$

has the following composition at perfect equilibrium at 600°C:

$$\begin{aligned} v_{CO} &= 0.1233, & v_{CO_2} &= 0.1608, & v_{H_2} &= 0.1988 \\ v_{H_2O} &= 0.1014, & v_{CH_4} &= 0.0183, & v_{N_2} &= 0.3974 \end{aligned}$$

The amount of gasifying agent from this is found to be

$$M_{(N_2)} = \frac{0.3974}{0.4740} = 0.8387$$

$$M_{(O_2)} = \frac{0.1608 + 0.0617 + 0.0507}{0.1260 + 0.2000} = \frac{0.2732}{0.3260} = 0.8381$$

$$M_{(H_2)} = \frac{0.1988 + 0.1014 + 0.0366}{0.4000} = \frac{0.3368}{0.4000} = 0.8420$$

There is a discrepancy in the last figures, caused by rounding them off, which would disappear if the analysis of the product gas was calculated with more significant figures.

To clarify, the starting equations for this calculation are summarized. The fuel composition, as expressed in % by weight,

is c, h, o, n, w or C_F , H_F , O_F , and N_F . The gasifying agent has the composition, as expressed in % by volume, v'_{O_2} , v'_{N_2} , v'_{H_2O} , v'_{CO_2} or C_M , H_M , O_M , and N_M . The composition of the product gas (at a given temperature and total pressure) and the requirements of fuel and gasifying agent per SCM of product gas are desired.

$$(I) \quad PK'_{PB} = \frac{v_{CO_2}}{(v_{CO})^2}$$

$$(II) \quad PK'_{PW} = \frac{v_{H_2O}}{v_{H_2}v_{CO}}$$

$$(III) \quad PK_{PM} = \frac{v_{CH_4}}{(v_{H_2})^2}$$

$$(IV) \quad v_{CO} + v_{CO_2} + v_{H_2} + v_{H_2O} + v_{CH_4} + v_{N_2} = 1$$

$$(V) \quad FC_F + MC_M = v_{CO} + v_{CO_2} + v_{CH_4}$$

where

$$C_F = \frac{22.416}{12.01} c = 1.8664 c = \frac{c}{0.5358}$$

$$(VI) \quad FH_F + MH_M = v_{H_2} + v_{H_2O} + 2v_{CH_4}$$

where

$$H_F = \frac{22.416}{2.016} \times h + \frac{22.416}{18.016} \times w = 11.121 h + 1.244 w$$

$$(VII) \quad FO_F + MO_M = 0.5v_{CO} + v_{CO_2} + 0.5v_{H_2O}$$

where

$$O_F = \frac{22.416}{32.000} \times o + \frac{22.416}{36.032} \times w = 0.7005 o + 0.6221 w$$

$$(VIII) \quad FN_F + MN_M = v_{N_2}$$

where

$$N_F = \frac{22.416}{28.016} = 0.8001 n$$

The solution of a system of eight equations with eight unknowns is possible in principle, though, of course, not easy. The calculation is inconvenient and time consuming so that it is necessary

to find methods of solution that are as rational as possible. Graphical and calculatory methods, such as the methods of Newton or Taylor by series development, or "trial and error" methods, can be used for this calculation. S. Traustel has reported different solutions in a series of publications,¹ proved their usefulness by numerical examples, and has discussed the fundamental relations between the different solutions, particularly the solutions derived from the material balances and the solution by degree of conversion (or dissociation). Traustel first suggested the following method of solution based on the preliminary work of Cerasoli,² Danulat,³ and Reiser.⁴ Assume one value, e.g., v_{CO} , calculate v_{CO_2} , $v_{\text{H}_2\text{O}}$, v_{CH_4} , v_{N_2} , M , check with Dalton's law (equation IV), and then correct the assumed value and repeat the calculation with the corrected assumed value, etc. In his second publication, Traustel changed his first suggestions slightly and gave his system of basic equations (see equations I to VIII). Again a v_{CO} value is assumed, and v_{CO_2} , v_{H_2} , $v_{\text{H}_2\text{O}}$, v_{CH_4} , v_{N_2} are determined by a system of converted formulas, as well as v_{CO} for checking. The deviation of the calculated value from the assumed one for carbon monoxide content is an indication of the improvement of the first estimation, which can also be evaluated graphically. The process is to be repeated, if necessary, until the desired accuracy has been achieved. Although this method is quite useful, it has been replaced by Traustel with a process which makes possible a more rational estimation. The derivation and the manipulation of these methods, which have stood practical test and will be used.

¹ Sergei Traustel, *Verbrennung, Vergasung und Verschlackung* (Thesis, Engineering University of Berlin), 1939. *Praktische Berechnung von Vergasungsgleichgewichten, Feuerungstechn.*, Vol. 29 (1941), No. 5, pp. 105-114. Grundsätzliches zur Berechnung von Vergasungsvorgängen, *Feuerungstechn.*, Vol. 30 (1942), No. 10, pp. 225-231. Zur Berechnung von Vergasungsgleichgewichten, *Feuerungstechn.*, Vol. 31 (1943), No. 7/8, pp. 111-114. Berechnung von Vergasungsgleichgewichten durch Lösung von 2 Gleichungen mit 2 Unbekannten, *Z. VDI*, Vol. 88 (1944), No. 51/52, pp. 688-690.

² T. Cerasoli, Il calcolo della composizione del gas misto, *Ann. di Chim. Applicata*, Vol. 13 (1923), pp. 257-270. Die Vergasung der Brennstoffe mittels Sauerstoff und Dampf, *Gas u. Wasserfach*, Vol. 70 (1927), No. 22, pp. 508-510.

³ Friedrich Danulat, *Die restlose Vergasung fester Brennstoffe mit Sauerstoff unter hohem Druck* (Thesis, Engineering University of Berlin, 1936). Frankfurt a/M, 1936.

⁴ H. Reiser, *Die Erzeugung eines kohlensäurefreien Gases durch Vergasung mit Sauerstoff* (Thesis, Engineering University of Berlin, 1939; not published)..

extensively throughout these pages, will be presented at length. The triangle method and the approximation method of Newton simplify the system by reducing it to two equations with two unknowns.

The triangle method of Traustel

The system of equations is not reduced to one equation with one unknown, as in the earlier method, but to two equations with two unknowns, which are considerably simpler and require less tedious calculations. This method has been used by Kühl⁵ and by Damköhler and Edse⁶ for the kindred problem of dissociation equilibria.

Two values must be estimated. The following were selected:

$$x = v_{\text{CO}} \quad y = v_{\text{H}_2}$$

The carbon dioxide, steam, and methane content can be determined from equations I, II, and III:

$$v_{\text{CO}_2} = PK'_{p_B}(v_{\text{CO}})^2 \quad (114)$$

$$v_{\text{H}_2\text{O}} = PK'_{p_W}v_{\text{CO}}v_{\text{H}_2} \quad (115)$$

$$v_{\text{CH}_4} = PK_{p_M}(v_{\text{H}_2})^2 \quad (116)$$

The nitrogen content is found from the nitrogen and oxygen balances by setting the expression for the ratio of nitrogen carriers to oxygen carriers in the gasifying agent equal to the same ratio in the produced gas:

$$\frac{FN_F + MN_M}{FO_F + MO_M} = \frac{N_G}{O_G} \quad (117)$$

In gasifying carbon, where $O_F = 0$ and $N_F = 0$, the unknown M cancels out and the nitrogen content of the gas becomes

$$v_{\text{N}_2} = \frac{N_M}{O_M} O_G \quad (118)$$

⁵ H. Kühl, Dissoziation von Verbrennungsgasen und ihr Einfluss auf den Wirkungsgrad von Vergasermaschinen, *Forschungsheft* 373 (*Forschung*, Vol. 6, 1935).

⁶ Gerhard Damköhler und Rudolf Edse, Zusammensetzung dissoziierender Verbrennungsgase und die Berechnung simultaner Gleichgewichte, *Z. Elektrochem.*, Vol. 49 (1943), No. 3, pp. 178-186.

As a check on the estimates, equations IV and VI are available, while equation V is reserved for the determination of the unknown F . By formulating ratios of hydrogen carriers to oxygen carriers in the gasifying agent and in the gas, by equating the two, the following expression results:

$$\frac{FH_F + MH_M}{FO_F + MO_M} = \frac{H_G}{O_G} \quad (119)$$

Gasifying carbon with H_F and $O_F = 0$.

$$\frac{H_M}{O_M} = \frac{H_G}{O_G} \quad (120)$$

If our estimates are correct, the following two equations of condition must be fulfilled:

$$\varphi = v_{CO} + v_{CO_2} + v_{H_2} + v_{H_2O} + v_{CH_4} + v_{N_2} - 1 = 0 \quad (121)$$

and

$$\psi = \frac{H_G}{O_G} - \frac{H_M}{O_M} = 0 \quad (122)$$

The correction of the estimated values by the triangle method will now be made, since the first estimate resulted in $\varphi \neq 0$ and $\psi \neq 0$. The encirclement of the correct solution is effected by the estimated location of three points with the coordinates x_1, y_1 (point 11), x_2, y_2 (point 22), and x_3, y_1 (point 31), in such a way that the differences between adjoining values are equal. Therefore,

$$\Delta = x_2 - x_1 = x_3 - x_2 = y_2 - y_1 \quad (123)$$

Each pair of values has a corresponding φ value according to equation 121, and the sum of all φ values represents a curved area in space which intersects the xy plane chosen as a reference plane in a curve. In the same way, each pair of values has a corresponding ψ value according to equation 122, and the ψ plane intersects the reference plane in another curve. If we consider sufficiently small sections of the reference planes, the areas in space become planes and the intersections of their curves with the

reference planes become straight lines (see Figure 12). The point of intersection P of the two straight lines is the desired solution, for in this point $\varphi = 0$ and $\psi = 0$; therefore, the two conditions

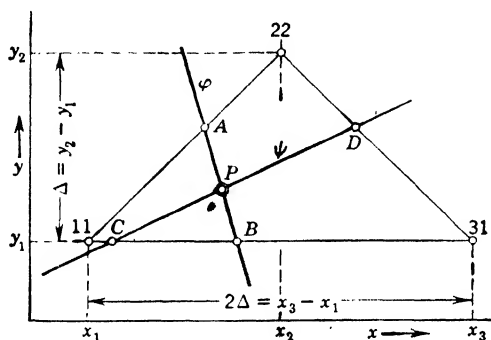


FIG. 12. Triangle method (S. Traustel).

11, 31, 22 = assumed couples of values

P = final result

are fulfilled. The points of intersection (A, B, C, D) of the two curves (straight lines) with the sides of the triangle 11-31-22 used for boxing in (or bracketing) the wanted solution each satisfy one of our condition equations and provide a relationship between x (or y) and φ (or ψ). For the 11-22 side of the triangle with the point of intersection A , the following equation holds, as can be seen in Figure 12 and still more clearly in Figure 13.

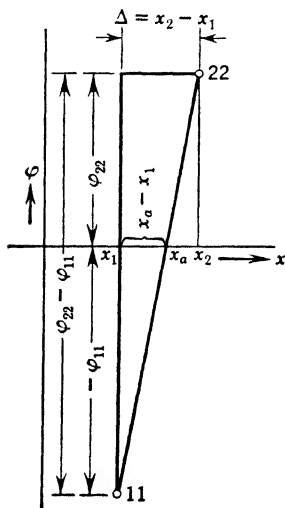


FIG. 13. Illustration of equation 124.

$$\frac{x_a - x_1}{x_2 - x_1} = \frac{-\varphi_{11}}{\varphi_{22} - \varphi_{11}} \quad (124)$$

$$x_2 - x_1 = \Delta \quad (123)$$

$$x_a = x_1 - \frac{\Delta \varphi_{11}}{\varphi_{22} - \varphi_{11}} \quad (125)$$

φ_{11} is a function of φ for the pair of values $x = x_1, y = y_1$. In the same way we find

$$y_a = y_1 - \frac{\Delta\varphi_{11}}{\varphi_{22} - \varphi_{11}} \quad (126)$$

The 11-31 side of the triangle with the point of intersection B of the φ curve becomes

$$\frac{x_b - x_1}{x_3 - x_1} = \frac{-\varphi_{11}}{\varphi_{31} - \varphi_{11}} \quad (127)$$

$$x_3 - x_1 = 2\Delta \quad (123)$$

$$x_b = x_1 - \frac{2\Delta\varphi_{11}}{\varphi_{31} - \varphi_{11}} \quad (128)$$

and

$$y_b = y_1 \quad (129)$$

The same calculation is made for the points C and D of the ψ curve (see Figure 14). For the 11-31 side of the triangle it is

$$\frac{x_3 - x_c}{2\Delta} = \frac{-\psi_{31}}{\psi_{11} - \psi_{31}} \quad (130)$$

$$x_c = x_3 + \frac{2\Delta\psi_{31}}{\psi_{11} - \psi_{31}} \quad (131)$$

$$y_c = y_1 \quad (132)$$

and for the 22-31 side with the point of intersection D :

$$\frac{x_3 - x_d}{\Delta} = \frac{-\psi_{31}}{\psi_{22} - \psi_{31}} \quad (133)$$

$$x_d = x_3 + \frac{\Delta\psi_{31}}{\psi_{22} - \psi_{31}} \quad (134)$$

and

$$\frac{y_d - y_1}{\Delta} = \frac{-\psi_{31}}{\psi_{22} - \psi_{31}} \quad (135)$$

$$y_d = y_1 - \frac{\Delta\psi_{31}}{\psi_{22} - \psi_{31}} \quad (136)$$

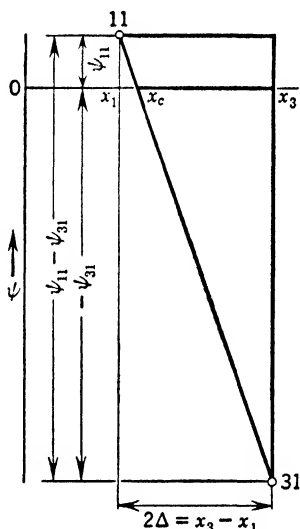


FIG. 14. Illustration of equation 130.

The equation of a straight line through points A and B , by which we have replaced the desired φ curve, if $y_b = y_1$, is

$$\frac{x - x_b}{x_a - x_b} = \frac{y - y_1}{y_a - y_1} \quad (137)$$

The straight line through the points C and D , if $y_c = y_1$, is

$$\frac{x - x_c}{x_d - x_c} = \frac{y - y_1}{y_d - y_1} \quad (138)$$

The intersection of the two straight lines is the desired solution. If these two equations, 137 and 138, are solved for x ,

$$x = \frac{y - y_1}{y_a - y_1} (x_a - x_b) + x_b \quad (139)$$

and

$$x = \frac{y - y_1}{y_d - y_1} (x_d - x_c) + x_c \quad (140)$$

If these expressions are equated, the y value is obtained:

$$\frac{y - y_1}{y_a - y_1} (x_a - x_b) + x_b = \frac{y - y_1}{y_d - y_1} (x_d - x_c) + x_c \quad (141)$$

$$y - y_1 \left[\frac{x_a - x_b}{y_a - y_1} - \frac{x_d - x_c}{y_d - y_1} \right] = x_c - x_b \quad (142)$$

$$y = \frac{\frac{x_c - x_b}{\frac{x_a - x_b}{y_a - y_1} - \frac{x_d - x_c}{y_d - y_1}}}{1} + y_1 \quad (143)$$

The values for x_a , x_b , x_c , x_d , y_a , y_d , from equations 125 to 134, are now inserted. For the sake of simplicity, the following condensed expressions are used:

$$A' = \frac{-\varphi_{11}}{\varphi_{31} - \varphi_{11}} \quad (144)$$

$$B' = \frac{\varphi_{22} - \varphi_{11}}{\varphi_{31} - \varphi_{11}} \quad (145)$$

$$C' = \frac{-\psi_{31}}{\psi_{11} - \psi_{31}} \quad (146)$$

$$D' = \frac{\psi_{22} - \psi_{31}}{\psi_{11} - \psi_{31}} \quad (147)$$

Therefore,

$$\begin{aligned} x_c - x_b &= x_3 + \frac{2\Delta\psi_{31}}{\psi_{11} - \psi_{31}} - x_1 + \frac{2\Delta\varphi_{11}}{\varphi_{31} - \varphi_{11}} \\ &= (x_3 - x_1) - 2\Delta C' - 2\Delta A' \end{aligned} \quad (148)$$

And, since $x_3 - x_1 = 2\Delta$ (see Figure 12),

$$x_c - x_b = 2\Delta[1 - (A' + C')] \quad (149)$$

$$\begin{aligned} x_a - x_b &= x_1 - \frac{\Delta\varphi_{11}}{\varphi_{22} - \varphi_{11}} - x_1 + \frac{2\Delta\varphi_{11}}{\varphi_{31} - \varphi_{11}} \\ &= \frac{-\Delta\varphi_{11}(\varphi_{31} - \varphi_{11}) + 2\Delta\varphi_{11}(\varphi_{22} - \varphi_{11})}{(\varphi_{22} - \varphi_{11})(\varphi_{31} - \varphi_{11})} \end{aligned} \quad (150)$$

$$y_a - y_1 = \frac{-\Delta\varphi_{11}}{\varphi_{22} - \varphi_{11}} \quad (151)$$

and

$$\frac{x_a - x_b}{y_a - y_1} = \frac{\frac{\varphi_{22} - \varphi_{11}}{-\Delta\varphi_{11}} [-\Delta\varphi_{11}(\varphi_{31} - \varphi_{11}) + 2\Delta\varphi_{11}(\varphi_{22} - \varphi_{11})]}{(\varphi_{22} - \varphi_{11})(\varphi_{31} - \varphi_{11})} \quad (152)$$

After simplifying as far as possible,

$$\begin{aligned} \frac{x_a - x_b}{y_a - y_1} &= \frac{(\varphi_{31} - \varphi_{11}) - 2(\varphi_{22} - \varphi_{11})}{\varphi_{31} - \varphi_{11}} \\ &= 1 - 2\frac{\varphi_{22} - \varphi_{11}}{\varphi_{31} - \varphi_{11}} = 1 - 2B' \end{aligned} \quad (153)$$

Furthermore,

$$\begin{aligned} x_d - x_c &= x_3 + \frac{\Delta\psi_{31}}{\psi_{22} - \psi_{31}} - x_3 - \frac{2\Delta\psi_{31}}{\psi_{11} - \psi_{31}} \\ &= \frac{\Delta\psi_{31}(\psi_{11} - \psi_{31}) - 2\Delta\psi_{31}(\psi_{22} - \psi_{31})}{(\psi_{22} - \psi_{31})(\psi_{11} - \psi_{31})} \end{aligned} \quad (154)$$

$$y_d - y_1 = \frac{-\Delta\psi_{31}}{\psi_{22} - \psi_{31}} \quad (155)$$

and

$$\begin{aligned} \frac{x_d - x_c}{y_d - y_1} &= \frac{\frac{\psi_{22} - \psi_{31}}{-\Delta\psi_{31}} [\Delta\psi_{31}(\psi_{11} - \psi_{31}) - 2\Delta\psi_{31}(\psi_{22} - \psi_{31})]}{(\psi_{22} - \psi_{31})(\psi_{11} - \psi_{31})} \\ &= \frac{-1[(\psi_{11} - \psi_{31}) - 2(\psi_{22} - \psi_{31})]}{\psi_{11} - \psi_{31}} \\ &= -1 + 2\frac{\psi_{22} - \psi_{31}}{\psi_{11} - \psi_{31}} \\ &= -1 + 2D' \end{aligned} \quad (156)$$

By inserting into the equation 143, the following simple expression is finally obtained:

$$y = y_1 + \frac{2\Delta[1 - (A' + C')]}{1 - 2B' + 1 - 2D'}$$

$$y = y_1 + \Delta \frac{1 - (A' + C')}{1 - (B' + D')} \quad (157)$$

The desired x value can be found from either equation 139 or equation 140. From

$$x = \frac{y - y_1}{y_a - y_1} (x_a - x_b) + x_b$$

by inserting the values from equations 150, 151, and 128, after a few simplifications, equation 158 is obtained:

$$x = x_1 + 2\Delta \frac{\varphi_{11}}{\varphi_{31} - \varphi_{11}} + \left(1 - 2 \frac{\varphi_{22} - \varphi_{11}}{\varphi_{31} - \varphi_{11}}\right) (y - y_1)$$

$$x = x_1 + 2\Delta A' + (1 - 2B')(y - y_1) \quad (158)$$

or, starting from equation 140,

$$x = x_3 - 2\Delta C' - (1 - 2D')(y - y_1) \quad (159)$$

Thereby, a value couple, x, y , has been found which is in better agreement with conditions than the first estimated value couple v_{CO}, v_{H_2} . The reason why $\varphi = 0$ and $\psi = 0$ are usually not satisfied completely is that the complicated functions $\varphi(x, y)$ and $\psi(x, y)$ were replaced by straight lines initially. By confining the estimated values, e.g., by making Δ in equation 123 one-tenth as large, reality is more closely approached. It is consequently possible to increase the accuracy of the result to any desired degree.

The simplification that carbon alone is gasified will now be dropped and the *general* case of fuel of arbitrary composition will be considered. The calculation is the same initially, but as soon as the material balances are considered, the formulas are expanded correspondingly. The nitrogen content is again obtained from the nitrogen balance; the two unknowns F and M , however, are eliminated by using the carbon and oxygen balances. From

$$FC_F + MC_M = C_G$$

and

$$FO_F + MO_M = O_G$$

the following expression is obtained by solving for F and equating the expressions after brief transformation:

$$M = \frac{C_F O_G - C_G O_F}{C_F O_M - C_M O_F} \quad (160)$$

From the same equations, by solving for M and equating the expressions,

$$F = \frac{C_G O_M - C_M O_G}{C_F O_M - C_M O_F} \quad (161)$$

Then -

$$v_{N_2} = N_G = F N_F + M N_M \quad (162)$$

When F and M have been found from equations 161 and 160, the somewhat minute form of the ψ function which has been chosen before, to make the unknown M disappear, may be dropped. Instead of this, ψ^* may be defined now as the difference of the hydrogen carriers of the gas and the hydrogen carriers of both the fuel and the gasifying agent (that is, the difference between output and input):

$$\psi^* = H_G - (F H_F + M H_M) = 0 \quad (163)$$

The numerical evaluation is facilitated because F and M for equation 162 have already been determined.

If the numerical evaluation of F and M which will be needed only for the final calculation with the ultimately ascertained reaction temperature is not desired, the expressions of equations 160 and 161 may be inserted into equation 117, which, after simplification, results in

$$v_{N_2} = \frac{(C_G O_M - C_M O_G) N_F + (C_F O_G - C_G O_F) N_M}{C_F O_M - C_M O_F} \quad (164)$$

With this value the φ function can now be calculated.

In a similar way, as Traustel also reports, the ψ value could be found; however, the numerical calculation of this expression is more laborious. Therefore, we start from the following definition of the ψ^{**} value:

$$\psi^{**} = \frac{H_G}{O_G} - \frac{(C_G O_M - C_M O_G) H_F + (C_F O_G - C_G O_F) H_M}{(C_F O_M - C_M O_F) O_G} = 0 \quad (165)$$

All expressions in parentheses already appear in equation 164, thus simplifying the numerical solution. With $H_F = O_F = 0$ (gasification of pure carbon), the definition of ψ^{**} is transformed into that of ψ , and equation 164 becomes equation 118.

The Newtonian approximation method developed by Traustel

Although the triangle method as described is very effective, clear and easy to manipulate in the evaluation of a suitable scheme of calculation, it presumes a rather close estimation of the first x, y couple, since otherwise the calculation has to be repeated several times before the desired final solution is found. This fact prompted Traustel, who was looking for a "perfectly mechanical" method, less dependent on the estimation, to apply Newton's method of successive approximation to his system of equations.

Considering the gasification of pure carbon first, we shall use the system of equations that are summarized on page 48, in addition to the following equations:

$$\varphi = v_{CO} + v_{CO_2} + v_{H_2} + v_{H_2O} + v_{CH_4} + v_{N_2} - 1 = 0 \quad (121)$$

and

$$\psi = \frac{H_G}{O_G} - \frac{H_M}{O_M} = 0 \quad (122)$$

The CO and H₂ contents are estimated, whereby a pair of values x, y are obtained different from the final results x_0, y_0 . Consequently,

$$\varphi(x, y) \neq 0 \quad \psi(x, y) \neq 0 \quad (166a; b)$$

Conversely,

$$\varphi(x_0, y_0) = 0 \quad \psi(x_0, y_0) = 0 \quad (167a; b)$$

The difference between these values is

$$x_0 - x = \Delta x \quad y_0 - y = \Delta y \quad (168a; b)$$

and, by making the difference infinitesimal,

$$x_0 - x = dx \quad y_0 - y = dy \quad (169a; b)$$

With two variables, x and y ,

$$d\varphi = \frac{\partial \varphi}{\partial x} dx + \frac{\partial \varphi}{\partial y} dy \quad (170)$$

$$d\psi = \frac{\partial\psi}{\partial x} dx + \frac{\partial\psi}{\partial y} dy \quad (171)$$

or, in more condensed form,

$$d\varphi = \varphi'_x dx + \varphi'_y dy \quad (170a)$$

$$d\psi = \psi'_x dx + \psi'_y dy \quad (171a)$$

The solution for dx and dy results in

$$dx = \frac{d\varphi}{\varphi'_x} - \frac{\varphi'_y}{\varphi'_x} dy \quad (172)$$

$$dy = \frac{d\psi}{\psi'_y} - \frac{\psi'_x}{\psi'_y} dx \quad (173)$$

$$dx = \frac{d\varphi}{\varphi'_x} - \frac{\varphi'_y}{\varphi'_x} \left[\frac{d\psi}{\psi'_y} - \frac{\psi'_x}{\psi'_y} dx \right] \quad (174)$$

After the members containing dx are combined and simplified,

$$dx = \frac{\psi'_y d\varphi - \varphi'_y d\psi}{\varphi'_x \psi'_y - \varphi'_y \psi'_x} \quad (175)$$

Furthermore, from equation 173,

$$dy = \frac{d\psi}{\psi'_y} - \frac{\psi'_x}{\psi'_y} \left[\frac{d\varphi}{\varphi'_x} - \frac{\varphi'_y}{\varphi'_x} dy \right] \quad (176)$$

$$dy = \frac{\varphi'_x d\psi - \psi'_x d\varphi}{\varphi'_x \psi'_y - \varphi'_y \psi'_x} \quad (177)$$

$$d\varphi = \varphi(x_0, y_0) - \varphi(x, y) = -\varphi(x, y) \quad (178)$$

$$d\psi = \psi(x_0, y_0) - \psi(x, y) = -\psi(x, y) \quad (179)$$

By inserting equations 169a, b, 178, and 179 into 175 and 177, the initial estimated values are corrected:

$$x_0 - x = \frac{\psi\varphi'_y - \varphi\psi'_y}{\varphi'_x \psi'_y - \varphi'_y \psi'_x} \quad (180)$$

$$y_0 - y = \frac{\varphi\psi'_x - \psi\varphi'_x}{\varphi'_x \psi'_y - \varphi'_y \psi'_x} \quad (181)$$

Inserting the estimated value pair x, y into the function $\varphi(x, y)$ and $\psi(x, y)$ of equations 121 and 122, we obtain the first partial derivatives φ'_x and ψ'_x at constant y , and φ'_y and ψ'_y at constant x . For this purpose the expressions in equations 121 and 122 are transformed in such a way that only v_{CO} and v_{H_2} appear in them.

From the relationship

$$\frac{N_M}{O_M} = \frac{N_G}{O_G} = \frac{v_{N_2}}{0.5v_{CO} + v_{CO_2} + 0.5v_{H_2O}} \quad (182)$$

we obtain

$$v_{N_2} = \frac{N_M}{O_M} (0.5v_{CO} + v_{CO_2} + 0.5v_{H_2O}) \quad (183)$$

Inserting equation 183 and equations 114 and 116 into equation 121 gives

$$\begin{aligned} \varphi = & \left(1 + 0.5 \frac{N_M}{O_M}\right) v_{CO} + \left(1 + \frac{N_M}{O_M}\right) v_{CO}^2 PK'_{PB} + v_{H_2} \\ & + \left(1 + 0.5 \frac{N_M}{O_M}\right) v_{CO} v_{H_2} PK'_{PW} + v_{H_2}^2 PK_{PM} - 1 \end{aligned} \quad (184)$$

$$\begin{aligned} \varphi'_x = & \left(1 + 0.5 \frac{N_M}{O_M}\right) + \left(1 + \frac{N_M}{O_M}\right) 2v_{CO} PK'_{PB} \\ & + \left(1 + 0.5 \frac{N_M}{O_M}\right) v_{H_2} PK'_{PW} \end{aligned} \quad (185)$$

$$\varphi'_y = 1 + \left(1 + 0.5 \frac{N_M}{O_M}\right) v_{CO} PK'_{PW} + 2v_{H_2} PK_{PM} \quad (186)$$

According to equation 122,

$$\psi = \frac{H_G}{O_G} - \frac{H_M}{O_M} = \frac{v_{H_2} + v_{H_2O} + 2v_{CH_4}}{0.5v_{CO} + v_{CO_2} + 0.5v_{H_2O}} - \frac{H_M}{O_M} \quad (122a)$$

and, by consideration of equations 114 to 118,

$$\begin{aligned} \psi = & v_{H_2} + \left(1 - 0.5 \frac{H_M}{O_M}\right) v_{H_2} v_{CO} PK'_{PW} + 2v_{H_2}^2 PK_{PM} \\ & - 0.5v_{CO} \frac{H_M}{O_M} - v_{CO}^2 \frac{H_M}{O_M} PK'_{PB} \end{aligned} \quad (187)$$

$$\psi'_x = \left(1 - 0.5 \frac{H_M}{O_M}\right) v_{H_2} PK'_{pw} - 0.5 \frac{H_M}{O_M} - 2v_{CO} \frac{H_M}{O_M} PK'_{pB} \quad (188)$$

$$\psi'_y = 1 + \left(1 - 0.5 \frac{H_M}{O_M}\right) v_{CO} PK'_{pw} + 4v_{H_2} PK_{pM} \quad (189)$$

The introduction of equations 184 to 189 into equations 180 and 181 provides the correction of the initially estimated values and represents a new pair of values which better satisfies the demands, though not yet perfectly. The repetition of the calculation results in an improved approximation of the final solution. In general, two steps bring about a good approximation.

If the simplification that pure carbon is gasified is dropped, the same method as in the previously described way is followed. The equation $\varphi = 0$ and $\psi^* = 0$ from equations 121 and 163 are transformed—by using equations 114 to 116 and 160 to 161—in such a way that only v_{CO} and v_{H_2} appear in the equations. If for reasons of simplicity the following abbreviations are introduced:

$$A'' = 1 + \frac{1}{C_F O_M - C_M O_F} (O_M N_F - 0.5 C_M N_F + 0.5 C_F N_M - O_F N_M) \quad (190)$$

$$B'' = 1 + \frac{1}{C_F O_M - C_M O_F} (O_M N_F - C_M N_F + C_F N_M - O_F N_M) \quad (191)$$

$$C'' = 1 - \frac{1}{C_F O_M - C_M O_F} (0.5 C_M N_F - 0.5 C_F N_M) \quad (192)$$

$$D'' = 1 + \frac{1}{C_F O_M - C_M O_F} (O_M N_F - O_F N_M) \quad (193)$$

Thus

$$\begin{aligned} \varphi = A'' v_{CO} + B'' v_{CO}^2 PK'_{pB} + v_{H_2} + C'' v_{CO} v_{H_2} PK'_{pw} \\ + D'' v_{H_2}^2 PK_{pM} - 1 \end{aligned} \quad (194)$$

$$\varphi'_x = A'' + B'' 2v_{CO} PK'_{pB} + C'' v_{H_2} PK'_{pw} \quad (195)$$

$$\varphi'_y = 1 + C'' v_{CO} PK'_{pw} + D'' 2v_{H_2} PK_{pM} \quad (196)$$

and, for the ψ^* functions after introducing the following substitutions:

$$A''' = \frac{1}{C_F O_M - C_M O_F} (O_M H_F - 0.5 C_M H_F + 0.5 C_F H_M - O_F H_M) \quad (197)$$

$$B''' = \frac{1}{C_F O_M - C_M O_F} (O_M H_F - C_M H_F + C_F H_M - O_F H_M) \quad (198)$$

$$C''' = 1 + \frac{1}{C_F O_M - C_M O_F} (0.5 C_M H_F - 0.5 C_F H_M) \quad (199)$$

$$D''' = 2 - \frac{1}{C_F O_M - C_M O_F} (O_M H_F - O_F H_M) \quad (200)$$

the following expressions are obtained:

$$\begin{aligned} \psi^*_x = v_{H_2} + C''' v_{H_2} v_{CO} PK'_{pW} + D''' v_{H_2}^2 PK_{pM} \\ - A''' v_{CO} - B''' v_{CO}^2 PK'_{pB} \end{aligned} \quad (201)$$

$$\psi'^*_x = C''' v_{H_2} PK'_{pW} - A''' - B''' 2 v_{CO} PK'_{pB} \quad (202)$$

$$\psi'^*_y = 1 + C''' v_{CO} PK'_{pW} + D''' 2 v_{H_2} PK_{pM} \quad (203)$$

The identical structure of the φ and ψ functions is evident. They differ only by the substituted quantities A'' , B'' , C'' , D'' , and A''' , B''' , C''' , D''' . The solution is facilitated by the fact that, in the substitution expressions, the quantities within the parentheses as well as those outside the parentheses are similar. Furthermore, it is evident that in the gasification of pure carbon—with $C_F = 1$ and $O_F = H_F = N_F = 0$ —the substitution expressions are simplified as follows:

$$\begin{aligned} A'' &= \left(1 + 0.5 \frac{N_M}{O_M}\right) & A''' &= 0.5 \frac{H_M}{O_M} \\ B'' &= \left(1 + \frac{N_M}{O_M}\right) & B''' &= \frac{H_M}{O_M} \\ C'' &= \left(1 + 0.5 \frac{N_M}{O_M}\right) & C''' &= 1 - 0.5 \frac{H_M}{O_M} \\ D'' &= 1 & D''' &= 2 \end{aligned}$$

Equations 194 to 196 and 201 to 203 simplify into the corresponding values for the gasification of carbon, i.e., equations 184 to 186 and 187 to 189. The gasification of carbon, therefore, may be considered to be a special case of the more general equations.

After trial and error methods starting from *one* assumed value yield to a complex system of very cumbersome algebraic expressions, and after the calculations based on the assumption of *two* unknowns lead into a relatively simple system which can be solved in a fraction of the time necessary for the first type of methods, it might be of, at least, academic interest to investigate if starting from *three* or *more* assumed values of unknowns is of advantage.

With three assumed values x, y, z we arrive at the following set of equations:

$$\varphi'_x dx + \varphi'_y dy + \varphi'_z dz = d\varphi \quad (204a)$$

$$\psi'_x dx + \psi'_y dy + \psi'_z dz = d\psi \quad (204b)$$

$$\chi'_x dx + \chi'_y dy + \chi'_z dz = d\chi \quad (204c)$$

and the final solution, considering

$$d\varphi = -\varphi \quad d\psi = -\psi \quad d\chi = -\chi$$

is

$$x_0 - x = \frac{\varphi[\chi'_y\psi'_z - \psi'_y\chi'_z] + \psi[\chi'_x\varphi'_y - \varphi'_x\chi'_y] + \chi[\psi'_x\varphi'_z - \varphi'_x\psi'_z]}{\varphi'_x\psi'_y\chi'_z + \varphi'_y\psi'_z\chi'_x + \varphi'_z\psi'_x\chi'_y - \chi'_x\psi'_y\varphi'_z - \chi'_y\psi'_z\varphi'_x - \chi'_z\psi'_x\varphi'_y} \quad (204d)$$

$$y_0 - y = \frac{\varphi[\chi'_z\psi'_x - \psi'_x\chi'_z] + \psi[\chi'_x\varphi'_z - \varphi'_x\chi'_z] + \chi[\psi'_x\varphi'_y - \varphi'_x\psi'_y]}{\varphi'_x\psi'_y\chi'_z + \varphi'_y\psi'_z\chi'_x + \varphi'_z\psi'_x\chi'_y - \chi'_x\psi'_y\varphi'_z - \chi'_y\psi'_z\varphi'_x - \chi'_z\psi'_x\varphi'_y} \quad (204e)$$

$$z_0 - z = \frac{\varphi[\chi'_x\psi'_y - \psi'_y\chi'_x] + \psi[\chi'_y\varphi'_x - \varphi'_y\chi'_x] + \chi[\psi'_x\varphi'_y - \varphi'_x\psi'_y]}{\varphi'_x\psi'_y\chi'_z + \varphi'_y\psi'_z\chi'_x + \varphi'_z\psi'_x\chi'_y - \chi'_x\psi'_y\varphi'_z - \chi'_y\psi'_z\varphi'_x - \chi'_z\psi'_x\varphi'_y} \quad (204f)$$

Instead of equations 180 and 181 with $2! = 2$ members in the numerator and in the denominator, we have $3! = 6$ members. The increase in calculatory manipulations outbalances the possible simplification of the equations. The selection of two assumed values of unknowns, therefore, is justified. (For a different method starting from more assumed unknowns, see Brinkley's method, page 103.)

The degree of reduction—a semigraphical method

Instead of starting from material balances, we also may consider the gasifying agent as it enters the reduction zone of the gas producer and the degree of reduction of the carbon dioxide and steam as well as the degree of methane formation. The methods are closely connected. The analytical treatment of this method, meanwhile, offers no distinct advantages compared to the previously described methods. Zeise⁷ reports an example of this kind.

⁷ H. Zeise, Thermodynamische Berechnung von Verbrennungstemperaturen und Umsätzen in Gasgemischen bei strenger Berücksichtigung aller Spaltungsmöglichkeiten, III. Mitt., *Feuerungstechn.*, Vol. 30 (1942), No. 2, pp. 25-29, and No. 10, pp. 231-234.

With graphical solutions, however, this method is of greater advantage.

If the gasifying agent is considered as it leaves the oxidation zone and enters the reduction zone of the producer, it will be assumed that all free oxygen has been converted to carbon dioxide and steam. Whether this is actually the case or not, incidentally, is of no consequence for the procedure and the results of the calculation. The gasifying agent, therefore, will have the following analysis:

$$v''_{\text{CO}_2} + v''_{\text{H}_2\text{O}} + v''_{\text{N}_2} = 1 \quad (205)$$

Part of the carbon dioxide is reduced according to the Boudouard reaction (equation 2). This degree of conversion or reduction is called α_B ; $\alpha_B v''_{\text{CO}_2}$ disappears and $(1 - \alpha_B) v''_{\text{CO}_2}$ remains; $2\alpha_B v''_{\text{CO}_2}$ parts of CO are formed. $\alpha_W v''_{\text{H}_2\text{O}}$ parts of steam disappear and $(1 - \alpha_W) v''_{\text{H}_2\text{O}}$ remain; $\alpha_W v''_{\text{H}_2\text{O}}$ parts of hydrogen and an equal amount of carbon monoxide are formed, according to the heterogeneous water-gas reaction (equation 3). Hydrogen can react with carbon according to equation 5 to form methane. At a degree of conversion α_M , $\alpha_M \alpha_W v''_{\text{H}_2\text{O}}$ of the formed hydrogen disappears and only $(1 - \alpha_M) \alpha_W v''_{\text{H}_2\text{O}}$ remains as hydrogen, whereas $\frac{\alpha_M}{2} \alpha_W v''_{\text{H}_2\text{O}}$ are the parts of newly formed methane. Nitrogen passes unchanged from the gasifying agent to the gas. The sum of the remaining and newly formed materials, therefore the amount of gas per SCM of gasifying agent, is then

$$\begin{aligned} \Sigma = & \underbrace{(1 - \alpha_B) v''_{\text{CO}_2}}_{\text{CO}_2} + \underbrace{(1 - \alpha_W) v''_{\text{H}_2\text{O}}}_{\text{H}_2\text{O}} + \underbrace{2\alpha_B v''_{\text{CO}_2} + \alpha_W v''_{\text{H}_2\text{O}}}_{\text{CO}} \\ & + \underbrace{(1 - \alpha_M) \alpha_W v''_{\text{H}_2\text{O}}}_{\text{H}_2} + \underbrace{\frac{\alpha_M}{2} \alpha_W v''_{\text{H}_2\text{O}}}_{\text{CH}_4} + \underbrace{v''_{\text{N}_2}}_{\text{N}_2} \quad (206) \end{aligned}$$

$$\Sigma = 1 + \alpha_B v''_{\text{CO}_2} + \alpha_W v''_{\text{H}_2\text{O}} - \frac{\alpha_M}{2} \alpha_W v''_{\text{H}_2\text{O}} \quad (207)$$

If the first simplified case in which no methane is present is considered or the slight amount of methane is neglected—this is the case of a gasification with dry air or at very low humidities at normal pressures—equation 207 is simplified as follows:

$$\Sigma = 1 + \alpha_B v''_{\text{CO}_2} + \alpha_W v''_{\text{H}_2\text{O}} \quad (207a)$$

and the mole fractions (partial volumes) in the product gas become:

$$v_{\text{CO}} = \frac{2\alpha_B v''_{\text{CO}_2} + \alpha_W v''_{\text{H}_2\text{O}}}{\Sigma} \quad (208)$$

$$v_{\text{CO}_2} = \frac{(1 - \alpha_B) v''_{\text{CO}_2}}{\Sigma} \quad (209)$$

$$v_{\text{H}_2} = \frac{\alpha_W v''_{\text{H}_2\text{O}}}{\Sigma} \quad (210)$$

$$v_{\text{H}_2\text{O}} = \frac{(1 - \alpha_W) v''_{\text{H}_2\text{O}}}{\Sigma} \quad (211)$$

$$v_{\text{N}_2} = \frac{v''_{\text{N}_2}}{\Sigma} \quad (212)$$

To find a relationship between α_B and α_W , the equilibrium constant for the homogeneous water-gas reaction is used, and the values from equations 208 to 211 are inserted. Then

$$K_W = \frac{v_{\text{CO}} v_{\text{H}_2\text{O}}}{v_{\text{CO}_2} v_{\text{H}_2}} = \frac{(2\alpha_B v''_{\text{CO}_2} + \alpha_W v''_{\text{H}_2\text{O}})(1 - \alpha_W) v''_{\text{H}_2\text{O}}}{(1 - \alpha_B) v''_{\text{CO}_2} \alpha_W v''_{\text{H}_2\text{O}}} \quad (213)$$

After simplification and transformation,

$$\alpha_B = \frac{K_W - \frac{v''_{\text{H}_2\text{O}}}{v''_{\text{CO}_2}} (1 - \alpha_W)}{K_W + 2 \left(\frac{1}{\alpha_W} - 1 \right)} \quad (214)$$

For the graphical solution the following preliminary calculations are required. Three values of α_W that most probably cover the range of the unknown degree of steam decomposition are estimated and used for the calculation of α_B according to equation 214. For a second equation of condition the definition of K_{pW} is used:

$$\frac{K_{pW}}{P} = \frac{v_{\text{CO}} v_{\text{H}_2}}{v_{\text{H}_2\text{O}}}$$

The values for v_{CO} , v_{H_2} , and $v_{\text{H}_2\text{O}}$ are calculated from equations 208, 210, and 211, the sum of the gas constituents from equation 207. Thereby three values of $K_{pW} P^{-1}$ are obtained which are plotted against α_W . The intersection with the value $K_{pW} P^{-1}$ is

the desired solution, which can be read on the abscissa. With the α_W value determined, α_B is calculated from equation 214 and the gas constituents from equations 208 to 212. In Figure 15 a solution of this kind is presented. Starting with a gasifying agent of the composition

$$v'_{O_2} = 0.1734 \quad v'_{H_2O} = 0.1745 \quad v'_{N_2} = 0.6521$$

and

$$v''_{CO_2} = 0.1726 \quad v''_{H_2O} = 0.1747 \quad v''_{N_2} = 0.6527$$

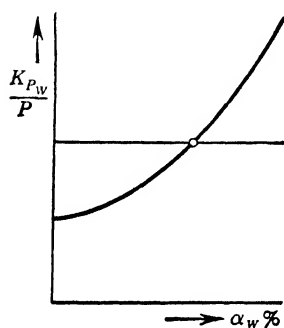


FIG. 15. Graphical determination of the degree of dissociation of steam.

α_W becomes 0.861 with the estimated values of 0.80, 0.85, 0.90 at $P = 1$ Atm, $t = 700^\circ\text{C}$. In the event that this result does not satisfy the requirements of accuracy, the graphical evaluation can be repeated with the three estimated values $\alpha_W = 0.860$, 0.861, 0.862, and the second place after the decimal point will be sufficiently accurate. With this value of α_W , α_B , and the other gas constituents are calculated according to equations 214 and 208 to 212.

The same process is applicable also in principle to the general case which includes methane formation. The mole fraction (partial volumes) of the product gas becomes in this case:

$$v_{CO} = \frac{2\alpha_B v''_{CO_2} + \alpha_W v''_{H_2O}}{\Sigma} \quad (215)$$

$$v_{CO_2} = \frac{(1 - \alpha_B) v''_{CO_2}}{\Sigma} \quad (216)$$

$$v_{H_2} = \frac{(1 - \alpha_M) \alpha_W v''_{H_2O}}{\Sigma} \quad (217)$$

$$v_{H_2O} = \frac{(1 - \alpha_W) v''_{H_2O}}{\Sigma} \quad (218)$$

$$v_{CH_4} = \frac{\frac{\alpha_M}{2} \alpha_W v''_{H_2O}}{\Sigma} \quad (219)$$

$$v_{N_2} = \frac{v''_{N_2}}{\Sigma} \quad (220)$$

Σ of equation 207 is to be used here.

The relationship between α_B and α_W is given by

$$\alpha_B = \frac{K_W(1 - \alpha_M) - \frac{v''_{H_2O}}{v''_{CO_2}}(1 - \alpha_W)}{K_W(1 - \alpha_M) + 2\left(\frac{1}{\alpha_W} - 1\right)} \quad (221)$$

It is not desirable to eliminate the unknown α_M analytically, since this would lead to awkward expressions. It is simpler to estimate three values for α_M . Nine values of α_W must then be calculated and not one but three points of intersection with $K_{pW}P^{-1}$ will be obtained. As a further equation of condition the definition of the equilibrium constant K_{pM} of the formation of methane is introduced, and α_B and the corresponding gas analysis for the values α_W of the three intersectional points which have been found before are calculated. Then $PK_{pM} = v_{CH_4}/v_{H_2}^2$ is evaluated and plotted against α_M . The intersection with PK_{pM} is the final solution which, inserted in equation 221, gives three values for a fourth curve, the intersection of which is the final value of α_W and—according to equation 221—also of α_B . The number of required calculations has increased from the previous four (neglecting methane) to thirteen for the general case.

To lessen the work of calculation, we can proceed in the following manner, which gives a good approximation. Methane is neglected at first, and α_B and α_W are calculated in the described manner, using equation 214. These are approximate values for α_B and α_W , if they cannot be estimated reliably (e.g., from previous calculations with every similar composition of the gasifying agent). With these approximative values α_M is calculated:

$$\alpha_M = \frac{K_{pM}K_{pW}(1 - \alpha_W)}{K_{pM}K_{pW}(1 - \alpha_W) + \alpha_B \frac{v''_{CO_2}}{v''_{H_2O}} + \frac{\alpha_W}{2}} \quad (222)$$

This equation was derived by choosing the definition for

$$K_{pM}K_{pW} = \frac{v_{CH_4}v_{CO}}{v_{H_2}v_{H_2O}} \quad (223)$$

as a starting equation, inserting the values of the gas constituents from equations 215–219, and solving for α_M . This α_M value is inserted into equation 221 or even into the following equation:

$$\alpha_B = \frac{v''_{H_2O}}{v''_{CO_2}} \left[K_{pM} K_{pW} (1 - \alpha_W) \frac{1 - \alpha_M}{\alpha_M} - \frac{\alpha_W}{2} \right] \quad (224)$$

The previous calculations are followed, the gas analysis of the product gas is determined, K_{pW} is calculated, these values plotted against α_W , which by way of equation 221 or 224 produces the final result. Although this is only an approximate solution, equation 224 is so sensitive to small deviations from α_M that the approximation is very close. Besides, if required, the calculation can be repeated with improved values of α_W and α_B .

In the sample calculation of Figure 15 α_W is 0.861 and α_B is 0.521, both approximately. With these values given, α_M becomes 0.0313 (equation 222) as compared with the more accurate value of 0.0314. The approximation, therefore, is quite satisfactory.

The graphical method may be used advantageously where the estimation of v_{CO} and v_{H_2} values necessary for the analytical methods is difficult and consequently might require a frequent repetition of the calculation, e.g., with quite unusual gasifying agents or under unusual conditions. With the first approximation a pair of values may be obtained which lead to an exact final solution, by proceeding with analytical methods.

The heat balance

So far, the problem has been to determine the equilibrium gas composition at known temperatures. The temperature of reaction, however, is unknown and has to be determined by heat balance of the reaction zones of the gas producer. The heat balance is solved graphically by means of the enthalpy-temperature diagram. The term *reaction zones* applies to the ash zone, the oxidation zone, and the reduction zone but does not include the preheating zone. In the ash zone, too, no reaction takes place; however, the gasifying agent is heated and the residues are cooled. By including this process of heat transfer in the reactions the basis of calculation is simplified, and the difficulty of having to fix the outlet temperature of the residues leaving the oxidation zone is avoided. Even if a small error is made by assuming the ash temperature to be equal to the fuel temperature (entering

the producer), it is within negligibly narrow limits. Only in slagging ash producers are conditions different since no preheating of the blast is affected by the slag, and the residue is issued at a temperature above slag fusion temperature. In this case the heat content of the residues has to be evaluated accordingly (including the heat of fusion of slag), and the slag zone, situated below the tuyères, is not considered to be part of the reaction zone. Generally speaking, the zones considered in the heat balance are limited at the lower end by the plane in which the blast enters the producer (lower plane of the grate in rotating grate producers or plane of the tuyère axis in slagging ash producers). The upper limit is that cross-section of the shaft where the temperatures of the gas and the fuel surface are practically equal (no more heat exchange) and where the exchange of material, and this means the gasification, is practically at a standstill. This is the end of the reduction zone. Further cooling leads to the freezing of the equilibria.* The path

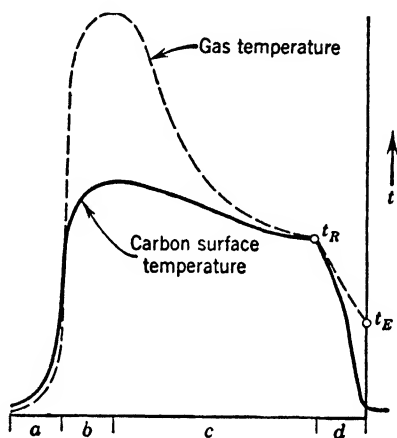


FIG. 16. Course of temperatures in a gas producer.

- a = ash zone
- b = oxidizing zone
- c = reducing zone
- d = preheating zone
- t_R = reaction temperature
- t_E = exit gas temperature

of the temperature in the gas producer, as it results from suppositions on the reactions taking place in it, is presented in Figure 16. Starting in the preheating zone, the solid fuel is first heated to *reaction temperature*. By this term is meant the surface temperature of the fuel at the end of the reduction zone. In the entire reaction zone the surface temperature of the solid fuel deviates only slightly from this value, if it is considered that this temperature is regulated mainly by the gas formation at the phase boundary. In the oxidation zone the

* For exceptions, reversible reactions in the preheating zone, particularly where the temperatures are still very high, see page 137.

surface temperature reaches a flat maximum. The absolute value has no influence upon the result of the calculation. In addition to the process of material and heat exchange by convection, the maximum is influenced by the exchange due to radiation between the plane of combustion (i.e., the place of reaction of incoming oxygen, and countercurrent gas from the phase boundary) and the surface of the solid fuel. In the ash zone, heat exchange takes place only between the gasifying agent (the blast) and the residue, whereby the temperature of the issuing material drops to a value little above the entering temperature of the blast.

We shall now consider the time available for the passage of the fuel through the gas producer, and whether heat exchange of the assumed extent can take place. If a gas producer operates at a throughput of F kg per m^2 hr of fuel and if the bulk density (the apparent density) of the fuel is d_f kg per m^3 , the fuel velocity is

$$w = \frac{F}{d_f} \quad [\text{m/hr}] \quad (225)$$

or the time for moving down one meter is

$$\Theta = \frac{d_f}{F} \quad [\text{hr}] \quad (226)$$

At a charging rate of 100, 200, 300, and 500 kg/m^2 hr to the gas producer and a bulk weight (apparent density) of 520 kg/m^3 of the coke, the fuel velocity is 0.192, or 0.385, 0.577, and 0.962 m/hr, respectively. The time for the fuel to move one meter is 5.2, 2.6, 1.4, and 1.04 hr. At the usual charging rate to rotating grate producers of 100 to 200 kg coke per m^2 per hour, very long times are therefore at disposal. The heating-through of a very coarse lump of fuel is therefore possible, and the assumption that the surface temperature equals the gas (reaction) temperature is justified.

The calculation of the surface temperatures⁸ shown on Figure 17 is based on the following assumptions. The lumps of fuel are considered to be spheres; in the temperature range between 0

⁸ Hans Bachmann, *Tafeln über Abkühlungsvorgänge einfacher Körper*, Berlin, 1938.

and 700°C the following data⁹ are used with high-temperature coke as the fuel:

Thermal conductivity (at the average temperature of 350°C)	$k = 1.957 \text{ kcal/m hr } ^\circ\text{C}$
True specific heat	$c_p = 0.3494 \text{ kcal/kg } ^\circ\text{C}$
Weight per unit volume	$\rho_s = 950 \text{ kg/m}^3$
Thermal diffusivity ($k/\rho_s c_p$)	$\alpha = 0.005896 \text{ m}^2/\text{hr}$

The heat transfer coefficients are assumed to be 20 to 11.7 kcal per m² hr °C for sphere diameters 15 to 70 mm, corresponding to

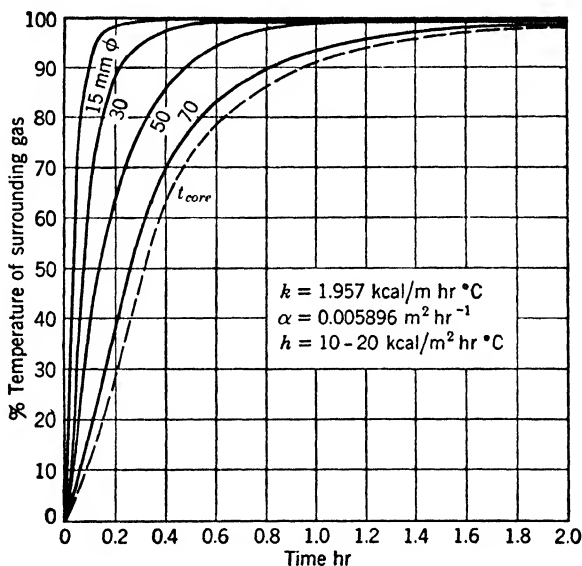


FIG. 17. Surface temperature of spherical coke particles when heated by the surrounding gas.

Inscribed diameters = particle diameter in millimeters

t_{core} = temperature of the core (70-mm particle)

average particle sizes of the different grades of industrial and domestic coke.

If a highly magnified section of the end of the reduction zone is viewed, it could be maintained that the equalization of the tem-

⁹ Walter Fritz und Hans Kneese, Wärmeleitfähigkeit, spez. Wärme und Temperaturleitfähigkeit von Koks, Koks und Braunkohle, *Feuerungstechn.*, Vol. 30 (1942), No. 12, pp. 273-279.

perature can never be complete and that a certain though small temperature difference would always exist at finite extension of the exchange surfaces. Consequently, there would also be a difference in gas and fuel surface temperature. If this is assumed, the gas temperature will not intersect the reduction exactly at a height h , but in a plane located above by the very small amount Δh . This is due to cooling in the preheating zone (see Figure 8, page 28). This is practically without any importance, because the height h of the reaction zone or $h + \Delta h$ serves merely for the determination of the external heat losses of the reaction zones, and the determination of this loss is unfortunately not accurate enough to make a shift of a few millimeters or even centimeters noticeable in measurement.

At low loads of the producer the preheating of the fuel (in a countercurrent gasification process) is complete. If, however, the rate is increased, the residence time in the preheating zone decreases, the reduction zone is repressed. Simultaneously, its heat loss decreases (since a larger amount of heat is converted in a smaller space) without changing the temperature of the cooling surface. The heat balance is thereby equalized and the reaction temperature remains nearly constant or rises only a small amount owing to the slightly preponderant decline of the external heat losses. These considerations are corroborated by the experiments of E. Hecker¹⁰ with a gas producer of 2.1 m inner diameter at $t_s = 62^\circ\text{C}$ saturation temperature of the blast (see Table 9).

TABLE 9

REACTION TEMPERATURES AS DERIVED FROM E. HECKER'S EXPERIMENTS

Fuel rate, $\text{kg/m}^2 \text{ hr}$	57.5	134.2	183.8	214.5
Fuel linear velocity, m/hr	0.12	0.27	0.38	0.44
v_{CO} (dry), %	28.33	28.93	28.47	29.07
Reaction temperature, $^\circ\text{C}$, derived from CO content, $^\circ\text{C}$	704	709	705	710

The slight deviations (e.g., reaction temperatures or CO contents at 134.2 and 183.8 $\text{kg/m}^2 \text{ hr}$) are caused by the difficulty in maintaining constant operation conditions for fuel and blast

¹⁰ Eberhard Hecker, Untersuchung an einem Hochdruckdampfkesselgenerator über den Einfluss der Leistungsveränderung, *Gas- u. Wasserfach*, Vol. 75 (1932), No. 18, pp. 329-335.

(temperature and degree of saturation) and in obtaining true average gas samples and gas analyses.

After the space outlines of the reaction zones are settled, their heat balances may be set up. According to Figure 18, the heat input is composed of:

- (1) The net calorific value of the fuel H_i . As far as pure carbon is considered, $H_i = 8080$ kcal/kg.
- (2) The enthalpy of the fuel after preheating to reaction temperature, H_C kcal/kg.
- (3) The enthalpy of the gasifying agent, H_M kcal/SCM.

The heat output consists of:

- (4) The heating value of the product gas, $H_{i,G}$ kcal/SCM.
- (5) The enthalpy of the product gas, H_G kcal/SCM.
- (6) The enthalpy of the discharged residue (slag), H_{sl} kcal/kg.
- (7) The external heat losses by radiation and convection, Q_{ext} .

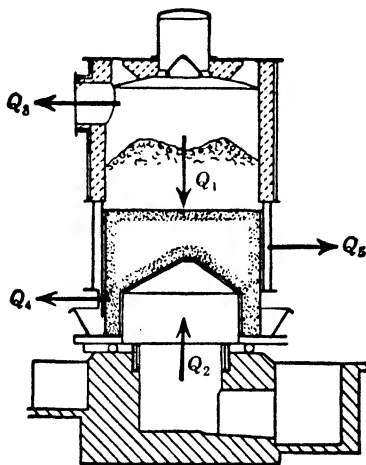


FIG. 18. Reaction zone of a gas producer.

$$Q_1 = H_{i,F} + H_C$$

$$Q_2 = H_M$$

$$Q_3 = H_{i,G} + H_G$$

$$Q_4 = H_{sl}$$

$$Q_5 = Q_{ext}$$

If we consider coke as the actual fuel gasified (even where coal is charged to the producer) and if we calculate only with the

combustible matter, the carbon (neglecting the ash content and the heat input by the ash), we can also neglect the enthalpy of

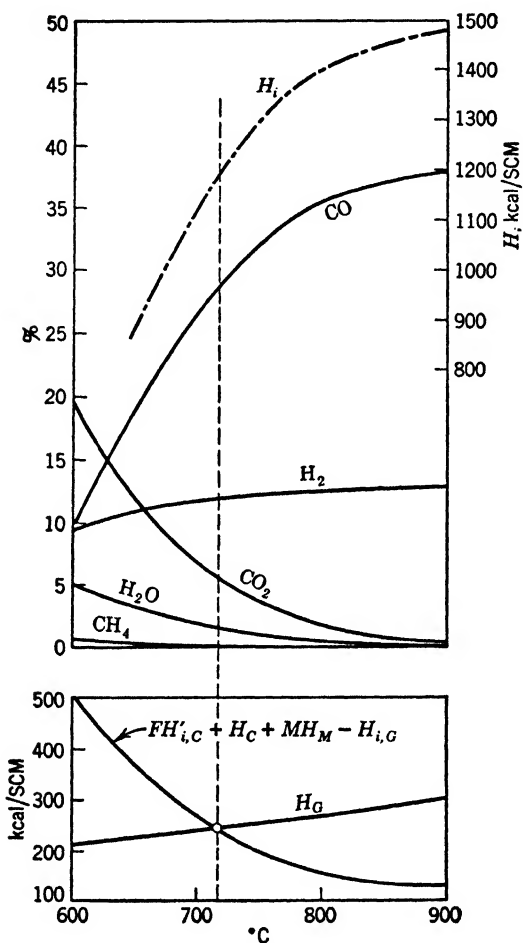


FIG. 19. Graphical heat balance (H - t diagram) and gas composition as a function of the reaction temperature.

the discharged residue (with the exception of liquid slag removal). The heat balance then looks like this:

$$FH_i + FH_C + MH_M = H_{i,G} + H_G - Q_{ext} \quad (227)$$

Allowance is made for the external heat losses by inserting a heat-

ing value of $H_i \left(1 - \frac{x}{100}\right)$ at $x\%$ heat loss (with reference to the gasified fuel). The enthalpy of carbon can be found in Table VII, page 306 of the appendix.

The external heat loss is influenced mainly by the temperature of the gas phase, particularly in the oxidation zone where the temperature is highest. A slight change in the height of the reduction zone is of no consequence. The heat input to the water or steam jacket, if such is used, gives a fair idea of the amount. The external heat loss of the jacket itself is to be added. As far as the water jacket is extended beyond the reaction zone, a proportional part of the losses is to be subtracted.* In normal-rated rotating grate gas producers with water jacket, Q_{ext} should be about 7 to 8%, in high-rated small gas producers (portable gas producers) between 9 and 10%, and in high-rated gas producers without water jacket (slagging ash producer) at 4 to 5% and less. (See also Figure 52, page 233.) If accurate heat balances of a gas producer are available, the value of Q_{ext} may be taken from them. It is expected to be little below the heat input to the jacket and its external heat loss.

For the graphical solution of the heat balance equation, the enthalpy of the product gas against temperature need only be plotted and intersected with curve. (See Figure 19.)

$$FH_i - Q_{ext} + FH_C + MH_M - H_{i,G} = \Sigma Q \quad (227a)$$

The reaction temperature and the gas analysis are then known, and the problem of gas composition and gas yield when gasifying a given fuel with given gasifying agent is solved. To obtain accurate numerical values, it is usually recommended to repeat the calculation with the reaction temperature thus determined, whereby a very close estimation of the expected values of CO and H₂ is possible.

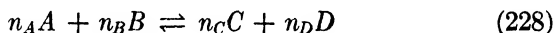
* This is to be noticed with reference to longer water or steam jackets and with extended tubes washed around by the hot gas like those in the Marischka type producer (see Figure 10).

3

GAS COMPOSITION AT INCOMPLETE EQUILIBRIUM

In the previous discussions it has been assumed that all equilibria are attained, and calculations have been based on this assumption. It remains to determine how the conditions are changed if equilibrium is not attained completely, and whether, or to what extent, equilibria are attained in gas producers. Only when this question has been settled and answered numerically does the calculation method reach its full practical importance and its general applicability.¹

If a reaction between components *A* and *B* is considered, leading to the products *C* and *D*, according to reaction



the velocity in one direction (v_1) is

$$v_1 \rightarrow k_1 n_A n_B \quad (229)$$

and, in the opposite direction,

$$v_2 \rightarrow k_2 n_C n_D \quad (230)$$

If the reaction is in equilibrium,

$$v_1 = v_2 \quad (231)$$

and the equilibrium is characterized by the equilibrium constant

$$K_p = \frac{k_1}{k_2} = \frac{(p_C)^{n_C} (p_D)^{n_D}}{(p_A)^{n_A} (p_B)^{n_B}} \quad (232)$$

The expression

$$(\Pi_p)^n = \frac{(p_C)^{n_C} (p_D)^{n_D}}{(p_A)^{n_A} (p_B)^{n_B}} \quad (233)$$

¹ Sergei Traustel und Wilhelm Gumz, "Über Vergasungsvorgänge bei unvollkommener Gleichgewichtseinstellung," *Bergbau u. Energiewirtschaft*, Vol. 2 (1949), No. 3, pp. 69-75, No. 4/5, pp. 85-87.

is called the *quotient of mass action*; at equilibrium it is equal to the equilibrium constant.

If, however, the reaction has not yet reached equilibrium, the rate of reaction from right to left in equation 228 dominates. The starting materials, therefore, are not converted as completely as would correspond to the equilibrium condition. The partial pressures or partial volumes of the gases are different, and the mass action quotient Π_p^n is *not* equal to the equilibrium constant but is smaller:

$$(\Pi_p)^n \neq K_p \quad (234)$$

If the degree of approach to the equilibrium is called x , where x is a number between 0 and 1, a *non-equilibrium condition* results:

$$(\Pi_p)^n = xK_p \quad (235)$$

We call the degree of approach of the Boudouard reaction (equation 2) x_B , that of the heterogeneous water-gas reaction (equation 3) x_W , and that of the methane formation reaction (equation 5) x_M . Then

$$x_B K_{pB} = \frac{p_{CO}^2}{p_{CO_2}} \quad (236)$$

$$x_W K_{pW} = \frac{p_{CO} p_{H_2}}{p_{H_2O}} \quad (237)$$

and

$$x_M K_{pM} = \frac{p_{CH_4}}{p_{H_2}^2} \quad (238)$$

If $x_B = x_W = x_M = 1$, equations 236 to 238 are changed into 20, 24, and 32, pages 10 and 11, i.e., a state of equilibrium exists.

In the form of the expressions we have the same situation as in combining the equilibrium constants of several reactions. As already mentioned, the state of equilibrium is included in our discussion if x approaches its limit of $x = 1$. Hence we can operate with the degrees of approach in the same way as we did previously with the equilibrium constants which could be reduced to the constants of the three basic gasification reactions or combinations thereof.

78 GAS COMPOSITION AT INCOMPLETE EQUILIBRIUM

Let us elucidate such a combination by considering the homogeneous water-gas shift reaction (degree of approach x_S):

$$x_S K_W = \frac{p_{CO} p_{H_2O}}{p_{CO_2} p_{H_2}} = \frac{p_{CO}^2}{p_{CO_2}} \frac{p_{H_2O}}{p_{CO} p_{H_2}} \quad (239)$$

$$x_S K_W = \frac{x_B K_{pB}}{x_W K_{pW}} \quad (240)$$

Thus

$$x_S = \frac{x_B}{x_W} \quad (241)$$

As a second illustration, we consider the formation of methane from carbon monoxide and hydrogen according to equation 25:

$$\begin{aligned} x_{25} K_{p_{25}} &= \frac{p_{CH_4} p_{H_2O}}{p_{CO} p_{H_2}^3} = \frac{p_{CH_4}}{p_{H_2}^2} \frac{p_{H_2O}}{p_{CO} p_{H_2}} \\ &= \frac{x_M K_{pM}}{x_W K_{pW}} \end{aligned} \quad (242)$$

$$x_{25} = \frac{x_M}{x_W} \quad (243)$$

The degrees of approach are therefore interrelated in the same way as the corresponding equilibrium constants, and it is sufficient to know the three degrees of approach of the basic reactions (equations 2, 3, 5) in order to find them for all reactions that can be derived from the basic ones.

If the expression xK_p is introduced into our scheme of calculation (page 48) instead of the known equilibrium constant K_p , the calculation is no way formally changed, but a new difficulty arises in that there are now three new unknowns in the equilibrium system. The general case

$$x_B \neq x_W \neq x_M \quad (244)$$

$$x_B < 1 \quad x_W < 1 \quad x_M < 1 \quad (245)$$

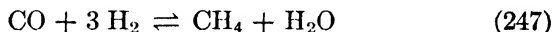
is therefore particularly difficult from a mathematical point of view, as long as the numerical degrees of approach are unknown. Traustel and Reuter² attempted to avoid this difficulty and to

² Sergei Traustel und Alfred Reuter, Die Gaswandlung in der Reduktionszone eines Gaserzeugers, *Feuerungstechn.*, Vol. 29 (1941), No. 7, pp. 159-161.

reach a simple working hypothesis by assuming that all homogeneous gas reactions reach complete equilibrium and that the approach of heterogeneous reactions to equilibrium, however, is less than 1. Assuming this, we have

$$x_B = x_W = x_M < 1 \quad (246)$$

i.e., the numerical values of the three degrees of approach are equal (and < 1) and there is just one new unknown. This assumption does not take into account the complicated methane formation, since it would also be assumed that the reaction



runs to completion. The methane formation, however, is a reaction in stages, and the above equation is to be considered as an overall equation. The stages may well be bimolecular, but in view of the complexity of the reaction we cannot expect it to proceed to completion. From experience we know that nickel catalysts are required for this reaction and that the presence of traces of ash particles to which one may attribute some catalytic action is by no means sufficient. It is therefore to be expected that $x_M < 1$, while

$$x_M \neq x_B \neq x_W \quad (248)$$

For the determination of the *degrees of approach* the comparison of calculated values and large-scale experiment is used.

For x_B and x_W , experiments are sufficient in which methane formation is negligibly small. In the sample calculations on page 86, the calculation of an experiment by Plenz³ is carried out and compared with the experimental values. It is seen that the agreement with a calculation where $x_B = x_W = 1$ is excellent, that therefore the assumption is fully justified, and that it leads to perfectly useful values. Such comparisons always produced the same result for numerous other gas production experiments.

For the determination of the degree of approach of the methane formation reaction x_M , the experiments, however, are not suited because

³ F. Plenz, Leistungsversuch an einer Koksvergasungsanlage auf dem Gaswerk Berlin-Neukölln, *Feuerungstechn.*, Vol. 15 (1926-1927), No. 20, pp. 232-234.

1. New formation of methane is extremely slight even at equilibrium.
2. The amount of methane from the small fraction of volatile matter of the coke—consisting mainly of hydrogen and methane—is generally higher than the amount of newly formed methane.
3. The analytical determination of low methane contents is difficult and therefore frequently faulty.

The picture is rather confusing owing to errors in analysis and differences in fuel composition (content of volatile matter and its composition). An additional factor is the temporary variation in the gas formed by devolatilization.

A numerical determination of x_M is possible only where the methane contents are so high that the uncertainty of measurement and the masking by the volatile constituents of the fuel are slight or negligible. The large-scale experiment of a pressure gasification of semi-anthracite coal with an oxygen-steam mixture is discussed below, since unfortunately no experiments with high-temperature coke have been reported. The coal analysis, the composition of the gasifying agent, and the raw gas analysis are given in Table 10.

In the attempt to recalculate this experimental result, a calculation with

$$x_B = x_W = x_M < 1$$

was as unsatisfactory as, for instance, the assumptions

$$x_B = x_W < 1 \quad x_M < 1$$

There is no reason at all to assume a lower degree of approach for the Boudouard and the heterogeneous water-gas reaction with this smaller-sized and even more reactive fuel in a high-pressure gas producer than for a rotating grate producer with gas coke (10- to 20-mm lump size) as used in the Plenz experiments. Therefore, a reasonable assumption may be

$$x_B = x_W = 1 \quad x_M < 1$$

The temperature of the reaction zone at the phase boundary which controls the analysis of the produced gas results from the heat balance on the reaction zones. The exact determination of the heat balance is quite difficult, and temperature exerts an extremely strong influence on the gas composition. Moreover, heat balances

of the whole gas producer include the external heat losses outside the reaction zones. In this case, the steam jacket was extended above the reaction zone, and the heat input from the producer to

TABLE 10
GASIFICATION OF SEMI-ANTHRACITE AT $P = 20$ ATM

<i>Fuel</i>	<i>Fixed Carbon</i>
Semi-anthracite	73.42% (88.56% ash and moisture free)
Mine "Alstaden," Sterkrade, Westphalia size 10/2 mm	
<i>Ultimate Analysis</i>	<i>Volatile Matter</i>
75.13 % C	9.48% (11.44% ash and moisture free)
3.56 % H ₂	
0.91 % S	<i>Heating Value (Raw Coal)</i>
3.30 % O ₂ + N ₂	$H_a = 7022$ kcal/kg
13.10 % ash	$H_i = 6807$ kcal/kg
4.00 % moisture	
100.00 %	<i>Raw Gas Analysis</i>
<i>Gasifying Agent</i>	14.36 % CO
7.779 % O ₂ }	31.30 % CO ₂
0.505 % N ₂ } room temperature	42.89 % H ₂
91.716 % H ₂ O $t_{H_2O} = 480^\circ\text{C}$	9.65 % CH ₄
	1.04 % N ₂
	0.27 % H ₂ S
	0.24 % C _n H _m
100.000 %	0.25 % O ₂
<i>Gas Yield</i>	
Pure gas (2% CO ₂) yield with reference to raw coal	100.00 %
1.560 SCM/kg	
Same with reference to pure (ash and moisture free) coal	
1.880 SCM/kg	

the jacket amounted to approximately 1% of the heat charged by the fuel. Including an allowance for heat input by the mineral matter, the deduction amounts to 0.8%.

To find the approach to the equilibrium we must bear in mind that different x values correspond to every reaction temperature.

82 GAS COMPOSITION AT INCOMPLETE EQUILIBRIUM

By a series of calculations with three different x_M values (with $x_B = x_W = 1$) and three different external heat losses, we found that the best conformity was reached by 0.8% external heat losses and with $x_M = 0.24$. Table 11 shows the result of the calculation with these assumptions, the graphically determined reaction temperature being 671.5°C.

TABLE 11
GASIFICATION OF CARBON AT 20 ATM
($x_B = x_W = 1$; $x_M = 0.24$; $Q_{ext} = 0.8\%$)

t_R	650°	675°	700°	671.5°C
$x_B PK'_{p_B}$	58.664	32.564	18.645	35.294
$x_W PK'_{p_W}$	29.952	18.756	12.035	19.998
$x_M PK_{p_M}$	1.15162	0.84914	0.63538	0.88528
% CO	6.06	8.04	10.43	7.74
% CO ₂	21.55	21.04	20.28	21.12
% H ₂	23.33	25.85	28.29	25.50
% H ₂ O	42.36	38.97	35.51	39.46
% CH ₄	6.27	5.68	5.08	5.76
% N ₂	0.43	0.42	0.41	0.42
	100.00	100.00	100.00	100.00
F kg/SCM	0.1815	0.1862	0.1918	0.1855
M SCM/SCM	0.8531	0.8306	0.8063	0.8338
H_G kcal/SCM	261.7	269.7	276.9	...
$H_{i,G}$ kcal/SCM	1318.7	1392.8	1476.4	...
ΣQ kcal/SCM	300.5	262.8	222.0	...

Unfortunately, the volatile constituents have a disturbing influence, and the difficulties of an exact determination are increased by the fact that no accurate pressure-distillation analysis of the fuel at reaction temperature is available. Merely from the distillation analysis at atmospheric pressure and from the known⁴ tendencies of the analysis to shift at higher pressures, we can assume that the volatile constituents at about 650 to 700°C and

⁴ F. Danulat, Wechselwirkungen zwischen Gas u. Brennstoff bei der Druckvergasung. *Gas- u. Wasserfach*, Vol. 85 (1942), No. 49-50, pp. 557-562.

20 Atm abs have the following gas analysis (dry basis): 1% CO₂, 76% H₂, 16% CH₄, 2% N₂. The volatile matter amounts to 11.44% by weight. The largest part of it is water of decomposition, a smaller fraction is tar and light oil, and only 2.2% by weight is gas corresponding to a yield of 0.07579 SCM per kilogram of coal. To compare gas yields, calculated and measured, as in Table 12, some further carbon losses have to be considered.

TABLE 12

PRESSURE GASIFICATION OF SEMI-ANTHRACITE

P = 20 Atm abs—comparison of calculation and measurement

Calculated		Measured
Gas of devolatilization	0.07579 SCM/lb fuel	...
Gas of gasification	5.39113 SCM/lb C _{fix}	...
Gas of gasification (dry)	2.76033 SCM/lb fuel	...
After 4.5% C loss		
Final gas	2.83612 SCM/lb fuel	...
After deduction of 1% pocket gas loss	2.80776 SCM/lb fuel	...
After washing out to 2% CO ₂	1.88429 SCM/lb fuel	1.880 SCM/lb
Gas composition (dry basis)		
12.58 % CO		14.36 % CO
33.99 % CO ₂		31.30 % CO ₂
43.02 % H ₂		42.89 % H ₂
9.68 % CH ₄		9.65 % CH ₄
0.73 % N ₂		1.04 % N ₂
		0.27 % H ₂ S
		0.24 % C _n H _m
		0.25 % O ₂
100.00 %		100.00 %

Carbon loss of 4.5% is assumed in residue and fly ash, and a loss of 1% is caused by the pocket gas losses. The pure gas (after CO₂ washed out under pressure to approximately 2%) is about 67.11% of the dry raw gas. Since pure gas was measured directly, these data can also be checked with the calculation, besides the gas analysis.

The agreement shown in Table 12 is good. The final gas is composed of 97.33% of gas from the gasification process and only 2.67% from devolatilization. An error in the assumption of the analysis of the volatile constituents is therefore not very impor-

tant. The agreement of the final analysis data is sufficient if not complete. The existing differences will be discussed briefly and critically.

The CO content of the calculation is slightly lower so that we might get the impression that the reaction temperature may have been slightly higher. This is perfectly possible, since some items of the heat balance are not very certain, e.g., the enthalpy of solid carbon. Small variations in the composition of the gasifying agent within the limits of error of flow measurements by orifices may also be the cause.

The CO₂ content, as calculated, is higher for the same reasons that the CO content is low. However, even a change of temperature to 690°C ($Q_{ext} = 0\%$) would still result in a CO₂ content that was too high. In view of the absolute value, it is not impossible that some CO₂ had already been washed out in the pre-cooler, after which the raw gas had been analyzed.

The H₂ content agrees fairly well with the measurement, especially if it is noted that H₂S has not been considered in the calculation. But H₂ + H₂S amounts to 43.16% as measured, and the H₂ content of the calculation, with only C as a body material, is 43.02%. The uncertainty of the composition of the gas of devolatilization is important since its H₂ content is particularly high and very dependent on temperature. Of the H₂ content of 43.02% in the final gas, 40.97% is due to gasification and 2.05% to devolatilization.

The CH₄ content cannot be used as a criterion since it was the starting point for the determination of the x_M value.

The nitrogen content of 0.73% is low, compared with 1.04% as measured. This difference is easily explained since the calculation was carried out for pure carbon. Considering the nitrogen content of the fuel (approximately 1%) and the slight NH₃ formation in the gas, a N₂ content is reached which agrees very well with the measured value. Some variation in the purity of the oxygen used may also have influenced the result to a certain degree.

When coke is gasified at atmospheric pressure, the amount of CH₄ formed is exceedingly small. It could be supposed that the consideration of x_M value < 1 has hardly a remarkable effect. A check calculation shows, however, that it is advisable in this (and any) case to calculate with an x_M value of the determined order of magnitude. The experimental results of F. Plenz * will once

* See p. 79, footnote 3.

again be used as an example. Table 13 shows the comparison of measurement and calculation. The following composition of the gasifying agent (air-steam mixture) has been used:

17.335% O₂, 65.214% N₂, 17.451% H₂O

corresponding to a saturation temperature of the blast of 57.5°C. The heat transfer to the water jacket plus other external heat

TABLE 13
GASIFICATION OF COKE ACCORDING TO PLENZ' EXPERIMENTS
(Comparison of Measurement and Calculation)

Experimental $t_s = 55-60^\circ\text{C}$	Average 57.5	Calculation	
		$x_M = 1$ $t_s = 57.5$ $t_R = 713$	$x_M = 0.24$ 57.5°C 713 °C
28.4-29.4	29.31	28.96	28.93 % CO
4.0- 5.7	5.17	5.82	5.81 % CO ₂
10.7-13.7	12.68	12.15	12.36 % H ₂
0.0- 1.2	0.41	0.17	0.04 % CH ₄
51.7-54.8	52.43	52.90	52.86 % N ₂
	100.00	100.00	100.00 %

losses of the reaction zones were assumed to be 8%, and the calculation was carried out with

$$(1) x_B = x_W = x_M = 1$$

$$(2) x_B = x_W = 1 \quad x_M = 0.24$$

In both cases the approach of the calculated to the measured values is satisfactory, but at $x_M = 0.24$ it is still better, although the agreement in both cases is quite satisfactory. The measured values, taken as an average, may not correlate completely, e.g., the CO and CO₂ contents as indicated. Differences are to be expected mainly because the operating conditions of the experiment were subject to certain variations and because the accuracy of the formulation of the average value is hard to control. Apparently the average value of the saturation temperature, for instance, does not agree perfectly with the average hydrogen content of the product gas, for the hydrogen content provides an accurate indication of the water content of the blast, so that it can even be

used for the calculated determination of the average saturation temperature. The deviation of the CO_2 content could be due to errors of measurement for formulation of the average value, since measurements (e.g., incomplete CO_2 absorption) will always lead to low values. The methane content from measurement varies extremely, indicating that this methane is mainly provided by the small amount of volatile matter in the coke.

As a result of the determination of the x value, it is to be noted that with the degrees of approach,

$$x_B = 1 \quad x_W = 1 \quad x_M = 0.24$$

in pressure as well as atmosphere gasification, perfectly satisfactory agreement between calculation and measurement has been effected. Thereby, the general usefulness of the calculation method is proved. Equilibrium in the heterogeneous reaction of carbon dioxide and steam reduction is practically complete; while methane formation reaches only approximately one-fourth the maximum value. As soon as further suitable experimental material is available, e.g., experiments with well-degasified high-temperature coke at very high pressures, the x_M value can be re-examined. However, neither a large shift nor a noticeable change of results is to be expected from such experiments.

Calculation scheme and sample calculations

Triangle method (see p. 50)

Fuel. Pure coke (100% C), neglecting the small amount of volatile constituents, and nitrogen, and sulfur.

Gasifying Agent. Air, saturated at 57.5°C , steam content 170 g/SCM (dry) = 0.2114 SCM/SCM dry air. The composition of the blast is:

$$\begin{array}{rcl} 0.2100 \text{ SCM} & \text{O}_2 = & 17.335 \% \text{ O}_2 \\ 0.7900 \text{ SCM} & \text{N}_2 = & 65.214 \% \text{ N}_2 \\ 0.2114 \text{ SCM} & \text{H}_2\text{O} = & 17.451 \% \text{ H}_2\text{O} \\ \hline & & 100.00 \% \end{array}$$

$$H_M = v'_{\text{H}_2\text{O}} = 0.17451 \quad O_M = v'_{\text{O}_2} + 0.5v'_{\text{H}_2\text{O}} = 0.260605$$

$$N_M = v'_{\text{N}_2} = 0.65214$$

$$\frac{H_M}{O_M} = 0.66963 \quad \frac{N_M}{O_M} = 2.50241$$

The calculation must be performed for several temperatures (at least three) in the neighborhood of the expected reaction temperature (e.g., between 700 and 750°C). Below is the calculation for 700°C.

At first a set of values for CO and H₂ is estimated, and the step Δ (the distance between points 11 and 22, 22 and 31 on the abscissa) is fixed. For instance $v_{\text{CO}} = 0.28$; $v_{\text{H}_2} = 0.12$; $\Delta = 0.01$. We then obtain three values for x and two for y :

$$x_1 = 0.27 \quad x_2 = 0.28 \quad x_3 = 0.29 \quad y_1 = 0.115 \quad y_2 = 0.125$$

If v_{CO} and v_{H_2} are known, that is, fixed by this assumption, the values for v_{CO_2} , $v_{\text{H}_2\text{O}}$, and v_{CH_4} are obtained from the definition of the equations of equilibrium constants (equations I to III, page 48). The value of v_{N_2} is obtained from the nitrogen and oxygen balance as

$$v_{\text{N}_2} = \frac{N_M}{O_M} \cdot O_G \quad (249)$$

and we now can set up the calculation scheme presented in Table 14. The last column and the bottom line (check) would be disregarded at first. N₂ (last column of scheme) is now calculated from equation 249, and the sum of the gas constituents (CO + CO₂ + H₂ + H₂O + CH₄ + N₂) from which the φ values result, according to equation 121, by subtraction of 1.

From equations 157 to 158,

$$y = 0.115 + 0.01 \frac{-0.58515}{-1.09412} = 0.115 + 0.00535 = 0.12035$$

$$\begin{aligned} x &= 0.26 + 2 \times 0.01 \times 0.45594 + (1 - 2 \times 0.66071) \times 0.00535 \\ &= 0.26 + 0.00912 - 0.00172 = 0.26740 \end{aligned}$$

With these values of $x = v_{\text{CO}} = 0.26740$ and $y = v_{\text{H}_2} = 0.12035$, the final calculation (check) is now carried out (see last line of scheme, Table 14), and the result in this case is

$$\psi = -0.00008 \quad \text{instead of} \quad = 0$$

$$\varphi = -0.00013 \quad \text{instead of} \quad = 0$$

If the calculation had to be made with three figures to the right of the decimal point, the accuracy of the result would be sufficient.

TABLE 14
CALCULATION SCHEME (TRIANGLE METHOD)

$t = 700^{\circ}\text{C}$	$K'_{p_B} = 0.93226$	$K'_{p_W} = 0.60176$	$\frac{N_M}{O_M} = 2.50241$	
$\Delta = 0.01$	$x_M K_{p_M} = 0.24 \times 0.13237 = 0.031769$			
Point	v_{CO}	v^2_{CO}	v_{CO_2}	v_{H_2}
11	0.26	0.0676	0.06302	0.115
22	0.27	0.0729	0.06796	0.125
31	0.28	0.0784	0.07309	0.115
Check	0.26740	0.071503	0.06666	0.12035
$v_{\text{CO}} \cdot v_{\text{H}_2}$	$v_{\text{H}_2\text{O}}$	$v^2_{\text{H}_2}$	v_{CH_4}	v_{N_2}
0.02990	0.01799	0.013225	0.00042	0.50544
0.03375	0.02031	0.015625	0.00050	0.53331
0.03220	0.01938	0.013225	0.00042	0.55749
0.032182	0.01937	0.014484	0.00046	0.52563

Point	11	22	31	Check
	0.11500	0.12500	0.11500	0.12035
	0.01799	0.02031	0.01938	0.01937
	0.00084	0.00100	0.00084	0.00092
$H_G =$	0.13383	0.14631	0.13522	0.14064
	0.13000	0.13500	0.14000	0.13370
	0.06302	0.06796	0.07309	0.06666
	0.00900	0.01016	0.00969	0.00969
$O_G =$	0.20202	0.21312	0.22278	0.21005
$H_G/O_G =$	0.66246	0.68651	0.60697	0.66955
$H_M/O_M =$	0.66963	0.66963	0.66963	0.66963
$\psi =$	-0.00717	+0.01688	-0.06266	-0.00008
$\Sigma v =$	0.96197	1.01708	1.04538	0.99987
$\varphi =$	-0.03803	+0.01708	+0.04538	-0.00013

From equations 144 to 147,

$$\begin{aligned}
 A' &= \frac{+0.03803}{0.08341} = 0.45594 & B' &= \frac{0.05511}{0.08341} = 0.66071 \\
 C' &= \frac{+0.06266}{0.05549} = 1.12921 & D' &= \frac{0.07954}{0.05549} = 1.43341 \\
 A' + C' &= 1.58515 & B' + D' &= 2.09412
 \end{aligned}$$

If this agreement is not satisfactory, the step Δ can now be lessened, e.g., $\Delta = 0.001$, and new values estimated from the previous result. The calculation is repeated as follows:

$$\begin{aligned}x_1 &= 0.2664 & x_2 &= 0.2674 & x_3 &= 0.2684 \\y_1 &= 0.11985 & y_2 &= 0.12085\end{aligned}$$

The result of this calculation (details may be omitted) according to the same scheme is

$$\begin{aligned}x &= v_{\text{CO}} = 0.26743 & y &= v_{\text{H}_2} - 0.12038 \\ \psi &= -0.00009 & \varphi &= -0.00002\end{aligned}$$

This accuracy is sufficient, even if four figures beyond the decimal point are used, and the unknown gas analysis at 700°C can be found in Table 15, where the results of calculations for more

TABLE 15
CALCULATION SCHEME FOR THE HEAT BALANCE *

t_R °C =	650°	700°	750°	800°	900°
Gas composition	19.22 10.83 11.37 3.27 0.07 55.24 100.00	26.74 6.67 12.04 1.94 0.04 52.57 100.00	32.40 3.49 12.41 1.06 0.03 50.61 100.00	35.65 1.66 12.64 0.56 0.02 49.47 100.00	37.97 % CO 0.37 % CO ₂ 12.83 % H ₂ 0.17 % H ₂ O 0.01 % CH ₄ 48.65 % N ₂ 100.00 %
H_G	224.0	236.6	250.0	265.0	298.4 kcal/SCM
$H_{i,G}$	878.6	1120.4	1300.0	1403.2	1477.3 kcal/SCM
F	0.1614	0.1792	0.1925	0.2000	0.2055 kg/SCM
M	0.8471	0.8061	0.7760	0.7586	0.7460 SCM/SCM
H_C =	207.6	228.2	249.4	270.9	315.2 kcal/kg
$F \cdot H_C$ =	33.5	40.9	48.0	54.2	64.8 kcal/SCM
$M \cdot H_M$ = (- 18.5)	15.7	14.9	14.4	14.0	13.8 kcal/SCM
$F \cdot H_i$ = (7433.6)	1199.8	1332.1	1431.0	1486.7	1527.6 kcal/SCM
ΣQ (equation 227a)	370.4	267.5	193.4	151.7	128.9 kcal/SCM

* As a rule, three points are sufficient to draw a curve and obtain a graphical heat balance; however, more points help to recognize the true character of this curve. Besides, these values may be needed for calculations with higher preheat of the blast.

temperatures between 650 and 900°C are also reported, omitting all details of calculation. This gives a good picture of the dependence of gas analysis on the reaction temperatures. Besides

this, Table 15 contains all necessary data for obtaining a heat balance. The quantity of fuel per SCM of wet gas (F) is calculated from the carbon balance, and the quantity of gasifying agent (M) from the nitrogen balance. The enthalpy of carbon is given by the formula *

$$H_C = 0.209333t + 0.2024 \times 10^{-3}t^2 - 50.933 \times 10^{-9}t^3 \quad (250)$$

t = temperature °C, H_C = kcal/kg carbon
(fixed carbon of coal or coke)

The external heat loss of the reacting zones has been assumed to be 8% of the fuel input; therefore, the net heating value of the carbon is

$$H_{iC} = 0.92 \times 8080 = 7433.6 \text{ kcal/kg}$$

The graphical solution (see Figure 19) arrives at a reaction temperature of 713°C, and the gas analysis (calculated for this temperature) is indicated below, in Table 16.

TABLE 16
CALCULATED FINAL GAS COMPOSITION
($x_M = 0.24$; $t_R = 713^\circ\text{C}$)

Wet Gas	Dry Gas
28.45	28.93 % CO
5.71	5.81 % CO ₂
12.16	12.36 % H ₂
1.67	... % H ₂ O
0.04	0.04 % CH ₄
51.97	52.86 % N ₂
<hr/> 100.00	<hr/> 100.00 %

According to equations 45 to 48 the equilibrium constants are the following:

$$K'_{pB} = 0.70560 \quad K'_{pW} = 0.48194$$

$$x_M \cdot K_{pM} = 0.24 \times 0.11447 = 0.027473$$

* This curve fits the three points:

$t = 500^\circ\text{C}$ $H_C = 148.9$ kcal/kg, according to measurements of W. Fritz and H. Kneese, *Feuerungstechn.*, Vol. 30 (1942), No. 12, p. 275.

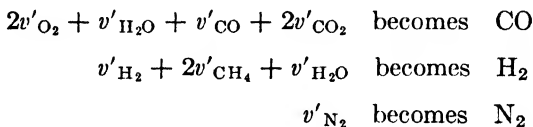
$t = 1000^\circ\text{C}$ $H_C = 360.8$ kcal/kg, according to Landolt-Bornstein, *Phys. Chem. Tab.*

$t = 1500^\circ\text{C}$ $H_C = 597.5$ kcal/kg, according to Landolt-Bornstein, *Phys. Chem. Tab.*

Since for the detailed presentation of this problem the same conditions of operation have been used as in Plenz' experiments, a comparison of calculation and measurement is possible (see Table 13, page 85).

General calculation rules

The calculations are carried out mainly in a series of three or more temperatures. The highest temperature is recommended as the starting temperature because the estimation is much easier and the complete reduction gives a clue to a reasonable assumption. A complete reduction (at temperatures above 1000°C) means that



In the preceding sample calculation, for instance,

$$\begin{aligned} 2 \times 0.17335 + 0.17451 &= 0.52121 = 38.67 \% \text{ CO} \\ 0.17451 &= 12.95 \% \text{ H}_2 \\ 0.65214 &= 43.38 \% \text{ N}_2 \\ \hline 1.34786 &= 100.00 \% \end{aligned}$$

At a temperature less than 1000°C the CO and H₂ values to be estimated must be below the above maximum value. The extrapolation into the lower temperature range is made fairly well by plotting the results for every temperature. We must bear in mind that the curve of hydrogen content is initially very flat with decreasing temperature and the curve of carbon monoxide somewhat steeper.

If a series of calculations has to be made for the same temperature (and pressure) but different composition of the blast, the CO and H₂ content changes proportionately with the values of complete reduction. After computation of one gas analysis all other first estimations can be made correctly by means of CO_{max} and H_{2 max} ratios.

If CO and H₂ values are located outside the triangle 11-22-31 or even very near the edge, decreasing the step Δ would make the next initial evaluation uncertain again. In such a case it is recommended that the calculation be repeated with unchanged step Δ,

but with a more suitable arrangement of the points of the triangle. Frequently, a sufficient accuracy is then realized in the result.

In a few cases the numerical calculation may fail, namely, if $(B' + D')$ in equation 157 = 1 or is slightly larger than 1. Then, if $(A' + C') > (B' + D')$, the expression $\frac{1 - (A' + C')}{1 - (B' + D')}$ is indefinite or a very big number. By a slight change of the first estimation or by using a different calculation method, this difficulty can be avoided.

Newton's approximation method

In order to have a means of comparison between the two methods, the same numerical example as before is chosen:

$$H_M = 0.17451$$

$$O_M = 0.26061$$

$$N_M = 0.65214$$

$$H_M/O_M = 0.66963$$

$$0.5(H_M/O_M) = 0.33482$$

$$N_M/O_M = 2.50241$$

$$0.5(N_M/O_M) = 1.25120$$

$$1 - 0.5(H_M/O_M) = 0.66518$$

$$1 + 0.5(N_M/O_M) = 2.25120$$

$$1 + (N_M/O_M) = 3.50241$$

The following value pair is now estimated:

$$x = v_{CO} = 0.27; \quad y = v_{H_2} = 0.12$$

At $t = 700^\circ\text{C}$, $P = 1 \text{ Atm}$,

$$K'_{pB} = 0.93226; \quad K'_{pW} = 0.60176; \quad x_M K_{pM} = 0.24 \times 0.13237 = 0.031769$$

From equation 186,

$$\varphi = 2.25120 \times 0.27 = 0.60782$$

$$+ 3.50241 \times \underbrace{0.0729 \times 0.93226}_{0.067962} = 0.23803$$

$$+ 0.12 = 0.12000$$

$$+ 2.25120 \times \underbrace{0.27 \times 0.12 \times 0.60176}_{0.019497} = 0.04389$$

$$\begin{array}{rcl}
 + \underbrace{0.0144 \times 0.031769} & = & 0.00046 \\
 0.0004575 & & 1.01020 \\
 - 1 & & -1.00000 \\
 \hline
 \end{array}$$

According to equation 187, $\varphi = +0.01020$

$$\begin{array}{rcl}
 \varphi'_x = & & 2.25120 \\
 + 3.50241 \times 2 \times \underbrace{0.27 \times 0.93226} & = & 1.76318 \\
 0.50342 & & \\
 + 2.25120 \times \underbrace{0.12 \times 0.60176} & = & 0.16256 \\
 0.072211 & & \\
 \varphi'_x = & + & 4.17694
 \end{array}$$

From equation 188,

$$\begin{array}{rcl}
 \varphi'_y = & & 1.00000 \\
 + 2.25120 \times \underbrace{0.27 \times 0.60176} & = & 0.36576 \\
 0.162475 & & \\
 + 2 \times \underbrace{0.12 \times 0.031769} & = & 0.00762 \\
 0.0076246 & & \\
 \varphi'_y = & + & 1.37338
 \end{array}$$

From equation 189,

$$\begin{array}{rcl}
 \psi = & & 0.12000 \\
 + 0.66518 \times 0.019497 & = & 0.01297 \\
 + 2 \times 0.0004575 & = & 0.00092 \\
 & & \hline
 & & +0.13389 \\
 - 0.33482 \times 0.27 & = & -0.09040 \\
 - 0.66963 \times 0.067962 & = & -0.04551 \\
 & & \hline
 & -0.13591 & -0.13591 \\
 & & \hline
 \end{array}$$

From equation 190, $\psi = -0.00202$

$$\begin{array}{rcl}
 \psi'_x = 0.66518 \times 0.072211 & = & +0.04803 \\
 - 0.33482 & = & -0.33482 \\
 - 0.66963 \times 0.50342 & = & -0.33711 \\
 & & \hline
 \psi'_x = & - & 0.62390
 \end{array}$$

94 GAS COMPOSITION AT INCOMPLETE EQUILIBRIUM

From equation 191,

$$\begin{array}{rcl}
 \psi'_y = 1 & & = 1.00000 \\
 +0.66518 \times 0.162475 & & = +0.10808 \\
 +2 \times 0.0076246 & & = +0.01525 \\
 & & \hline
 \psi'_y = +1.12333
 \end{array}$$

Note the repeated occurrence of expressions in ψ as in φ , in ψ'_x as in φ'_x , and in ψ'_y as in φ'_y .

According to equations 180 and 181,

$$\begin{aligned}
 x_0 - x &= \frac{\psi\varphi'_y - \varphi\psi'_y}{\varphi'_x\psi'_y - \varphi'_y\psi'_x} \\
 &= \frac{-0.00202 \times 1.37338 - 0.01020 \times 1.12333}{4.17694 \times 1.12333 + 0.62390 \times 1.37338} \\
 &= \frac{-0.014232}{5.548934} = -0.00256
 \end{aligned}$$

$$x = 0.27 - 0.00256 = 0.26744$$

$$\begin{aligned}
 y_0 - y &= \frac{\varphi\psi'_x - \psi\varphi'_x}{\varphi'_x\psi'_y - \varphi'_y\psi'_x} \\
 &= \frac{-0.01020 \times 0.62390 + 0.00202 \times 4.17694}{5.548934} \\
 &= \frac{+0.0020736}{5.548934} = +0.00037
 \end{aligned}$$

$$y = 0.12 + 0.00037 = 0.12037$$

Repeating the calculation results in φ and ψ values ≤ 0.00004 , or 26.74% CO, 12.04% H₂ in full agreement with the triangle method.

For the numerical solution it is recommended that the computer write down the entire calculation scheme—if possible, the ψ values by the side of the φ values—and then proceed with the multiplication. This is of advantage because the same multiplicands occur several times, and, with one multiplicand setting of the calculating machine, several multiplications may be carried out.

Another decisive advantage of this method is the fact that subsequent series of computations with improved x and y values can be calculated in an abbreviated form. Small adjustments of x and y do not influence ϕ'_x , ϕ'_y , ψ'_x , ψ'_y very much; repeated calculations, therefore, may be limited to ϕ , ψ , $x_0 - x$, and $y_0 - y$. Thus this method is considerably faster than the triangle method.

This method is specially recommended for calculations of gasification processes with pure steam or steam-oxygen mixtures, where the whole scheme is considerably simplified.

4

OTHER CALCULATION METHODS

Calculations based on the gas analysis

If a gas having a given ratio of two components is to be produced, it is preferable to calculate the feed requirements by proceeding backwards from the given product composition, rather than attempting to arrive at the proper feed by assuming a feed composition and determining whether or not it will yield the desired product gas. In some cases the calculation is simplified considerably by choosing as a basis the production of 1 SCM of gas. We calculate the amount of blast and its composition by means of hydrogen and oxygen balances, and the fuel (which is assumed to be carbon) by the carbon balance. Finally the heat balance is used to find the correct reaction temperature, the calculation being repeated for at least three temperatures. Examples of this type of problem are the following.

(1) Hydrocarbon synthesis. The Fischer-Tropsch process¹ using a cobalt catalyst requires a synthesis gas with a ratio of $H_2/CO = 2$, as high a $(CO + H_2)$ content as possible, and as low a sulfur content as possible ($S \leq 2$ mg/SCM).

(2) Reduction of iron ores in a shaft furnace according to Wiberg's process² requires a reducing gas with a CO/H_2 ratio of 4, and CO_2 , H_2O , and sulfur as low as possible. About 60 to 70% of the spent gas is recycled.

(3) Ammonia synthesis requires a gas having a H_2/N_2 ratio of 3, prepared either by mixing water gas and producer gas or

¹ B. H. Weil and J. C. Lane, *Synthetic Petroleum from the Synthine Process*, Brooklyn, N. Y., 1948.

² Martin Wiberg, A new method for the production of iron sponge, *Trans. Am. Electrochem. Soc.*, Vol. 51 (1927), pp. 279-304. Einer Améen, Framställning av järnsvamp i Söderfors enligt Wiberg-metoden, *Jernkont. Ann.*, Vol. 127 (1943), p. 227. Einer Améen, Swedish sponge iron, *Iron Age*, Vol. 153 (1944), No. 3, pp. 55-59, 150; No. 4, pp. 56-65.

by gasification with oxygen-enriched air and steam, followed by water gas shift reaction and purification.

(1) If a CO/H_2 ratio of ε is desired, the equilibrium gas composition is calculated from equations I, II, III, page 48, equation 238, and

$$v_{\text{CO}} = \varepsilon v_{\text{H}_2} \quad (251)$$

$$v_{\text{CO}_2} = v_{\text{CO}}^2 K'_{pB} = \varepsilon^2 v_{\text{H}_2}^2 K'_{pB} \quad (252)$$

$$v_{\text{H}_2\text{O}} = v_{\text{CO}} v_{\text{H}_2} K'_{pW} = \varepsilon v_{\text{H}_2}^2 K'_{pW} \quad (253)$$

$$v_{\text{CH}_4} = v_{\text{H}_2}^2 x_M K_{pM} \quad (254)$$

$$v_{\text{CO}} + v_{\text{CO}_2} + v_{\text{H}_2} + v_{\text{H}_2\text{O}} + v_{\text{CH}_4} = 1 \quad (255)$$

Express all constituents in terms of v_{H_2} , substitute in equation 255, and solve for v_{H_2} . Equations 251 to 254 will give the concentrations of the other gas components.

$$\varepsilon v_{\text{H}_2} + \varepsilon^2 v_{\text{H}_2}^2 K'_{pB} + v_{\text{H}_2} + \varepsilon v_{\text{H}_2}^2 K'_{pW} + v_{\text{H}_2}^2 x_M K_{pM} = 1 \quad (255a)$$

$$v_{\text{H}_2} = -a + \sqrt{a^2 + b} \quad (256)$$

$$b = \frac{1}{\varepsilon^2 K'_{pB} + \varepsilon K'_{pW} + x_M K_{pM}} \quad (257)$$

$$a = \frac{1 + \varepsilon}{2} b \quad (258)$$

The blast is presumed to be a mixture of oxygen (v'_{O_2}) and steam ($v'_{\text{H}_2\text{O}}$). Other constituents could easily be considered, e.g., v'_{CO_2} or v'_{N_2} , as an impurity of the oxygen used and therefore in a fixed ratio to v'_{O_2} . From the hydrogen and oxygen balances the gasifying agent, M , is found as follows.

$$M v'_{\text{H}_2\text{O}} = v_{\text{H}_2} + v_{\text{H}_2\text{O}} + 2v_{\text{CH}_4} \quad (\text{hydrogen balance}) \quad (259)$$

$$v'_{\text{H}_2\text{O}} = \frac{v_{\text{H}_2} + v_{\text{H}_2\text{O}} + 2v_{\text{CH}_4}}{M} \quad (260)$$

$$v'_{\text{O}_2} = 1 - v'_{\text{H}_2\text{O}} \quad (261)$$

$$M(v'_{\text{O}_2} + 0.5v'_{\text{H}_2\text{O}}) = v_{\text{CO}_2} + 0.5v_{\text{CO}} + 0.5v_{\text{H}_2\text{O}} \quad (\text{oxygen balance}) \quad (262)$$

$$M(1 - v'_{\text{H}_2\text{O}} + 0.5v'_{\text{H}_2\text{O}}) = v_{\text{CO}_2} + 0.5v_{\text{CO}} + 0.5v_{\text{H}_2\text{O}} \quad (262a)$$

$$M - 0.5(v_{\text{H}_2} + v_{\text{H}_2\text{O}} + 2v_{\text{CH}_4}) = v_{\text{CO}_2} + 0.5v_{\text{CO}} + 0.5v_{\text{H}_2\text{O}} \quad (262b)$$

$$M = v_{\text{CO}_2} + 0.5(v_{\text{CO}} + v_{\text{H}_2}) + v_{\text{H}_2\text{O}} + v_{\text{CH}_4} \quad (263)$$

$$F = 0.5358(v_{\text{CO}_2} + v_{\text{CO}} + v_{\text{CH}_4}) \quad (102)$$

v'_{O_2} and $v'_{\text{H}_2\text{O}}$ are found by using the hydrogen balance, equation 260. By assuming three different temperatures the heat balance is examined graphically to arrive at a solution which satisfies the material balances as well as the heat balance.

(2) As a somewhat more complicated case the production of a reduction gas for a Wiberg shaft furnace will be discussed in a sample calculation. A certain reaction temperature is fixed as lower limit in order to obtain a gas with low CO_2 content ($t_R = 900^\circ\text{C}$), $\epsilon = \text{CO}/\text{H}_2 = 4$, and gas of the following composition (after knocking out moisture by condensation) is recycled:

$$\begin{array}{r} 20.5 \% \text{ CO}_2 \\ 61.5 \% \text{ CO} \\ 18.0 \% \text{ H}_2 \\ \hline 100.0 \% \end{array}$$

Neglect the recycle gas at first and obtain:

From equation 257:

$$b = \frac{1}{16 \times 0.025896 + 4 \times 0.034286 + 0.00476} = 1.7978$$

From equation 258: $a = 2.5 \times 1.7978 = 4.4945$

From equation 256:

$$v_{\text{H}_2} = -4.4945 + \sqrt{20.2004 + 1.7978} = 0.19572$$

From equation 251: $v_{\text{CO}} = 4 \times 0.19572 = 0.78288$

From equation 252: $v_{\text{CO}_2} = 0.61290 \times 0.025896 = 0.01587$

From equation 253:

$$v_{\text{H}_2\text{O}} = 0.78288 \times 0.19572 \times 0.034286 = 0.00525$$

From equation 254, with $X_M = 0.24$:

$$v_{\text{CH}_4} = 0.038298 \times 0.00476 = 2.00018$$

From equation 263: $M = 0.51060 \text{ SCM/SCM}$

From equation 260: $v'_{\text{H}_2\text{O}} = \frac{0.20112}{0.51060} = 0.3939$

From equation 261: $v'_{O_2} = 1 - 0.3939 = 0.6061$

$$O_M = 0.6061 + 0.1970 = 0.8031$$

$$H_M = 0.3939$$

$$\frac{O_M}{H_M} = 2.0388$$

A blast of 60.61% O_2 + 39.39% H_2O would result in extremely high and impractical temperatures. Besides, a main object of the process is the recycling and reducing of as much gas as possible.

We have fixed the reaction temperature and will adjust the heat balance by a proper choice of the amount of gas recycled and of steam added. Therefore we assume different ratios of v'_{H_2O} to recycle gas, calculate H_M , and add the necessary amount of oxygen to have a O_M/H_M ratio as calculated above. This gives us, by recalculating for the basis 100%, the composition of the blast which fits all material balances. By a complete heat balance (at 900°C) we find the H_2O /recycle ratio and hence the blast analysis, which also satisfies the heat balance.

Assuming 30% H_2O and 70% recycle gas (composition as given above), we have:

$$0.30 \quad H_2O$$

$$0.70 \times 0.205 = 0.1435 \text{ CO}_2$$

$$0.70 \times 0.615 = 0.4305 \text{ CO}$$

$$0.70 \times 0.18 = 0.1260 \text{ H}_2$$

$$\Sigma H_M = 0.4260$$

$$O_M = 2.0388 \times 0.426 = 0.86853$$

Part of this oxygen is delivered by the CO_2 and CO in the recycle gas, and the H_2O added; this part amounts to

	0.50875	
There remains	0.35978	to be supplied as O_2 .
	0.86853	

The final blast analysis, therefore, is given in the second column of the following tabulation.

Steam Recycle gas	25 75	30 70	35 65	40 60
	36.16	31.66	27.68	24.15 % CO
	12.06	10.55	9.23	8.05 % CO ₂
	10.58	9.27	8.10	7.07 % H ₂
	19.60	22.06	24.24	26.17 % H ₂ O
	21.60	26.46	30.75	34.56 % O ₂
	100.00	100.00	100.00	100.00 %
$H_{i,M}$	1363.9	1194.4	1044.1	911.0 kcal/SCM
M^*	0.6673	0.6478	0.6228	0.6059 SCM/SCM
$F =$	0.5358($C_G - MC_M$)			
$=$	0.2557	0.2827	0.3049	0.3236 kg/SCM

* By hydrogen balance.

Calculating the heat balance [$(Q_{ext} = 6\%)$, average preheating of the blast (recycle gas + steam + oxygen) to 50°C (no preheat), 400, 600, 800°C] results in the following H₂O/recycle gas ratios for which blast composition, M , F , and O₂ consumption are calculated in the same way.

$t_M =$	800°C	600°	400°	50° (no preheat)
$\frac{v'_{H_2O}}{v \text{ recycle}}$	0.28	0.328	0.375	0.45
	0.72	0.672	0.625	0.55
	33.39	29.38	25.87	20.98 % CO
	11.13	9.79	8.62	6.99 % CO ₂
	9.78	8.60	7.57	6.14 % H ₂
	21.11	23.31	25.23	27.91 % H ₂ O
	24.59	28.92	32.71	37.98 % O ₂
	100.00	100.00	100.00	100.00 %
$M =$	0.6520	0.6312	0.6140	0.5915 SCM/SCM
$F =$	0.2726	0.2957	0.3146	0.3395 kg/SCM
O ₂ consumption	0.1603	0.1825	0.2009	0.2246 SCM/SCM
Steam consumption	0.1107	0.1183	0.1246	0.1327 kg/SCM

A certain excess of recycle gas is available (rising amount with falling preheat temperature) which may be used to raise the gas temperature entering the shaft furnace.

(3) Ammonia synthesis gas calculation cannot be simplified to the same degree as in the two previous examples because $\epsilon = N_2/H_2 = 0.333 \dots$ leaves the two unknowns of the gas analysis v_{H_2} and v_{CO} . We therefore proceed in the same way as described on pages 50 to 62, using either the triangle method or the Newtonian approximation.

Assume v_{CO} and v_{H_2} and calculate the other gas components as well as φ (according to equation 121, page 51). Calculate M from equation 263, which in this case (including nitrogen) reads:

$$M = v_{CO_2} + 0.5(v_{CO} + v_{H_2}) + v_{H_2O} + v_{CH_4} + v_{N_2} \quad (264)$$

(v'_{H_2O} is from equation 260.)

$$v'_{N_2} = \frac{v_{N_2}}{M} \quad (265) *$$

$$v'_{O_2} = 1 - v'_{N_2} - v'_{H_2O} \quad (266)$$

$$\psi = \frac{N_M}{H_M} - \frac{N_G}{H_G} = 0 \quad (267)$$

$$\psi = \frac{v'_{N_2}}{v'_{H_2O}} - \frac{v_{N_2}}{v_{H_2} + v_{H_2O} + 2v_{CH_4}} = 0 \quad (267a)$$

With $\varphi \neq 0$; $\psi \neq 0$, improved estimates are made and the calculation is repeated until satisfactory small differences are reached. The heat balance is made in the usual way.

If an oxygen-air mixture is used to produce the synthesis gas directly from carbon (coke), the amounts of oxygen and air are determined as follows:

Oxygen from the air $\frac{21}{79} \times v'_{N_2}$, hence

$$\text{air} = 1.2658v'_{N_2} \quad (268)$$

$$\text{oxygen} = v'_{O_2} - 0.2658v'_{N_2} \quad (269)$$

If the oxygen itself has some nitrogen content as impurity and its purity is x or $100x\%$, the amount of impure oxygen will be:

$$O_{2(\text{impure})} = \frac{v'_{O_2} - 0.2658v'_{N_2}}{0.7342 + 0.2658x} \quad (270)$$

$$\text{air} = (v'_{O_2} - xO_{2(\text{impure})})4.7619 \quad (271)$$

* Pure carbon assumed as fuel, N_2 content of fuel neglected.

Other solutions proposed

The calculation methods described so far are based partly on Traustel's work (triangle method, Newtonian approximation method), partly on the author's previous work, and partly on a paper published in cooperation with Traustel.* Other methods, entirely independent of these papers, have been proposed but they have not been referred to here because they either offer no advantage over the methods discussed or they postulate a greater knowledge of mathematics than the methods presented.

Schlaepfer and Tobler³ were the first to publish calculation results of a theoretical investigation of portable gas producers using wood fuel, but they did not disclose all the details of their methods of computation.

Starting with Schlaepfer and Tobler's work, Hubendick and co-workers⁴ published a complete and improved derivation as a method of their own. For good reason they criticized Schlaepfer and Tobler's assumption of a given equilibrium temperature and the statement that there would be only little difference between 700 and 1000°C (*sic!*). Traustel's work was not mentioned although the authors have presented a brief sketch of the development of gas producer theory. Hubendick and co-workers neglected methane formation for the sake of simplification and used the following six basic equations: carbon, hydrogen, oxygen, and heat balance, the homogeneous water-gas equilibrium, and the producer gas (Boudouard) equilibrium. The computation is made on molar quantities, the moisture added by the blast is expressed in kilograms per kilogram of combustible matter of the fuel. The two assumptions made are the reaction temperature and the sum of the mole numbers of the product gas. These are later corrected by trial and error methods until the result satisfies the equations.

* See footnote 1, page 76.

³ P. Schlaepfer und T. Tobler, *Theoretische und praktische Untersuchungen über den Betrieb von Motorfahrzeugen mit Holzgas*, Bern, Switzerland, 1937.

⁴ E. Hubendick, Stig Olsson, and Sven Axelson, Gasgenererings teori, *Teknisk Tidskr.*, Vol. 72 (1942); *Automobil och Motorteknik*, No. 10, pp. 73-80, No. 11, pp. 81-88. E. Hubendick and T. B. Lundström, Gasgenererings teori II, Kolgasförfarandet, *Teknisk Tidskr.*, Vol. 74 (1944), pp. 741-746. E. Hubendick and K. A. Löfroth, Gasgenererings teori III, Kålleförfarandet, *Teknisk Tidskr.*, Vol. 74 (1944), pp. 1073-1078. E. Hubendick, Gasgenererings teori IV, Vedgasförfarandet, *Teknisk Tidskr.*, Vol. 75 (1945), pp. 321-326.

Entirely different ways to deal with the equilibrium composition of a system with several constituents are proposed by Brinkley,⁵ who uses matrix methods. Many mechanical engineers and chemists are unfamiliar with these methods, but they might find them of special merit for machine computation. These computational details, however, cannot be considered within the scope of this book.*

Other "theories," the authors of which dispose of equilibrium conditions, need no further attention.⁶ Prettre and Magat⁷ ventured upon a calculatory attack on reaction kinetics. (See also Chapter 10, page 275.) In spite of their claim of satisfactory agreement with practical results a number of their basic assumptions are problematical, such as the settling of CO₂ and CO formation in the combustion zone, the extrapolation of Mayers' formula,⁸ and its application to entirely different physical operating conditions, neglecting the difference between Mayers' experimental device and actual performance conditions, etc. It seems

⁵ Stuart R. Brinkley, Jr., Note on the conditions of equilibrium for systems of many constituents, *J. Chem. Physics*, Vol. 14 (1946), No. 9, pp. 563-564. Calculation of the equilibrium composition of systems of many constituents, *J. Chem. Physics*, Vol. 15 (1947), No. 2, pp. 107-110.

* After work on this manuscript had been completed, Harold J. Kandiner and Stuart R. Brinkley, Jr., issued a paper, *A Systematic Method for Calculating Complex Equilibrium Relationships* (read at the fall meeting of the American Chemical Society, Atlantic City, N. J., September, 1949), which presents a more detailed outline of the Brinkley method. Three different solutions of the working equations (material balances, equilibrium constant definitions, Dalton's law) are discussed: the simple iteration method, a modified iteration method, and the Newton-Raphson method. Only the last mentioned is generally applicable to most of the gasification problems. The main difference as compared with the methods used in this book is the start from more than two assumed values ("primary unknowns"), e.g., four in their sample calculation, in order to ease subsequent evaluation of the remaining ("secondary") unknowns. The total time for setting up the equations and for the calculatory work is not less than in the methods presented here, as far as can be judged from this paper.

⁶ Fernand Denis, *Théorie du gazogène*, *Rev. univ. mines*, Vol. VIII, Ser. 18 (1942), No. 8, pp. 353-363.

⁷ Marcel Prettre and Michel Magat, A kinetic theory for air-producer-gas formation, *J. Inst. Fuel*, Vol. 21 (1947), No. 116, pp. 35-43.

⁸ Martin A. Mayers, The rate of reduction of carbon dioxide by graphite, *J. Am. Chem. Soc.*, Vol. 56 (1934), pp. 70-76.

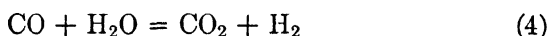
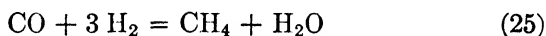
sufficient to predict the overall performance of a gas producer within certain limits of accuracy. The attempt to reproduce the whole temperature and concentration field (at any point within the producer) is a daring enterprise which must fail because of the need of making too many unsubstantiated assumptions, although it would be of great scientific interest.

5

APPLICATIONS OF THE SEMIGRAPHICAL METHOD FOR ASSOCIATED PROBLEMS

Methanization

Besides gasification the semigraphical method offers a convenient solution for some associated problems. Consider the methanization of a water gas as a process to increase the heating value. The two main reactions upon which the calculation is based are:



If

α_1 = the factor of conversion of CO into CH_4

α_2 = the factor of conversion of CO into CO_2

v'_{CO} = CO content (volume %) of the fresh feed

v'_{H_2} = H_2 content (volume %) of the fresh feed

the total gas composition will be

$$\begin{aligned} \Sigma = & \underbrace{(1 - \alpha_1 - \alpha_2)v'_{\text{CO}}}_{\text{CO}} + \underbrace{\alpha_2 v'_{\text{CO}}}_{\text{CO}_2} + \underbrace{v_{\text{H}_2} + \alpha_2 v'_{\text{CO}} - 3\alpha_1 v'_{\text{CO}}}_{\text{H}_2} \\ & + \underbrace{\alpha_1 v'_{\text{CO}} - \alpha_2 v'_{\text{CO}}}_{\text{H}_2\text{O}} + \underbrace{\alpha_1 v'_{\text{CO}}}_{\text{CH}_4} \quad (272) \end{aligned}$$

The equilibrium constant of the water-gas shift reaction is

$$K_W = \frac{v_{\text{CO}} v_{\text{H}_2\text{O}}}{v_{\text{CO}_2} v_{\text{H}_2}} \quad (16)$$

and, by inserting the gas constituent according to equation 272, after canceling v'_{CO} ,

$$K_W = \frac{(1 - \alpha_1 - \alpha_2)(\alpha_1 - \alpha_2)}{\alpha_2 \left(\frac{v'_{\text{H}_2}}{v'_{\text{CO}}} + \alpha_2 - 3\alpha_1 \right)}$$

$$= \frac{\alpha_1 - \alpha_1^2 - \alpha_1\alpha_2 - \alpha_2 + \alpha_1\alpha_2 + \alpha_2^2}{\frac{v'_{\text{H}_2}}{v'_{\text{CO}}} \alpha_2 + \alpha_2^2 - 3\alpha_1\alpha_2} \quad (273)$$

$$\alpha_2^2(1 - K_W) - \alpha_2 \left(1 + K_W \frac{v'_{\text{H}_2\text{O}}}{v'_{\text{CO}}} - 3K_W\alpha_1 \right) + \alpha_1 - \alpha_1^2 = 0 \quad (274)$$

$$\alpha_2^2 - \alpha_2 \left[\frac{1 + K_W \frac{v'_{\text{H}_2}}{v'_{\text{CO}}} - 3K_W\alpha_1}{1 - K_W} \right] + \frac{\alpha_1 - \alpha_1^2}{1 - K_W} = 0 \quad (275)$$

$$\alpha_2 = \frac{a}{2} - \sqrt{(a/2)^2 - b} \quad (276)$$

$$a = \frac{1 + K_W \frac{v'_{\text{H}_2}}{v'_{\text{CO}}} - 3K_W\alpha_1}{1 - K_W} \quad (277)$$

$$b = \frac{\alpha_1 - \alpha_1^2}{1 - K_W} \quad (278)$$

Assume α_1 , and calculate α_2 according to equations 276 to 278; hence

$$v_{\text{CH}_4} = \alpha_1 \quad (279)$$

$$v_{\text{CO}} = 1 - \alpha_1 - \alpha_2 \quad (280)$$

$$v_{\text{CO}_2} = \alpha_2 \quad (281)$$

$$v_{\text{H}_2} = (v'_{\text{H}_2}/v'_{\text{CO}}) + \alpha_2 - 3\alpha_1 \quad (282)$$

$$v_{\text{H}_2\text{O}} = \alpha_1 - \alpha_2 \quad (283)$$

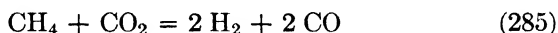
From these values the quotient

$$\Pi = \frac{v_{\text{CH}_4} v_{\text{H}_2\text{O}}}{v_{\text{CO}} (v_{\text{H}_2})^3} = P^2 K_{p_{28}} \quad (284)$$

is calculated and compared with the right side of equation 284. With three assumptions for α_1 , three values of Π are found, and this curve will intersect $P^2K_{p_{25}}$ in the desired α_1 value. Equations 279 to 283 yield the final gas composition after conversion to the basis $\Sigma v = 1$.

Reforming of methane

If methane (or natural gas) is reformed to deliver a gas, consisting mainly of CO and H_2 with a certain CO/ H_2 ratio, for which CO_2 has to be provided by recycling or any other means, the same method may be applied. Starting from the two main reactions,



with

α_1 = the factor of conversion of CH_4 to $CO + H_2$

α_2 = the factor of conversion of H_2 to CO

v'_{CH_4} = CH_4 content (volume %) of the feed gas

v'_{CO_2} = CO_2 content (volume %) of the feed gas

$$\begin{aligned} \Sigma = & \underbrace{(1 - \alpha_1)v'_{CH_4}}_{CH_4} + \underbrace{v'_{CO_2} - \alpha_1 v'_{CH_4} - 2\alpha_1\alpha_2 v'_{CH_4}}_{CO_2} \\ & + \underbrace{2\alpha_1 v'_{CH_4} + 2\alpha_1\alpha_2 v'_{CH_4}}_{CO} + \underbrace{(1 - \alpha_2)2\alpha_1 v'_{CH_4}}_{H_2} \\ & + \underbrace{2\alpha_1\alpha_2 v'_{CH_4}}_{H_2O} \end{aligned} \quad (287)$$

Assume again α_1 ; hence α_2 derived from the water-gas shift reaction equilibrium constant is

$$\alpha_2 = -\frac{a}{2} \pm \sqrt{(a/2)^2 + b} \quad (288)$$

$$a = \frac{2\alpha_1^2 \left(1 - K_W \left[1 + \frac{v'_{CO_2}}{v'_{CH_4}} \right] \right)}{4\alpha_1^2(1 - K_W)} \quad (289)$$

$$b = \frac{K_W \left(2\alpha_1^2 - 2\alpha_1 \frac{v'_{CO_2}}{v'_{CH_4}} \right)}{4\alpha_1^2(1 - K_W)} \quad (290)$$

108 SEMIGRAPHICAL METHOD FOR ASSOCIATED PROBLEMS

To reach a certain CO/H₂ ratio (see the problem of producing reduction gases for shaft furnaces, page 98), repeat the calculation for the temperature chosen (e.g., 1500°C if thermal reforming, or less if catalytic reforming is planned) for different α_1 values (which are nearly 1.0 in the case of thermal reforming).

The choice of α_1 is checked by three estimated values. Calculate the gas composition from

$$v_{\text{CH}_4} = (1 - \alpha_1) \quad (291)$$

$$v_{\text{CO}_2} = \frac{v'_{\text{CO}_2}}{v'_{\text{CH}_4}} - \alpha_1 - 2\alpha_1\alpha_2 \quad (292)$$

$$v_{\text{CO}} = 2\alpha_1 + 2\alpha_1\alpha_2 \quad (293)$$

$$v_{\text{H}_2} = (1 - \alpha_2)2\alpha_1 \quad (294)$$

$$v_{\text{H}_2\text{O}} = 2\alpha_1\alpha_2 \quad (295)$$

$$\Pi = \frac{v_{\text{H}_2}^2 v_{\text{CO}}^2}{v_{\text{CH}_4} v_{\text{CO}_2}} = P^{-2} K_{pM(288)} \quad (296)$$

By varying the $v'_{\text{CO}_2}/v'_{\text{CH}_4}$ ratio the gas analysis of the desired CO/H₂ ratio can be picked out and the necessary feed gas composition be determined.

6

MATHEMATICAL TREATMENT OF GAS-PRODUCER PERFORMANCE

Influence of the moisture content of the gasifying agent

The previously described methods of calculation permit the mathematical investigation of the performance of gas producers. Many problems of gas making can actually be solved by calculation. Of the many problems a few of special interest may be selected.

The effect of steam in the air blast is well known from various experimental programs and publications.¹⁻³

The result of the computation is in excellent agreement with the results of the experiments, which at times were painstaking

¹ William Arthur Bone and Richard Vernon Wheeler, The use of steam in gas producer practice, *Engineering*, Vol. 83 (1907), pp. 639-659, 664. Further experiments upon gas producer practice, *Engineering*, Vol. 86 (1908), pp. 837-838, 874-876.

² Arnold Hartley Gibson and Reginald Duncan Gwyther, The effect of varying degree of saturation of the air-supply to a suction-gas producer, *Minutes of Proc. Inst. Civil Eng.*, Vol. CLXXVII (1909), pp. 264-283.

³ E. A. Allcut, The effect of varying proportions of air and steam on a gas-producer, *Proc. Inst. Mech. Eng.* (1911), Part 1-2, pp. 349-397.

⁴ Kurt Neumann, Die Vorgänge im Gasgenerator auf Grund des zweiten Hauptsatzes der Thermodynamik, *Forsch. Ing. Wes.*, No. 140, Berlin, 1913. *Z. VDI*, Vol. 57 (1913), No. 8, pp. 291-298, No. 9, pp. 338-342.

⁵ R. V. Wheeler, Producer-gas and gas-producer practice, II, *Fuel Sci.*, Vol. 2 (1923), No. 4, pp. 106-110.

⁶ R. T. Haslam, I. T. Ward, and R. F. Mackie, Reactions in the fuel bed of a gas producer, III, Effects of steam-coal ratio, *Ind. Eng. Chem.*, Vol. 19 (1927), No. 1, pp. 141-144.

⁷ M. Fulda and G. Gehlhoff, Ueber den Einfluss der Betriebsbedingungen auf die Erzeugung von Generatorgas, *Glastechn. Ber.*, Vol. 10 (1932), No. 3, pp. 131-149.

⁸ H. Wohlschläger, Untersuchungen an Schwachgaserzeugern, *Feuerungstechn.*, Vol. 26 (1938), No. 4, pp. 102-106.

and time consuming. The advantages and limitations of steam addition to the blast are shown clearly from the results tabulated in Table 18 and presented in Figures 20 and 21. Throughout Tables

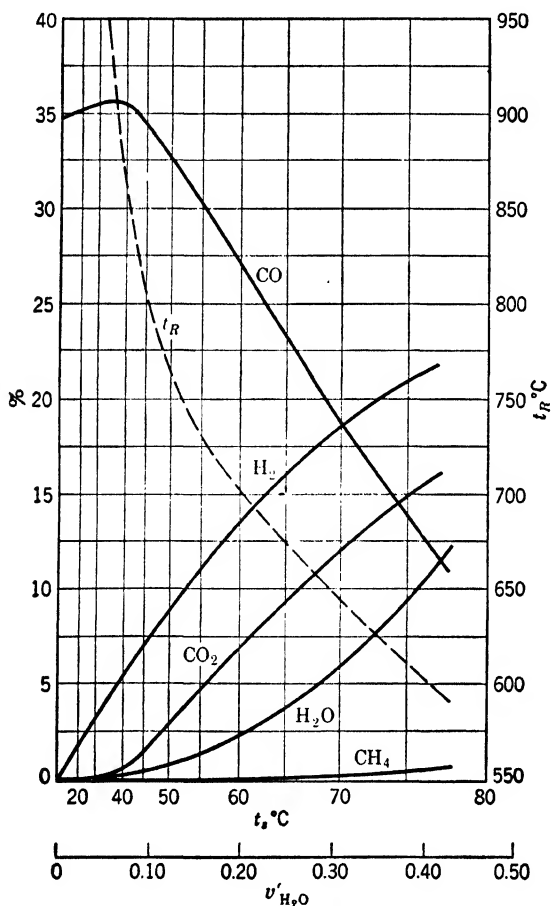


FIG. 20. Gas components and reaction temperature (t_R) as a function of the moisture content of the blast (v'_{H_2O}) or the saturation temperature of the blast (t_s). (Gasification of carbon.)

17 and 18 the fuel is assumed to be pure carbon, the external heat loss 8%.

However, it is not only the heating value which characterizes the efficiency of a gasification process but the gas yield multiplied

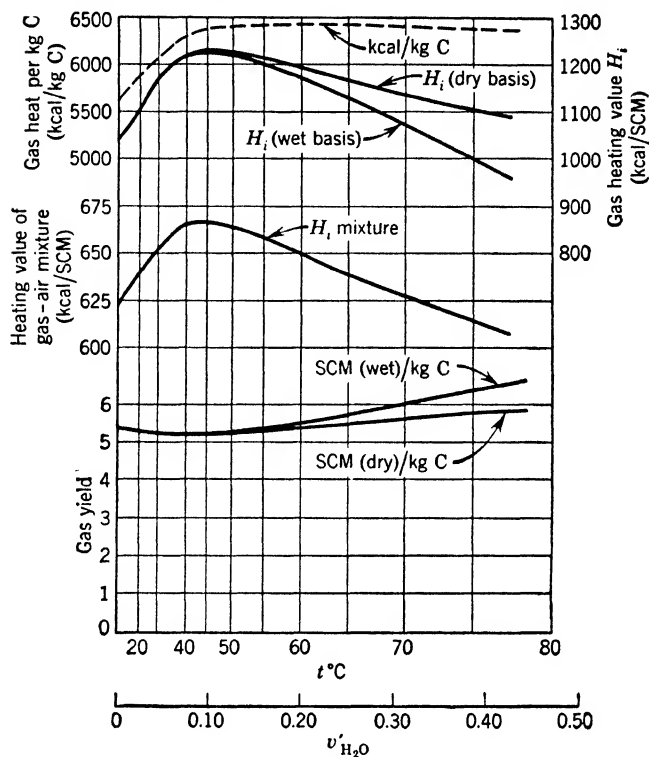


FIG. 21. Gas heating value per SCM and per kg C, heating value of the stoichiometric gas-air mixture, and gas yield as a function of the moisture content of the blast. (Gasification of carbon.)

TABLE 17
GASIFICATION OF CARBON (WET BLAST)

$v'_{H_2O} = 0.40$ $t = 550^\circ$	600°	650°	$t_R = 601^\circ C$
6.34	12.17	20.12	12.31 % CO
17.89	15.64	11.88	15.57 % CO ₂
18.40	21.45	23.54	21.50 % H ₂
15.04	10.80	7.09	10.72 % H ₂ O
0.78	0.51	0.32	0.51 % CH ₄
41.55	39.43	37.05	39.39 % N ₂
100.00	100.00	100.00	100.00 %

TABLE 17 (Continued)
GASIFICATION OF CARBON (WET BLAST)

$v'_{\text{H}_2\text{O}} = 0.30$ $t = 600^\circ$	650°	700°	$t_R = 646^\circ\text{C}$
12.02	19.74	27.76	19.09 % CO
15.26	11.43	7.19	11.77 % CO ₂
16.74	18.43	19.43	18.33 % H ₂
8.32	5.45	3.25	5.66 % H ₂ O
0.31	0.20	0.12	0.20 % CH ₄
47.35	44.75	42.25	44.95 % N ₂
100.00	100.00	100.00	100.00 %
$v'_{\text{H}_2\text{O}} = 0.20$ $t = 650^\circ$	700°	750°	$t_R = 698.5^\circ\text{C}$
19.33	26.96	32.74	26.75 % CO
10.96	6.78	3.56	6.98 % CO ₂
12.87	13.61	14.02	13.60 % H ₂
3.72	2.21	1.21	2.25 % H ₂ O
0.09	0.06	0.04	0.06 % CH ₄
53.03	50.38	48.43	50.45 % N ₂
100.00	100.00	100.00	100.00 %
$v'_{\text{H}_2\text{O}} = 0.10$ $t = 750^\circ$	800°	850°	$t_R = 795^\circ\text{C}$
31.37	34.36	35.80	34.15 % CO
3.27	1.54	0.72	1.67 % CO ₂
7.42	7.52	7.65	7.55 % H ₂
0.62	0.33	0.17	0.35 % H ₂ O
0.01	0.01	0.00	0.01 % CH ₄
57.31	56.19	55.66	56.27 % N ₂
100.00	100.00	100.00	100.00 %
$v'_{\text{H}_2\text{O}} = 0.08$ $t = 800^\circ$	850°	900°	$t_R = 850.5^\circ\text{C}$
34.00	35.40	36.04	35.41 % CO
1.51	0.70	0.34	0.70 % CO ₂
6.13	6.19	6.22	6.19 % H ₂
0.26	0.14	0.08	0.14 % H ₂ O
0.00	0.00	0.00	0.00 % CH ₄
58.10	57.57	57.32	57.56 % N ₂
100.00	100.00	100.00	100.00 %

TABLE 17 (Continued)
 GASIFICATION OF CARBON (WET BLAST)

$v'_{\text{H}_2\text{O}} = 0.06$ $t = 850^\circ$	900°	950°	$t_R = 912.5^\circ\text{C}$
34.98	35.60	35.88	35.69 % CO
0.69	0.33	0.16	0.27 % CO ₂
4.70	4.73	4.75	4.74 % H ₂
0.10	0.06	0.03	0.05 % H ₂ O
59.53	59.28	59.18	59.25 % N ₂
100.00	100.00	100.00	100.00 %
$v'_{\text{H}_2\text{O}} = 0.05$ $t = 900^\circ$	950°	1000°	$t_R = 960^\circ\text{C}$
35.37	35.65	35.78	35.69 % CO
0.32	0.16	0.09	0.14 % CO ₂
3.97	3.98	3.99	3.98 % H ₂
0.05	0.03	0.02	0.03 % H ₂ O
60.29	60.18	60.12	61.16 % N ₂
100.00	100.00	100.00	100.00 %
$v'_{\text{H}_2\text{O}} = 0.025$ $t = 1000^\circ$	1050°	1100°	$t_R = 1096^\circ\text{C}$
35.19	35.25	35.29	35.29 % CO
0.08	0.05	0.03	0.03 % CO ₂
2.03	2.03	2.03	2.03 % H ₂
0.01	0.00	0.00	0.00 % H ₂ O
62.69	62.67	62.65	62.65 % N ₂
100.00	100.00	100.00	100.00 %
$v'_{\text{H}_2\text{O}} = 0.000$ $t = 1100^\circ$	1250°	1500°	$t_R = 1200^\circ\text{C}$
34.67	34.70	34.71	34.69 % CO
0.03	0.01	0.00	0.01 % CO ₂
65.30	65.29	65.29	65.30 % N ₂
100.00	100.00	100.00	100.00 %

TABLE 18
GASIFICATION OF CARBON (WET BLAST)

ν H ₂ O	0.40	0.30	0.20	0.17451	0.10	0.08	0.06	0.05	0.025	0.000
t_R °C	601	646	698.5	716	795	850.5	912.5	960	1086	1200
Wet Gas Analysis	% CO	12.31	19.09	28.82	34.15	35.41	35.69	35.69	35.29	34.69
	% CO ₂	15.57	11.77	6.89	5.50	0.70	0.27	0.14	0.03	0.01
	% H ₂	21.50	18.33	13.60	12.19	6.19	4.72	3.98	2.03	0.00
	% H ₂ O	10.72	5.66	2.25	1.61	0.14	0.05	0.03	0.00	0.00
	% CH ₄	0.51	0.20	0.06	0.04	0.01	0.00	0.00	0.00	0.00
Dry Gas Analysis	% N ₂	39.39	44.95	50.45	51.84	56.27	59.25	61.16	62.65	65.30
		100.00	100.00	100.00	100.00	100.00	100.00	100.00	100.00	100.00
	% CO	13.79	20.23	27.37	29.29	34.27	35.71	35.69	35.29	34.69
	% CO ₂	17.44	12.48	7.05	5.59	1.68	0.27	0.14	0.03	0.01
	% H ₂	24.08	19.43	13.91	12.39	7.58	4.74	3.99	2.03	0.00
H ₂ (wet gas) kcal/SCM H ₂ (dry gas) kcal/SCM F kg C/SCM M SCM/SCM G SCM/kg C G _{dry} SCM/kg C GH ₂ kcal/kg C η_e % ξ %	% CH ₄	0.57	0.21	0.06	0.04	0.01	0.00	0.00	0.00	0.00
	% N ₂	44.12	47.65	51.61	52.69	56.46	59.28	60.18	62.65	65.30
		100.00	100.00	100.00	100.00	100.00	100.00	100.00	100.00	100.00
		968	1065	1163	1187	1226	1199	1180	1118	1048
		1084	1128	1189	1206	1231	1200	1180	1118	1048
		0.1521	0.1664	0.1806	0.1841	0.1920	0.1927	0.1920	0.1892	0.1859
		0.8309	0.8129	0.7982	0.7951	0.7915	0.7979	0.8016	0.8134	0.8264
		6.575	6.009	5.538	5.432	5.209	5.168	5.190	5.209	5.284
		5.870	5.669	5.413	5.345	5.191	5.188	5.207	5.284	5.379
		6365	6400	6441	6448	6386	6223	6147	5907	5637
		78.8	79.2	79.7	79.8	79.0	77.0	76.1	73.1	69.8
		67.7	76.8	85.9	88.4	95.6	99.0	99.3	100.0	...

by the gas heating value (the calorific content), indicating the amount of heat as gas per unit fuel gasified. This calorific content (Figure 20) shows at first a trend similar to that of the heating value, but it remains nearly constant after reaching its maximum at a slightly higher moisture content of the blast. Therefore it seems to be more reasonable and safer for any kind of gas producer with dry ash removal to operate with higher saturation temperatures (on the right branch of the curve) as long as cheap steam is available (from steam jackets, waste heat boilers, saturator-washer, etc.).

The use of steam from outside sources is usually not economical and should be limited to the least possible amount. Steam addition mainly affords the slagging control, and the fuel and its mineral matter dictate the minimum necessary for safe operation.

If hot gas is used, care must be taken that the dew point of steam and tar vapors possibly contained in the gas (which are absent if pure carbon is gasified) is not reached. The dew point, including different amounts of moisture content of the fuel, is shown in Figure 22. If coal (not carbon) is gasified the gas of devolatilization and the water vapor of decomposition have to be considered. The influence of SO_3 in traces increases the dew point considerably. In this case the limit of permissible gas cooling would be given by the condensation of tar and light oil vapors.

In internal-combustion engines—especially in any kind of portable gas producer—it is preferable to avoid the addition of water (or steam) in order to simplify the operation and the equipment

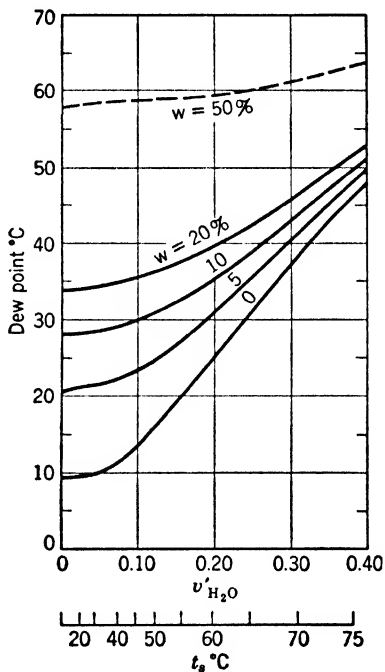


FIG. 22. Dew point of gas (produced from carbon) at different moisture contents of the blast ($v' \text{H}_2\text{O}$) and of the fuel ($w \%$).

and to avoid carrying water ballast. The differences in output and efficiency are actually very slight since the heating value of the (stoichiometric) gas-air mixture is the important factor, and not the gas heating value. To stress the difference more, the percentage of the optimum has been used as the ordinate in Figure 23. The mixture actually falls off more quickly than the gas heating value. For the problem of "dry" or "wet" gasification

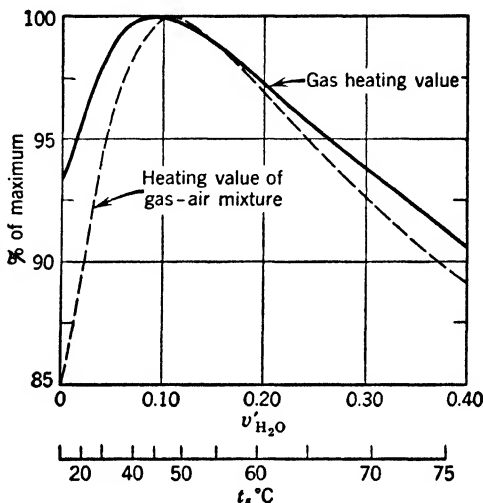


FIG. 23. Course of the heating value (in percentage of the maximum) of gas and gas-air mixture as a function of the moisture content of the blast.

in portable gas producers, other viewpoints, such as inflammability, "softness" of combustion, ease of operation, and possibilities of purification are likewise important.

Figure 24 presents another relationship between the net heating value and the degree of moisture decomposition and the steam/fuel ratio. The value recommended by Neumann,* i.e., 0.4 kg H_2O /kg C, actually corresponds to the highest heating value but not to the maximum calorific content. The degree of decomposition of the moisture introduced with the blast is defined as

$$\xi = \frac{Mv'_{H_2O} - v_{H_2O}}{Mv'_{H_2O}} 100 \quad [\%] \quad (297)$$

* See footnote 4 of this chapter, p. 109.

The moisture of the fuel, of course, must not be included in a countercurrent system, since this amount of water does not pass through the reaction zone. The degree of steam decomposition has sometimes been confused with the approach to the equilibrium.

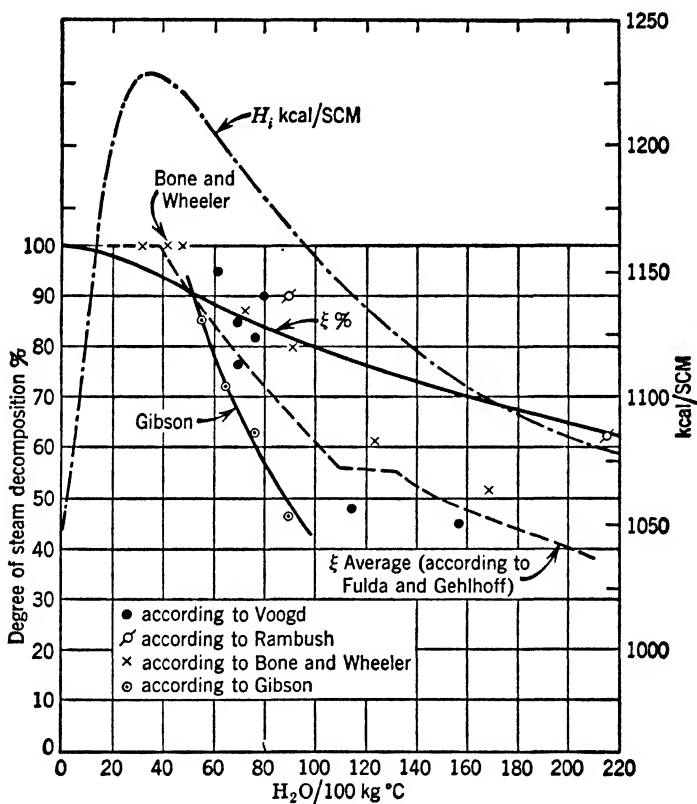


FIG. 24. Gas heating value and degree of steam decomposition as a function of the steam/fuel ratio. (Gasification of carbon or coke.)

The ξ value, here presented, refers to equilibrium conditions of the gas producer (Boudouard) and water-gas reaction. It agrees well with data of Voogd⁹ and Rambush,¹⁰ even though their measurements are quite dispersed. The average values of Fulda

⁹ G. Voogd, *Het Gas*, Vol. 8 (1928), p. 214, referred to by Fulda and Gehlhoff, footnote 7, p. 109.

¹⁰ N. E. Rambush, *Modern Gas Producers*, London, 1923.

and Gehlhoff * (dotted line) were obtained by laboratory experiments (semicommercial scale with 490-mm shaft diameter), with external heat losses far exceeding 8% as calculated. Therefore vastly different values can be expected with commercial-scale operation.

Effect of preheating the blast

In the previous calculations the temperature of the blast was equal to the saturation temperature. If, however, the blast is preheated further by means of waste heat or by other sources of heat, the reaction temperature is raised and the product gas improves. The increase of the heating value is particularly large in that section where the curves (particularly CO content) are steep, but the increase is very small, or even zero, in the high-temperature region where the curves have almost reached their maximum and have flattened out. The advantage of preheat is therefore different in every range and is very noticeable, even with moderate preheating, in the medium temperature range where most of the standard gas producers and shaft furnaces are operated. Preheating is of no additional value in a slagging ash producer (dry blast), except in a down-draft producer with moist fuels. In this case the gasification is by no means "dry," as the moisture is supplied by the fuel, not by the blast. Preheating has proved very effective in portable wood gas producers.

Since the addition of steam and the utilization of preheating have opposite effects, they can be adjusted in such a way that certain reaction temperatures, and therefore certain maximum temperatures, are maintained in the oxidation zone, and so that the gas heating value reaches the permissible maximum for a given fuel and set of operating conditions. A glance at Figure 25 shows that preheating does not affect the gasification of carbon with dry air. At saturation temperature of 57.5° every increase of 100°C preheat results in an improvement of the heating value of approximately 35 kcal/SCM. At a very high degree of saturation of the blast ($v'_{H_2O} = 40\%$ $t_s = 76.2^\circ\text{C}$) the average increase is twice as much and amounts to approximately 70 kcal per SCM. Gas technology, so far, has made little use of the possibilities of operating with high steam addition and simultaneously high preheat. At $t_s = 76.2^\circ\text{C}$ and $t_M = 450^\circ\text{C}$, the same heating value

* See footnote 7, p. 109.

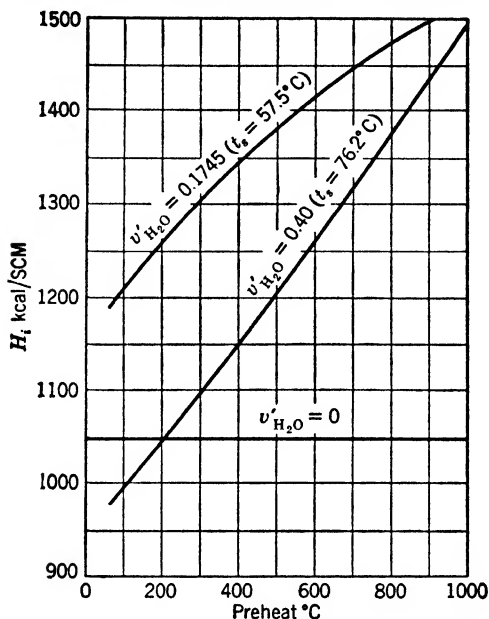


FIG. 25. Influence of preheat to the heating value of the product gas at three different moisture contents of the blast.

is reached as at $t_s = 57.5^\circ\text{C}$ without preheat. The advantage is shown in Table 19 as an increase of 8.8% in the gas yield or the calorific content.

TABLE 19

COMPARISON OF LOW-SATURATION AND HIGH-SATURATION, HIGH-PREHEAT GAS
(Fuel: Carbon)

t_s	t_M	t_R	H_i (wet)	Yield	Calorific Content
$^\circ\text{C}$	$^\circ\text{C}$	$^\circ\text{C}$	kcal/SCM	SCM/kg	kcal/kg
57.5	57.5	716	1187	5.432	6448
76.2	450	641.5	1187	5.91	7015

Since steam cost may play an important part in the total cost of gas, the economic picture may be different and has to be con-

sidered in every individual case with reference to steam cost and first cost of the preheater. In any event, it always pays to utilize completely every available source of waste heat or by-product steam.

Recycling off-gas

Saturation of the blast influences the slagging performance in the gas producer, in addition to improving the gas quality. Simple and effective as this expedient is, there have been many proposals—in portable as well as in stationary installations—to introduce gases other than steam (CO_2 or products of combustion) into the producer. Although the addition of CO_2 has a strong temperature-reducing effect, it is usually not available as a pure gas or is too expensive to compete with water for this purpose. Combustion gases, however, containing both CO_2 and steam, are available at no expense, but also contain a large amount of nitrogen. Their introduction costs something for pressuring to inlet pressure; a considerable advantage in portable producer (in vehicles) is the elimination or drastic reduction of the water ballast. Another advantage is the possible utilization of the enthalpy of this off-gas if a preheater is provided.

Table 20 compares the two processes to illustrate the differences between "wet" gasification and "dry" gasification with recycling of combustion gases. Operation conditions are set in such a way that equal conditions (equal reaction temperatures) prevail.

If exhaust gases (from the motor) are added to the dry blast, the heating value of the gas decreases about 24%, the calorific content only 3.6%. The efficiency is nearly maintained, but the most important factor regarding the output of the internal-combustion engine is the heating value of the gas-air mixture entering the motor. It drops down 12.8% to 505 kcal/SCM, which is only 63% of standard gasoline operation practice (800 kcal/SCM).

In some practical cases a smaller addition of exhaust gas may be sufficient, depending upon the nature of the fuel used, but in principle recycling of combustion gases is inferior to wet blast operation, although it has some other advantages. According to W. J. Walker¹¹ the maximum heating value and the minimum

¹¹ William John Walker, A generalized theory of gas producer reactions with suggestions for research and development, *Trans. Inst. Chem. Eng.*, Vol. 13 (1935), pp. 121-130.

nitrogen content are reached at 25% exhaust gas, which may not always be enough to control slag formation.

TABLE 20
COMPARISON OF WET BLAST AND DRY BLAST WITH RECYCLING OF
EXHAUST GASES

(Fuel: Carbon, $Q_{ext} = 10.7\%$, $t_R = 700^\circ\text{C}$)

<i>Case 1</i>		<i>Case 2</i>	
Addition of Steam		Addition of 0.5 SCM Exhaust Gas per SCM Dry Air	
$t_s = 56.7^\circ\text{C}$		$v'_{\text{H}_2\text{O}} = 0.0531$	
$v'_{\text{H}_2\text{O}} = 0.1681$		$v'_{\text{CO}_2} = 0.0464$	
$v'_{\text{O}_2} = 0.1747$		$v'_{\text{O}_2} = 0.1420$	
$v'_{\text{N}_2} = 0.6572$		$v'_{\text{N}_2} = 0.7584$	
$t_M = 56.7^\circ\text{C}$		$t_M = 100^\circ\text{C}$	
<i>Gas Composition</i>			
Wet	Dry	Wet	Dry
26.69	27.20	24.78	24.93 % CO
6.64	6.77	5.73	5.76 % CO ₂
11.64	11.86	3.95	3.97 % H ₂
1.87	...	0.59	... % H ₂ O
0.04	0.04	0.00	0.00 % CH ₄
53.12	54.13	64.95	65.34 % N ₂
100.00	100.00	100.00	100.00 %
<i>Gas Heating Value</i>			
$H_i = 1109$	1130	850	855 kcal/SCM
<i>Gas Yield</i>			
5.593		7.033	SCM/kg
<i>Calorific Content</i>			
6203		5978	kcal/kg
<i>Gasification Efficiency</i>			
76.77%		73.99%	
<i>Heating Value of Gas-Air Mixture</i>			
579		505	kcal/SCM

Effect of external heat losses

In contrast to the effect of preheating the blast, the external heat losses (radiation and convection, cooling water, etc.) act in the opposite direction. In the range of high reaction temperature

a change in external losses means little to the heating value of the product gas. The more we approach the steep section of the curves (H_i or CO, H_2 curve) the more noticeable is the effect of heat losses. Figure 26 shows these conditions for three typical cases of a dry, a medium, and a wet blast.

In small gas producers the losses play an appreciable part and cause a considerable difference in the result of pilot plant and

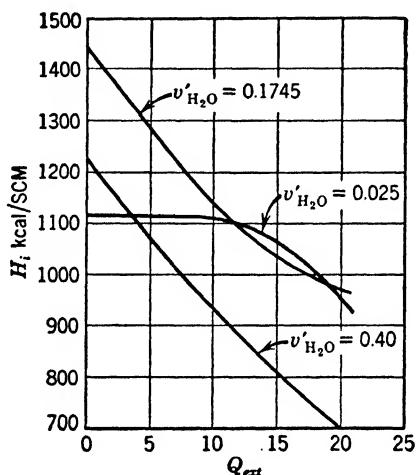


Fig. 26. Influence of the external heat loss to the heating value of the product gas at different moisture contents of the blast.

commercial-scale operation (see, e.g., Figure 24), especially if moist fuels like wood, lignite briquettes, or peat are used in down-draft producers or in cases of high moisture content of the blast. A decrease in external losses by careful insulation or by protective fuel layers (attainable by a suitable introduction of the blast into the fuel and a central gas outlet) greatly improves the gas quality and the heating value of the gas-air mixture, and therefore the power output.¹²

¹² See, e.g., H. Lutz, Die Verbesserung des Fahrzeug-Holzgaserszeugers durch wärmetechnische Massnahmen, *Automobiltechn. Z.*, Vol. 43 (1940), No. 23, pp. 589-595, Vol. 44 (1941), No. 6, pp. 142-148; *Feuerungstechn.*, Vol. 29 (1941), No. 8, pp. 186-189.

Concurrent and down-draft gasification

The type of gasification, so far considered, was countercurrent. Hot gases from the oxidation zone moved up, countercurrent to the down-coming fuel. Excellent heat exchange, low exit gas temperatures, and devolatilizing and drying of the green fuel are characteristics of this process. The gas moves very fast (normal gas velocity at mean temperature is 1 m/sec, referring to the

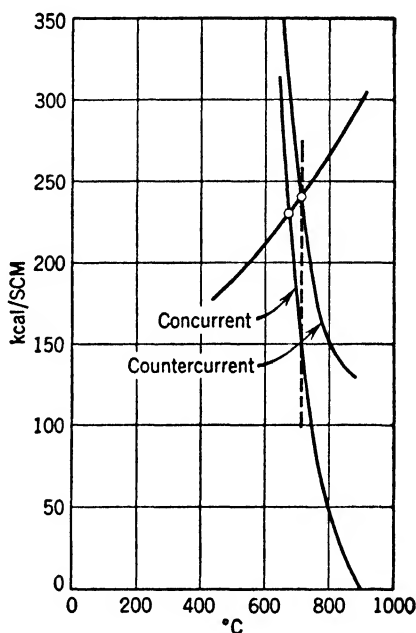


FIG. 27. $H-t$ diagram of the countercurrent and concurrent gasification.

empty producer cross-section, or 2.5 m/sec, assuming 40% void space) and the fuel very slowly (average fuel velocity 10^{-4} m/sec). The residence time of the gas is about 0.4 sec and residence time of the fuel 9000 sec. The presence of an immense excess of carbon as the body material of the main reactions is noteworthy.

As soon as this principle is abandoned the heat balance will be changed considerably. Not only will there be no heat input by the fuel heated to reaction temperature in the preheating zone, but also this amount of heat has to be delivered from other sources

(from the heating value of the fuel) and there is no heat exchange between gas and fuel behind the reaction zone, except where a special device for preheating and devolatilization is provided. For this reason the exit gas temperature of a concurrent type gas producer is much higher than that of a countercurrent type, and the efficiency correspondingly less.

There are two main gas producer types of the concurrent system, the gasification of powdered coal or small-size coals in suspension, and the down-draft gas producer.

Gasification in Suspension. Gasification of carbon in a fluidized bed of sufficient height, containing enough excess carbon surface to insure full reduction, will result in a much lower reaction temperature. From the sample calculations of a gasification of carbon (in a countercurrent system) on page 86, the intersection point of the graphical solution of the heat balance is shown for both cases in Figure 27. In a concurrent producer the reaction temperature would be 679°C, or 37° below the countercurrent system. Table 21 compares the gas analysis for both cases, at otherwise equal operating conditions. To raise the reaction temperature

TABLE 21
GAS ANALYSIS (CALCULATED), COUNTERCURRENT AND CONCURRENT
GASIFICATION OF CARBON

($v'_{\text{H}_2\text{O}} = 0.17451$; $Q_{\text{ext}} = 8\%$)

Countercurrent	Concurrent
$t_R = 716$	$t_R = 679^\circ\text{C}$
28.82	23.71 % CO
5.50	8.36 % CO ₂
12.19	11.80 % H ₂
1.61	2.44 % H ₂ O
0.04	0.06 % CH ₄
51.84	53.63 % N ₂
100.00	100.00 %
H_i 1187	1024 kcal/SCM
F 0.1841	0.1722 kg/SCM
M 0.7951	0.8224 SCM/SCM
F/M 0.2315	0.2094 kg/SCM

of the concurrent system to the same level as the countercurrent, 87.5 kcal/SCM had to be added, for instance, by raising the pre-

heat of the blast to about 400°C. Actually, if coal or char is used (not pure carbon), additional amounts of heat are necessary for drying, for heating of the volatile matter, moisture, and ash to reaction temperature, and for devolatilization of the coal. Therefore, the temperature of the blast must be raised to 1000°C or more. Another difficulty is provision of the necessary excess carbon as a body material, a practical handicap, especially, for the sweep-type pulverized fuel gas producer.

An analysis of the results of the Koppers process in gasifying a predried lignite is shown in Table 22. In a concurrent system the fuel—first its volatile matter—will burn until the oxygen of the blast is consumed. Gases of combustion together with the residual fuel start to react with each other. To complete reduction (down to equilibrium) two main conditions must be fulfilled: first, there must be enough carbon to reduce the carbon dioxide and the steam to CO and H₂, according to equilibrium, including enough excess carbon to keep the reactions going; and, second, the temperature must be sufficiently high so that the reaction rate will be great enough to permit approach to equilibrium within the short residence time. In a countercurrent system both these stipulations are easily fulfilled. The residence time of the solid fuel, several thousandfold greater, provides enough reducing agent, huge surfaces, and a turbulent flow with large heat and mass exchange rates. The temperature in the gas phase drops continuously down from its peak in the oxidizing zone and provides a stimulating impulse to the reactions.

A fluidized bed contains considerably less carbon and operates at a more uniform temperature, thus slowing down the reactions,

TABLE 22

ANALYSIS OF THE KOPPERS PROCESS OF POWDERED COAL GASIFICATION

Fuel: Lignite, predried; analysis of fuel, as fed	Gasifying agent: Oxygen-steam mixture, preheated to 900°C
56.20 % C	30.72 % O ₂
0.33 % S	1.28 % N ₂
4.71 % H ₂	68.00 % H ₂ O
20.58 % O ₂ + N ₂	
5.18 % ash	100.00 %
13.00 % H ₂ O	
<hr/> 100.00 %	

TABLE 22 (Continued)

ANALYSIS OF THE KOPPERS PROCESS OF POWDERED COAL GASIFICATION

Composition of the volatile matter; in % of fuel as fed	Composition of the volatile matter burnt (= 74% total combustible volatile matter)
12.78 % C	22.8 % C
0.33 % S	0.6 % S
4.71 % H ₂	8.4 % H ₂
19.58 % O ₂	1.8 % N ₂
1.00 % N ₂	35.0 % O ₂
13.00 % H ₂ O	31.4 % H ₂ O
	100.0 %
Products of combustion (exit oxidizing zone)	Composition of remaining char (= C _{fix} + 26% volatile matter)
13.20 % CO ₂	87.5 % C
1.28 % N ₂	2.3 % H ₂
85.52 % H ₂ O	0.2 % S
	0.5 % N ₂
	9.5 % O ₂
100.00 %	100.0 %
Gas composition at 800°C	Fuel/reducing agent ratio at 800°C
48.4 % CO	$\frac{0.274}{0.4965} = 0.551$
3.1 % CO ₂	
44.9 % H ₂	
2.7 % H ₂ O	
0.2 % CH ₄	
0.7 % N ₂	
100.0 %	
	Fuel/reducing agent ratio (as fed), 0.400
	Carbon deficiency:
	0.151 = 37.8% of carbon actually fed
	= 27.4% of carbon necessary
Dry gas composition calculated at $t_R = 688^\circ\text{C}$	Measured
35.8	35 % CO
14.0	14 % CO ₂
48.4	50 % H ₂
0.8	— % CH ₄
1.0	1 % N ₂
100.0	100 %

and in a sweep-type producer the carbon present is still much less (the reaction chamber is a nearly empty space), thus definitely applying a brake to the reaction. Consequently, since the endothermic reactions are retarded, the gas temperature remains high, and an unsuitable gas (with high CO_2 and H_2O content) at high temperature, low efficiency, and a restrained gas yield will result.

Figure 28 shows these conditions in an impressive way. Although the exit gas temperature is very high (magnitude of 1000°C), the gas analysis is far from the equilibrium gas composition at these temperatures. Table 22 gives the gas analysis (as calculated) at 800°C . The necessary fuel (carbon) per SCM of product gas of this analysis is 0.274 kg/SCM, the gasifying agent 0.4965 SCM/SCM, and the ratio of F/M is 0.551. Actually, according to the feed, this ratio was only 0.4. This means that the gas leaving the oxidizing zone never will reduce its CO_2 and H_2O content to the extent calculated; the reaction

is stopped at that point at which the carbon is practically used up because of the deficiency of carbon. The results of repeating the calculation for several temperatures appear in Figure 28. The temperature at which the actual F/M ratio is reached is 688°C ; and the gas analysis as measured coincides fairly well with the calculation at this temperature (see bottom of Table 22).

It has been stated in the technical literature that the temperature of the exit gas has to be kept 320 to 420°C higher than equilibrium temperature, but no plausible explanation for this empirical stipulation has been given.¹³ Figure 28 gives the answer. There

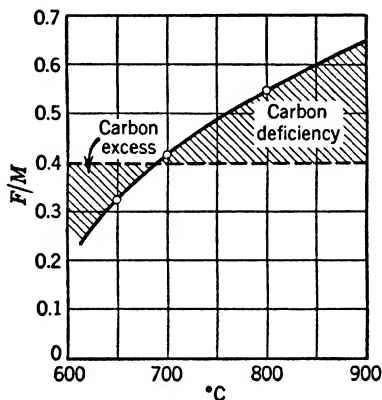


FIG. 28. Ratio of fuel/gasifying agent versus reaction temperature, showing the ranges of excess carbon and carbon deficiency in a concurrent gasification process (Koppers process).

¹³ L. L. Newman, Oxygen in the production of hydrogen and synthesis gas, *Ind. Eng. Chem.*, Vol. 40 (1948), No. 4, pp. 559-582 (p. 567). Harold V. Atwell, Koppers powdered coal gasification process, *FIAT Final Report* 1303 (September 2, 1947).

is no arbitrary relationship between equilibrium analysis and actual analysis. This is not a problem of the kinetics of these reactions but a problem of proper proportioning of blast (or oxygen) and carbon and of the heat balance. Carbon deficiency has stopped the progress of the reducing reaction.

Another example is given in Figure 29. A series of experiments ¹⁴ is shown with widely different F/M ratios. The tendency of

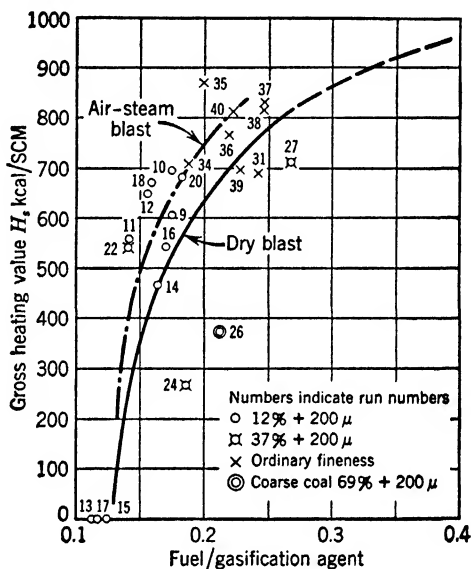


FIG. 29. Gasification of pulverized bituminous coal. Heating value of product gas vs. F/M ratio.

temperature to increase as the F/M ratio is raised is quite obvious. Higher ratios have not been applied (in spite of the known beneficial effect of a higher coal feed) because of the dropping of temperatures due to this excess fuel or, in other words, the inadequacy of the heat balance. Only by balancing this temperature decrease by higher preheat (which was limited in the existing experimental outfit) can a better approach be made to the equilibrium and more reasonable results be obtained.

¹⁴ For more details of these experiments (otherwise unpublished because unfinished), see Harold V. Atwell, Gumz powdered coal process, FIAT *Final Report* 1304 (September 15, 1947).

The sweep-type powdered coal gas producer (with a once-through operation) is handicapped by the facts that feeding the right amount of reducing carbon necessitates very high preheat and that all carbon should be consumed.

In theory essentially all the carbon can be gasified, but at the end of the process the quantity of reducing agent (C) becomes so small that the rates of the reducing reactions approach zero. In practice, a rather appreciable quantity of unconsumed, finely divided carbon remains at the end of the reaction, thus limiting gas yield and gas quality. Gas cleaning, or washing out these fine carbon particles, is one of the most difficult engineering problems.

Recycling excess carbon is one way to improve operating conditions. This is done automatically by the fluidized bed operation. This technique, with its tendency to level out temperatures of gaseous and solid components, renders the problem of deashing or deslagging more difficult. By partial withdrawal of inventory, or in a more effective way by the combination of a sweep-type and an adjoining fluidized bed operation, the slag removal and ash level can be controlled (as proposed by Hydrocarbon Research, Inc., New York).^{*} In the sweep-type oxidizing zone, the molten or plastic slag is easily removed, as shown by the Szikla-Rozinek furnace.¹⁵

Down-Draft Gasification of Wood. Wood is a gas-producer fuel rich in moisture and volatile matter. The ratio of hydrogen and oxygen content to carbon is very high. If gasified in a down-draft producer, as is standard practice, to transform the higher hydrocarbons and oxygenates into CO and H₂, the products of combustion of the volatile matter as well as the vaporized moisture enter the gasification zone. The gasification corresponds, therefore, to a very wet blast process. Table 23 presents the result of calculations for wood with varying moisture (0 to 30%). The external

^{*} Patent applications pending.

¹⁵ Géza Szikla and Arthur Rozinek, Die Entwicklung des Schwebvergaser Bauart Szikla-Rozinek, *Feuerungstechn.*, Vol. 26 (1938), No. 4, pp. 97-102. Arthur Rozinek, Weiterentwicklung des Schwebvergaser Bauart Szikla-Rozinek, *Feuerungstechn.*, Vol. 30 (1942), No. 7, pp. 153-161. Wilhelm Gumz, Der Schwebvergaser Bauart Szikla-Rozinek als Feuerung und als Gaserzeuger, *Archiv für bergbauliche Forschung.*, Vol. 3 (1942), No. 2, pp. 122-129. Arthur Rozinek, The Szikla-Rozinek floating gasifier, a new system of coal combustion, *Machinery Lloyd*, Vol. XIX (1947), No. 1/A.

TABLE 23

DOWN-DRAFT GASIFICATION OF WOOD WITH DIFFERENT MOISTURE CONTENT

Moisture, % Net Heating Value, kcal/kg	0 4430	10 3927	20 3424	30 2921
Reaction Temp., °C	661	631	600	555
Gas Analysis (Wet)				
% CO	21.04	16.50	12.02	6.83
% CO ₂	9.99	12.68	15.24	17.88
% H ₂	18.18	18.73	18.94	17.45
% H ₂ O	4.65	6.68	9.41	13.65
% CH ₄	0.69	1.07	1.66	2.72
% N ₂	45.45	44.34	42.73	41.47
	100.00	100.00	100.00	100.00
Gas Analysis (Dry)				
% CO	22.07	17.68	13.27	7.91
% CO ₂	10.48	13.59	16.82	20.71
% H ₂	19.07	20.07	20.19	20.21
% CH ₄	0.72	1.15	1.83	3.15
% N ₂	47.66	47.51	47.17	48.02
	100.00	100.00	100.00	100.00
Gas net heating value, kcal/SCM	1161.6	1071.1	991.7	887.3
Gas yield, SCM/kg	2.967	2.800	2.604	2.401
Gasifying agent, SCM/SCM	0.5858	0.5715	0.5507	0.5344
Fuel consumption, kg/SCM	0.3371	0.3571	0.3841	0.4164
Gas yield × heating value, kcal/kg	3446.5	2999.1	2582.4	2130.4
Gasification efficiency, %	77.8	76.4	75.4	72.9
Equivalent blast saturation temperature, °C *	68.0	69.6	74.3	85.0

* By *equivalent blast saturation temperature* is meant the saturation temperature of the blast, gasifying pure carbon, which gives the same reaction temperature.

heat loss is assumed to be 7.5%, no preheat, entering air 80% saturated at 20°C, $x_B = x_W = x_M = 1$. As expected, gas heating value, gas yield, and calorific content decrease with increasing moisture, corresponding to lower reaction temperatures. The last line indicates equivalent saturation temperatures in a counter-current system to compare with carbon gasification and wet blast.

A moisture content of 30% is about the limit if no additional heat is supplied by high preheat. At about 36% moisture the equivalent saturation reaches 100% and a water gas is produced, but the reaction temperature drops below 500°C and all heat necessary must be supplied by external sources. Raising the reaction temperature by external heat sources (exhaust gases, improved insulation, etc.) to 650°C causes a gas to form, as shown in the right column of Table 24. Wood with 30% moisture is used.

TABLE 24
GASIFICATION OF WOOD, 30% H₂O
(Influence of External Heating)

Without External Heat $t_R = 555^\circ\text{C}$	With External Heat $t_R = 650^\circ\text{C}$
Gas analysis (dry basis)	
7.91	23.0 % CO
20.71	13.9 % CO ₂
20.21	35.5 % H ₂
3.15	2.6 % CH ₄
48.02	25.0 % N ₂
<hr/>	<hr/>
100.00	100.0 %
Heating value	
H_i (dry) = 1028	1829 kcal/SCM
Gas yield (wet basis)	
2.401	1.847 SCM/kg
(Dry basis)	
2.073	1.664 SCM/kg
Calorific content (dry basis)	
2131	3043 kcal/kg
Gas-air mixture, heating value	
450.5	665.6 kcal/SCM

F. Fischer¹⁶ refers to results of a Fouchet-type gas producer utilizing oak wood wastes with 20% moisture in a down-draft operation. With 8.94% external heat loss the reaction temperature is 600°C. Table 25 shows a comparison of calculated values and experimental results.

At first sight the agreement seems quite satisfactory. However, it must be noted that the experimental gas analysis indicates a

¹⁶ Ferdinand Fischer, *Kraftgas*, 2nd ed., edited by J. Gwosdz, Leipzig, 1921, p. 391.

certain amount of higher hydrocarbons (illuminants) and more methane than theoretically possible under the most favorable assumptions ($x_M = 1$). It could be assumed that CH_4 is formed only with $x_M < 1$. It follows, therefore, that apparently the volatile matter is *not* completely burnt to CO_2 and H_2O , and the product gas still contains some unreformed constituents of the original devolatilization products. These deviations have been attributed to incomplete reactions and shortness of contract time.

TABLE 25

GASIFICATION OF WOOD (FOUCHET GAS PRODUCER)
(Comparison of Calculatory and Experimental Results)

Fouchet Gas Producer Gas Analysis as Reported	Adjusted to O_2 -free Basis	Calculated ($t_R = 600^\circ\text{C}$)
13.27	13.29	13.27 % CO
15.96	15.98	16.82 % CO_2
20.97	20.99	20.91 % H_2
2.61	2.61	1.83 % CH_4
46.80	46.85	47.17 % N_2
0.28	0.28	... % Illuminants
0.11 % O_2

More reasonable, however, is the explanation that this incompleteness is due to purely physical causes. Gas and air were not perfectly mixed. Because of the large quantities of water vapor and devolatilization products, intimate mixing of a rather limited amount of air is difficult. At least locally (not in the average) a deficiency of free oxygen prevented complete combustion, and a fraction of these gases pass the oxidizing zone unburnt. Even if the producer hearth is constricted in the reducing zone, as in most constructions, the temperature at this zone is not high enough for complete decomposition of hydrocarbons, especially of methane.

This incomplete combustion of the products of devolatilization becomes even more noticeable in another type of wood gas producer. In the Fouchet type the air is distributed relatively well over the cross-section, but the Imbert type and its imitators are fed with air through lateral nozzles or slots. H. Lutz * has reported

* See footnote 12, p. 122.

experimental data of an Imbert producer which, at first sight, seems to deviate widely from the calculations. See Table 26 and

TABLE 26
IMBERT GAS PRODUCER; WOOD FUEL 20% MOISTURE

Experimental Results (H. Lutz)	Calculated $H_2O = 0\%$; $t_R = 650^\circ C$
20.50	20.2 % CO
11.20	11.5 % CO_2
17.00	18.2 % H_2
2.00	0.8 % CH_4
49.30	49.3 % N_2
<hr/> 100.00	<hr/> 100.0 %

compare with the 20% moisture fuel in Table 23. It is particularly striking that the former achieves higher CO and lower CO_2 contents, a rather constant CH_4 content, and a lower H_2 content with different fuel moisture and different rates. However, it should be remembered that in the Imbert producer hot product gas passes upward through a double jacket, thus minimizing the external heat losses. Hence, the reaction temperature rises appreciably, by approximately 50° , the gas quality improves, and the importance of the jacket is thereby well established. The oxidation zone is formed in front of each tuyère (see Figure 30). Between the nozzles near the wall as well as in the center are spots which are not reached by oxygen, staying at lower temperatures. All products of devolatilization passing here remain necessarily unburnt because no oxygen is present. They may be partly cracked in the reduction zone, but temperatures (approximately $650^\circ C$) are by no means sufficient for complete reforming. Methane, for example, is still stable at this temperature. Steam not having

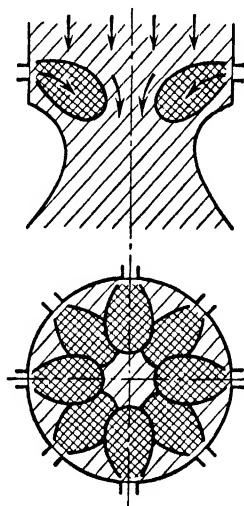


FIG. 30. Hearth of an Imbert gas producer.

Shaded = fuel bed
Cross-hatched = oxidation zones

Steam not having

passed the oxidation zone hits the reduction zone with much too low a temperature and consequently cannot react; it acts rather as a cooling medium and remains more or less undecomposed. Incomplete equilibrium, too low reaction velocity, and short contact time, often quoted as possible causes, have nothing to do with this condition. The steam has not been brought into a state to react from merely physical reasons, because of non-uniform distribution of oxygen and a non-uniform temperature pattern. Therefore the reaction cannot proceed in the same way as calculation—assuming perfect uniformity—indicates.

A comparison of Lutz' data with calculated results shows that a fuel with 20% moisture and 650°C reaction temperature corresponds to a negative heat loss of -7%. This heat is supplied by the enthalpy of the exit gas. The gas composition, however, refers to a gas of which only 70% of the products of devolatilization (including moisture) have passed the oxidation zone. This would be a gas which theoretically corresponds to a gas from wood with zero moisture content. (See Table 26.)

As far as heating value is concerned, the incomplete decomposition is apparently no disadvantage; in the heating value of the gas-air mixture entering the motor a difference of only 1.9% occurs. Incomplete decomposition, however, entails condensation of hydrocarbons, losses, operation trouble, and formation of corrosive precipitates.

It is, therefore, preferable to reach complete decomposition of all volatile constituents and to increase the heating value and performance by raising the reaction temperature by known means.*

The down-draft wood gas producer should be constructed on the following bases:

- (1) Assurance of uniform charge of the air blast to the cross-section. The larger the diameter the more difficult is this achieved by lateral nozzles. Introduction of the air above the fuel bed is preferable.
- (2) Avoidance of all heat losses, utilization of the enthalpy of the exit gas (double jacket), careful insulation.
- (3) Preheat of the blast, utilization of the exhaust gases of the integrated motor.
- (4) Addition of heat by other sources (if available) for blast or jacket heating.

* See footnote 12, p. 122.

In stationary installations where the limitations of motor vehicles with regard to space and weight do not apply, external heat supply (4) is most promising. Preheating of the blast, however, has a rather limited effect. With 30% moisture of the fuel, even 800°C increases the reaction temperature only 27°C owing to the decreasing amount of blast. The external heat, therefore, has to be applied by other methods. This is possible (1) by recycling gas and heating the recycle gas before reintroducing, (2) by external heating, possibly by subdividing the producer into chamber (similar to coke ovens) with heating flues between.

Table 24 presents an example of a process using wood waste with 30% H₂O introducing 20% of heat externally, a preheat of 200°C by exhaust gases, resulting in 650°C reaction temperature. Power output is increased more than 30% by the thermal improvements.

In wood gasification, charcoal is formed by the wood and is the actual fuel entering the reaction zone. If the rates of formation of charcoal and of its consumption are equal, the charcoal level remains constant, carry-over losses disregarded. If less charcoal is gasified than newly formed (or if charcoal is removed as practiced in some processes), the gasification corresponds to that of a fuel with more moisture. On the other hand, if more charcoal is gasified than newly formed, that is, if fire bed charcoal is consumed, this operation corresponds to a gasification of a drier fuel. Consumption of bed coal tends to make the gas leaner, to lower the hydrogen content, and to raise the temperature. Inequality of the rates of carbonization and of gasification occurs mainly with low loads and frequent load variations.

Lutz found a fairly close agreement between measured and calculated data at full load and at two-thirds load; at one-third load the CO content is somewhat lower, the CO₂ and H₂ content higher. This gas composition indicates a lower temperature (higher heat loss) and higher charcoal formation. The rate of carbonization is a function of the temperature of the oxidation zone. This zone, however, retains its depth and temperature approximately over a fairly wide load range. Consequently at one-third load, for example, the formation of charcoal continues at a higher rate whereas the gasification diminishes. At overloads, the reverse happens, fire bed charcoal is consumed faster than delivered, the hydrogen content diminishes, and the temperature rises.

Different types of wood are characterized by the quality and density of their charcoal. Beechwood gives a strong coarse charcoal. The charcoal of pines and all coniferous trees disintegrates easily and splits. These trees form smaller pieces of charcoal; consequently the zones of oxidation are smaller, and the attainment of uniform gas distribution is more difficult.

Slagging-ash gas producers

Gas producers with liquid slag removal, the oldest type of producers, have a number of advantages: ^{17, 18, 19}

- (1) They can be operated with high blast pressures, hence with a very high specific production (regardless of the lower seal which sometimes limits rotating grate producer output).
- (2) They can be built in very large units, thus cutting down operation cost. The blast furnace, the prototype of a slagging-ash producer, is built in standard capacities of 1000 tons per day.
- (3) They can utilize low-grade fuels with very high ash content, which would result in very high carbon losses in standard rotating grate producers; they even handle the residues of water gas and similar producers successfully.
- (4) Their operation can be handled in a way to obtain valuable by-products such as cement and cement raw materials, glass, pig iron, and such special iron as phosphoric spiegel iron ferrosilicon ²⁰ and non-ferrous metals.²¹

¹⁷ Carl D. Smith, The slagging type of gas producer, *Bureau of Mines Tech. Paper* 20 (1912).

¹⁸ Jules Deschamps, *Les gazogènes*, Paris, 1902 (Ch. Dunod).

¹⁹ N. E. Rambush, *Modern Gas Producers*, London, 1923, pp. 133-148.

²⁰ Julius Lamort, Die Erzeugung von Eisen und Glas im Abstichgaserzeuger aus Hochofenschlacke und ähnlichen Gesteinen, *Stahl u. Eisen*, Vol. 56 (1936), No. 36, pp. 1006-1007, *Glastech. Ber.*, Vol. 14 (1936), No. 2, pp. 54-60.

²¹ According to H. Philippon (*Rev. de l'industrie minérale*, Vol. 14 [1934], No. 317, pp. 125-127) the Société de la Vieille Montagne at Vivier (Aveyron), France, operates a slagging-ash producer of 200 tons per day from which 100 t are residues of the Zn-electrolysis (with 15 to 20% metal content), resulting in 25 t/day of a 70% concentrate. Furthermore, three gas producers are operated at Baelen, Belgium, each having a capacity of 300 t/day for lead slag refining.

- (5) Their operation is very flexible and shows good adaptability to any gas demand, including high overloads.²²

Nevertheless, slagging-ash producers have not been very popular until now because of the lower efficiency (if operated with dry air), low heating value of the gas, and the unfamiliarity of many consumers with correct choice of the burden and the slag tapping operation. The burden has to be mixed with fluxes (like limestone, blast furnace, or open hearth slag) in such a way that easy tapping and low slag viscosity are reached. These disadvantages, however, are more or less easily overcome, and the slagging-ash producer will be the gas producer of the future, if developed to high yield and efficiency. This is positively true where large quantities of gas are desired at lowest heat cost as, for example, for gas turbine operation.

Comparisons of slagging-ash producer performance and calculation disclose a new characteristic. In spite of extremely high "reaction temperatures" (about 1100 to 1200°C if dry air is used) the CO₂ content in the exit gas does not approach zero, but stays considerably higher. The main reason is the high temperature level in the preheating zone which renders the coke very reactive. Therefore, the equilibria do not freeze, but they follow the decreasing temperatures down to the gas exit temperature (see Table 30).

The following calculation takes into account the small amount of volatile matter of the coke (which has some influence because of the low H₂ level in the gas). In addition, the effect of the ash components will be considered in a way discussed in more detail in blast furnace calculations (see page 225).

The performance of a slagging-ash producer of the Georgs-Marien-Hütte type²³ will be used as reference. Table 27 reports the analyses of the fuel (ash-free basis) as well as of the burden, consisting of 25% coke ash + 75% open hearth slag. Table 28 gives the composition of the blast. Table 29 presents the calculated gas analyses, and Table 30 compares long-run operational data with the calculation.

²² Hans Voellmecke, Schlackenabstich-Gaserzeuger als Ausgleichsmittel in der Wärmewirtschaft, *Stahl u. Eisen*, Vol. 31 (1937), No. 36, pp. 503-509.

²³ J. Henselmann, Der Abstichgenerator Bauart Georgsmarienhütte, *Centralbl. d. Hütten- u. Walzwerke*, Vol. 31 (1927), No. 36, pp. 503-509.

TABLE 27

SLAGGING-ASH PRODUCER, FUEL ANALYSIS

Coke (Ash-free Basis)	Burden (25% coke ash + 75% open hearth slag)	Fictitious Fuel (Coke + O ₂ from burden)
99.25 % C	19.41 % SiO ₂	94.013 % C
0.30 % H ₂	9.94 % Al ₂ O ₃	0.284 % H ₂
0.31 % O ₂	4.57 % Fe ₂ O ₃	5.570 % O ₂
0.14 % N ₂	3.55 % FeO	0.133 % N ₂
	29.96 % CaO	
	5.74 % MgO	
	7.20 % MnO	
	18.40 % P ₂ O ₅	
	0.29 % alkali	
	0.94 % SO ₂	
<hr/> 100.00 %	<hr/> 100.00 %	<hr/> 100.000 %

TABLE 28

SLAGGING-ASH PRODUCER, BLAST ANALYSIS, BLAST AND FUEL MOLAL DATA

$v'_{O_2} = 0.20821$	$C_M = 0$	$C_F = 1.75466$
$v'_{N_2} = 0.78325$	$H_M = 0.00854$	$H_F = 0.03158$
$v'_{H_2O} = 0.000854$	$O_M = 0.21248$	$O_F = 0.03902$
	$N_M = 0.78325$	$N_F = 0.00106$

TABLE 29

SLAGGING-ASH PRODUCER

(Calculated Gas Analyses in Equilibrium)

$t = 800^\circ$	850°	900°	1000°	1500°C
33.28	34.59	35.18	35.58	35.73 % CO
1.45	0.67	0.32	0.09	0.00 % CO ₂
1.27	1.30	1.31	1.32	1.33 % H ₂
0.05	0.03	0.02	0.01	0.00 % H ₂ O
0.00	0.00	0.00	0.00	0.00 % CH ₄
63.95	63.41	63.17	63.00	62.94 % N ₂
<hr/> 100.00	<hr/> 100.00	<hr/> 100.00	<hr/> 100.00	<hr/> 100.00 %

TABLE 30

SLAGGING-ASH PRODUCER

(Comparison of Performance Data with Calculations)

As Measured		As Calculated	
Monthly Average	Yearly Average	At $t_E = 840^\circ$	At $t_R = 1184^\circ\text{C}$
32.20	31.4 ... 32.3	34.41	35.70 % CO
0.76	0.7 ... 1.02	0.78	0.01 % CO ₂
1.19	1.19 ... 1.65	1.30	1.33 % H ₂
1.07	1.07 ... 1.08	0.00	0.00 % CH ₄
		63.51	62.96 % N ₂
		<hr/> 100.00	<hr/> 100.00 %

With 10% ash content, 90 kg of C correspond to 10 kg of ash + 30 kg of open hearth slag, or 44.44 kg/100 kg C.

Calculated per 1 kg of pure coke:

$$0.4444 \times 0.0457 = 0.02031 \text{ kg FeO}_3 \text{ or } 0.00610 \text{ kg O}_2$$

$$0.4444 \times 0.0355 = 0.01578 \text{ kg FeO or } 0.00351 \text{ kg O}_2$$

$$0.4444 \times 0.01840 = 0.08178 \text{ kg P}_2\text{O}_5 \text{ or } 0.04609 \text{ kg O}_2$$

$$\underline{\hspace{1.5cm}} \\ 0.05570 \text{ kg O}_2$$

This amount of oxygen also goes into the gas. Therefore, the calculation can be carried out as if a fictitious fuel, correspondingly richer in oxygen, were gasified. This fuel, fictitiously synthesized, would have the composition (if calculated per 100%) given in the third column of Table 27.

The blast is dry air, but not completely free of moisture, and even small percentages of moisture produce some hydrogen in the product gas. A saturation temperature of 10°C and $\varphi = 70\%$ degree of saturation are assumed, resulting in a blast composition as tabulated in Table 28.

The method of calculation is principally the same as in previous problems. M and F , v_{N_2} , and ψ^* are determined from equations 160 to 163. The results are given in Table 29 and Fig. 31.

It is to be noted that the relatively high contents of mineral matter, the reduction of the oxides, including the phosphoric acid, and the tapping of liquid slag and metal (temperature 1400°C)

have to be considered thoroughly when calculating the heat balance.* The external heat losses are only 4%, since these calculations are based on a high specific rate. According to Figure 31, the reaction temperature is 1184°C, the exit gas temperature—on top of the fuel bed—840°C. Table 30 compares Henselmann's performance data with these calculations.

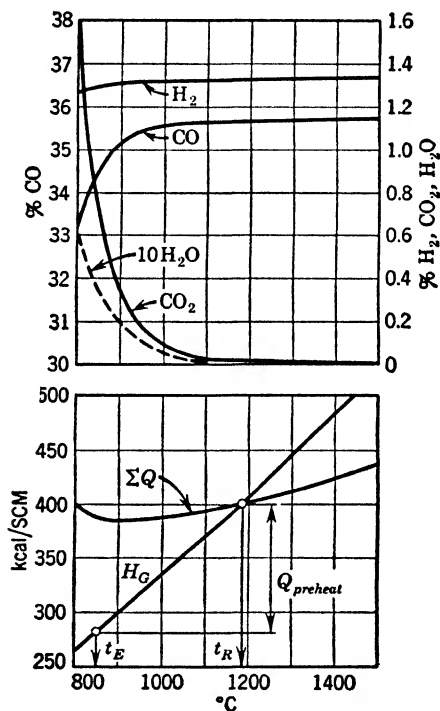


FIG. 31. Slagging-ash gas producer. H - t diagram and gas composition.

This comparison justifies the assumption that the reactions do not freeze at the existing high reaction temperatures but that they reverse and deliver a gas corresponding to the fuel bed top temperatures. Here the calculation is not in full agreement with the measured performance, but they are close enough to be quite satisfactory. The analytical results are somewhat doubtful, especially the constant high methane content. This methane can originate

* These problems are discussed in detail in Part II, see p. 173. Therefore, only the final results are reported here.

only from the volatile matter of the coke and cannot possibly be so high. A correction would bring the CO and CO₂ contents nearer agreement in calculation and performance.

The suitability of the slagging-ash producer to handle extremely low-grade fuels will be discussed in connection with the problem of gasifying coal wastes. When a low-rank bituminous coal is washed a dirt with 25 % C (after devolatilization) and 75% mineral matter remains. Ash and fuel analyses are given in Table 31.

TABLE 31
SLAGGING-ASH PRODUCER
(Fuel: Coal Waste)

Mineral Analysis	Ash Analysis
16 % quartz	49.87 % SiO ₂
58 % clay	26.57 % Al ₂ O ₃
12 % iron oxide	13.92 % Fe ₂ O ₃
7 % lime	4.55 % CaO
5 % magnesite	2.77 % MgO
2 % phosphoric acid	2.32 % P ₂ O ₅
<hr/> 100 %	<hr/> 100.00 %
Fuel Analysis (Including O ₂ and C from the burden)	
83.26 % C	C _F = 1.55396
0.25 % H ₂	H _F = 0.02780
16.38 % O ₂	O _F = 0.11474
0.11 % N ₂	N _F = 0.00088
<hr/> 100.00 %	

In the preheating zone certain amounts of material pass into the gas: 8.10% water of hydration, 2.61% CO₂ from decomposition of magnetite and formed by reduction of Fe₂O₃ into Fe₃O₄ (consuming a corresponding amount of CO).

In the reaction zone the CO₂ from limestone and the oxygen content of the iron oxides and the phosphoric acid are added. The original fuel may be assumed to be the same as in the preceding example (after its devolatilization), and the fictitious fuel (adding the C and O₂ from the burden) corresponds to an analysis as tabulated above.

A calculation utilizing the same blast as mentioned in Table 28 yields the results given in Table 32.

TABLE 32

SLAGGING ASH PRODUCER

(Fuel: Coal Waste. Calculated Gas Analysis at Equilibrium.)

$t = 750^\circ$	800°	850°C
32.33	35.50	37.02 % CO
3.48	1.65	0.77 % CO ₂
1.22	1.28	1.31 % H ₂
0.10	0.06	0.03 % H ₂ O
0.00	0.00	0.00 % CH ₄
62.87	61.51	60.87 % N ₂
<hr/> 100.00 <hr/>	<hr/> 100.00 <hr/>	<hr/> 100.00 % <hr/>
H _i 1008	1105	1152 kcal/SCM
F 0.2304	0.2390	0.2432 kg/SCM
M 0.8024	0.7851	0.7768 SCM/SCM

With 5.2% external heat loss, the graphically obtained reaction temperature will be 800°C . Because of the much higher ratio of burden to fuel, this temperature is much lower than in the previous problem.

In addition to the gas leaving the reaction zone (5.114 SCM kg pure coke), we have 0.336 SCM/kg gas of devolatilization and the gas from the burden: 0.0195 SCM of CO disappearing and changing into 0.0195 SCM CO₂ by reduction of Fe₂O₃, and 0.0462 SCM CO₂ from MgCO₃. The gas of devolatilization (at 800°C) is assumed to have 5.0% CO, 3.0% CO₂, 52.0% H₂, 5.0% N₂, 30% CH₄, and 5.0% C_nH_m. The results are tabulated in Table 33.

The efficiency (gasification efficiency), not including the relatively small tar yield but including the gas of devolatilization, with 8100 kcal/kg net heating value of the fuel (moisture and ash-free basis, 35% volatile matter, 65% C_{fix}), amounts to

$$\eta = \frac{0.65 \times 5.496 \times 1314 \times 100}{8100} = 58\%$$

In this case the reactions are assumed not to reverse themselves since the reaction temperature is only 800°C and the exit gas temperature probably is in the range of only 200 to 400°C .

At these operating conditions the slag is self-flowing; no addition of flux is necessary. If so, the temperature limit of operation without preheat seems to be reached; any further item of heat consumption (by addition of limestone, or scrap, ore or slag to produce more pig iron or special iron) requires a balancing of the heat input by preheating. H. Philipon²⁴ proposes to use about 15% of the product gas for this purpose and to heat the blast to 400 to 600°C in a tubular preheater. It might be more economical

TABLE 33

SLAGGING ASH PRODUCER

(Fuel: Coal Waste. Calculated Final Gas Analysis.)

Gas Leaving Reaction Zone	Product Gas	Experimental Results (by H. Philipon)
35.52	33.00	31.0 % CO
1.65	2.91	3.5 % CO ₂
1.28	4.37	3.0 % H ₂
61.55	57.57	61.5 % N ₂
0.00	1.84	1.0 % CH ₄
0.00	0.31	... % C _n H _m
<hr/> 100.00	<hr/> 100.00	<hr/> 100.0 %
Heating value:	1314	1099 kcal/SCM
Gas yield:	5.96	SCM/kg (pure coke)

in some cases to use coal fines or slack coal sieved from the producer fuel, thus eliminating excessive carry-over losses, or enabling higher loads, saving the total product gas for consumption.

The calculation permits in some ways a comparison with results reported by H. Philipon. In his case the burden consisted of

45.50 % slate
 28.80 % coke with high (28%) ash content
 26.50 % limestone

100.00 %

In addition, 8% cast-iron scrap was charged. The product gas is tabulated in Table 33 (last column). Other products are spec-

²⁴ H. Philipon, Le gazogène à fusion des cendres soufflé au vent réchauffé à haute température, *Revue de l'industrie minière*, Vol. 14 (1934), No. 317, pp. 125-137.

ular iron (spiegel) with 4 to 10% Si, and a slag with 40 to 43% CaO, well suited for cement production. The charge contained 25% fixed carbon in both cases. The fuel, however, used in Philipon's experiments, has far less volatile matter, his burden more iron and limestone; therefore the gas is expected to be leaner, the reaction temperature somewhat lower, CO and H₂ lower, and CO₂ higher. Yet, the results compare favorably as far as their order of magnitude is concerned, and check fairly well.

The suitability of slagging-ash producers for the utilization of low-grade high-ash fuels may be considered proved and economical. The liquid state of the slag facilitates its further use, and the overall efficiency, including all possible by-product, renders the process economically sound and attractive.

The main disadvantage of the slagging-ash producer, the lower gasification efficiency compared with rotating grate gas producers with optimum steam addition, can easily be overcome if steam is added to the slagging-ash producer too. The manner in which this is accomplished is, however, decisive. Earlier types, e.g., the Wuerth producer, shows devices for introduction of steam above the tuyères, but they were unsuccessful. Steam, even if superheated, is still much colder than the surface of the coke in the reaction zone. Steam decomposition, besides, is a highly endothermic reaction and needs heat, or the surface temperatures decrease rapidly. The conventional introduction of slightly superheated steam at appreciable pressure displaces the gas and cools the coke hit by the steam jet; no noticeable reaction could reasonably be expected. Most of the steam passes the fuel bed undecomposed, even favoring uneven gas distribution and decreasing temperatures. Conversely, the moisture of the blast entering a standard gas producer passes the oxidation zone and is raised to the maximum temperature of the gas phase (order of magnitude 1500 to 1800°C). The steam, thus highly preheated, is ready to react quickly and to furnish the necessary heat of reaction; it decomposes until equilibrium is reached.

This experience shows that it is unprofitable and, considering the cost of steam generation, economically unsound to introduce only steam into a gas producer. Steam should always be fed admixed with oxygen (or air) to create an oxidation zone and high temperatures. In a slagging-ash producer the slag zone must be hot enough to permit tapping; too much steam addition would

be detrimental. The reaction zone, meanwhile, should be operated with as much steam addition as practically possible to lower the exit temperatures and increase the chemically bound heat. The following method is suggested. Part of the blast, dry or with limited amount of moisture, but preferably highly preheated, is introduced into the hearth of the producer at its melting zone; part of the blast essentially richer in moisture, but containing enough oxygen to form an oxidation zone of appreciable size, is fed in above the melting zone. The producer, thus, is operated with two oxidation zones, one slightly above the other, at different temperatures. The upper zone is supposed to carry enough moisture to avoid liquefaction of the slag. If, for example, the lower tuyères operate "dry," the upper row with 50% of the air and 60°C saturation temperature (200 g/SCM), the average moisture content of the entire blast will be 100 g/SCM ($t_s = 48^\circ\text{C}$), $v'_{\text{H}_2\text{O}} = 0.10$. The result can be read from Table 28: gas-heating value 1226 kcal/SCM, reaction temperature 795° , and exit gas temperature correspondingly lower, gasification efficiency 79%. Thus the undisputed advantages of the slagging-ash producer may be combined with the benefit of a wet blast. Characteristics of this producer are large units, high efficiency even with low-grade fuels, little mechanical trouble by eliminating the grates, low first cost, and lower gas exit temperatures favorable for effective gas cleaning,

Gasification with oxygen and oxygen-enriched air

Reaction temperature and gas quality increase and the amount of inerts is reduced if the blast is enriched with oxygen, or if oxygen steam mixtures or even pure oxygen are used. The whole range of 21 to 100% O_2 in the blast and 0 to 80% H_2O has two limited areas of practical interest. If the reaction temperatures are confined to 600 to 1100°C , the area *A* in Figure 32 (800 to 1100°C) covers slagging-ash producers, area *B* rotating grate gas producers or dry bottom operation. It is entirely possible to operate standard types of rotating grate gas producers with oxygen and to keep the temperatures within safe limits by adjusting the steam content of the blast. The heating value (see Figure 33) is mainly influenced by the oxygen content in the dry blast, far less by the steam content. Apart from limiting the temperatures, the steam content is an important economical factor as it replaces part of the rather expensive oxygen. All measures that result in higher reaction

temperatures permit higher steam percentages and may greatly influence the economics. Such measures are highest possible pre-heat, addition of heat by recycled gases and external heating, and, above all, increase of the pressure (see p. 160).

Continuous production of water gas by gasification of coke (or coal) with mixtures of oxygen and steam may be regarded as one

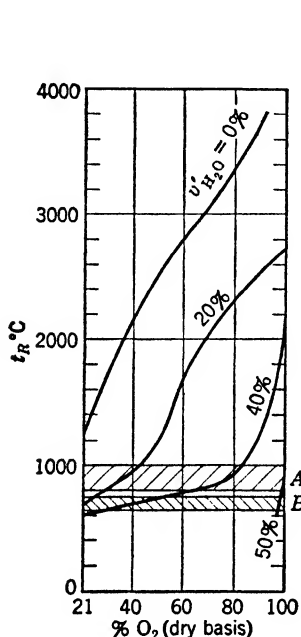


FIG. 32. Reaction temperatures of oxygen-steam blast gasification of carbon.

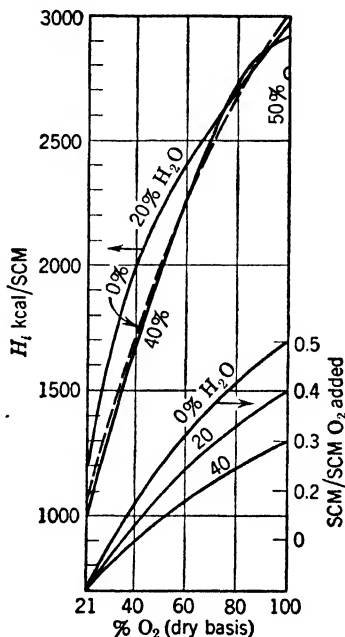


FIG. 33. Net heating value and oxygen consumption. (Dry and wet blast with various O_2 content.)

of the main sources of future synthesis gas production. Table 34 summarizes a series of calculations covering the slagging-ash producers (50 to 60% H_2O , 50 to 40% O_2) or reaction temperatures from 1200 to 800°C, as well as dry removal (65 to 80% H_2O , 35 to 20% O_2) or reaction temperatures from about 750 to less than 650°C. Pure carbon is assumed as fuel; external heat losses of 4% have been used throughout the calculation. Besides gas analyses, gas heating values, H_2/CO ratio, fuel consumption (kg/SCM [wet]), blast (M SCM/SCM [wet]), analyses of dry gas, gas yields, gasification efficiencies, based upon gross (η_g) and

net heating value (η_i), degree of steam decomposition (ξ), and oxygen and steam requirements are reported. (See also Figure 34.)

Slight changes are caused by using actual coke with a small percentage of volatile matter (0.5 to 1%) and nitrogen ($\sim 1\%$)

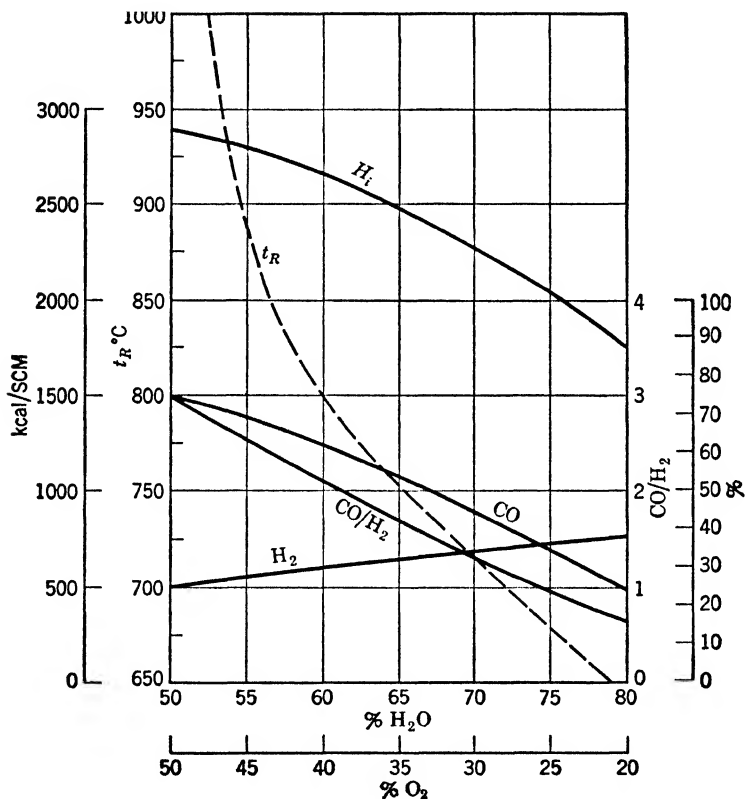


FIG. 34. Oxygen-steam gasification of carbon. CO, H₂, CO/H₂ ratio, t_R , and H_i as a function of the blast composition.

and impure oxygen (95 to 98% purity), resulting in a certain nitrogen content of the product gas.

The high gasification efficiencies of 88 to 90% attained by continuous gasification with oxygen give a fuel saving of 25 to 16%, compared with the standard discontinuous water-gas process which reached 65 to 75%.

TABLE 34

CONTINUOUS GASIFICATION OF CARBON WITH OXYGEN-STEAM MIXTURES

	Liquid Slag Removal				Dry Slag Removal			
v_{H_2O} %	50	52.5	55	60	65	70	75	80
v_{O_2} %	50	47.5	45	40	35	30	25	20
t_R °C	1200	989	887	800	753.5	715	680	640.5
Gas Analysis								
(Wet)								
CO %	75.0	73.18	70.33	62.69	54.17	44.56	34.71	24.06
CO ₂ %	...	0.41	1.56	5.14	9.09	13.43	17.50	21.43
H ₂ %	25.0	26.14	27.30	29.73	32.19	34.52	36.43	37.40
H ₂ O %	...	0.25	0.77	2.34	4.37	7.17	10.83	16.20
CH ₄ %	...	0.02	0.04	0.10	0.18	0.32	0.53	0.91
%	100.0	100.00	100.00	100.00	100.00	100.00	100.00	100.00
H_s kcal/SCM	3028	3009	2961	2810	2635	2429	2210	1954
H_i kcal/SCM	2908	2884	2829	2666	2479	2260	2030	1766
H ₂ /CO	0.333	0.36	0.39	0.47	0.59	0.77	1.04	1.55
F kg/SCM	0.4019	0.3944	0.3854	0.3640	0.3399	0.3125	0.2826	0.2486
M SCM/SCM	0.5000	0.5034	0.5118	0.5379	0.5682	0.6046	0.6443	0.6927
Gas Analysis								
(Dry)								
CO %	75.0	73.36	70.88	64.19	56.64	48.00	38.93	28.71
CO ₂ %	...	0.41	1.57	5.27	9.51	14.47	19.63	25.57
H ₂ %	25.0	26.21	27.51	30.44	33.66	37.19	40.85	44.63
CH ₄ %	...	0.02	0.04	0.10	0.19	0.34	0.59	1.09
%	100.0	100.00	100.00	100.00	100.00	100.00	100.00	100.00
Gas Yield								
$G_{(wet)}$ SCM/kg C	2.489	2.536	2.595	2.748	2.942	3.200	3.539	4.022
$G_{(dry)}$ SCM/kg C	2.489	2.529	2.575	2.683	2.813	2.971	3.156	3.371
$G_{(wet)} \times H_i$ kcal/kg	7235	7311	7341	7325	7293	7233	7184	7104
$G_{(wet)} \times H_s$ kcal/kg	7534	7630	7682	7719	7752	7774	7820	7859
η_i %	89.6	90.4	90.9	90.7	90.3	89.5	88.9	87.9
η_s %	89.6	94.4	95.1	95.5	95.3	96.2	96.8	97.3
ξ %	100	99.1	97.3	92.7	88.2	83.1	77.6	70.8
Oxygen Consumption								
SCM/SCM (wet)	0.25	0.2391	0.2303	0.2152	0.1989	0.1814	0.1611	0.1385
SCM/kg C	0.6221	0.6063	0.5976	0.5912	0.5850	0.5805	0.5701	0.5573
SCM/10 ³ kcal	0.0860	0.0829	0.0814	0.0807	0.0805	0.0803	0.0793	0.0784
Steam Consumption								
SCM/SCM (wet)	0.25	0.2643	0.2815	0.3227	0.3693	0.4232	0.4832	0.5542
kg/SCM (wet)	0.201	0.2125	0.2263	0.2595	0.2969	0.3403	0.3885	0.4456
kg/kg C	0.5002	0.5388	0.5873	0.7129	0.8735	1.089	1.375	1.792

Gasification of anthracite with oxygen-steam mixture, compared with experimental results

As an example of a rotating grate gas producer operated with oxygen, one of the test runs reported by C. C. Wright, K. M. Barclay, and R. F. Mitchell²⁵ as well as by C. C. Wright and L. L. Newman²⁶ will be used. These experiments were run with two different sizes of anthracite and with coke in a Wellman-Galusha rotating grate gas producer at Trail, British Columbia (Consolidated Mining and Smelting Company of Canada, Ltd.). The test run with rice anthracite (run A) is picked out for comparison of calculation and experimental result because of the completeness of its record.* The blast during this run † was

23.36 % O ₂
75.75 % H ₂ O
0.11 % H ₂
0.78 % N ₂
<hr/>
100.00 %

The small amount of hydrogen originates from the bottled oxygen, the nitrogen from a slight air infiltration. The fuel actually gasified is assumed to be fixed carbon only. No complete measurements of the amount of gas, the products of devolatilization, and its analysis at reaction temperature of about 680 to 700°C are available, and some assumptions are necessary. Based on similar conditions, a carbonization gas quantity of 0.0474 SCM/SCM of

²⁵ C. C. Wright, K. M. Barclay, and R. F. Mitchell, Production of hydrogen and synthesis gas by the oxygen gasification of solid fuel, *Ind. Eng. Chem.*, Vol. 40 (1948), No. 4, pp. 592-600.

²⁶ C. C. Wright and L. L. Newman, The oxygen gasification of anthracite in the Wellman-Galusha producer, American Gas Association Joint Conference of Production, Chemical Committees (June, 1947). Abstracted: *Chem. Eng.*, Vol. 54 (1947), No. 6, pp. 114-115.

* Additional information by Kenneth M. Barclay, Division of Fuel Technology, The Pennsylvania State College, is duly acknowledged.

† These figures are slightly adjusted, including an allowance for losses of moisture in the ash pit. Hereby the oxygen and hydrogen balances are improved.

gas produced from the fixed carbon in the reaction zone is assumed with the following analysis:

28.0 % CO
17.0 % CO ₂
41.9 % H ₂
8.0 % CH ₄
3.7 % N ₂
1.4 % O ₂
<hr/>
100.0 %

Even if this analysis is considered to be somewhat arbitrary, the influence of the devolatilization gases is very limited, as is seen by comparing "reaction gas" and "final gas" in Table 36.

TABLE 35
OXYGEN GASIFICATION OF ANTHRACITE
(23.36% O₂, 75.75% H₂O, 0.11% H₂, 0.78% N₂)

	<i>t</i> = 680	690	700°C
<hr/>			
	34.18	36.57	38.89 % CO
	16.97	15.52	14.10 % CO ₂
	36.97	37.19	37.35 % H ₂
	10.83	9.74	8.74 % H ₂ O
	0.55	0.49	0.44 % CH ₄
	0.50	0.49	0.48 % N ₂
	<hr/>		
	100.00	100.00	100.00 %
<i>F</i>	0.2770	0.2817	0.2863 kg/SCM
<i>M</i>	0.6446	0.6316	0.6192 SCM/SCM
<i>F</i> × <i>H'</i> _C *	2227	2265	2302 kcal/SCM
<i>F</i> <i>H_F</i>	61	63	65 kcal/SCM
<i>M</i> <i>H_M</i>	15	15	15 kcal/SCM
<i>H_{i,g}</i>	2029	2102	2172 kcal/SCM
Σ <i>Q</i>	274	241	210 kcal/SCM
<i>H_G</i>	245	246	248 kcal/SCM
<i>t_R</i> = 689°C			

* The total external heat loss has been slightly reduced, compared with the reported heat balance. A deduction has also been made for heat put in by the enthalpy of mineral matter and unburnt carbon. This brings the loss down to a fictitious number of 0.5% or *H'*_C = 8039.6 kcal/kg.

TABLE 36

OXYGEN GASIFICATION OF ANTHRACITE

(Comparison of Calculated [at 689°C] Value with Experimental Data [Dry Basis])

Calculated		Measured	
"Reaction Zone"	Final (Exit) Gas	Corrected Analysis *	Original Analysis
40.30 %	39.73 %	39.90 %	39.75 % CO
17.38 %	17.36 %	17.77 %	17.70 % CO ₂
41.23 %	41.25 %	40.71 %	40.55 % H ₂
0.55 %	0.89 %	0.85 %	0.85 % CH ₄
0.54 %	0.70 %	0.70 %	1.00 % N ₂
...	0.07 %	0.07 %	0.15 % O ₂
100.00 %	100.00 %	100.00 %	100.00 %

* The correction made refers to the assumption that 0.07% excess oxygen is due to a slight air infiltration during analyzing. Accordingly this amount of oxygen and a corresponding amount of nitrogen have been deducted.

The remaining differences are within the limits of deviation of measurements and constants used for calculation. The temperature of 689°C gives a satisfactory approach to the experimental data so that the slight correction of the heat balance is justified.

The Thyssen-Gálocsy process

Oxygen gasification of solid fuels according to the Thyssen-Gálocsy-Koller process consists of two-stage oxygen introduction in such a manner that gas (recycle gas or extraneous gas) is burned in a pre-chamber with an appreciable excess of oxygen, with simultaneous addition of steam. This gas mixture, containing oxygen, is introduced into the coke bed of the gas producer. The inventors claim as a main advantage of this process that the temperature peaks are eliminated and can be handled by ordinary commercial means (water cooling), and that the additional amount of heat introduced by recycling part of the product gas is equivalent to more than 1700°C preheat of the blast. Therefore high reaction temperatures are reached in spite of the addition of large amounts of steam. The process affords all advantages of the slagging-ash producer; its economic possibilities are dependent on the cost of oxygen.

Operating results of a Thyssen-Gálocsy gas producer of 1.1 m inner diameter of the hearth during a 72-hr period are as follows: *

Coke charged	1496.07 kg/hr
Carbon charged	1271.66 kg/hr
Carbon per square meter of hearth area	1338 kg C/m ² hr
Oxygen (raw)	1038.2 SCM/hr
Purity	90%
Saturation temperature	79.9°C
Recycle gas	679.4 SCM/hr
Saturation temperature	29°C
Steam	750.38 kg/hr

Calculations have shown that the blast possibly was not 100% saturated or lost part of its moisture due to temporary cooling. If we assume an average saturation of 95%, the blast consisting of oxygen, steam, and recycle gas has this analysis:

35.91 % O ₂
34.04 % H ₂ O
18.42 % CO
0.68 % CO ₂
6.05 % H ₂
0.05 % CH ₄
4.85 % N ₂

$$100.00 \%$$

$$H_{iM} = 716 \text{ kcal/SCM}$$

This unusual blast, including C, H, O, N, makes it necessary to use equations 160–163, but involves no principal difficulty. Table 37 shows the result of the calculation including the gas composition at 856°C, reaction temperature if the external heat losses amount to 8.17% of the heating value of the carbon.

In the comparison of calculated and measured data, it is obvious that the approach of the methane reaction is possibly close to $x_M = 1$. The higher methane content may be attributed to the volatile matter of the coke (a more complete coke analysis was not available), and the higher x_M value may be accounted for by the fact that for smooth slag tapping operation iron oxide and open hearth slag had been added as a flux. This, indeed, is known

* Courtesy of Thyssen'sche Gas- und Wasserwerke G.m.b.H., Duisburg-Hamborn, Germany.

TABLE 37

GAS COMPOSITION (THYSSEN-GÁLOCSY PRODUCER)

$t =$	800°	850°	900°	856°C
% CO	65.78	69.70	71.58	70.00
% CO ₂	5.66	2.72	1.33	2.49
% H ₂	23.23	23.26	23.30	23.25
% H ₂ O	1.92	1.03	0.57	0.98
% CH ₄	0.06	0.04	0.03	0.04
% N ₂	3.35	3.25	3.19	3.24
	100.00	100.00	100.00	100.00
H _i kcal/SCM	2763	2706	2589	2715
M SCM/SCM	0.5954	0.6064	0.6289	0.6046
F kg/SCM	0.3335	0.3298	0.3223	0.3304

as an effective catalyst for methane formation and may help to raise x_M to or closer to 1.

With these operating conditions, and $x_M = 1$, fuel consumption is 0.33140 kg/SCM of total product gas, gas yield is 3.0175 SCM/kg, blast is 0.60536 SCM/SCM. 26.06% of the blast is

TABLE 38

THYSSEN-GÁLOCSY PROCESS

(Comparison of Calculation and Experimental Results)

	Calculated Analysis (Dry Basis)		Measured Analysis	
	$x_M = 0.24$ $x_M = 1$		Reduced to Zero	As Reported
			O ₂	
% CO	70.69	70.78	70.67	70.6
% CO ₂	2.51	2.52	2.60	2.6
% H ₂	23.48	23.28	23.22	23.2
% CH ₄	0.04	0.15	0.20	0.2
% N ₂	3.27	3.27	3.20	3.3
% O ₂	0.1
%	100.00	100.00	100.00	100.0

recycled gas, 38.94% O₂(+N₂), 35.00% H₂O; therefore 0.15776 SCM/SCM has to be recycled, 84.224% of the gas yield or 2.5415 SCM/kg C are actually available product gas. With these figures and 2721.6 kcal/SCM net heating value of the gas,

$$F = 0.3935 \text{ kg/SCM product gas}$$

$$\begin{aligned} \text{O}_2 \text{ consumption} &= \frac{0.60536}{0.84224} \times 0.3591 \\ &= 0.2581 \text{ SCM/SCM product gas} \\ \eta &= \frac{2.5415 \times 2721.6}{8080} \times 100 = 85.6\% \end{aligned}$$

if based on carbon alone.

Fuel and oxygen consumption are slightly higher and gasification efficiency somewhat lower than the continuous gasification with 40% O₂ + 60% H₂O without gas recycling. Recycling has no thermal advantage; its only virtue is that it introduces oxygen without excessive heat peaks and hot spots.

Water-gas production

The composition of water gas, obtained by gasification of carbon (coke) with steam, is 50% CO, 50% H₂ at complete decomposition. Since the formation of water gas (see equation 3) is a strongly endothermic reaction, the required amount of heat has to be introduced into the process somehow. This is done conventionally by alternately blowing with air to produce heat and with steam to gasify. Other ways, operating continuously, are (1) external heating (indirect heating by heating surfaces); (2) heating by gas recycling (direct heating with recycle or purge gases); (3) electric heating; and (4) combinations of methods (1), (2), (3).

Finally the continuous gasification with oxygen-steam mixtures produces a semi water gas somewhat richer in CO (see Table 34); with 74.25% H₂O + 25.75% O₂ the CO/H₂ ratio of 1 is reached. The continuous process, therefore, includes (5) gasification with oxygen-steam mixtures and (6) combinations of methods (1) to (5).

Table 39 shows the calculated analysis of water gas at various temperatures, based on $x_B = x_W = 1$; $x_M = 0.24$. Fuel consumption (F), steam blast (M), and gas yields relate to the gas period only, not to the whole cycle. (See also Figures 35 and 36.)

When the air blast phase of the operating cycle starts, after the fuel bed has been cooled down in the preceding gas period, a rather low-grade producer gas is made. As the temperature rises, and as the heat equilibrium is re-established, the gas is improved (this

TABLE 39

WATER-GAS PRODUCTION FROM CARBON BY STEAM

t_R °C	1000	900	800	750	700	650	600	550	500°C
% CO	49.64	48.72	44.81	39.75	31.68	21.86	12.92	6.57	2.90
% CO ₂	0.16	0.61	2.63	5.25	9.36	14.02	17.62	19.26	19.14
% H ₂	49.86	49.72	49.50	49.36	48.88	47.33	43.88	38.29	31.02
% H ₂ O	0.28	0.83	2.78	5.19	9.32	15.50	23.44	32.48	41.86
% CH ₄	0.06	0.12	0.28	0.45	0.76	1.29	2.14	3.40	5.08
%	100.00	100.00	100.00	100.00	100.00	100.00	100.00	100.00	100.00
Dry Analysis									
% CO	49.78	49.13	46.09	41.93	34.94	25.87	16.87	9.74	4.99
% CO ₂	0.16	0.62	2.70	5.54	10.32	16.59	23.02	28.52	32.62
% H ₂	50.00	50.13	50.92	52.06	53.90	56.01	57.31	56.71	53.35
% CH ₄	0.06	0.12	0.29	0.47	0.84	1.53	2.80	5.03	8.74
	100.00	100.00	100.00	100.00	100.00	100.00	100.00	100.00	100.00
F^* kg/SCM	0.2672	0.2650	0.2556	0.2436	0.2240	0.1992	0.1751	0.1566	0.1454
M SCM/SCM	0.5025	0.5078	0.5284	0.5545	0.5972	0.6541	0.7160	0.7757	0.8304
$G_{(wet)}$ SCM/kg	3.743	3.774	3.912	4.106	4.465	5.021	5.711	6.385	6.880
$G_{(dry)}$ SCM/kg	3.733	3.743	3.803	3.893	4.049	4.243	4.372	4.311	4.000
ξ %	99.4	98.4	94.7	90.6	84.4	76.3	67.3	58.1	49.6

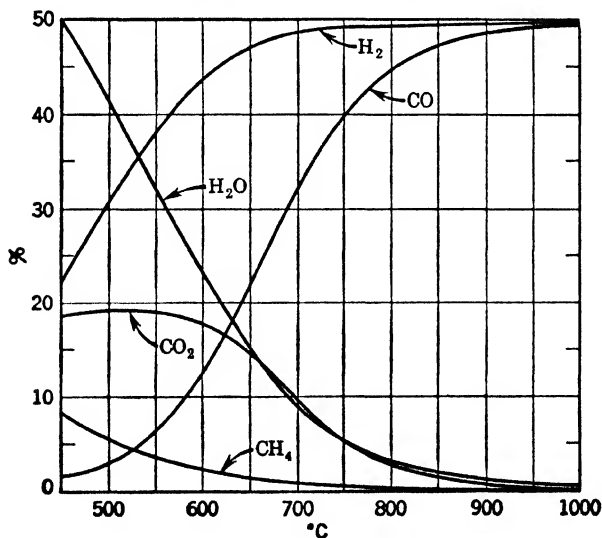


FIG. 35. Water-gas from carbon (wet basis).

is not desirable, however, because of the poorer heat utilization). Even if the resulting gas is burnt by secondary air, and its chemical heat is used for preheating the blast or raising steam in waste heat boilers, this standard water-gas process, although still prevailing today, is thermally and mechanically unsatisfactory. The future will see this process outmoded and replaced by continuous methods.

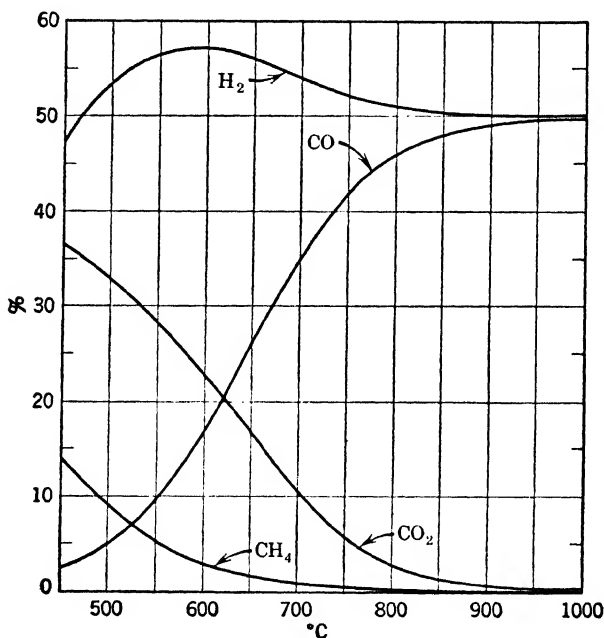


FIG. 36. Water-gas from carbon (dry basis).

The calculation of the whole cycle of the discontinuous water-gas process is a rather difficult problem. In contrast to the problem of heat accumulation with inactive surfaces, this is a process which combines heat accumulation and gasification, in which the surface temperatures are not primarily dependent upon heat transfer considerations because of the active surface but tend to remain at or approach equilibrium with the gas. The fuel bed could be considered a regenerative heat exchanger with limited maximum temperatures.

In reverse order, it is quite easy to draw conclusions from the gas analysis regarding the surface temperature (reaction tempera-

ture) of the coke. The average temperature of the coke is usually approximately 750 to 780°C, which results in the following limits of the (dry) gas composition:

5.5 to 3.6%	CO ₂
41.9 to 44.2%	CO
52.1 to 51.2%	H ₂
0.5 to 0.4%	CH ₄

In practice water gas is a mixture of water gas of this analysis and a certain amount of producer gas, which dilutes the product gas if the cycle is switched from air blow to steam blow. If a relatively high-grade producer gas ($t_R = 750^\circ\text{C}$, 31% CO, 2% H₂, 3% CO₂, 64% N₂) and 6% admixture of blow gas are assumed, the following final analysis results (at 750°C): 41.3% CO, 5.4% CO₂, 49.1% H₂, 0.4% CH₄, 3.8% N₂.

Experimental results on an old-type water-gas producer²⁷ show 7.04 to 1.60% CO₂ during the blow period, corresponding to a temperature fluctuation of 120°C. During the gas period, 1.8 to 5.6% CO₂ were measured, corresponding to only 80°C. The change-over of the cycles takes place slowly, and considerable time elapses between the end of the blow period and the beginning of the gasification with steam. Meanwhile, part of the temperature level attained is lost by heat-equalizing processes. The development, therefore, turned to short blow periods and rapid (mechanized) shifting, improving gas quality, and economy.

One of the first steps in this direction was made by the Dellwik-Fleischer water-gas producer.²⁸ CO₂ contents of 0.4 to 14.1% are reported in the gasification period, corresponding to 900 to 670°C, $\Delta t = 230^\circ\text{C}$. These high temperatures were made possible by blowing with dry air and by preheating of the steam at the beginning of the gasification period.

The mineral matter of the fuel, although undesirable in general, plays an important part in water-gas production. As long as free carbon is present, temperatures of the solids are limited. After the carbon has disappeared there is no more limitation in temperature, and the mineral matter can be heated to much higher temperatures, unhindered by endothermic reactions, and thus will con-

²⁷ Paul Dolch, *Wassergas. Chemie und Technik der Wassergasverfahren*, Leipzig, 1936, p. 123.

²⁸ P. Dolch, *op. cit.*, p. 130.

tribute to greater heat accumulation in the gas producer stock column. For this reason a limited ash content is even desirable, although the softening temperature should be as high as possible in order to allow high temperatures during the blow period without clinkering trouble.

Temperature fluctuations up to 670°C ²⁹ cannot be interpreted as a fluctuation of the temperatures proper of the solids but as influence mainly of the gas phase temperature. The findings of Foster and Vorum,³⁰ who have reported temperature fluctuations of 417 to 472°C in the lower sections and 167 to 250°C in the higher sections of the fuel bed of a water-gas generator, indicate not only an influence of the hot gas film but also a higher solids temperature in the lower sections where ash content is enriched.

The heat balance of a water-gas process, regardless of the kind of heat supply, shows that, at 6% external heat losses and at a reaction temperature of 750°C , the enthalpy of the steam entering with 300°C represents only 2.2% of the total heat requirement. If the superheat of the entering steam is increased to 900 and 1500°C , the percentages become 6.9 and 12.5. Although preheating of the blast is very beneficial to the economics of the gasification process and to the gas quality, these figures show clearly that this method of covering the heat requirements by superheating, as suggested by Pattenhausen, is impractical.

In any recycle process, therefore, the amount of gas circulated must be much larger than the normal blast. If the final temperature of the recycled gas is taken as 1200 to 1300°C , the amount of recycle gas required will be 4.6 SCM/SCM of water gas. The principal disadvantage of all recycle processes is the limitation of the gas temperature or maximum temperature of the materials of the heating regenerators. In powdered coal recycle gasification (Schmalfeldt-Wintershall process), where conditions are unfavorable because of concurrent exchange, this is specially true, and the gas quality is affected unfavorably. If this process is combined with other heat production processes, such as partial addition of oxygen, the gas quality and yield can be materially improved.

Finally, the heat supply by electricity, preferably where it is available at low cost from water power or cheap fuels, is to be

²⁹ *Ibid.*, p. 193.

³⁰ John F. Foster and Donald A. Vorum, Research on the mechanism of the water-gas reaction, *Proc. A.G.A.*, 1947, pp. 723-732.

mentioned. The carbon necessary for heat supply can be replaced by electric current; the carbon necessary for reduction has to be supplied as coke or similar solid fuel. Ivar Hole³¹ reports the following analysis of electro water gas, given in the right-hand column of Table 40.

TABLE 40
ELECTRO WATER GAS

Calculated ($t_R = 850^\circ\text{C}$)		Reported by I. Hole
Wet	Dry	Dry
47.45	48.17 % CO	48% CO
1.26	1.28 % CO ₂	1% CO ₂
49.61	50.37 % H ₂	51% H ₂
1.50	... % H ₂ O	...
0.18	0.18 % CH ₄	...
<hr/> 100.00	<hr/> 100.00 %	0.1% SO ₂
		0.1% N ₂
H_i 2723	2765 kcal/SCM	2760 kcal/SCM
F 0.262		0.260 kg/SCM
M 0.402		0.420 kg/SCM
G 3.82		3.84 SCM/kg
Q_{El} 1.10		1.47 kw/SCM
Q_{ext} 10% (assumed)		

The fuel was anthracite (analysis not reported) with 3.5 to 5% ash content. The fuel consumption is 300 kg/1000 SCM of dry gas (corresponding to 0.296 kg/SCM [wet] or 0.283 kg/SCM [wet] ash-free, moisture-free basis = 0.260 kg C, assuming 91.5% fixed carbon + 8.5% volume matter in the fuel). The steam consumption of 420 kg/1000 SCM (wet) is an average round figure and possibly too high (or including losses by condensation). The gas analyses are in good correlation. The power consumption of 1.10 kw/SCM is calculated with an assumed external heat loss of 10% of the fuel heat input, 400°C steam inlet temperature. The actual consumption (1.47 kw/SCM) was higher, which may be due to higher external heat losses and some moisture of the fuel neglected in the calculation and to less steam superheating (temperature not reported).

³¹ Ivar Hole, Der Elektrogaserzeuger, Bauart Hole, *Feuerungstechn.*, Vol. 27 (1939), No. 9, pp. 259-260.

Effect of pressure on gasification

Water Gas at High Pressure. One possible operating variable for influencing the result of gasification is the use of higher pressures. Whereas only pressures of 8 at (gage) were mentioned in earlier proposals,³² proposals which were not carried out in practice, the Lurgi Gesellschaft für Wärmetechnik m.b.H., Frankfurt/Main, Germany, first used pressures of 20 at for the gasification of solid fuels with oxygen, a process originated by O. Hubmann.

Installations on a commercial scale were erected at Hirschfelde and Böhlen, Saxony, and Brüx (Most), Bohemia. The advantages of high pressure gasification are:

- (1) The dimensions of the gas producer and all piping are smaller.
- (2) The capacity is higher (theoretically proportional to pressure but practically on account of limited flow rates and higher carry-over losses about proportional to the square root of the pressure).
- (3) The gas heating value can be increased (sacrificing gas yield) by removing CO_2 by pressure washing and H_2O by condensation.
- (4) A heating value of 4000 kcal/SCM, dry, CO_2 -free basis, equal to standard city gas, can be reached at pressures which can be handled commercially (20 at with dry lignite, 50 at with pure carbon), using oxygen-steam mixtures as a blast.

The effect of pressure is based on the shift of the gas equilibria. According to the principle of least resistance (see p. 15), the Boudouard equilibrium is shifted toward the CO_2 side, the heterogeneous water-gas equilibrium is shifted toward the H_2O side, and the methane equilibrium toward CH_4 formation. Consequently, the gasification takes place on a higher temperature level.

To demonstrate the influence of pressure at a constant temperature, Table 41 shows calculated water-gas analyses at constant temperatures.

These calculations have been based on the assumption that the fuel is pure carbon and that the influence of pressure upon the

³² Jules Deschamps, *Les gazogènes*, Paris, 1902, pp. 258-272 (gas producer type "Gardie").

TABLE 41

INFLUENCE OF PRESSURE UPON THE WATER-GAS ANALYSIS

$t_R = 700^\circ\text{C}$	Pressures in Atmospheres				
	1	10	25	50	100
% CO	31.68	13.19	8.60	6.15	4.38
% CO ₂	9.36	16.21	17.23	17.62	17.84
% H ₂	48.88	36.94	29.36	23.64	18.44
% H ₂ O	9.32	29.32	37.97	43.72	48.54
% CH ₄	0.76	4.34	6.84	8.87	10.80
	100.00	100.00	100.00	100.00	100.00
Dry Basis					
% CO	34.94	18.66	13.86	10.92	8.50
% CO ₂	10.32	22.94	27.78	31.31	34.67
% H ₂	53.90	52.27	47.33	42.00	35.84
% CH ₄	0.84	6.13	11.03	15.77	20.90
	100.00	100.00	100.00	100.00	100.00
$H_i(\text{wet})$ kcal/SCM	2278	1719	1599	1552	1530
$H_i(\text{dry})$ kcal/SCM	2512	2431	2578	2758	2972
$H_i(\text{dry, CO}_2\text{-free})$ kcal/SCM	2801	3155	3570	4015	4549
$t_R = 800^\circ\text{C}$					
% CO	44.81	27.99	20.13	15.11	11.11
% CO ₂	2.63	10.25	13.24	14.93	16.14
% H ₂	49.50	44.08	38.30	32.79	26.95
% H ₂ O	2.78	15.48	24.18	31.00	37.58
% CH ₄	0.28	2.20	4.15	6.08	8.22
	100.00	100.00	100.00	100.00	100.00
Dry Basis					
% CO	46.09	33.12	26.54	21.92	17.80
% CO ₂	2.70	12.12	17.46	21.66	25.86
% H ₂	50.92	52.16	50.52	47.59	43.17
% CH ₄	0.29	2.60	5.48	8.83	13.17
	100.00	100.00	100.00	100.00	100.00
$H_i(\text{wet})$ kcal/SCM	2649	2166	1947	1819	1731
$H_i(\text{dry})$ kcal/SCM	2725	2563	2568	2640	2773
$H_i(\text{dry, CO}_2\text{-free})$ kcal/SCM	2801	2917	3112	3370	3740
$t_R = 900^\circ\text{C}$					
% CO	48.72	40.77	33.74	27.63	21.69
% CO ₂	0.61	4.31	7.37	9.88	12.19
% H ₂	49.72	47.25	43.90	39.84	34.64
% H ₂ O	0.83	6.61	12.70	18.87	25.76
% CH ₄	0.12	1.06	2.29	3.78	5.72
	100.00	100.00	100.00	100.00	100.00
Dry Basis					
% CO	49.13	43.65	38.65	34.06	29.22
% CO ₂	0.62	4.61	8.44	12.18	16.42
% H ₂	50.13	50.60	50.28	49.10	46.66
% CH ₄	0.12	1.14	2.63	4.60	7.70
	100.00	100.00	100.00	100.00	100.00
$H_i(\text{wet})$ kcal/SCM	2759	2536	2343	2182	2034
$H_i(\text{dry})$ kcal/SCM	2782	2716	2684	2689	2740
$H_i(\text{dry, CO}_2\text{-free})$ kcal/SCM	2799	2847	2931	3062	3278

enthalpy of the gases as well as upon the equilibrium constant of the water-gas reaction is negligible. Because at high pressures there is a marked difference between "real" and "ideal" gas, there is also an effect on the homogeneous water-gas reaction equilibrium constant. According to Sartori and Newitt,³³ the equilibrium constant of the homogeneous water-gas reaction is at 400°C, and

$P =$	10	60	80	100 Atm
$K =$	0.096	0.106	0.109	0.112

For the sake of simplification these influences and possible improvements of the calculation are not taken into account.

Water Gas at Pressures below 1 Atm. The deep influence of pressure is reversed if gasification under vacuum is considered. Such processes are of little practical and economical value because all items registered as advantages of the pressure operation are disadvantages of a vacuum process, especially if high vacua are used.

From a merely theoretical point of view the trend of influence of pressure is more clearly and impressively demonstrated if the shift in both directions is shown. Table 42 shows the gas analyses

TABLE 42
GASIFICATION UNDER VACUUM

$t_R = 700^\circ\text{C}$	$P = 0.1$	0.01	0.001 Atm
% CO	46.34	49.58	49.96
% CO ₂	2.00	0.23	0.02
% H ₂	50.18	50.03	50.00
% H ₂ O	1.40	0.15	0.01
% CH ₄	0.08	0.01	0.01
	<hr/>	<hr/>	<hr/>
	100.00	100.00	100.00
Dry Basis			
% CO	47.00	49.66	49.97
% CO ₂	2.03	0.23	0.02
% H ₂	50.89	50.10	50.00
% CH ₄	0.08	0.01	0.01

calculated at pressures below atmospheric; and Figure 37 presents the whole range of 0.001 to 100 Atm at 700°C reaction temperature.

³³ G. Sartori and D. M. Newitt, The influence of pressure upon water gas and other equilibria, *Engineering*, Vol. 149 (1940), No. 3865, p. 157.

Producer Gas under Pressure. A gas producer operated under the same conditions, except for elevated pressure, will attain a

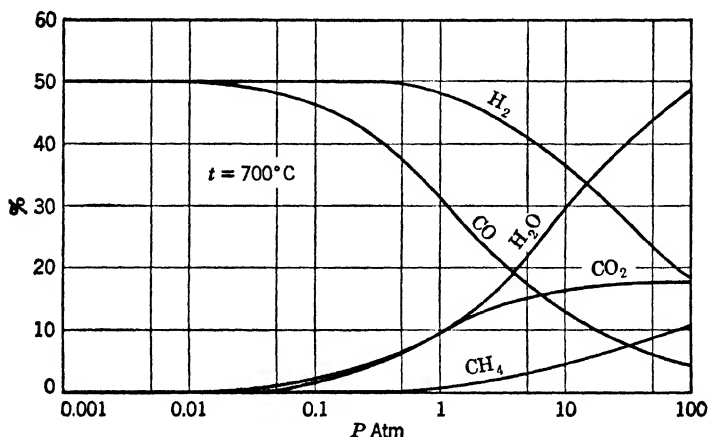


FIG. 37. Water gas from carbon. Influence of pressure ($t_R = 700^{\circ}\text{C}$, $P = 0.001$ to 100 Atm).

higher reaction temperature, balanced by a decrease of the heating value due to higher CO_2 and H_2O contents. The result of a gasification of carbon at atmospheric pressure with air-steam mixture

TABLE 43

PRESSURE GASIFICATION WITH AIR-STEAM MIXTURE

$$(v'_{\text{H}_2\text{O}} = 0.17451)$$

$$P = 20 \text{ Atm}; Q_{\text{ext}} = 1.79\%$$

$t = 700^{\circ}$	800°	900°	1000°	$t_R = 932^{\circ}\text{C}$
9.08	19.61	29.85	35.39	32.16 % CO
15.38	10.05	4.62	1.67	3.38 % CO_2
7.33	9.70	11.30	12.17	11.65 % H_2
8.01	4.77	2.31	0.99	1.78 % H_2O
0.34	0.21	0.12	0.07	0.10 % CH_4
59.86	55.66	51.80	49.71	50.93 % N_2
100.00	100.00	100.00	100.00	100.00 %
H_i (wet) 492	859	1202	1388	1279 kcal/SCM
F 0.1329	0.1601	0.1853	0.1989	0.1910 kg/SCM
M 0.9179	0.8535	0.7942	0.7622	0.7809 SCM/SCM

($v'_{\text{H}_2\text{O}} = 0.17451$) is shown in Table 44, left-hand column. Under the same conditions, but at a total pressure of 20 Atm, the reaction temperature rises to 932°C ; the result is shown in the right-hand column of Table 44. At these temperatures, however, the operation of a rotating grate is impossible.

TABLE 44

COMPARISON OF ATMOSPHERIC AND PRESSURE GASIFICATION OF CARBON
(CALCULATED)

($v'_{\text{H}_2\text{O}} = 0.17451$; see Tables 18 and 43)

$P =$ $Q_{\text{ext}} =$ $t_R =$	1 Atm 8% 716°C		20 Atm 1.79% 932°C	
	(Wet)	(Dry)	(Wet)	(Dry)
% CO	28.82	29.29	32.16	32.74
% CO ₂	5.50	5.59	3.38	3.34
% H ₂	12.19	12.39	11.65	11.86
% H ₂ O	1.61	...	1.78	...
% CH ₄	0.04	0.04	0.10	0.10
% N ₂	51.84	52.69	50.93	51.85
	100.00	100.00	100.00	100.00
H_i kcal/SCM	1187	1206	1279	1302

From a comparison of Tables 43 and 44, we arrive at the following conclusions:

- (1) At the same reaction temperature the gas under pressure will be much poorer than at atmospheric pressure (1 Atm 1184 kcal/SCM; 20 Atm \sim 500 kcal/SCM); meanwhile the reaction temperature will rise with increasing pressure.
- (2) The reaction temperature (by self-adjustment) is considerably higher under pressure; hence the heating value will be of about the same magnitude or even higher than at atmospheric pressure. Since such high temperatures are sometimes undesirable, we may conclude as in (3).

- (3) Gasification under pressure allows a much higher steam content in the blast; it demands a high steam ratio if dry slag removal is applied.

The influence of a higher steam ratio is represented in Table 45. Judging from the reaction temperature, a steam content of the

TABLE 45
PRESSURE GASIFICATION WITH AIR-STEAM MIXTURES
($P = 20$ Atm; $Q_{ert} = 1.79\%$; $v'_{H_2O} = \text{variable}$)

v'_{H_2O} t_R	0.17451 * 932	0.50 815	0.60 775	0.70 734°C
CO	32.16	22.55	17.64	12.84
CO ₂	3.38	10.23	12.82	15.07
H ₂	11.65	24.57	26.20	26.64
H ₂ O	1.78	11.27	16.69	23.32
CH ₄	0.10	1.19	1.98	3.11
N ₂	50.93	30.19	24.67	19.02
	100.00	100.00	100.00	100.00
H_i kcal/SCM	1279	1414	1375	1338
F kg/SCM	0.1910	0.1820	0.1738	0.1662
G SCM/kg	5.236	5.495	5.754	6.017
GH_i kcal/kg	6697	7770	7912	8051
η_g %	82.9	96.2	97.9	99.6
η_{therm} %	80.1	84.2	82.3	80.2
M SCM/SCM	0.7810	0.7644	0.7808	0.8026
Steam kg/SCM	0.1096	0.3073	0.3767	0.4517

* See Table 44.

blast of about 70% is necessary to operate with dry ash removal and rotating grates. The gasification efficiency rises as this ratio is increased. The only disadvantage is that the higher steam requirement cannot be provided by the steam jacket, as is generally the case for gasification at atmospheric pressure, so that other sources of steam have to be utilized. If a separate production of steam by generation in a boiler is considered, as the quantity obtained in the jacket is insufficient, the thermal efficiency

may be defined as the ratio of heat delivery (in the product gas) to the heat supplied to the gas producer and to the boiler.

$$\eta_{therm} = \frac{GH_i}{H_F + \frac{E}{\eta_B}} \quad (298)$$

where E represents the enthalpy of any external heat source (raising steam or superheating the blast) and η_B the boiler (or superheater, air preheater) efficiency. The difference between η_g and η_{therm} increases with the steam content of the blast. With $v'_{H_2O} = 0.70$, the jacket steam (assuming the total heat loss of 1.79% used for raising steam in the jacket) provides only 8% of the total requirements; 92% must be delivered by a steam boiler. A boiler efficiency of 85% is assumed in the calculations given in Table 45. The picture looks somewhat more favorable if exhaust steam is used or if other sources of waste heat are available, such as the cooling of the combination chamber of a gas turbine.

Another advantage of pressure gasification is the simple and inexpensive transmission and utilization of the pressured gas. No gas compressor is required. Compression is limited to the air and the boiler feedwater, pipes are small in diameter, permissible pressure drop due to friction may be high. For this reason the combination of pressure gasification and gas turbine has been recommended as an obviously simple device for the production of energy.³⁴ However, the question of steam production outside the system needs more careful consideration.

The gas turbine offers a much simpler setup than the modern high-pressure steam plant; on the other hand, pressure gasification with rotating grates and its high steam requirements is by no means as simple as desirable. It is to be noted also that the higher heating value and CH_4 content of the pressure gas require more combustion air (which also has to be compressed to gas turbine inlet pressure), balancing the advantage of a smaller air requirement for gasification (see Table 46). As the theoretical combustion temperature is too high, combustion with extremely high excess air ratios or admission of additional cooling air is

³⁴ L. Musil, Vereinheitlichung und technische Entwicklung im Bau von Wärmekraftwerken, *Arch. Wärmewirtsch.*, Vol. 25 (1944), No. 7/8, pp. 111-114.

required to keep the gas inlet temperature at 700°C (or higher, according to turbine blade material and development). The total air requirement is thus about 29.5 SCM/kg C. With this quantity of total air, the differences shown in the third line of Table 46 are not of economic significance.

The development of a high-rate gas producer in connection with gas turbines is as urgent a problem as the turbine itself. If by raising inlet temperatures and utilizing the waste heat, the inlet pressure of the turbine is kept low, pressure gasification offers no

TABLE 46
PRESSURE GASIFICATION AND COMBUSTION

P v'_{H_2O}	20	20	20	20	1
	0.17451	0.50	0.60	0.70	0.17451
Air requirement:					
For gasification	3.376	2.100	1.797	1.449	3.565
For combustion	5.512	6.526	7.091	7.423	5.325
Total SCM/kg C	8.888	8.626	8.888	8.872	8.890

decisive advantage. If higher pressures are used, a limitation of outside steam is imperative, and a slagging ash type (with quite a number of unsolved engineering problems) is preferable. With regard to utilization of the gas enthalpy, future development depends upon the possibility of a hot gas cleaning (under pressure) effective enough to avoid excessive blade wear.

These questions, to which brief reference has been made, show that in the future there will be numerous problems in gas technology for which solutions must be found. The incorporation of gas production into the field of power poses problems which require new solutions because of their completely different economic and technical background.

Pressure Gasification with Oxygen-Steam Mixtures. Pressure gasification with oxygen and steam has so far been the most important application of pressure in gas technology from a practical point of view. Results obtained in Lurgi high-pressure gas pro-

ducers with various fuels have appeared in the technical literature to some extent.³⁵⁻⁴⁰

To isolate the influence of pressure without the disturbing effect of volatile matter, the following calculations assume pure carbon as the fuel, $\alpha_B = \alpha_W = 1$; $\alpha_M = 0.24$; Q_{ext} a function of \sqrt{P} .

$P = 1$	10	100	1000 Atm
$Q_{ext} = 8$	2.53	0.8	0.253%

Reaction temperature is kept constant throughout Table 47 by adjusting the steam-oxygen ratio.

The results of these somewhat laborious calculations are presented in Figure 38, which clarifies the advantages and the limits of the application of high pressures. With appropriate measures (extremely high pressures, scrubbing out CO_2) gas heating values of more than 6000 kcal/SCM can be obtained. If coal is used instead of pure carbon, higher heating values or equal results at lower pressures are obtained which are due to the effect of the volatile matter.*

From the engineering standpoint, the design of gasification for operation at extremely high pressures has two problems, the provision of materials of construction which will withstand the pressure and the provision of materials which will withstand contact with hot gases. The practicability of gasification at extreme pressures is open to future development. Capacity of gas producers as well as pipe lines reaches a magnitude unknown in previous practice, but a series of difficult construction problems

³⁵ Fr. Danulat, *Die restlose Vergasung fester Brennstoffe mit Sauerstoff unter hohem Druck*, Thesis, Berlin, 1935.

³⁶ Fr. Danulat, *Die Sauerstoff- Druckvergasung fester Brennstoffe, Gas- u. Wasserfach*, Vol. 84 (1941), No. 40, pp. 549-552.

³⁷ Fr. Danulat, Wechselwirkungen zwischen Gas und Brennstoff bei der Druckvergasung, *Gas- u. Wasserfach*, Vol. 85 (1942), No. 49/50, pp. 557-562.

³⁸ Rudolf Drawe, Erfolge der Druckvergasung mit Sauerstoff, *Arch. Wärmewirtsch.*, Vol. 19 (1938), No. 8, pp. 201-203.

³⁹ Horace M. Weir, High pressure gasification in Germany, *Ind. Eng. Chem.*, Vol. 39 (1947), No. 1, pp. 48-54.

⁴⁰ L. L. Newman, Oxygen in the production of hydrogen or synthesis gas, *Ind. Eng. Chem.*, Vol. 40 (1948), No. 4, pp. 559-582 (Lurgi Pressure-Gasification Process, pp. 571-577).

* The composition of gas of devolatilization is affected by pressure in much the same manner as gasification gas. As the pressure is raised, the CH_4 , CO_2 , and H_2O contents are increased and the H_2 and CO contents are lowered.

TABLE 47

PRESSURE GASIFICATION OF CARBON WITH STEAM-OXYGEN MIXTURES

t_R °C	700				800
P Atm	1000	100	10	1	100
H ₂ O %	96.52	94.10	87.70	71.15	90.0
Wet basis					
% CO	1.46	4.71	15.03	40.70	12.44
CO ₂	19.85	20.67	21.06	15.44	20.25
H ₂	6.62	17.06	31.86	34.92	23.78
H ₂ O	58.14	48.32	28.82	8.55	37.13
CH ₄	13.93	9.24	3.32	0.39	6.40
	100.00	100.00	100.00	100.00	100.00
H_i kcal/SCM	1191	1371	1549	2160	1534
F kg/SCM	0.1888	0.1855	0.2107	0.3029	0.2095
M SCM/SCM	0.9596	0.8912	0.7655	0.6219	0.8178
G SCM/kg	5.297	5.391	4.747	3.302	4.774
ξ %	37.2	42.4	57.1	80.7	49.6
$\eta_{gasif} (H_i)$ %	78.1	91.4	91.0	88.3	90.6
O ₂ consumption					
SCM/SCM	0.0334	0.0526	0.0942	0.1794	0.0883
SCM/10 ³ kcal	0.0280	0.0384	0.0608	0.0831	0.0576
Dry Basis					
% CO	3.49	9.11	21.11	44.50	19.79
CO ₂	47.42	40.00	29.59	16.89	32.21
H ₂	15.82	34.01	44.77	38.19	37.82
CH ₄	33.27	17.88	4.53	0.42	10.18
	100.00	100.00	100.00	100.00	100.00
H_i kcal/SCM	3357	2652	2176	2362	2440
G SCM/kg	2.217	2.786	3.379	3.019	3.001
Dry; CO ₂ -free basis					
% CO	6.63	15.19	29.98	53.54	29.20
H ₂	30.09	55.01	63.58	45.95	55.79
CH ₄	63.28	29.80	6.44	0.51	15.01
	100.00	100.00	100.00	100.00	100.00
H_i kcal/SCM	6384	4421	3090	2841	3599
G SCM/kg	1.166	1.671	2.379	2.510	2.035

must be solved in the course of this new development.* Besides increasing heating value, the decreasing of oxygen consumption

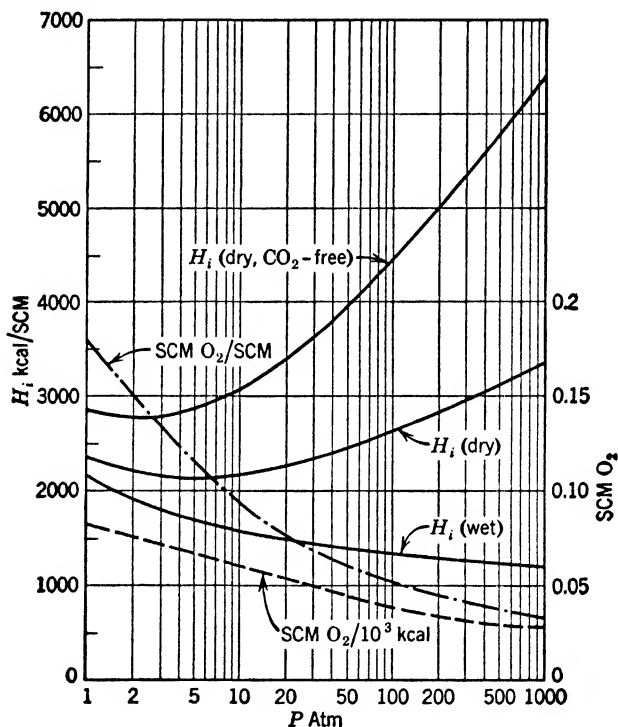


FIG. 38. Pressure gasification of carbon with oxygen-steam mixtures ($t_R = 700^\circ C$).

renders high-pressure gasification very attractive because oxygen is an important factor in the cost of product gas.

* In practice the chemical industry, e.g., hydrogenation and ammonia synthesis, is familiar with pressures up to 700 Atm.

P A R T T W O

Blast Furnaces

7

COMPOSITION OF GAS IN BLAST FURNACES

Reactions in the blast furnace

Blast furnaces may be regarded as gas producers in which other reactions, such as sintering, smelting, dehydrating, deacidifying, and reducing, take place at the same time. These reactions affect the heat balance of the furnace, as well as the gas composition, chiefly insofar as gaseous constituents are separated from the charge, for example, or exchanges take place between the gases and the burden, as in the reduction of the solid oxides in the burden. Conversely, gas producers are also blast furnaces in which all the reactions mentioned above either do not occur at all or play hardly any part in the heat balance because of the low proportions of such substances as oxides, carbonates, and sulfates, even though they are present in all fuel ash. The slag-tap gas producer, which is fired with high-ash fuel and special fluxes, is an intermediate stage between the gas producer proper and the blast furnace. The fluxes are chiefly intended to increase the fusibility of the slag, thus facilitating tapping. They consist either of limestone or, preferably, of furnace slag rich in iron and phosphorus, e.g., open-hearth slag, to make the iron easily fusible and to aid in heat transfer from the zone of maximum temperature (at the tuyères) to the slag bath by means of the iron trickling down. The fuel ash and the fluxes are "smelted" in the gas producer, i.e., the oxides are reduced, the carbon dioxide in the carbonates driven off, and the slag constituents fused. These are seen to be the same reactions that occur in the blast furnace, with the sole difference that in the gas producer the proportion of coke in the charge is considerably higher.

These reactions are not without influence on the composition of the gas. Not only is the heat balance affected by the fuel ash and the fluxes but the charge also contains oxygen carriers, especially ferric oxide, ferrous oxide, and phosphoric acid, which

contribute their additional oxygen to the gas in the reducing process. In practice, this is manifested in an increase in the oxygen carriers of the gas, that is, of the CO , CO_2 , and H_2O contents. In this process, no arbitrary allocation of this charge oxygen among these three constituents of the gas is possible; the heat balance and the law of mass action, rather, regulate this automatically. If we should try to determine this allocation experimentally, employing other dimensions than those of the producer or the furnace for which these questions are to be solved (semi-industrial experiment), the results would be worthless, since the basically changed external heat loss Q_{ext} would have caused a considerable change in the reaction temperatures, and thus in the equilibrium and in the composition of the gas. But this affects the result decisively, and for this reason the application of small-scale experiments to industrial installations is permissible only if great care and caution are used.

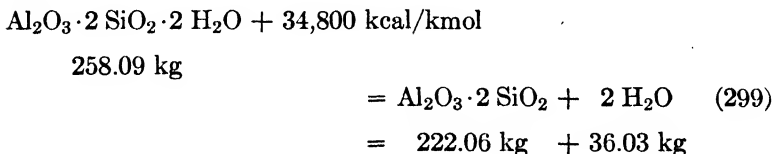
If we start with these considerations and methods of calculation, it is but a short step from the smelting of fuel ash and fluxes in a slag-tap gas producer to the smelting of ore in a blast furnace or to the slagging of the flux and smelting of the pig iron in a cupola furnace. First some general remarks on the differences between gas producers and blast furnaces. Though they are similar in external structure and general mode of operation, there are major basic differences between them in purpose and in the gas composition obtained. Whereas the purpose of the gas producer is to provide a gas with the highest possible heating value, it is the aim of blast furnaces to obtain as high smelting and combustion outputs as possible in the complete dehydration, deacidification, and reduction of the charge, and at the same time to make use of the fuel as efficiently as possible, thus not gasifying it into carbon monoxide, but burning it to carbon dioxide and steam as far as possible. Hence, in certain respects, gas producers and blast furnaces require opposite operating procedures. Aside from stoichiometric assumptions, the ratio of carbon monoxide to carbon dioxide is governed by the supply of oxygen in the blast, the steam, the charge, and, chiefly, by the reaction temperature. This temperature, in turn, is plainly fixed by the heat balance in the reaction zones. Thus the lines along which the gas composition can be effectively influenced are clearly traced out for us. This influence is exerted by:

- (1) The amount of coke added, i.e., the ratio of coke or of carbon to the other constituents of the charge.
- (2) The blast temperature.
- (3) The loss of heat outwards through radiation and conduction (cooling, absolute size of the furnace, and load).
- (4) The heat supply or loss through supplementary recycled gases fed into the furnace (hot gases or cold, combustible gases, which are to be burned in the shaft).
- (5) To a slight degree, by the fuel.

Other variations are made possible by an arbitrary change in the coke charge, e.g., the addition of inert solids (addition of slag, recycling the charge), by additional heating or increased cooling, by the employment of oxygen and oxygen-enriched air, by pressure variation, and by endothermic reactions. Examples of opportunities of this sort will be pointed out as the occasion arises.

As has been said, the reactions in blast furnaces, so far as material changes are concerned, are driving off the water of hydration, decomposing the carbonates, reducing the metallic oxides, and slagging reactions—all of which will be taken up in detail.

The *water of hydration* (water of crystallization) is adsorptively combined with solids. Hence the dissolving of this bond requires more than supplying the heat of vaporization; a quantity of heat must be supplied that corresponds to the heat of hydration. Let us take kaolin, for instance, as a representative of the clays. We have

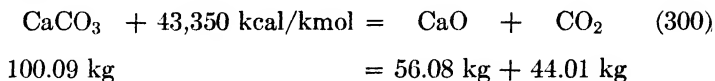


For 1 kg of clay (kaolin) 135 kcal are required, or 965.8 kcal are required for 1 kg of water driven off. Pure evaporation would have required only 583.4 kcal for 1 kg of H_2O ; hence freeing the water of hydration from its bond has required an additional 382.4 kcal/kg.¹

¹ The value of 75 kcal/kg H_2O given by Senfter [*Arch. Eisenhüttenwes.*, Vol. 12 (1938–1939), No. 2, pp. 549–564, especially Table 1, p. 552], as well as Wesemann's value [*Arch. Eisenhüttenwes.*, Vol. 13 (1939–1940), No. 3, pp. 113–122, especially Figure 3, p. 116] appear to be too low.

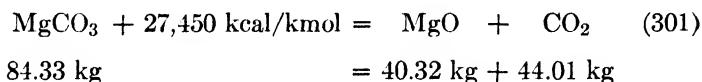
The *decomposition of the carbonates* occurs in accordance with the following equations:²

(a) *Lime*



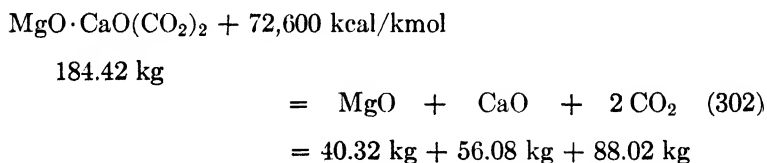
433.1 kcal of heat are required for 1 kg CaCO_3 .

(b) *Magnesite*



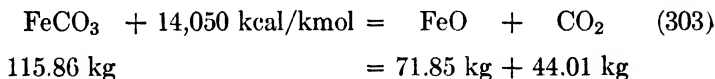
326 kcal of heat are required for 1 kg MgCO_3 .

(c) *Dolomite*



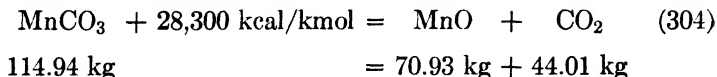
394 kcal of heat are required for 1 kg of dolomite.

(d) *Ferrous Carbonate* (spathic iron ore)



121 kcal of heat are required for 1 kg FeCO_3 .

(e) *Manganese Carbonate*



246 kcal of heat are required for 1 kg MnCO_3 .

² Since the data in the literature differ considerably, all the heats of reaction have been recalculated, using the heat contents listed in the *Taschenbuch für Chemiker und Physiker* (edited by J. D'Ans and E. Lax), Berlin, 1943, Table 3114; also cf. p. 6 and Table IV in the Appendix, p. 303. The only exception was the heat content of formation for coking carbon, which was taken from Table 1, p. 6. On the other hand, the tables of the *Taschenbuch* were used for all compounds of carbon.

Manganese carbonate decomposes at very low temperatures, especially in the presence of moisture. As a result, it never reaches the reaction zone of the furnace, and hence its carbon dioxide passes off as such fairly unchanged. Likewise, for magnesite and ferrous carbonate, in the range of about 200 to 400°C, the decomposition pressure is so low—0.1 to 1 at—that the separation of the

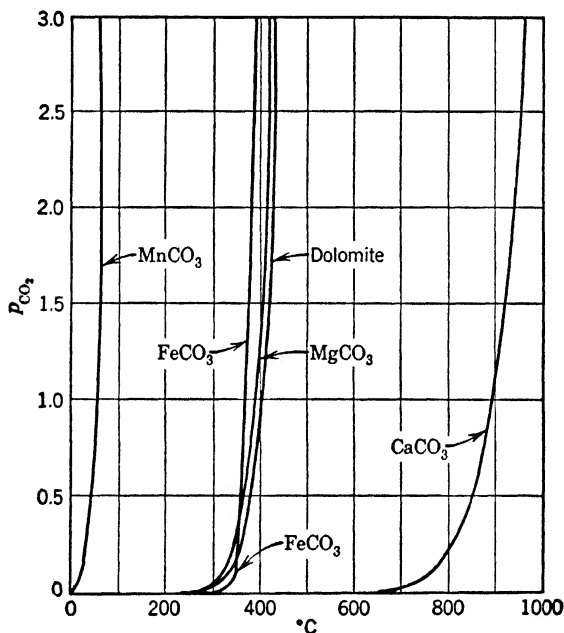
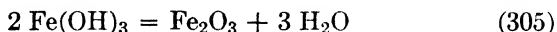


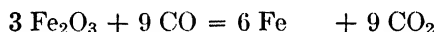
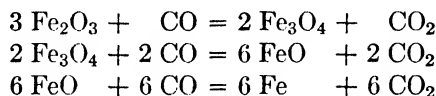
FIG. 39. Pressure of decomposition of various carbonates.

carbon dioxide may take place outside the reaction zone (Figure 39). On the other hand, with lime we may count on the separation of carbon dioxide occurring in the reaction zone itself, especially when it is borne in mind that the large pieces of lime require a considerable length of time to heat up, and that the subsequent supply of carbon dioxide from the interior of the pieces as their cores heat up occurs but slowly, the pieces reaching the lower zones of the furnace in the meantime. As a result, the driven-off carbon dioxide also participates in the reactions, and this must accordingly be taken into account in our calculations.

Reduction of ores consists of a step-by-step removal of the oxygen in the ore by the reducing agents. Let us take as our first example ferric oxide (Fe_2O_3), the highest oxide of iron. It is the chief constituent of hematite, whereas iron hydroxide, the principal constituent of limonite (minette), is converted into iron oxide by dehydration:



The reduction of iron oxide to metallic iron (Fe) takes place as follows, via ferroferric oxide (Fe_3O_4) and ferrous oxide (FeO):



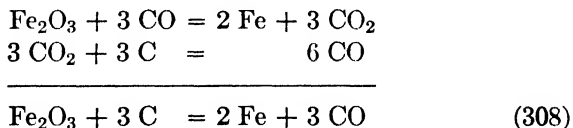
or



Listing these reactions together leads us to the overall molecular formula of equation 306, which is the only one of interest to us in calculation. As the carbon dioxide produced can and will react further with the carbon according to

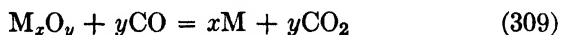


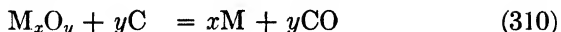
depending solely upon the temperature at which the reactions occur, equations 306 and 307 may also be combined as follows:



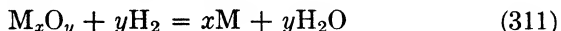
In the literature on the metallurgy of iron, overall equation 306 is called *indirect reduction*, whereas overall equation 308 is called *direct reduction*. These terms, however, are undesirable and superfluous. Moreover, they were of no assistance in promoting correct views of the reactions in the reducing process, as proved by the fruitless debates in the literature on the problem of "direct" or "indirect" reduction or the extent of each (also see p. 190).

We may also write the reactions of equations 306 and 308 in the general form





thus including the reduction of the lower stages of the oxidation of iron and of other metallic oxides. Another reducing agent in addition to carbon monoxide, hydrogen, is at our disposal* in accordance with the general pattern:

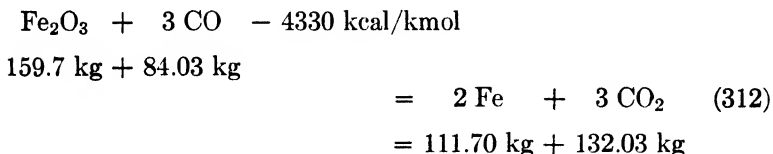


Overall equation 311 is considered to be mostly unimportant in normal blast-furnace operation.

A heterogeneous reaction in accordance with overall equation 310 is quite inconceivable. The solid (M_xO_y) can react with the spatially distant solid (C) only through an intermediate gaseous medium (CO , H_2), and the gaseous reaction products (CO_2 , H_2O) may then be further reduced by solid carbon to CO and H_2 . The concepts of direct and indirect reduction are superfluous insofar as assumptions of that sort are unnecessary in making the calculation, as the method set forth below will indicate. Determining the $CO:CO_2$ ratio, for example, on the basis of experience or even of a small-scale experiment, would anticipate the results of calculation and thus make the aim of the calculation actually illusory. Since, as we have emphasized, the $CO:CO_2$ ratio depends on the heat balance in the reaction zone, an experimental determination by means of a small-scale experiment must indicate the contribution of indirect reduction absolutely falsely.

Let us examine the reduction of the oxides in detail.

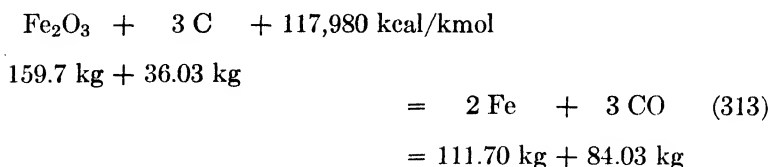
(a) *Ferric Oxide*



27.1 kcal are available per kg of Fe_2O_3 , and 38.8 kcal per kg of

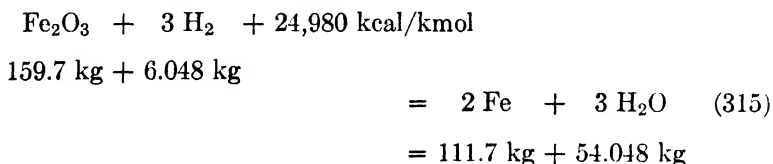
* Whereas hydrogen is a significant and practically used reducing agent—although it is mostly ignored in conventional blast furnace calculations—there are other reducing agents, such as the hydrocarbons, which are usually too valuable to be employed for this purpose, to be sure. In countries possessing little coal, but rich in natural gas, however, reducing agents of this type may also be of practical importance, mostly after conversion into a $CO + H_2$ mixture.

iron produced. The reaction is slightly exothermic (heat of reaction negative!).



738.8 kcal of heat are required for 1 kg of Fe_2O_3 , whereas 1056.2 kcal are required for 1 kg of iron produced; the reaction is endothermic (heat of reaction positive!). The heat required by the reaction is represented by the equation

$$H'_{\text{Fe}_2\text{O}_3} = 765.9 \frac{\text{CO}}{\text{CO} + \text{CO}_2} = 27.1 \text{ kcal/kg Fe}_2\text{O}_3 \quad (314)$$



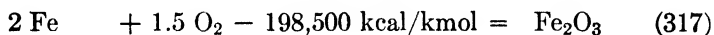
156.4 kcal of heat are required for 1 kg Fe_2O_3 , and 223.6 kcal for 1 kg of iron produced. In the joint reduction by carbon monoxide and hydrogen is

$$\begin{aligned} H''_{\text{Fe}_2\text{O}_3} = 765.9 \frac{\text{CO}}{\text{CO} + \text{CO}_2 + \text{H}_2 + \text{H}_2\text{O}} \\ + 183.5 \frac{\text{H}_2\text{O}}{\text{CO} + \text{CO}_2 + \text{H}_2 + \text{H}_2\text{O}} \\ - 27.1 \text{ kcal/kg Fe}_2\text{O}_3 \quad (316) \end{aligned}$$

This is the equation of a plane in space, passing through the three required heat points: 27.1 kcal/kg for 100% CO_2 formation, 738.8 kcal/kg for 100% CO formation, and 156.4 kcal/kg for 100% H_2O formation. In practice, this joint reduction by carbon monoxide and hydrogen always occurs in the blast furnace, but reduction by hydrogen is usually ignored because of the slight hydrogen content of the blast. But when we examine the smelting of oxides in a water-gas producer, e.g., in the Thyssen-Gálocsy

generator, it is essential that the extremely high percentage of reduction due to hydrogen be borne in mind.

From the standpoint of computation, however, this variation of the heat required with the gas composition, caused by the combination of the decomposition of the metallic oxides with the recombination of the oxygen with the carbon and the hydrogen, is quite inconvenient. It is therefore simpler, and of equal value so far as the final result is concerned, to consider the heat expended to decompose the oxides and the absorption of heat in the new oxygen compounds successively. The equation

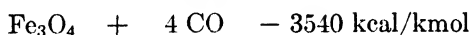


$$2 \times 55.85 \text{ kg} + 48 \text{ kg} = 159.7 \text{ kg}$$

states that iron, when oxidized (burned) to Fe_2O_3 , has a "heating value" of $\frac{198,500}{111.7} = 1777.1 \text{ kcal/kg Fe}$. Conversely, a heat ex-

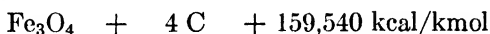
penditure of $\frac{198,500}{159.7} = 1243.0 \text{ kcal/kg Fe}_2\text{O}_3$, or $1777.1 \text{ kcal/kg Fe}$, referred to the iron set free, is necessary.

(b) *Ferroferric Oxide*



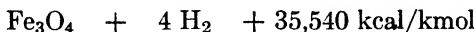
$$\begin{aligned} 231.55 \text{ kg} + 112.04 \text{ kg} &= 3 \text{ Fe} + 4 \text{ CO}_2 \quad (318) \\ &= 167.55 \text{ kg} + 176.04 \text{ kg} \end{aligned}$$

15.3 kcal are available per kg of Fe_3O_4 , or 21.1 kcal available per kg of iron produced.



$$\begin{aligned} 213.55 \text{ kg} + 48.04 \text{ kg} &= 3 \text{ Fe} + 4 \text{ CO} \quad (319) \\ &= 167.55 \text{ kg} + 112.04 \text{ kg} \end{aligned}$$

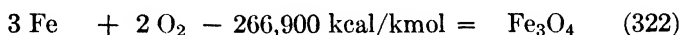
The heat required per kg of Fe_3O_4 is 689.0 kcal, or 952.2 kcal/kg of iron produced.



$$\begin{aligned} 231.55 \text{ kg} + 8.064 \text{ kg} &= 3 \text{ Fe} + 4 \text{ H}_2\text{O} \quad (320) \\ &= 167.55 \text{ kg} + 72.064 \text{ kg} \end{aligned}$$

The heat required per kg of Fe_3O_4 is 153.5 kcal, or 212.1 kcal/kg of iron produced. The heat of reaction is

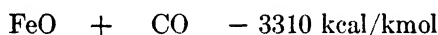
$$H''_{\text{Fe}_3\text{O}_4} = 704.3 \frac{\text{CO}}{\text{CO} + \text{CO}_2 + \text{H}_2 + \text{H}_2\text{O}} + 168.8 \frac{\text{H}_2\text{O}}{\text{CO} + \text{CO}_2 + \text{H}_2 + \text{H}_2\text{O}} - 15.3 \text{ kcal/kg} \quad (321)$$



$$167.55 \text{ kg} + 64 \text{ kg} = 231.55 \text{ kg}$$

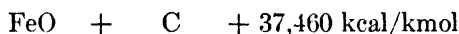
The heat required per kg of Fe_3O_4 is 1152.7 kcal/kg. The heat required per kg of Fe is 1573.0 kcal/kg.

(c) *Ferrous Oxide*



$$\begin{aligned} 71.85 \text{ kg} + 28.01 \text{ kg} &= \text{Fe} + \text{CO}_2 \quad (323) \\ &= 55.85 \text{ kg} + 44.01 \text{ kg} \end{aligned}$$

46.1 kcal are available per kg of FeO, and 29.3 kcal/kg of iron produced.



$$\begin{aligned} 71.85 \text{ kg} + 12.01 \text{ kg} &= \text{Fe} + \text{CO} \quad (324) \\ &= 55.85 \text{ kg} + 28.01 \text{ kg} \end{aligned}$$

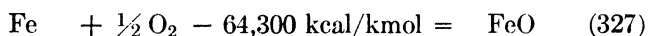
The heat required per kg of FeO is 521.4 kcal, or 670.7 kcal/kg of iron produced.



$$\begin{aligned} 71.85 \text{ kg} + 2.016 \text{ kg} &= \text{Fe} + \text{H}_2\text{O} \quad (325) \\ &= 55.85 \text{ kg} + 18.016 \text{ kg} \end{aligned}$$

The heat required per kg of FeO is 89.9 kcal, or 115.7 kcal/kg of iron produced. The heat of the reaction is

$$H''_{\text{FeO}} = 567.5 \frac{\text{CO}}{\text{CO} + \text{CO}_2 + \text{H}_2 + \text{H}_2\text{O}} + 136.0 \frac{\text{H}_2\text{O}}{\text{CO} + \text{CO}_2 + \text{H}_2 + \text{H}_2\text{O}} - 46.1 \text{ kcal/kg} \quad (326)$$

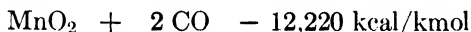


$$55.85 \text{ kg} + 16 \text{ kg} = 71.85 \text{ kg}$$

$$\text{Heat required per kg of FeO} = 89.9 \text{ kcal/kg}$$

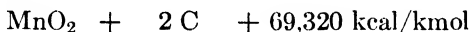
$$\text{Heat required per kg of Fe} = 115.7 \text{ kcal/kg}$$

(d) *Manganese Dioxide* (pyrolusite, brown stone)



$$\begin{aligned} 86.93 \text{ kg} + 56.02 \text{ kg} &= \text{Mn} + 2 \text{CO}_2 \quad (328) \\ &= 54.93 \text{ kg} + 88.02 \text{ kg} \end{aligned}$$

140.6 kcal are available per kg of MnO₂, 222.5 kcal/kg of manganese produced.



$$\begin{aligned} 86.93 \text{ kg} + 24.02 \text{ kg} &= \text{Mn} + 2 \text{CO} \quad (329) \\ &= 54.93 \text{ kg} + 56.02 \text{ kg} \end{aligned}$$

The heat required is 797.4 kcal/kg of MnO₂, or 1262.0 kcal/kg of manganese produced.



$$\begin{aligned} 86.93 \text{ kg} + 4.032 \text{ kg} &= \text{Mn} + 2 \text{H}_2\text{O} \quad (330) \\ &= 54.93 \text{ kg} + 36.032 \text{ kg} \end{aligned}$$

The heat required is 84.2 kcal/kg of MnO_2 , or 133.3 kcal/kg of manganese produced. The heat of reaction is

$$H''_{\text{MnO}_2} = 938.0 \frac{\text{CO}}{\text{CO} + \text{CO}_2 + \text{H}_2 + \text{H}_2\text{O}} + 224.8 \frac{\text{H}_2\text{O}}{\text{CO} + \text{CO}_2 + \text{H}_2 + \text{H}_2\text{O}} - 140.6 \quad (331)$$

$$\text{Mn} + \text{O}_2 - 123,000 \text{ kcal/kmol} = \text{MnO}_2 \quad (332)$$

$$54.93 \text{ kg} + 32 \text{ kg} = 86.93 \text{ kg}$$

$$\text{Heat required per kg of MnO}_2 = 1414.9 \text{ kcal/kg}$$

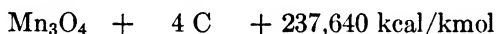
$$\text{Heat required per kg of Mn} = 2239.2 \text{ kcal/kg}$$

(e) *Manganomanganic Oxide*



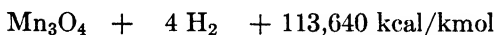
$$\begin{aligned} 228.79 \text{ kg} + 112.04 \text{ kg} &= 3 \text{ Mn} + 4 \text{ CO}_2 \quad (333) \\ &= 164.79 \text{ kg} + 176.04 \text{ kg} \end{aligned}$$

The heat required is 325.9 kcal/kg of Mn_3O_4 , or 452.4 kcal/kg of manganese produced.



$$\begin{aligned} 228.79 \text{ kg} + 48.04 \text{ kg} &= 3 \text{ Mn} + 4 \text{ CO} \quad (334) \\ &= 164.79 \text{ kg} + 112.04 \text{ kg} \end{aligned}$$

The heat required is 1038.7 kcal/kg of Mn_3O_4 , or 1442.1 kcal/kg of manganese produced.



$$\begin{aligned} 228.79 \text{ kg} + 8.064 \text{ kg} &= 3 \text{ Mn} + 4 \text{ H}_2\text{O} \quad (335) \\ &= 164.79 \text{ kg} + 72.064 \text{ kg} \end{aligned}$$

The heat required is 496.7 kcal/kg of Mn_3O_4 , or 689.6 kcal/kg of manganese produced.

The heat required by the reaction is found from equation

$$H''_{\text{Mn}_3\text{O}_4} = 712.8 \frac{\text{CO}}{\text{CO} + \text{CO}_2 + \text{H}_2 + \text{H}_2\text{O}} + 170.8 \frac{\text{H}_2\text{O}}{\text{CO} + \text{CO}_2 + \text{H}_2 + \text{H}_2\text{O}} + 325.9 \quad (336)$$

$$3 \text{ Mn} + 2 \text{ O}_2 - 345,000 \text{ kcal/kmol} = \text{Mn}_3\text{O}_4 \quad (337)$$

$$164.79 \text{ kg} + 64 \text{ kg} = 228.79 \text{ kg}$$

$$\text{Heat required per kg of Mn}_3\text{O}_4 = 1507.9 \text{ kcal/kg}$$

$$\text{Heat required per kg of Mn} = 2093.6 \text{ kcal/kg}$$

(f) *Manganous Oxide*

$$\text{MnO} + \text{CO} + 29,090 \text{ kcal/kmol}$$

$$\begin{aligned} 70.93 \text{ kg} + 28.01 \text{ kg} &= \text{Mn} + \text{CO}_2 \quad (338) \\ &= 54.93 \text{ kg} + 44.01 \text{ kg} \end{aligned}$$

The heat required is 410.1 kcal/kg of MnO, or 529.6 kcal/kg of manganese produced.

$$\text{MnO} + \text{C} + 69,860 \text{ kcal/kmol}$$

$$\begin{aligned} 70.93 \text{ kg} + 12.01 \text{ kg} &= \text{Mn} + \text{CO} \quad (339) \\ &= 54.93 + 28.01 \text{ kg} \end{aligned}$$

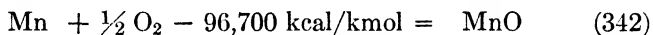
The heat required is 984.9 kcal/kg of MnO, or 1271.8 kcal/kg of manganese produced.

$$\text{MnO} + \text{H}_2 + 38,860 \text{ kcal/kmol}$$

$$\begin{aligned} 70.93 \text{ kg} + 2.016 \text{ kg} &= \text{Mn} + \text{H}_2\text{O} \quad (340) \\ &= 54.93 \text{ kg} + 18.016 \text{ kg} \end{aligned}$$

The heat required is 547.9 kcal/kg of MnO, or 707.4 kcal/kg of manganese produced. In a mixed reduction the heat required by the reaction is given by

$$H''_{\text{MnO}} = 574.8 \frac{\text{CO}}{\text{CO} + \text{CO}_2 + \text{H}_2 + \text{H}_2\text{O}} + 137.8 \frac{\text{H}_2\text{O}}{\text{CO} + \text{CO}_2 + \text{H}_2 + \text{H}_2\text{O}} + 410.1 \text{ kcal/kg} \quad (341)$$

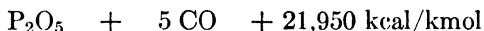


$$54.93 + 16 \text{ kg} = 70.93 \text{ kg}$$

$$\text{Heat required per kg of MnO} = 1363.3 \text{ kcal/kg}$$

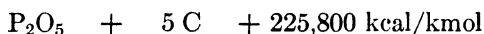
$$\text{Heat required per kg of Mn} = 1760.4 \text{ kcal/kg}$$

(g) *Phosphoric Acid*



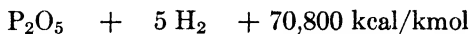
$$\begin{aligned} 141.96 \text{ kg} + 140.05 \text{ kg} &= 2 \text{P} + 5 \text{CO}_2 \quad (343) \\ &= 61.96 \text{ kg} + 220.05 \text{ kg} \end{aligned}$$

The heat required is 154.6 kcal/kg of P_2O_5 , or 354.3 kcal/kg of phosphorus.



$$\begin{aligned} 141.96 \text{ kg} + 60.05 \text{ kg} &= 2 \text{P} + 5 \text{CO} \quad (344) \\ &= 61.96 \text{ kg} + 140.05 \text{ kg} \end{aligned}$$

The heat required is 1590.6 kcal/kg of P_2O_5 , or 3644.3 kcal/kg of phosphorus.



$$\begin{aligned} 141.96 \text{ kg} + 10.08 \text{ kg} &= 2 \text{P} + 5 \text{H}_2\text{O} \quad (345) \\ &= 61.96 \text{ kg} + 90.08 \text{ kg} \end{aligned}$$

The heat required is 498.7 kcal/kg of P_2O_5 , or 1142.7 kcal/kg of phosphorus. In a mixed reduction by carbon and hydrogen, the heat reaction is

$$H''_{P_2O_5} = 143.6 \frac{CO}{CO + CO_2 + H_2 + H_2O} + 344.1 \frac{H_2O}{CO + CO_2 + H_2 + H_2O} + 154.6 \text{ kcal/kg} \quad (346)$$

$$2 P + 2.5 O_2 - 360,000 \text{ kcal/kmol} = P_2O_5 \quad (347)$$

$$61.96 \text{ kg} + 80 \text{ kg} = 141.96 \text{ kg}$$

$$\text{Heat required per kg of } P_2O_5 = 2535.9 \text{ kcal/kg}$$

$$\text{Heat required per kg of P} = 5810.2 \text{ kcal/kg}$$

If we ignore the bosh and slagging reactions for the present, we can make the picture of the manifold reactions in a blast furnace clearer by simplifying it in our minds. This simplification involves no sacrifice of the accuracy of our calculations of the reactions, since we are interested only in the overall result. Nor does the manner in which we obtain the result or the reactions involved affect the chemical interchanges or the overall heat balance of the furnace.* We therefore arrange the reactions in the blast furnace according to Figure 40. The entering blast, consisting of oxygen, nitrogen, and a slight amount of steam, first encounters carbon in excess and converts its oxygen into CO_2 until all the available oxygen is consumed—analogous to the reactions in the oxidation zone of a gas producer—after which the carbon dioxide and the steam are reduced to carbon monoxide and hydrogen (box 1 in Figure 40). This reaction takes place directly in front of the tuyères, as we know from the results of measurements made on blast furnaces. Under normal blast-furnace operating conditions the oxidation zone has the shape of a sphere about 0.8 to

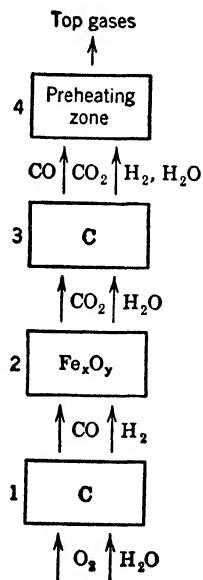


FIG. 40. Principle of reactions in a blast-furnace shaft.

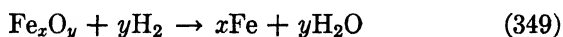
* Conditions are somewhat different if we want to deal with partial reactions in the furnace separately, for instance, the hearth, bosh, and shaft reactions. It is then necessary to differentiate between the various reactions.

1.0 m (2.6 to 3.3 ft) in diameter. We shall ignore for the present the fact that reoxidation of iron and other reactions (the *hearth reactions*) may also take place here. For the end result of our computation, it is immaterial that in practice there is no complete separation between the oxidation and the reduction zones but that these two zones interpenetrate each other, of course. In all discussions of chemical interchanges it is advisable to assume a complete oxidation to CO_2 , followed by a reduction of the CO_2 to CO , whereas, when considering the maximum temperatures to be expected, we must take the synchronism of oxidizing and reducing reactions into account. Because of this fact different fuels, having different surfaces and different reactivities, yield different combustion temperatures. For if the CO_2 produced by combustion is very quickly reduced to CO , so that the combustion of the carbon monoxide formed at the surface of the coke in the oxidation zone can no longer take place under the given conditions of measurement, flow, and mixture, we get a gas mixture rich in carbon monoxide, and a lower temperature owing to the binding of the chemical energy. This is the reason for the difference between the temperature in front of the tuyères when highly reactive fuels are used, such as charcoal, which burns at a low temperature, and the corresponding temperature when the more slowly reactive coke, which burns at a higher temperature, is employed.

In what follows, however, we shall consider only the chemical interchanges, proceeding step by step and assuming a complete separation of the reactions as symbolized by the little boxes in Figure 40. Owing to the high temperature of the blast, the low steam content of the blast, and the strongly endothermic reducing reactions of the furnace stack (which do not yet occur at this point), the oxidation zone and the reduction zone at the tuyères, shown in box 1, exhibit such high temperatures as to insure complete reduction of the carbon dioxide and steam, especially since this must be in a temperature range above the melting points of the iron and the slag. The gases formed here serve as reducing agents for the next layers, as shown in box 2, in which we consider the ores to be reduced to be also present in excess. The reactions involved are



and



We assume, to begin with, that this reduction is complete, i.e., proceeding until equilibrium is established. This assumption will have to be checked later on. However, the probability that the reactions are complete is very great, since, as we know, excess iron oxides are not retained in the blast-furnace hearth, with the exception of the quantity in the slag, which we can assign to the refining action of manganese oxide, as will be shown later. In accordance with the equilibrium conditions, part of the carbon monoxide has been converted into carbon dioxide, and part of the hydrogen into steam. We shall imagine all the shaft reactions involving the ore concentrated in box 2. In the layers located higher up, which we assume concentrated in box 3, the carbon dioxide and the steam are then again reduced to carbon monoxide and hydrogen, depending on the reaction temperature. Thus the carbon re-establishes the gas equilibrium upset by the reduction of the ore, so that after leaving this box, or the whole reaction zone, the gas mixture we have consists of CO , CO_2 , H_2 , H_2O , and N_2 . The traces of CH_4 that are present may be ignored for the moment. Finally, in the preheating zone (box 4), the carbon dioxide in the carbonates (MgCO_3 , MnCO_3 , and FeCO_3) appears, as well as the moisture in the fuel and the burden, and tiny quantities of water of hydration, together with the volatile constituents of the fuel. This entails a certain change in the analysis of the reaction gases, the magnitude of which, however, can easily be estimated.

In reality, however, instead of these four little boxes we have a manifold stratification of coke and burden charges. The oxygen is consumed step by step, and what we have combined into boxes 1 to 3 in Figure 40 would have to be spread over numerous boxes in succession, with the reduction of the gases by the carbon and reduction of the ore by the gases. This reduction is followed by another reduction of the gases thereby produced by the carbon, repeated over and over, leading finally to the end result, which we have determined with our simplifying and summarizing concepts of the composition of the charge gases.

Mechanism of furnace reactions

As we have constructed a picture of the gasification reaction (see p. 25) to aid our conceptions, let us now again briefly consider the reactions in the blast-furnace shaft as a supplement to

what has gone before, as well as a justification for the framework of our calculations. The calculations and the conception on which they are based provide us with an insight into the reactions occurring and yield numerical data that serve to indicate all the measures required for the operation and control of blast furnaces.

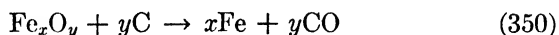
The reduction of the ore is a physicochemical process in which the physical portion of the process plays an outstanding part, for the reducing agents must first be brought into contact with the piece of ore before the chemical reaction can begin. That is why we have already rejected the notion of the so-called direct reduction by the solid carbon as a representation of the overall process that does not correspond to the actual reactions. Moreover, the progress of the reaction is impeded by the covering over of the surfaces by the reduction products (from ferroferrie oxide to metallic iron, which have to be overcome by the diffusion of the reactive agents through these outer coatings as the process continues).³ The moot question whether indirect reduction takes place in accordance with equations 306, 309 or direct reduction takes place in accordance with equations 308, 310 is clearly settled in this concept, since access of the reducing agent to the surface of the piece of ore and especially to the interior of the ore is conceivable only if the agent is gaseous. Action of solid carbon in the coke upon solid iron oxide is out of the question, for the two do not lie so close to each other in the blast furnace as to be able to react together directly. At the prevailing temperatures, particularly in the hearth and bosh of the furnace, the conditions necessary for the deposition of carbon on the ore by the decomposition reaction of carbon monoxide do not exist. Here we have temperatures at which only carbon monoxide and hydrogen are stable. If the reaction



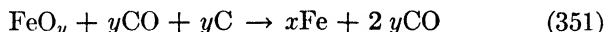
takes place on the surface of a piece of ore that has reached this zone, the carbon dioxide formed on the surface is immediately

³ W. Baukloh, *Die Roheisengewinnung durch den Hochofenprozess* (The Production of Pig Iron by the Blast-Furnace Process), in A. Eucken and M. Jacob, *Der Chemie-Ingenieur* (The Chemical Engineer), Vol. 3, Part 5, Leipzig, 1940; W. Baukloh and R. Durrer, *Archiv Eisenhüttenwes.*, Vol. 4 (1930-1931), No. 10, pp. 455-460.

reduced to CO as soon as it encounters carbon, and then the (overall) reaction seems to be



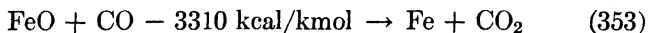
since we can find only CO in the gas phase. But if we consider a portion of the space, containing ore and coke, we may also express the reaction that takes place by the formula



which indicates that even according to the formula there need be no direct action of the carbon upon the ore. If the split-off carbon is still frequently considered to be the carrier of the direct reduction, as has even been actually demonstrated in reduction experiments (in laboratory or small-scale experiments), the carbon being formed in the decomposition reaction



it should be borne in mind that we are here dealing with a reaction that is promoted by a falling temperature and thus can be shown to exist in a laboratory experiment because of the enormous percentage of heat losses there. It cannot, however, occur in a blast furnace. When ore and coke travel through the furnace, the surface temperature of the coke will always be lower than that of the ore, other conditions and their height in the furnace being the same, since very strongly endothermic reactions occur in the coke while slightly exothermic reactions occur in the ore. In the lower part of the furnace, which we should now consider for a moment, the removal of the oxygen in the ore will have already proceeded so far that only ferrous oxide is present, and the reaction therefore is



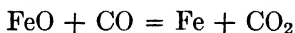
Thus carbon monoxide, which here reaches the surface of the ore, will have no occasion to split into carbon dioxide and carbon in accordance with equation 352, depositing nascent carbon, which in turn could react with the oxygen in the ore. Since we have been able to prove that the reduction is a process essentially dependent upon the physical conditions, the reducibility of the ore is likewise dependent chiefly upon the physical properties of the ore and without any appreciable influence upon the composi-

tion of the waste gases or upon the nature of the reduction, just as the reactivity of the coke has no effect upon the quality of the gas. The contrary opinion is repeatedly found in the literature. A slowly reacting coke, such as high-temperature coke, yields the same gas as a very reactive coke (e.g., low-temperature char or charcoal), aside from the slight effect entailed by the variation in the amount and composition of the volatile constituents, which at bottom has nothing at all to do with reaction of the carbon proper. Nor does the reactivity of the coke affect the performance of gas producers and furnaces, so far as the steady state is concerned. The same is true of the reducibility of the ore. Ores containing Fe_2O_3 are easily reducible, as is shown by the equilibrium state; Fe_3O_4 ores are reducible with difficulty, ferrous oxide is even less reducible, and manganous oxide is not at all reducible by CO in the blast-furnace shaft. It is incorrect to assign a definite share in direct or indirect reduction to an ore on the basis of its reducibility, as is at once understandable from what has been stated. A considerable role is played by the physical state of the ore (density, behavior under heat), grain size (granulation characteristic, form stability at high temperatures), and its proportion in the gangue. When a particularly large and dense piece of ore sinks deep down in the furnace before being completely reduced, it reaches temperature zones in which under certain circumstances no carbon dioxide is stable any longer in the presence of carbon. All nascent carbon dioxide is then immediately reduced again to carbon monoxide. It would be wrong to infer from this, however, that ores that are hard to reduce are reduced only "directly." For the same ore, suitably crushed, can also be reduced in the shaft in a temperature range of 700 to 800°C, yielding a correspondingly higher CO_2 percentage, indicating that the "indirect reduction" is apparently greater. Thus it is evident that we are not dealing with any specific property of the given ore, which proves the undesirability, stressed above, of relating the concepts of direct or indirect reduction in any way with the reducibility of the ore.

Shaft reactions and their localization in the blast furnace

It is not enough, however, to know what reactions occur and to prove which reactions cannot occur. We also have to indicate where and when they occur in order to be able to enter the reaction

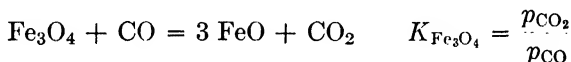
products in our calculations at the proper places. This information is supplied by the constants of equilibrium. The equilibrium constants for the reductions of iron oxide were computed as outlined by H. Schenck:⁴ *



$$K_{\text{FeO}} = \frac{p_{\text{CO}_2}}{p_{\text{CO}}}$$

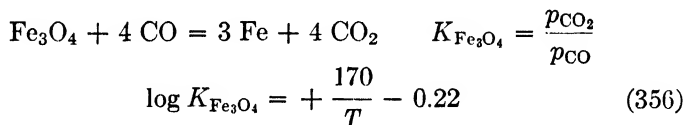
$$\log K_{\text{FeO}} = + \frac{381}{T} - 2.110 \log T + 0.395 \times 10^{-3}T + 5.357 \quad (354)$$

for



$$\log K_{\text{Fe}_3\text{O}_4} = - \frac{1373}{T} - 0.341 \log T + 0.41 \times 10^{-3}T + 2.303 \quad (355)$$

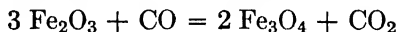
and for



We then get the CO content of the gas that is in equilibrium with the oxides as

$$v_{\text{CO}} = \frac{1 - v_{\text{N}_2}}{1 + K} \quad (357)$$

The constant of equilibrium of the reaction



is so large that the CO content almost vanishes. Thus in Figure 41 it practically coincides with the abscissa axis. This means that this reaction stage already occurs at very low CO concentra-

⁴ Hermann Schenck, *Einführung in die physikalische Chemie der Eisenhüttenprozesse*, Vol. 1, Berlin, 1932.

* Schenck defines the K value as the reciprocal of the value employed here. For the sake of uniformity of our representation, however, we place the components to the right of the equal sign in the denominators of the equilibrium constants.

tions and low temperatures. In Figure 41 the CO contents of the reduction reactions are plotted as functions of temperature, together with the curve for the Boudouard reaction; both curves are plotted for a reaction with dry air. This diagram throws

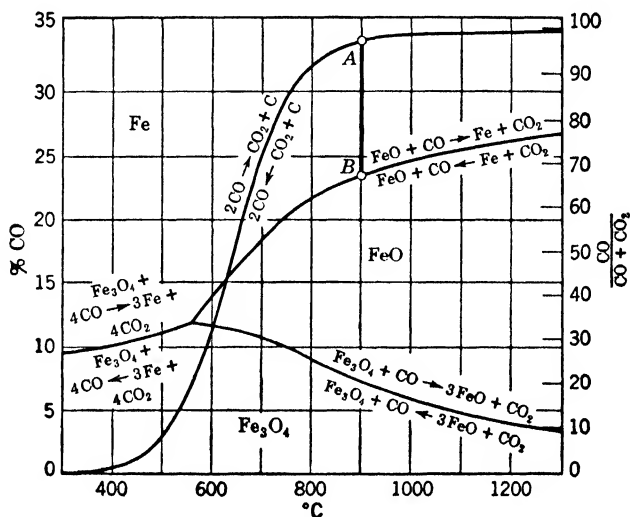
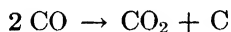


FIG. 41. Equilibrium curves of iron oxides. Reduction by carbon monoxide.

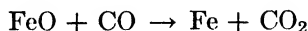
much light on the reactions in the blast furnace; it indicates that, for example, at 900°C the reaction



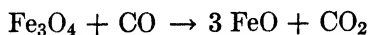
must occur above a CO content of 34.19%, whereas below this content the reaction must be



Above 23.53% of CO the ferrous oxide is reduced in accordance with



Below this CO concentration it is not reduced at all. Above 7.36% CO, at a temperature of 900°C, the ferroferric oxide is reduced to ferrous oxide in accordance with



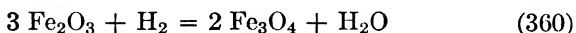
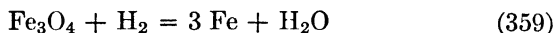
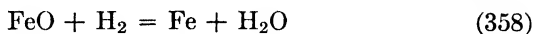
whereas iron oxide, Fe_2O_3 , is not stable at this temperature. Below 560°C the ferrous oxide stage is skipped, the reduction of the ferroferric oxide proceeding directly to metallic iron in accordance with the overall formula of equation 356, but this requires a CO concentration of more than 11%. But such a concentration does not exist in the blast furnace at this temperature, and consequently the reaction cannot take place in the furnace. The removal of the oxygen in the ferroferric oxide takes place only at temperatures above 600°C , and then solely via the ferrous oxide stage.

If a hot gas at a temperature of 900°C in equilibrium with the coke carbon (point *A* in Figure 41) is brought to the surface of the ore, it will react with the FeO until its CO content has sunk to the value fixed by the equilibrium conditions of the reaction $\text{FeO} + \text{CO} \rightarrow \text{Fe} + \text{CO}_2$, namely 23.55% CO (point *B*). Now this gas is no longer in equilibrium with the carbon, but it will again be brought into equilibrium as soon as it comes in contact with carbon in the next higher layer, etc., etc. In so doing, it will cool off owing to the heat requirements of this exchange and come into equilibrium at a correspondingly lower temperature. Thus the gas is cooled (at the surface of the coke), although the reaction $\text{FeO} + \text{CO} \rightarrow \text{Fe} + \text{CO}_2$ is an exothermic one. The combination of this reaction with the strongly endothermic Boudouard reaction is still highly endothermic, as is confirmed by the gross equation $\text{FeO} + \text{C} \rightarrow \text{Fe} + \text{CO}$. It is not the reduction of the ore, but the re-establishment of the Boudouard equilibrium, that is responsible for the heat consumption of the overall reaction.

The distance between the Boudouard curve and the other curves is a measure of the magnitude of the reducing effect of the reducing agent (CO). If ferroferric oxide should reach the temperature zone of 900°C before being converted into ferrous oxide, it would be reduced extremely violently and rapidly to FeO, and immediately thereafter to metallic iron. Thus high blast-furnace performance depends on high temperatures (high CO contents). If the furnace is too cold, the difference in concentration of the reducing agent between the gas phase and the surface of the ore diminishes more and more, the reactions slow down or come to a dead stop, and the furnace is "running cold," i.e., it delivers the ore incompletely reduced. The remedy is raising the temperatures

(increasing the coke charge, raising the blast temperature, and enriching it with oxygen).

For the reduction of the iron oxides by hydrogen according to the equations



we obtain their associated equilibrium constants simply by coupling these reactions with the corresponding constants for the CO reduction through the equilibrium constants for the homogeneous gas reaction. If

$$K_{\text{FeO}(\text{CO})} = \frac{v_{\text{CO}_2}}{v_{\text{CO}}} \quad (361)$$

$$K_{\text{FeO}(\text{H}_2)} = \frac{v_{\text{H}_2\text{O}}}{v_{\text{H}_2}} \quad (362)$$

we get

$$K_{\text{FeO}(\text{H}_2)} = K_{\text{FeO}(\text{CO})} K_W = \frac{v_{\text{CO}_2}}{v_{\text{CO}}} \frac{v_{\text{CO}}}{v_{\text{CO}_2}} \frac{v_{\text{H}_2\text{O}}}{v_{\text{H}_2}} = \frac{v_{\text{H}_2\text{O}}}{v_{\text{H}_2}} \quad (363)$$

The same holds true for $K_{\text{Fe}_3\text{O}_4}$, and here too $K_{\text{Fe}_2\text{O}_3}$ becomes so small that it does not show up in the diagram (see Figure 42);

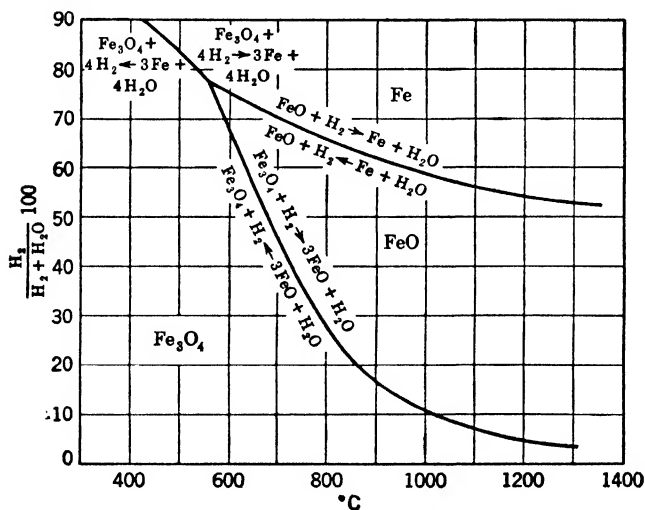


FIG. 42. Equilibrium curves of iron oxides. Reduction by hydrogen.

TABLE 49
REDUCTION OF IRON OXIDES BY HYDROGEN
(Equilibrium Constants and Gas Composition in the State of Equilibrium)

t °C	K_{FeO} (as in Equations 354, 363, 364)	$K_{Fe_3O_4}$ (as in Equations 355, 363, 364)	$K_{Fe_3O_4}$ (as in Equations 356, 363, 364)	ψ_{H_2}		
				As in Equations 354, 363, 364	As in Equations 355, 363, 364	As in Equations 356, 363, 364
450	0.1414	0.8761
500	0.2046	0.8302
550	0.2808	0.7808
600	0.3355	0.4767	...	0.7488	0.6772	...
700	0.4345	1.2070	...	0.6971	0.4531	...
800	0.5265	2.5822	...	0.6551	0.2792	...
900	0.6178	4.8838	...	0.6181	0.1700	...
1000	0.6998	8.4083	...	0.5883	0.1063	...
1100	0.7747	13.4499	...	0.5635	0.0692	...
1200	0.8412	20.2683	...	0.5431	0.0470	...
1300	0.8977	29.0279	...	0.5270	0.0333	...

i.e., very low percentages of hydrogen already suffice to reduce ferric oxide to ferrous oxide.

If the iron oxides were subjected to the reducing action of *pure* hydrogen (in the absence of carbon), we should have as a gas a mixture of H_2 and H_2O , the composition of which is found from the equation

$$v_{H_2} = \frac{1}{1 + K} \quad (364)$$

The numerical values are listed in Table 49. In the blast furnace, to be sure, H_2 does not occur by itself, and carbon is present, so

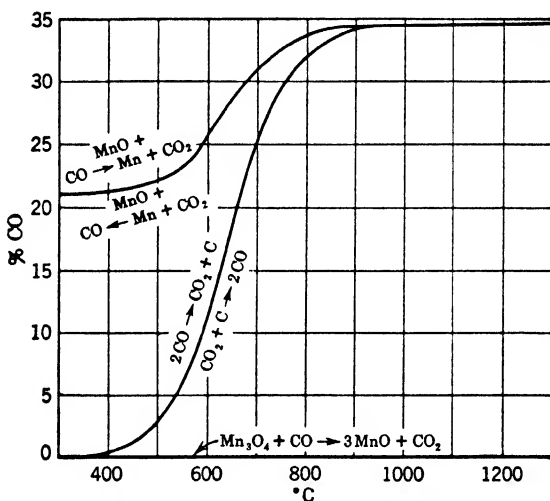


FIG. 43. Equilibrium curves of manganese oxides. Reduction by carbon monoxide.

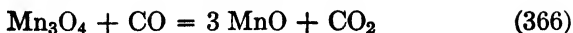
that Figure 42 does not reproduce the reactions actually occurring in the blast furnace.

When the same considerations are applied to the manganese oxides, we get Figure 43. According to H. Schenck * the equilibrium constants for the reduction of manganese oxides are

$$\log K_{Mn_3O_4} = \frac{2668}{T} - 0.3 \quad (365)$$

for the reaction

* See footnote 4, p. 193.



and

$$\log K_{\text{MnO}} = -\frac{6300}{T} + 0.3 \quad (367)$$

for the reaction

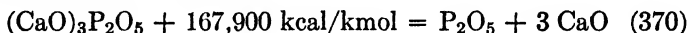


The equilibrium constant according to equation 365 is very large. At 700°C, for example ($K_{\text{Mn}_3\text{O}_4} = 552$), v_{CO} will consequently be very small in accordance with equation 357. At $t = 700^\circ\text{C}$, for example, $v_{\text{CO}} = 0.06\%$, which means that Mn_3O_4 is completely unstable. On the other hand, the equilibrium constant computed from equation 367 is very small with the CO content about $(1 - v_{\text{N}_2})$, since $1 + K \sim 1$, and thus the CO content is above the amount that the furnace can supply, as Figure 43 indicates. Thus no concentration gradient exists in the blast furnace under any circumstances, and consequently manganous oxide cannot be reduced in a blast-furnace shaft. The only feasible method is reduction by iron in accordance with the reaction equation



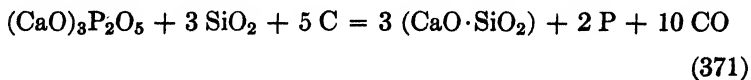
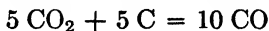
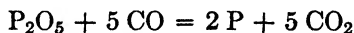
This is a reaction that occurs in the hearth (cf. p. 207), but does not affect the composition of the gas, as only an exchange of oxygen between manganese and iron takes place.

Phosphoric acid is present mostly in the form of phosphates, such as $(\text{CaO})_3\text{P}_2\text{O}_5$ or $(\text{CaO})_4\text{P}_2\text{O}_5$, which are decomposed in accordance with the equation

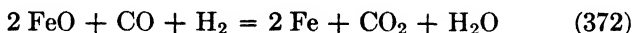


corresponding to a heat demand of 1182.7 kcal per kg of P_2O_5 .

Silicic acid and iron promote the reduction of phosphorus. The decomposition of the phosphates may take place according to the following equations:



Now let us turn to the reactions involved in the simultaneous use of CO and H₂ as reducing agents, for the sake of simplicity assuming a mixture of equal parts of CO and H₂. The reduction of the ferrous oxide then proceeds in accordance with



Assume the mixture to have been produced by the employment of an oxygen-steam mixture in the blast furnace. From the equations

$$v_{\text{CO}} + v_{\text{CO}_2} + v_{\text{H}_2} + v_{\text{H}_2\text{O}} = 1 \quad (373)$$

$$v_{\text{CO}} = v_{\text{H}_2} \quad (374)$$

we obtain

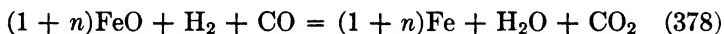
$$v_{\text{CO}} + v_{\text{CO}}K_{\text{FeO}(\text{CO})} + v_{\text{CO}} + v_{\text{CO}}K_{\text{FeO}(\text{H}_2)} = 1 \quad (375)$$

$$v_{\text{CO}} = \frac{1}{2 + K_{\text{FeO}(\text{CO})} + K_{\text{FeO}(\text{H}_2)}} \quad (376)$$

Likewise, we can treat the reduction of ferroferric oxide in accordance with the equation



The results are listed in Table 50. In general, for a ratio of $\frac{\text{H}_2}{\text{CO}} = n$, we may write



$$v_{\text{CO}} = \frac{1 - v_{\text{N}_2}}{1 + n + K_{\text{FeO}(\text{CO})} + nK_{\text{FeO}(\text{H}_2)}} \quad (379)$$

with analogous expressions for the other oxides.

Figure 44 gives the curves, which are very flat, especially for the reduction of FeO. Compared to reduction with CO and H₂, the high-temperature reduction could have been expected to be most active with hydrogen and slowest with carbon monoxide, with a mixture of both occupying an intermediate position. The relationship is reversed at low temperatures. The relative remoteness from the concentration of the equilibrium state may be considered a measure of the reaction's impulse, in the diagram of

Figure 44, that is, the distance from the upper edge of the figure (which represents 100% of the reducing agent). Wiberg⁵ has ascertained that reduction with carbon monoxide-hydrogen mixtures is most favorable. It is true that the hydrogen reduction proceeds faster at first, but later on it slows down more, so that the carbon monoxide and hydrogen reduction curves intersect.

TABLE 50

REDUCTION OF IRON OXIDES BY A 1:1 CARBON MONOXIDE-HYDROGEN MIXTURE

(Gas Composition in the State of Equilibrium)

°C	$v_{CO}(v_{H_2})$		
	(FeO)	(Fe ₃ O ₄)	(Fe ₃ O ₄)
450	0.3148
500	0.3121
550
600	0.3133	0.2707	...
700	0.3218	0.1970	...
800	0.3252	0.1375	...
900	0.3242	0.0946	...
1000	0.3220	0.0654	...
1100	0.3190	0.0461	...
1200	0.3158	0.0332	...
1300	0.3128	0.0246	...

He assumes that, when mixtures are used, the reducing power of the hydrogen is utilized at first, whereas toward the end of the process the reducing power of the carbon monoxide is employed. A possible explanation of this statement may be the fact that, as the reduction proceeds, the temperature drops more rapidly when hydrogen is employed, thus carrying the reaction into the range where the reaction slows down. When H₂-CO mixtures are used, on the other hand, the impetus of the reaction remains fairly

⁵ Martin Wiberg, Om reduktion av järnmalm med koloxid, väte och metan, *Jernkontorets Annaler*, Vol. 124 (1940), No. 5, pp. 179-212, especially Figure VIII.

constant in a very wide temperature range, as indicated by Figure 44.

In the blast furnace, as in the gas producer, we consider not the whole furnace, but solely the reaction zone proper, which in the blast furnace includes the hearth, the bosh, and a part of the shaft. Thus we differentiate between a *main reaction zone* and a *preheating and pre-reaction zone*, which we shall call the preheating zone for short, even though certain reactions occur here too, such as the

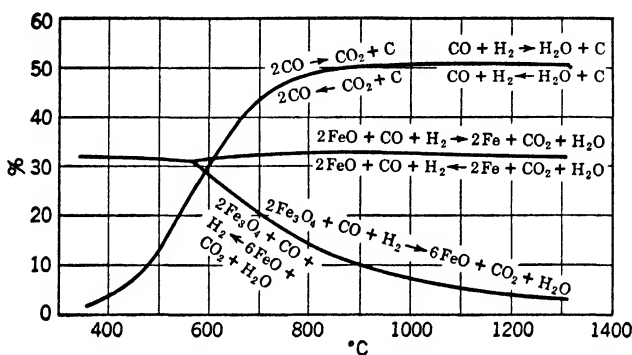


FIG. 44. Equilibrium curves of iron oxides. Reduction by a CO-H_2 mixture (1:1).

deacidification of the carbonates (with the exception of CaCO_3), the reduction of ferric oxide (Fe_2O_3) to ferroferric oxide (Fe_3O_4), etc. All other reactions take place in the main reaction zone that occur only at an elevated temperature, such as the reduction of ferrous oxide (FeO), of ferroferric oxide (Fe_3O_4), and of phosphoric acid (P_2O_5), the removal of carbon dioxide from the lime, etc. In this temperature range, the establishment of equilibrium is assured, for otherwise the reduction of the ore would have to remain incomplete, which experience teaches us is not the case.* Here, at the end of the reaction zone, the gas composition is not yet the same as that found at the furnace throat, since important shifts still occur in the preheating zone, depending on the nature of the fuel (especially its volatile content) and of the burden (especially the percentage of carbonates and ferric oxide in the burden). Thus in the preheating and pre-reaction zones we deal

* The FeO content of the slag is explained by the hearth reaction, e.g., the reduction of manganous oxide by iron in accordance with equation 369.

with the release of carbon dioxide from MgCO_3 , MnCO_3 , dolomite ($\text{MgO} \cdot \text{CaO}(\text{CO}_2)_2$), and FeCO_3 , the reduction of Fe_2O_3 to Fe_3O_4 , and of MnO_2 , Mn_2O_3 , and Mn_3O_4 to MnO , and, last, drying and the release of the water of hydration. We assume that these reactions occur in box 4 in the schematic diagram of Figure 40.

In accordance with the equation

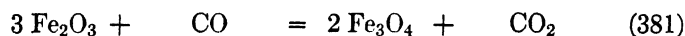


$$\begin{aligned} 84.33 \text{ kg} &= 40.32 \text{ kg} + 44.01 \text{ kg} \\ &22.263 \text{ SCM} \end{aligned}$$

there is, corresponding to 1 kg of burden:

$$\frac{22.263}{84.33} \text{MgCO}_3 = 0.26400 \text{ MgCO}_3 \text{ SCM CO}$$

According to the reduction equation



$$\begin{aligned} 479.1 \text{ kg} + 28.01 \text{ kg} &= 463.10 \text{ kg} + 44.01 \text{ kg} \\ 22.408 \text{ SCM} &22.263 \text{ SCM} \end{aligned}$$

the CO consumed is

$$\frac{22.408}{479.1} \text{Fe}_2\text{O}_3 = 0.04677 \text{ Fe}_2\text{O}_3 \text{ SCM}$$

yielding in exchange

$$\frac{22.263}{479.1} \text{Fe}_2\text{O}_3 = 0.04647 \text{ Fe}_2\text{O}_3 \text{ SCM CO}_2$$

All together, in the preheating zone the following quantities of carbon dioxide are produced per kilogram of burden:

$$\begin{aligned} \Sigma(\text{CO}_2) &= 0.26400 \text{ MgCO}_3 + 0.12072 \text{ MgO} \cdot \text{CaO}(\text{CO}_2)_2 \\ &+ 0.19369 \text{ MnCO}_3 + 0.19215 \text{ FeCO}_3 \\ &+ 0.04647 \text{ Fe}_2\text{O}_3 + 0.25610 \text{ MnO}_2 \\ &+ 0.09731 \text{ Mn}_3\text{O}_4 \quad (\text{SCM CO}_2/\text{kg burden}) \quad (382) \end{aligned}$$

On the other hand, the following quantities of carbon monoxide vanish:

$$\begin{aligned}\Sigma(\text{CO}) = & 0.04677 \text{ Fe}_2\text{O}_3 + 0.25777 \text{ MnO}_2 \\ & + 0.09794 \text{ Mn}_3\text{O}_4 \quad (\text{SCM CO/kg burden}) \quad (383)\end{aligned}$$

During this process the initial weight of the burden has diminished to

$$\begin{aligned}B = & 0.47812 \text{ MgCO}_3 + 0.52272 \text{ MgO} \cdot \text{CaO}(\text{CO}_2)_2 \\ & + 0.61710 \text{ MnCO}_3 + 0.96660 \text{ Fe}_2\text{O}_3 + 0.81594 \text{ MnO}_2 \\ & + 0.93007 \text{ Mn}_3\text{O}_4 \quad (\text{kg/kg burden}) \quad (384)\end{aligned}$$

or by the following amount:

$$\begin{aligned}\Delta B = & +0.52188 \text{ MgCO}_3 + 0.47728 \text{ MgO} \cdot \text{CaO}(\text{CO}_2)_2 \\ & + 0.38290 \text{ MnCO}_3 + 0.03340 \text{ Fe}_2\text{O}_3 + 0.18406 \text{ MnO}_2 \\ & + 0.06993 \text{ Mn}_3\text{O}_4 \quad (\text{kg}) \quad (385)\end{aligned}$$

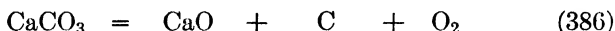
In these equations the most important element is the Fe_2O_3 content; the other constituents are usually present only in small quantities in the burden. It should also be noted whether the carbon dioxide of the carbonates is included in weight and analyses data or not.

All the other reactions take place in the reaction zone proper. They include the release of carbon dioxide from lime (CaCO_3), the reduction of Fe_3O_4 and FeO to Fe , the reduction of the phosphoric acid to phosphorus, reactions in which material changes take place, since oxygen and carbon dioxide pass off from the burden as gases. The nascent oxygen is bound by the carbon, partly as CO_2 and partly as CO . The extent to which this occurs is unmistakably governed by the law of mass action and the heat balance, without requiring any arbitrary assumptions. Compared to the majority of the computation methods known up to the present time, this elimination of arbitrary assumptions—such as the magnitude of “direct” and “indirect” reduction—represents the most substantial advance comprised in the method of computation set forth here. The assumptions recommended in the literature of ferrous metallurgy are often contradictory and possess no clear justification. Thus the proportion of direct reduction is sometimes supposed to be fairly constant ($= 59\%$);⁶ at other

⁶ Bernhard Osann, *Stahl u. Eisen*, Vol. 36 (1916), No. 20, pp. 477–484, and No. 22, pp. 530–536, as well as *Lehrbuch der Eisenhüttenkunde*, 2nd ed., Leipzig, 1923–1926.

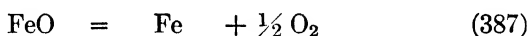
times cases are reported in which direct reduction is totally absent.⁷ The last case involved an experimental furnace with a hearth diameter of 508 mm and correspondingly very high heat losses, which explains the deviation from the value that is usual in furnaces of commercial size. This indicates what false inferences may be made from a semi-industrial experiment.

The quantities of oxygen passing off as gas (in terms of weight) are found directly from the structure of the formula. For example,



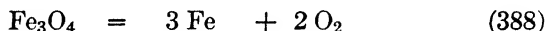
$$100.09 \text{ kg} = 56.08 \text{ kg} + 12.01 \text{ kg} + 32 \text{ kg}$$

Hence $(32/100.09) \text{ CaCO}_3 = 0.31971 \text{ CaCO}_3 \text{ kg}$ of oxygen correspond to 1 kg of CaCO_3 . In addition, the lime furnished $(12.01/100.09) \text{ CaCO}_3 = 0.1200 \text{ CaCO}_3 \text{ kg}$ of carbon per kg of burden. Furthermore,



$$71.85 \text{ kg} = 55.85 \text{ kg} + 16 \text{ kg}$$

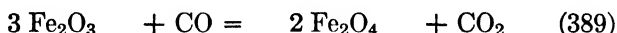
$(16/71.85) \text{ FeO} = 0.22269 \text{ FeO kg}$ of oxygen corresponds to 1 kg of FeO :



$$231.55 \text{ kg} = 167.55 \text{ kg} + 64 \text{ kg}$$

Hence $(64/231.55) \text{ Fe}_3\text{O}_4 = 0.27640 \text{ Fe}_3\text{O}_4 \text{ kg}$ of oxygen per kg of Fe_3O_4 .

In the case of Fe_2O_3 , it should be borne in mind that, according to equation



$$3 \times 159.70 \text{ kg} = 2 \times 231.55 \text{ kg}$$

$$479.10 \text{ kg} \qquad \qquad 463.10 \text{ kg}$$

one kg of Fe_2O_3 has already been converted in the pre-reaction zone into 0.96660 kg of Fe_3O_4 . Consequently, the ferric oxide furnishes us with an additional

$$(0.96660 \times 0.27640) \text{ Fe}_2\text{O}_3 = 0.26717 \text{ Fe}_2\text{O}_3 \text{ kg O}_2 \quad (390)$$

⁷ P. H. Royster, T. L. Joseph, and S. P. Kinney, *Stahl u. Eisen*, Vol. 44 (1924), No. 27, pp. 793-795. *Blast Furnace and Steel Plant*, Vol. 12 (1924), Nos. 1-3, pp. 35, 98, 154 ff. Also cf. Franz Sauerwald, *Physikalische Chemie der Metallurgischen Reaktionen*, Berlin, 1930, p. 129.

Altogether, therefore, we get the following quantities of oxygen, referred to the burden originally charged into the furnace:

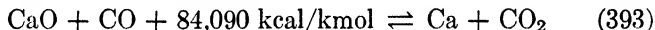
$$\Sigma(\text{O}_2)_{\text{burden}} = 0.31971 \text{ CaCO}_3 + 0.26717 \text{ Fe}_2\text{O}_3 + 0.27640 \text{ Fe}_3\text{O}_4 \\ + 0.22269 \text{ FeO} + 0.56354 \text{ P}_2\text{O}_5 \quad (\text{kg O}_2/\text{kg burden}) \quad (391)$$

which now pass off as gas and react with the coke carbon just as the blast oxygen does. This must be taken into account in the computation. From the lime a certain amount of carbon is delivered, i.e.,

$$\frac{12.01}{100.09} \text{ CaCO}_3 = 0.1199 \text{ CaCO}_3 \quad (\text{kg C/kg burden}) \quad (392)$$

For the reason given, we need not consider the manganoous oxide (MnO) reduction, since it furnished no additional constituents to the gas.

The question might also arise whether all the stack reactions have thus been covered, and why still other reactions might not be possible. Let us discuss, by way of example, whether a CaO reduction in accordance with the equation



is possible as a counterpart to the reduction of FeO. From the thermochemical data * we find the equilibrium constant of this reaction,

$$K = \frac{p_{\text{CO}_2}}{p_{\text{CO}}} \quad (394)$$

to be

$$\log K = 1.0694 - \frac{18,388}{T} - 0.0004899T \quad (395)$$

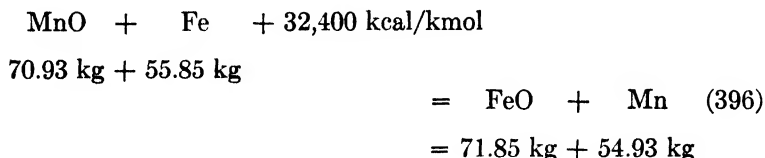
For $T = 1500^\circ\text{K}$, we get, for instance, the numerical value $\log K = -12$, K thus being of the order of magnitude of $10^{-12} p_{\text{CO}}$. Thus CaO cannot be reduced, and practically no CO_2 is produced.

The hearth reactions

We have already encountered one of the hearth reactions: the reduction of manganoous oxide by iron, which does not affect the chemical balance of the shaft but is of importance when we investi-

* See Table IV, Appendix, p. 303.

gate the quantities of manganese that enter into the iron quantities of manganous and iron oxide that enter into the slag. According to equation



589.8 kcal of heat are required per kilogram of manganese in the pig iron. In reality, the heat required for manganese production is still higher, since now we re-form FeO, though the production of Fe had required a corresponding quantity of heat. We may, however, proceed on the supposition that all the oxygen in the ferric oxide had been removed, and consider the heat requirements of the manganous oxide reaction in accordance with the foregoing equation 396.

Considered from the purely physical standpoint, reactions in the liquid state must take place considerably more slowly than gas reactions or heterogeneous reactions in which gases take part; they facilitate a rapid exchange because of their mobility. Hence we may expect that the hearth reactions, which occur principally in the iron-slag bath, take place slowly and do not reach a state of equilibrium. The more viscous, hence the colder, the bath or the melt, the farther they remain from the equilibrium stage.

From thermochemical data * we find the equilibrium constant of equation 396,

$$K = \frac{(\text{FeO})(\text{Mn})}{(\text{MnO})(\text{Fe})} \quad (397)$$

to be approximately †

$$\log K = -\frac{7085}{T} + 0.1312 \quad (398)$$

On the other hand, Körber and Oelsen ⁸ found in laboratory experiments that

* See Table IV, Appendix, p. 303.

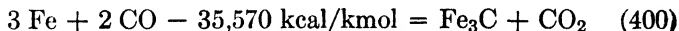
† With the assumption that $\sum \nu c_p = 0$.

⁸ Friedrich Körber, Untersuchungen über das Verhalten des Mangans bei der Stahlerzeugung, *Stahl u. Eisen*, Vol. 52 (1932), No. 6, pp. 133-142. Also see H. Schenck, *Einführung in die physikalische Chemie der Eisenhüttenprozesse*, Berlin, 1932, p. 241, Figure 124.

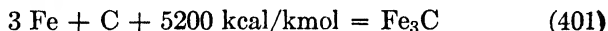
$$\log K = -\frac{6234}{T} + 1.0263 \quad (399)$$

At $t = 1700^\circ\text{C}$, K' (the reciprocal) is 2883 according to equation 398, but only 136 according to equation 399 and the experiments of Körber and Oelsen. Probably equilibrium has not yet been established * owing to the slowness of the reaction, and the value of x_{Mn} would then be 0.047. These figures must be taken with the necessary caution, of course, since they still require a theoretical and experimental foundation.

Carbon forms with iron an iron carbide, Fe_3C , which can be imagined as produced by the reaction



as well as by the gross reaction



Hence $5200/12.01 = 433.0$ kcal are required per kilogram of C in the pig iron.

The equilibrium constant of the reaction according to equation 400,

$$K = \frac{(\text{Fe}_3\text{C})(\text{CO}_2)}{(\text{Fe})^3(\text{CO})^2} = \sim \frac{v_{\text{CO}_2}}{P(v_{\text{CO}})^2} \quad (402)$$

in which P is the total pressure of this pressure-controlled reaction, can be computed from the heat of reaction and the entropy. We get

$$\log K = \frac{7880.61}{T} + 0.79048 \cdot \log T - 10.68767 \quad (403)$$

The carbon monoxide content (percentage by volume) in the equilibrium state is then computed by means of

$$v_{\text{CO}} + v_{\text{CO}_2} + v_{\text{N}_2} = 1$$

from equation 400 as

* Even though the computation from the thermochemical data is uncertain, and in particular we cannot prove exactly the justification for the assumption made in footnote †, the difference found is food for thought, especially since the first term in equation 397 leads to a heat of reaction of only 28,520 kcal/kmol, contrary to the higher value cited above, which is also buttressed by measurements. There is no justification, therefore, for accepting Körber's and Oelsen's value as the true equilibrium constant. Cf. H. Schenck, *Einführung in die Physikalische Chemie der Eisenhüttenprozesse*, Vol. 2, Berlin, 1934, pp. 105-106.

$$v_{\text{CO}} = -\frac{1}{2KP} \pm \sqrt{\left(\frac{1}{2KP}\right)^2 + \frac{(1 - v_{\text{N}_2})}{KP}} \quad (404)$$

and, for $v_{\text{CO}} + v_{\text{CO}_2} = 1$, and $P = 1$ Atm,

$$v_{\text{CO}} = -\frac{1}{2K} \pm \sqrt{\left(\frac{1}{2K}\right)^2 + \frac{1}{K}} \quad (405)$$

This enables us to make an interesting comparison with the values measured by H. Schenck and J. Bökmann.⁹ The results of the

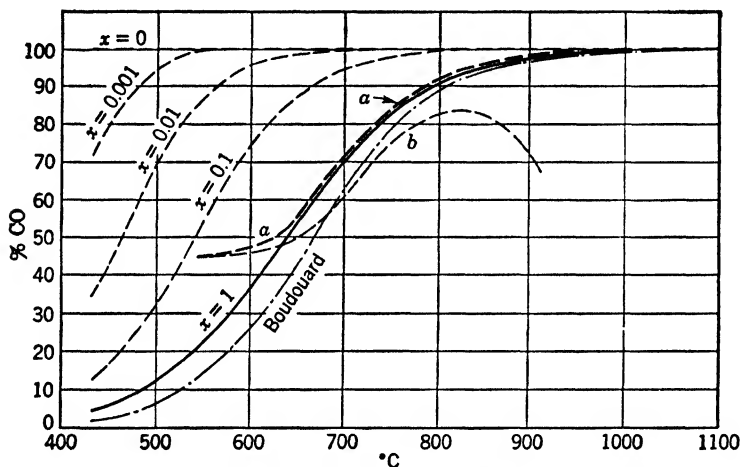


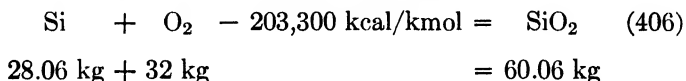
FIG. 45. Equilibrium diagram $3 \text{ Fe} + 2 \text{ CO} = \text{Fe}_3\text{C} + \text{CO}_2$.

computation are shown in Figure 45, for $p_{\text{CO}} + p_{\text{CO}_2} = 1$ Atm. At the left the curve runs beside the (dashed and dotted) Bou-douard curve, coinciding with it at high temperatures. The curve *a* measured by Schenck completely coincides with the theoretical curve above 650°C ; below 650°C it suddenly makes a sharp bend to the left. The explanation for this is the fact that below this temperature equilibrium is no longer achieved. The v_{CO} curve was plotted in Figure 45 for various degrees of completeness between $x = 0$ and $x = 1$ (equilibrium) in order to indicate disequilibrium conditions. According to the curve, x would be slightly more than 10% at 550°C .

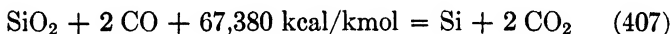
⁹ Cited from H. Schenck, *Einführung in die physikalische Chemie der Eisenhüttenprozesse*, Vol. 1, Berlin, 1932, p. 148, and Table I.

The equilibrium conditions for equilibrium with the α and γ mixed crystals occurring in the temperature range of 700 to 900°C (curve *b*) cannot be handled theoretically as yet, owing to our lack of caloric data. According to measurements, this curve *b* lies below the Boudouard curve. It is only this that makes a recarburizing reaction possible in the blast-furnace shaft, provided the iron is present in the form of this modification, whereas, according to curve *a*, this reaction does not take place in the blast furnace because of the absence of a concentration gradient.

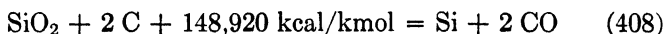
The reduction of silicon dioxide requires 3384.9 kcal/kg of SiO_2 , or 7245.2 kcal/kg of Si, according to the equation



We have intentionally ignored silicon in the shaft reactions, since it is only in the hearth (and perhaps as early as in the bosh, in part) that conditions exist under which the reduction of silica appears to be possible. A reduction in accordance with the equation



or



is impossible in the blast furnace. For physical reasons the "direct" reduction of silica according to equation 408 should really be considered only the overall equation of a reaction in accordance with equation 407, with subsequent carbon dioxide reduction as indicated by Boudouard. Equation 407 cannot occur in the blast furnace, however, as is shown by the following considerations. The equilibrium constant of this reaction,

$$K = \frac{(\text{Si})(\text{CO}_2)^2}{(\text{SiO}_2)(\text{CO})^2} = \sim \frac{v_{\text{CO}_2}}{v_{\text{CO}}} \quad (409)$$

in the temperature range of 500° to 1700°K, is 10^{-21} to 6×10^{-10} , as determined from the thermochemical data, or

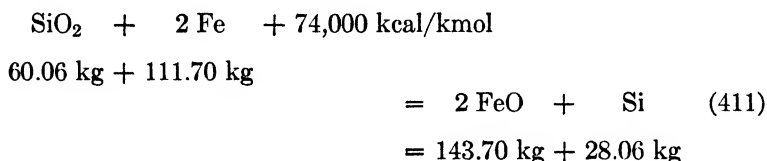
$$K' = \frac{v_{\text{CO}}}{v_{\text{CO}_2}} = 10^{21} \text{ to } 0.167 \times 10^{10}$$

and

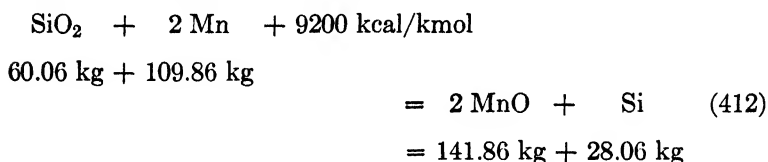
$$v_{\text{CO}} = (1 - v_{\text{N}_2}) \frac{K'}{1 - K'} = (1 - v_{\text{N}_2}) \quad (410)$$

We thus have the same situation as with manganous oxide (Figure 43). There is no effective concentration gradient in the blast-furnace shaft between the gas and the surface of the silica to be reduced, not even in the area of the highest temperatures, so that the reduction cannot take place in accordance with equation 407.

Thus the reduction of the silica takes place only via the iron, that is, in the hearth bath, at best in the granulated metal in the bosh, in accordance with equation



Heat required per kilogram of Si (in pig iron) is 2637 kcal; or, via the manganese, in accordance with



Heat required per kilogram of Si (in pig iron) is 328 kcal.

The equilibrium constant of equation 411 is

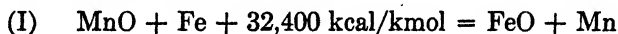
$$K = \frac{(\text{FeO})^2(\text{Si})}{(\text{SiO}_2)(\text{Fe})^2}; \quad \log K = -\frac{16,182}{T} + 2.088 \quad (413)$$

In the temperature range of 1200° to 2100°K it is 4.01×10^{-12} to 2.41×10^{-6} ; the equilibrium constant according to equation 412 is

$$K = \frac{(\text{MnO})^2(\text{Si})}{(\text{SiO}_2)(\text{Fe})^2}; \quad \log K = -\frac{2012}{T} + 1.826 \quad (414)$$

In the same temperature range it varies from 1.409 to 7.370.

If we combine all the equations 394, 411, and 412 once again, together with the numerical values of the equilibrium constants for the temperature $t = 1700^\circ\text{C}$,



$$K_I = 0.35 \times 10^{-4}$$



$$K_{II} = 7.7 \times 10^{-7}$$



$$K_{III} = 6.4$$

The equilibrium constants are related through the equation

$$K_{III} = \frac{K_{II}}{(K_I)^2} \quad (415)$$

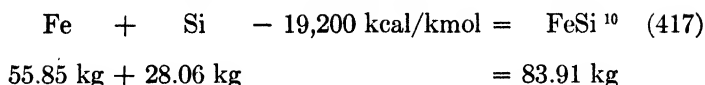
Indeed, K_{III} is derived from equation II, and equation I is derived from equation 416,

$$K_{III} = \frac{7.7 \times 10^{-7}}{1.225 \times 10^{-7}} = 6.4 \quad (416)$$

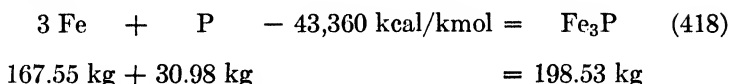
in agreement with the numerical value from equation 414.

What do these equations signify? The larger the equilibrium constant, the higher the yield of the substances at the right of the equal sign. Thus manganese is a stronger reducing agent for silica than iron, which is definitely a weak agent. Consequently, a burden poor in manganese yields a weakly silicized pig iron, and vice versa. In the manufacture of silicon spiegel, it is advantageous to have a burden rich in manganese; it makes possible obtaining high silicon contents in the product. The positive heat of reaction signifies that these are endothermic reactions; raising the temperature intensifies the course of the reactions from left to right. This corresponds to the well-known fact that very high hearth temperatures are required for the manufacture of ferroalloys, that in fact we must resort to the electric furnace if high-percentage alloys are to be produced. Equation III also indicates that for a given temperature the higher the silicon content, the lower the percentage of manganese; if both percentages are to be increased (production of silicon spiegel), very high temperatures must be employed (electric furnace).

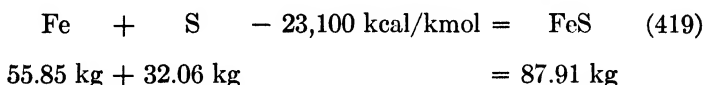
The formation of iron silicides, phosphates, and sulfides yields considerable heat of formation, since these are highly exothermic reactions; but the actual values have not yet been definitely determined at the present time.



Heat generated per kilogram of Si (in pig iron) is 686 kcal.

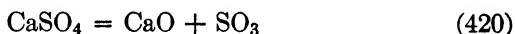


Heat generated per kilogram of P (in pig iron) is 1400 kcal.

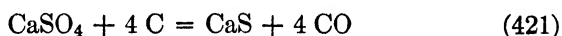


Heat generated per kilogram of S (in pig iron) is 720 kilocalories.

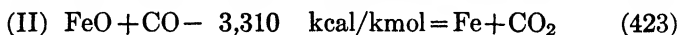
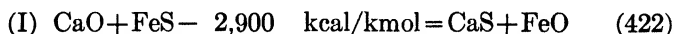
Only a slight amount of sulfur comes from the burden. Most of it comes from the fuel and the ash constituents of the fuel, where it is present chiefly as pyrites (FeS), and in smaller percentages as sulfate and as organic sulfur. The sulfates yield up their water of hydration readily. Subsequent decomposition may take place in accordance with reaction



but SO₃ rarely occurs in the waste gas. The sulfur, rather, passes as a rule into the slag or the iron:



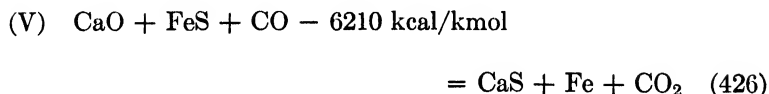
In the presence of carbon, the pyrites sulfur forms CaS, Fe, and CO in accordance with the following reactions:



¹⁰ Friedrich Körber, Die Beziehungen zwischen Bildungswärme, Aufbau und Eigenschaften technisch wichtiger Legierungen, *Stahl u. Eisen*, Vol. 56 (1936), No. 48, pp. 1401-1411.

* The discrepancy between this heat of reaction and our equation 2, p. 3, is due to the modification of carbon (diamond) employed in the tabular values of the *Taschenbuch für Chemiker und Physiker*.

Combining the first and second partial reactions, we get



i.e., desulfurization of lime and reduction of ferrous oxide by carbon monoxide. This reaction can also be obtained by subtracting equation III from equation IV. Correspondingly, the equilibrium constants of the various reaction stages may be obtained from one another as follows:

$$K_{IV} = K_I K_{II} K_{III} \quad (427)$$

$$K_V = K_I K_{II} = \frac{K_{IV}}{K_{III}} = K_{IV} K'_{p_B} \quad (428)$$

and

$$K_I = \frac{K_V}{K_{II}} = K_V K'_{II} \quad (429)$$

As one may easily demonstrate, K'_{II} is identical with Schenck's equation 354 * (cf. p 193). If the equilibrium constant of the summary equation (IV), calculated from thermochemical data, is found to be roughly †

$$\log K_{IV} = - \frac{7557}{T} + 8.825 \quad (430)$$

by combining it with the equilibrium constants of the Boudouard reaction and of ferrous oxide reduction as indicated, we can obtain the values of Table 51.

The actual desulfurization reaction (partial reaction I) is slightly exothermic, as these equations indicate. Hence, at higher temperatures the desulfurizing effect is diminished, even though only slightly, since the order of magnitude of the equilibrium constant of reaction I changes only slightly. But there is no doubt that the desulfurizing reaction in the blast furnace requires the assistance of the gases; and the intermediate reaction of

* Schenck employs the reciprocal form of the equilibrium constants.

† Assuming that $\sum \nu c_p = 0$, since the c_p values of CaS at high temperatures are unknown.

equation V, which is somewhat exothermic, is therefore particularly interesting. This reaction is plotted in Figure 46, together with the Boudouard curve (for air). The diagram indicates that the

TABLE 51

EQUILIBRIUM CONSTANTS OF THE REACTIONS OF EQUATIONS 423 TO 426

$T =$	1000	1250	1500	1750	2000°K
Reaction IV: $K_{IV} =$	18.54	601.2	6124	32,140	111,200
Reaction V: $K_V =$	9.773	5.373	3.773	3.021	2.595
Reaction I: $K_I =$	15.38	12.86	11.88	11.40	11.01

effective concentration gradient of carbon monoxide has a maximum in the temperature range of 800 to 1050°C; it is here that the reaction will be liveliest. At higher temperatures the drop is slight, whereas it is quite considerable at lower temperatures, so

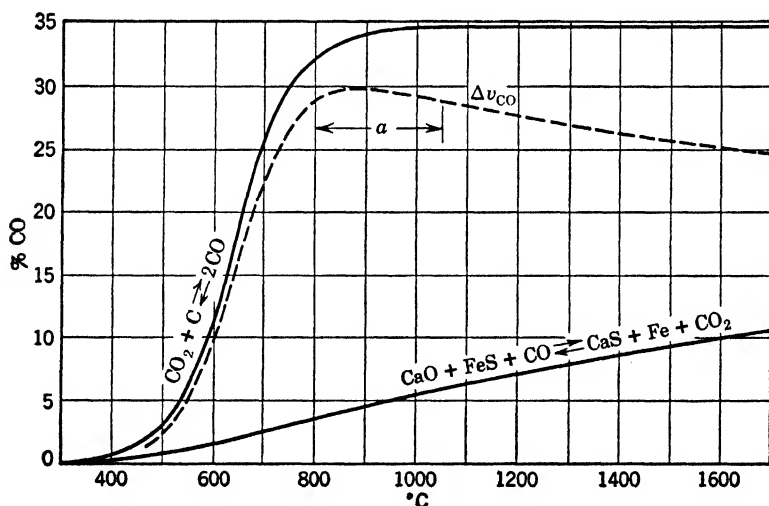
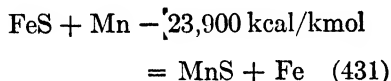


FIG. 46. Desulfurization by carbon monoxide in the presence of lime.

that desulfurization presupposes temperatures of 800°C or higher, which are easily available in the bosh and hearth of the blast furnace. Thus lime is the given desulfurizing agent, and a very effective one, but a corresponding basicity of the slag must be

insured.* Since, at higher temperatures, the CaO is broken down increasingly, for example, by formation of calcium ortho and meta-silicate, and finally of calcium trisilicate, as well as by the formation of aluminates and ferrites, it is not available for desulfurization, of course. The "free" CaO attains a maximum in the temperature range of 900 to 1000°C, as shown in Figure 47 for the example of cement formation according to data by Kühl and Lorenz,¹¹ so that this temperature span is best for desulfurization for this reason as well.

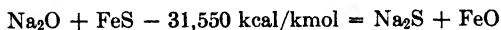
Manganese is another desulfurizing agent. The desulfurizing reaction proceeds in accordance with the equation



The reaction is rather highly exothermic. The heat generated † is 271.9 kcal/kg of FeS, or 745.5 kcal/kg of slagged sulfur in the manganese desulfurization of equation 431, as contrasted with only 33.0 kcal/kg of FeS, or 90.5 kcal/kg of slagged sulfur, in the lime desulfurization of equation 422.

Slag formation is an exothermic process. According to Ulich,

* We shall not enter into a discussion at this point of *acid smelting*, as employed for an ore burden poor in iron, where a suitable addition of lime is not feasible because the burden would then be impoverished still more. The desulfurizing is then effected outside the blast furnace, for instance, by the addition of soda in accordance with the reaction



This reaction is even more exothermic than those of lime and manganese desulfurization.

¹¹ H. Kühl, *Zementchemie in Theorie und Praxis*, Berlin, 1929, *Tonind. Z.*, Vol. 53 (1929), No. 78, p. 1397.

† Heat generated in soda desulfurization is 358.9 kcal/kg of FeS, or 984.1 kcal/kg of slagged sulfur.

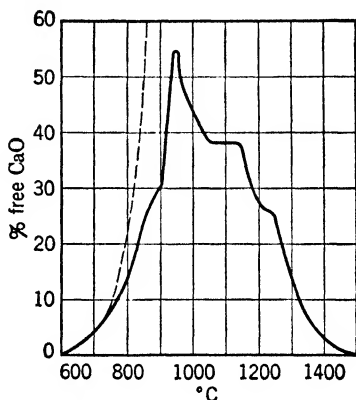


FIG. 47. Free CaO in cement formation (according to data of Lorenz and Kühl).

Schwarz, and Cruse ¹² the heat of formation is 140 kcal/kg. Körber and Oelsen ¹³ have constructed a diagram for determining the heat of formation, giving the following values for typical blast-furnace slags:

Basic slag = -161 kcal/kg

Acid slag = -145 kcal/kg

for crystalline slag. The difference between crystalline and vitreous slag (heat of devitrification) is given as 40 to 80 kcal/kg,

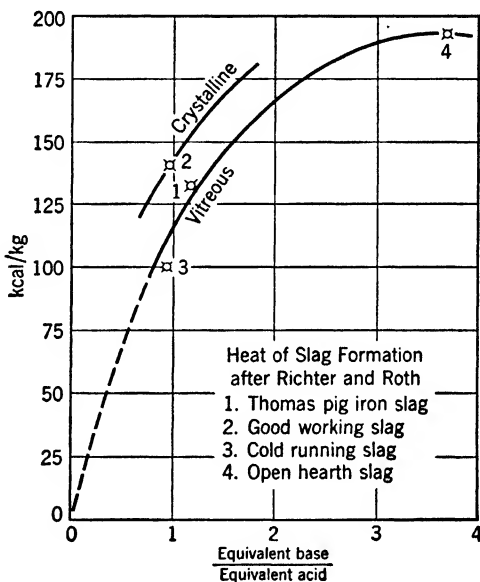


FIG. 48. Heat of slag formation after Richter and Roth.

while Richter and Roth ¹⁴ state that it is at least 30 kcal/kg. The measurements by Richter and Roth are in very good agreement with these figures (see Figure 48).

¹² Herman Ulich, Carl Schwarz, and Kurt Cruse, Wärmetönungen metallurgischer Reaktionen II, *Arch. Eisenhüttenwes.*, Vol. 10 (1936-1937), No. 11, pp. 493-500.

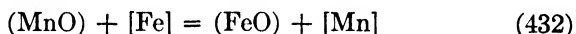
¹³ Friedrich Körber and Willy Oelsen, Die Schlackenkunde als Grundlage der Metallurgie der Eisenerzeugung, *Stahl u. Eisen*, Vol. 60 (1940), No. 42, pp. 921-929, No. 43, pp. 948-955.

¹⁴ Helmuth Richter and Walther A. Roth, Die Bildungswärme von Eisenschlacken aus den Oxyden, *Arch. Eisenhüttenwes.*, Vol. 11 (1937-1938), No. 9, pp. 417-419.

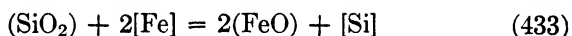
Yield

Since the top gas is considered merely a by-product of the blast furnace, although we are devoting most of our attention to it in connection with our computations, the yield figures must also be discussed to provide an answer to the question (so important to the material balance) of how the substances in the total burden are divided among the product (pig iron in the blast furnace), the slag, and the top gas.

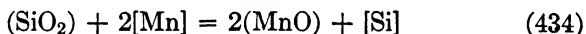
Since the iron oxides can be reduced fairly easily, the iron yield is nearly 100%. Indeed, it may be assumed that it is actually 100%, and that the amounts of ferrous oxide appearing in the slag have merely been subsequently formed in the hearth as a result of the reduction of manganese and silicon:



and



The brackets signify that the substance in question is contained in the metal; the parentheses, that it enters the slag or is contained in the ore. But, as silica is also reduced by manganese (and energetically, too), in accordance with



the Mn produced in accordance with equation 132 can re-enter the slag to improve the Si content. Since 2 moles of Fe are consumed for 1 mole of Si, whereas 1 mole of Si also requires 2 moles of Mn, and 1 mole of Mn requires 1 mole of Fe, 1 mole of Si in the pig iron always corresponds to the consumption of 2 moles of Fe, irrespective of the nature of the extraction process. Only the percentages of FeO and MnO in the slag can vary, being governed by equation 432 (cf. p. 208). Hence the iron yield is

$$\epsilon = 1 - [\text{Mn}] - 2[\text{Si}] \quad (435)$$

In accordance with the equilibrium constants, the higher the percentages of silica and manganese in the charge, the higher the percentages of silicon and manganese. Consequently, the yield of silicon and manganese depends on the basicity of the burden or of the slag, as well as on the hearth temperature. But since our observations (see p. 209) justify the assumption that the reaction of equation 432 does not proceed until equilibrium is

reached, time (residence time in the furnace) and the agitation of the bath, which is hard to influence in the blast furnace, are additional factors. Since high temperature produces a high fluidity of the bath, temperature acts doubly to promote the silicon and manganese yield. Hot furnaces therefore exhibit a correspondingly poor iron yield, a slag richer in FeO, and a pig iron richer in Si and Mn. Insofar as conditions of disequilibrium are involved, these effects cannot be dealt with mathematically, unless the degree of approach to the equilibrium of the reaction were determined by experiments. This uncertainty does not affect our calculation, in the first place, because the gas formed from the burden is the same as if all the iron oxides had been reduced 100%, in which connection the effects of the Mn and Si may be neglected.

In the case of phosphoric acid we may assume 100% P yield; the reaction $3\text{Fe} + \text{P} = \text{Fe}_3\text{P}$ will not be complete if the furnace is operating cold, however. The Mn, Si, and P in the pig iron must be taken into account in the heat balance only in the heat required for the hearth reactions, the experimentally determined Si, P, and Mn percentages in the pig iron furnishing a basis for estimating the extent of the reaction. We shall ignore the other constituents of the burden. The corresponding figures may be found in Table 52.

According to the observations made on page 216, the higher the acidity and the lower the basicity of the slag, the higher the sulfur yield.* In acid melts, for example, we are not interested in the product after desulfurization (outside the furnace), but just as it is tapped from the furnace. According to the desulfurizing reaction of equations 424 and 426, 1.749 kg of CaO or 3.122 kg of CaCO_3 are required per kilogram of sulfur, while many times this quantity is available in the blast furnace. This CaO, however, is not free; the higher the silica content, the more of this CaO is removed. Hence both a definite absolute quantity of lime as well as a definite degree of basicity are necessary. With a burden poor in iron the amount of slag is high, but at the same time the fuel consumption rises, and with it the absolute amount of sulfur.

* We speak of "yields" of sulfur, arsenic, etc., in order to make our terminology conform with our previous terminology, although these are undesirable constituents.

It is difficult to get a criterion—aside from experience—for the carbon passing into the pig iron, especially as the formation of Fe_3C is confined to a narrow temperature range, as indicated by Figure 45 (curve *b*). We must, therefore, assume that the C percentages in the pig iron produced are such as we know from

TABLE 52

YIELD FIGURES IN %

Fe	95–100 *	
Mn	60–75	in normal furnace operation
	80–90	in a hot furnace
Si	2–15	2 to 3% for basic or slightly acid burden; up to 15% for strongly acid burden very deficient in lime.
P	100 †	
Ti	0–10	
V	60–90	
Ni	100	
Cu	100	
Cr	~100	
As	70–95	
Pb	100	(not in the pig iron)
Zn	100	(not in the pig iron)
S	20–50	(high for acid melts; low for basic melts)

* Equals 100% in calculating the quantity of gas, ignoring the Mn and Si in the pig iron.

† In the case of basic Bessemer iron, 97% for a hot furnace and 97 to 70% for a cold one.

experience (3.5 to 4.0%). A high silicon content counteracts the formation of Fe_3C by favoring the formation of FeSi , which equation 417 indicates is considerably more endothermic and is favored by high temperature.

The *slag yield* is found from the difference between the substances charged and the substances constituting the pig iron and the top gas. The principal slag-forming constituents are: SiO_2 , less the amount of SiO_2 reduced, whose Si has passed into the pig iron and whose O_2 has gone off with the gas; Al_2O_3 ; CaO ; MgO ; MnO , insofar as it has not been reduced to Mn; and FeO , insofar as it has passed over from the metal into the slag as a result of the

MnO reduction. Hence the amount of slag per kilogram of burden (the slag yield) is

$$\epsilon'' = (1 - \epsilon_{\text{SiO}_2})\text{SiO}_2 + \text{Al}_2\text{O}_3 + \text{CaO} + \text{MgO} + \text{MnO} \quad (436)$$

If the carbonates and higher oxides are specified in the analysis of the burden, they are to be recalculated accordingly, e.g.:

$$\begin{aligned} \epsilon'' = (1 - \epsilon_{\text{SiO}_2})\text{SiO} + \text{Al}_2\text{O}_3 + 0.56030 \text{ CaCO}_3 \\ + 0.4712 \text{ MgCO}_3 + 0.61710 \text{ MnCO}_3, \text{ etc.} \end{aligned} \quad (437)$$

The FeO in the burden or in the slag and the CaS in the slag need not be considered in detail, because they have already been dealt with when we considered the MnO and the CaO.

Thus the amount of slag depends wholly upon the nature of the ores smelted, and the ores must be so constituted and, if necessary, must be supplied with such fluxes as to make the resulting slag comply with the following two conditions:

- (1) The burden must produce a well-fused, easily tapped slag.
- (2) The slag must be basic in order to insure desulfurization.

The second condition may be ignored only if desulfurization is effected outside the furnace and the only goal aimed at is low melting temperature and high liquidity of the slag (*acid smelting*). It is convenient to use the slag ratio

$$p = \frac{\text{acids}}{\text{bases}} 100 = \frac{\text{CaO} + \text{MgO} + \text{FeO} + \text{MnO}}{\text{Si} + \text{Al}_2\text{O} + (\text{TiO}_2)} 100 \quad (438)$$

as a measure of the basicity. In view of the large number of slag constituents, it is not entirely easy to obtain an accurate picture of the relationships between melting temperature and composition of the slag, but it is usually sufficient to confine ourselves to the triple system $\text{CaO-SiO}_2\text{-Al}_2\text{O}_3$, since very high precision is unnecessary. Figure 49 shows the melting-point isotherms according to Rankin and Wright¹⁵ and the lines of equal slag ratios

$$\frac{\text{CaO}}{\text{SiO}_2 + \text{Al}_2\text{O}_3}$$

As Figure 50 indicates, the basic slags (as defined by O. Glaser¹⁶)

¹⁵ A. Rankin and E. Wright, *Zeitschrift für anorganische Chemie*, Vol. 92 (1915), p. 213.

¹⁶ Otto Glaser, *Neuere Untersuchungsverfahren zur Erkennung des Schlackenbaues*, *Arch. Eisenhüttenwes.*, Vol. 2 (1928-1929), No. 2, pp. 73-79.

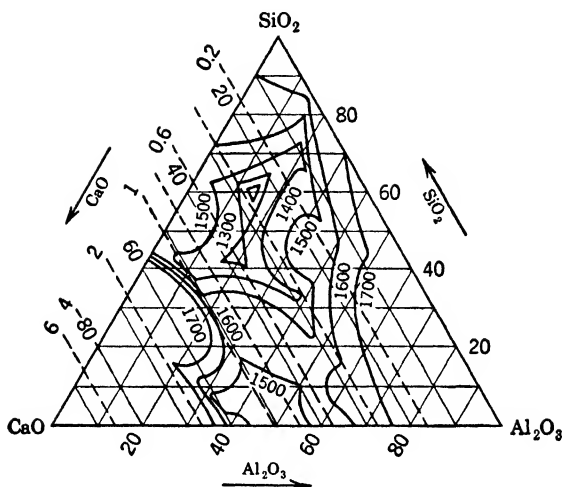


FIG. 49. Diagram of the system $\text{SiO}_2 + \text{Al}_2\text{O}_3 + \text{CaO}$.

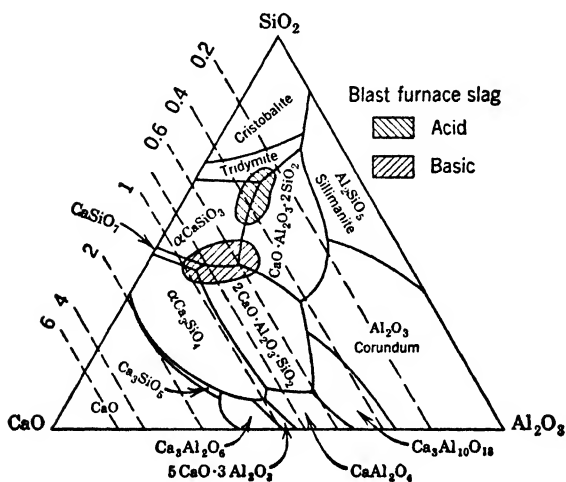


FIG. 50. Slag diagram showing typical blast-furnace slags. (Numbers indicate the $\text{CaO}/(\text{SiO}_2 + \text{Al}_2\text{O}_3)$ ratio.)

lie in the region of $\text{CaO}/(\text{SiO}_2 + \text{Al}_2\text{O}_3) = 0.5$ to 1.0, whereas the acid slags are located between 0.2 and 0.5. The melting temperatures of the acid slags are somewhat lower than those of the basic ones. When the basicity is very high, $\text{CaO}/(\text{SiO}_2 + \text{Al}_2\text{O}_3) = 1$, there is the danger that the slag will no longer flow. From this we see that high sulfur contents cannot be controlled by increasing the basicity indefinitely, as finally they can no longer be handled by the blast furnace. The computation of the burden¹⁷ comprises the development of the desired temperature ranges by means of suitable composition of the ore and the fluxes. The ash constituents of the coke may be, and for high ash contents they must be, included in the computation.

The *pig iron yield* or *burden yield* (not identical with the above-mentioned iron yield), the figure mostly used in economic calculations, is the sum of the yields of Fe, Mn, Si, P, and C, as well as of the other undesirable constituents, such as S, As, etc., referred to the ore burden.

¹⁷ For graphical methods, see Walter Mathesius, *Die physikalische und chemische Grundlagen des Eisenhüttenwesens*, 2nd ed., Leipzig, 1924, pp. 207-221; and *Stahl u. Eisen*, Vol. 28 (1908), No. 32, pp. 1121-1142.

8

METHOD OF COMPUTATION

After having endeavored to obtain an idea of the reactions in the blast furnace * and to clarify the necessary conditions for material balances and for the heat balance sheet, we may commence the computation proper, using the gas producer as a model. In both instances we take 1 SCM of product gas as the reference value, thus departing somewhat from the usage in other accounts, which usually employ the ton of pig iron produced as the reference basis. The most important prerequisite for any method of computation is the determination of the equilibria. Without them or without knowing the approximation to the equilibria, calculation would be impossible and its results useless or, at best, an unattainable ideal picture. In gas producers, equilibria are fully achieved in essence. This may also be expected to occur in blast furnaces, so far as we are dealing with reaction temperatures of the same order of magnitude as in gas producers. The comparison of calculation and measurement will indicate the extent to which this assumption is actually correct. We take no stand on the assertions made almost uniformly throughout the literature that equilibria are not established in shaft furnaces (and hence in the blast furnace),† especially since justifications (not to mention proofs) of these assertions are not given at all or are quite inadequate. The examples for which we have carried out computations indicate that the reaction temperatures in a rotary-grate gas producer and in a pig-iron blast furnace are actually of the same order of magnitude. In the rotary-grate gas producer the reaction temperature of about 700°C is produced by the pronounced effect

* If we have discussed chiefly the conditions prevailing in blast furnaces, we have done so because in the blast furnace all the types of reactions are encountered that are found in part in other shaft furnaces. Thus the blast furnace serves merely as the most typical example of shaft furnaces in general.

† Cf. p. 246.

of the moisture in the blast (saturation temperature about 60°C). In the blast furnace this reaction temperature is produced, with a dry blast preheated to 600 to 700°C, by the heat required for heating up the burden, for the reactions within the furnace, and for melting down the slag and the pig iron.

The task of performing a shaft-furnace computation may start from various formulations of the problem. Conditions are simplest when the ratio of burden weight * to fuel weight,

$$\mu = \frac{\text{Kilograms of burden}}{\text{Kilograms of fuel}} \quad (439)$$

is known. This will always be the case if merely the influence of a high ash content or of fluxes is to be investigated in a slagging ash gas producer or a calculation is to be carried out for a blast furnace, a cupola, or similar shaft furnace with a given amount of coke per charge (quantity of coke per kilogram of burden = $1/\mu$): Case 1.

On the other hand, if the amount of coke per charge is unknown and is first to be determined by the computation (since a burden whose effect on the heat balance as yet unknown is to be treated), the computation must be performed for at least three assumed numerical values of μ , and the amount of coke per charge or the applicable value of μ determined for the overall heat balance sheet: Case II. For unknown burdens or unusual temperatures, this must be accompanied by an examination of the question of whether the hearth temperature suffices to carry out the job assigned to the blast furnace. Thus, in the production of ferroalloys in the blast furnace, it is not the heat required by the reactions (especially the shaft reactions) that governs the coke per charge, but the necessary hearth temperatures, and hence the extent of the hearth reactions. In this case, the blast furnace is employed not only for the reduction of the ore but also chiefly for the manufacture of a very specific product, and this double task determines

* In the subsequent discussion we employ this term, commonly used in blast-furnace operation, for all shaft furnaces, defining the "burden" as all the components of the charge except the combustible part of the fuel. Thus, in the blast furnace, the "ore burden" + fluxes + fuel ash. The term *total burden* is sometimes used for the whole charge put into the furnace, but, by our definition, we shall always understand the burden to mean the total burden minus the combustible portion, or the carbon, of the fuel.

its coke requirements. The most suitable quantity of coke per charge is one that results in the lowest possible charge temperature, together with a sufficiently high hearth temperature, corresponding to the tapping requirements. The chief value of a calculation lies in the fact that it makes it possible to judge unusual procedures and to estimate the value of operational measures correctly and not merely by guesswork.

The work of computation involved is not inconsiderable, which makes it all the more important to estimate the order of magnitude of the value of μ in such computations so as to keep as close as possible to the expected value. If a mathematical investigation is applied to variables whose effect upon the heat balance is easily visible—for instance, to various degrees of blast preheating—it is easier to estimate the expected value of μ or of the coke required. In this case, to be sure, the coke per charge should not be entered into the calculation like heat added by the higher preheating. It should rather be borne in mind that the reduction of the coke per charge entailed greatly reduces the ratio of the ascending volume of gas to the descending charge, so that the cooling effect of the gas becomes greater as the blast temperature increases.* The same observation applies to the enrichment of the blast with oxygen. Reducing the nitrogen ballast diminishes the fuel consumption and increases the burden/fuel ratio. In addition, the volume of the ascending gas is smaller owing to the lower percentage of nitrogen, as a result of which the temperature is lowered very rapidly and considerably.†

To make a preliminary estimate of the fuel consumption we can make use of a diagram in which a graphic heat balance sheet is set up per kilogram of burden, with estimated values of the reaction temperature t_R (or, what amounts to the same, of heating value of the top gases) and of the charge temperature t_G .¹ The heat required consists of a quantity that is independent of the fuel (the “theoretical heat requirement” of the burden, comprising drying, deacidification, reduction, and slagging of the burden,

* Cf. the example of the hot-blast cupola furnace, p. 267.

† Cf. p. 253 for the consequences of this.

¹ This mode of representation has been employed successfully wherever this estimate is easy to make ($H_i = 0$, t_G known), as in rotary cement kilns. Cf. W. Gumz, *Handbuch der Brennstoff- und Feuerungstechnik*, Berlin, 1942, p. 178, Figure 45. *Beiträge zur wärmetechnischen Berechnung von Zementdrehöfen*, *Zement*, Vol. 22 (1933), No. 49, pp. 677–682, No. 50, pp. 691–694.

and melting of the slag and the pig iron) and a quantity depending on the fuel, comprising the heat losses in the palpable and latent heat of the top gas and the heat losses through radiation, conduction, and the cooling water. The sum of these two quantities represents the heat required, which is plotted against the heat supplied (fuel consumption = $1/\mu$ times the heating value). A

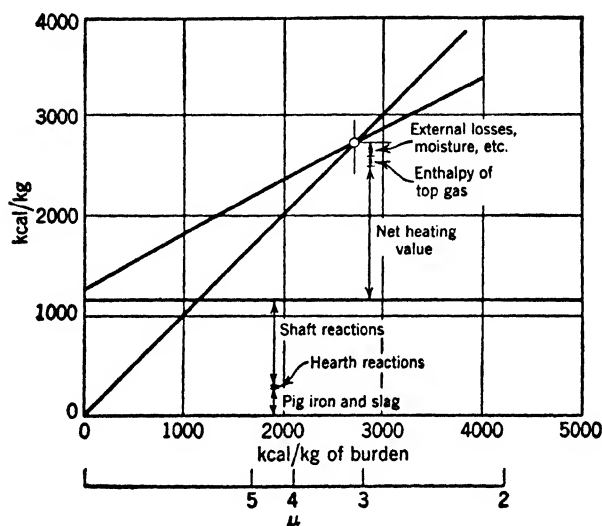


FIG. 51. Heat-input, heat-output diagram used for estimating the burden/fuel ratio.

45-degree straight line (assuming equal scales for heat supplied and heat required) then intersects the curve at the sought-for heat supply that covers this requirement (Figure 51). But as we have merely estimated the heating value of the gas and the top gas temperature, we must now carry out the precise calculation with three values of μ that bracket the expected result. With the more accurate values thus obtained, the heat balance may then be corrected and the final correct value of consumption obtained.

The computation is carried out as follows. We conceive the total charge to be a hypothetical (fictitious) fuel, which contains—besides its carbon (coke carbon)—additional carbon c' , namely, the carbon derived from the calcium carbonate, and additional

oxygen o' (the burden oxygen).* By equations 391, 392, page 207, these additional constituents, referred to 1 kg of actual fuel, are found to be

$$c' = 0.12\mu\text{CaCO}_3 \quad (440)$$

$$o' = \mu(0.31971 \text{ CaCO}_3 + 0.22269 \text{ FeO} + 0.27640 \text{ Fe}_3\text{O}_4 \\ + 0.26716 \text{ Fe}_2\text{O}_3 + 0.56354 \text{ P}_2\text{O}_5) \quad (441)$$

We are not considering the whole furnace, but—as in the gas-producer calculation—we are merely setting up material and heat balance sheets for the *reaction zone* (main reaction zone). The hypothetical fuel F_h entering this zone is characterized by the equation

$$F_h = F(1 + c' + o') \quad (442)$$

If the carbon content of the actual fuel (F) itself is C (or $C = 100\%$), in the hypothetical fuel it is changed into

$$c_h = \frac{C + c'}{1 + c' + o'} \quad (443)$$

the hydrogen content is changed into

$$h_h = \frac{H}{1 + c' + o'} \quad (444)$$

the oxygen content is changed into

$$o_h = \frac{O + o'}{1 + c' + o'} \quad (445)$$

and so forth. With this new composition of the fuel, which is characterized chiefly by a large increase in oxygen, the fuel values

$$C_F = 1.8664 c_h \quad (446)$$

$$H_F = 11.121 h_h \quad (447)$$

$$O_F = 0.7005 o_h \quad (448)$$

$$N_F = 0.8001 n_h \quad (449)$$

are found in equations V to VIII, page 48.

* Instead of adding the constituents of the burden that pass over into the gas to the fuel, we could also combine them with the gasifying agents. Then the problem would be dealt with as if the coke were reacting with a blast that was correspondingly richer in oxygen.

If the fuel used is not carbon or a fully devolatilized coke, allowance must be made for the fact that the fuel must be devolatilized or additionally devolatilized in the preheating zone and that a devolatilized (but possibly not entirely devolatilized) fuel, which is not identical with the fuel supplies in the charge, enters the main reaction zone. This must be borne in mind when charcoal is used, for instance.*

With the expression developed in equations 446 to 449, we now enter the equations developed for gas producers, several modes of proceeding to a solution being open to us. For example, we now determine F_h , M , and v_{N_2} from equations 160 to 162.

$$F_h = \frac{C_{GO_M} - C_{MO_G}}{C_{FO_M} - C_{MO_F}} \quad (450)$$

$$M = \frac{C_{FO_G} - C_{GO_F}}{C_{FO_M} - C_{MO_F}} \quad (451)$$

$$v_{N_2} = F_h N_F + M N_M \quad (452)$$

and

$$\psi^* = H_G + (F_h H_F + M H_M) \quad (453)$$

The actual fuel consumption per SCM of gas is found from equation 442 to be

$$F = \frac{F_h}{1 + c' + o'} \quad (454)$$

The heat balance sheet is quite different from that of the gas producer. In addition to the terms in equation 227, the following other terms appear:

H_μ = Heat content of the burden after heating up to the reaction temperature t_R (kcal/kg burden).

Q_Σ = Sum of the additional heat required for the blast-furnace reactions, comprising the quantities Q_{shaft} , Q_{hearth} , and Q_{sl} .

Q_{shaft} = Heat required for the shaft reactions (kcal/kg burden).

Q_{hearth} = Heat required for the hearth reactions (kcal/kg burden).

* Cf. the sample calculation on p. 236.

Q_{sl} = Heat required for slag formation (negative since the slagging reactions are exothermic on the whole) (kcal/kg burden).

H_{prod} = Heat content of the manufactured product—in the blast furnace, the tapped pig iron, including its heat of fusion, at the tapping temperature (kcal/kg pig iron).

H_{sl} = Heat content of the slag, including its heat of fusion, at the tapping temperature (kcal/kg slag).

The complete heat-balance equation is then

$$FH_i + FH_C + F\mu H_\mu + MH_M = H_{i,G} + H_G + F\mu(Q_\Sigma + \epsilon' H_{prod} + \epsilon'' H_{sl}) + Q_{ext} \quad (455)$$

The left side of this equation represents the quantities of heat supplied in the reaction area, namely:

FH_i = Fuel heat introduced (heating value).

FH_C = Enthalpy of the fuel * introduced to t_R . This includes not only the carbon that forms gas, but also the carburization carbon that enters the pig iron.

$F\mu H_\mu$ = Enthalpy of the burden † introduced by the preheating of the burden (μF) to the reaction temperature t_R .

MH_M = Enthalpy of the blast introduced (enthalpy of the gasifying agent).

The right side of the equation includes the quantities of heat produced; first, the net heating value and the heat content of the generated gas at the temperature t_R in kilocalories per SCM of gas, then the quantities of heat consumed in the various reactions, and Q_{ext} the heat lost externally by radiation, conduction, and in the cooling water.

ϵ' signifies the pig-iron yield (burden yield) ‡

* Since we call the pure coke the fuel, assigning its ash constituents to the burden, whereas the moisture and the volatiles pass off in the preheating zone, we may consider H_C to be pure carbon and take the numerical values from Table VII in the Appendix, p. 306.

† For the devolatilized burden considered here we may employ the tabular values for blast-furnace slag contained in Table VII in the Appendix, p. 306.

‡ Cf. p. 219. We take the burden yield to be 100% iron yield, plus the yield of carbon, silicon, phosphorus, and sulfur, but neglecting the manganese yield, since the latter is obtained at the expense of the iron yield.

ϵ'' signifies the slag yield. *

H_{prod} and H_{sl} for pig iron and blast-furnace slag are to be taken from Table VII—in the appendix, p. 306.

If all the terms are brought over to the left side of the equation in order to plot the H - t diagram, leaving only $H_{i,G} + H_G$ on the right side, making an allowance for Q_{ext} by means of a percentage reduction of the heat supplied in the fuel (reduced net heating value H'_i), we obtain

$$FH'_i + FH_C + F\mu[H_\mu - Q_\Sigma - \epsilon'H_{prod} - \epsilon''H_{sl}] + MH_M = H_{i,G} + H_G \quad (456)$$

The equation ²

$$H_i = 81.3 C + 243 H + 15 N - 23.5 O + 45.6 S \quad (457)$$

may be used to find the net heating value of the fuel. First the heat losses must be estimated. In doing this it is found to be particularly desirable to base the heat balance on 1 SCM of gas or (what amounts to the same thing) on 1 kg of fuel burned, since the fluctuations involved are smaller than when 1 ton of pig iron produced is used as a basis. Senfter ³ gives values of 100 to 682 kcal/ton of pig iron; thus there is practically nothing that can be used as a basis. It is obvious that this value must be quite different, depending on whether we are dealing with a poor or a rich burden. On the other hand, if these losses are based on 1 kg of fuel, say, by a percentage reduction of the heating value, a much better allowance is made for the variety of operating conditions. The heat losses may be estimated from Figures 52 and 53 for gas producers and blast furnaces. The heat exchange per unit volume is greatest in gas producers, and hence the radiation and conduction losses lowest. In gas producers under very high loads these losses may fall below 1%, and even lower in high-pressure gas producers (proportional to \sqrt{P}) (see p. 160). In blast furnaces, the higher the ratio μ = burden/fuel and the less the coke per charge, the lower is the heat exchange per unit volume. Consequently

* Cf. p. 222. The dust losses are included in the slag, so far as they are not dealt with separately.

² Cf. *Feuerungstechnik*, Vol. 26 (1938), No. 10, pp. 322–323.

³ Eduard Senfter, *Die Vorausberechnung des Koksverbrauch im Hochofen*, *Arch. Eisenhüttenwes.*, Vol. 12 (1938–1939), No. 2, pp. 549–564.

in a blast furnace ($\mu \sim 3$) it is higher than in a gas producer, and in a cupola furnace ($\mu \sim 6$ to 10) still higher than in a blast furnace.

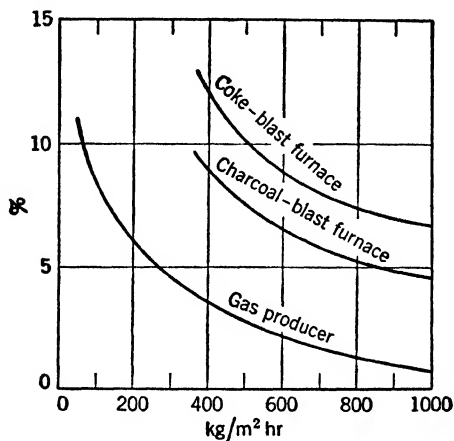


FIG. 52. External heat losses (in percentage of heat input by the fuel).

For equal blast, low bulk weight of the fuel signifies faster throughput than high bulk weight, which is why charcoal furnaces have shorter throughput times than coke blast furnaces. Figure 53 shows the influence of the burden/fuel ratio (μ), whereas the curves of Figure 52 are drawn for a ratio of about 3 or $1/(1 + \mu) = 25\%$. Furnaces running at particularly high temperatures (such as ferromanganese furnaces) have lower percentage losses than colder-working furnaces.

If the gas composition has been determined for at least three temperatures, and the reaction temperature determined graphically, we know the gas composition for the end of the reaction zone for the corresponding value, but we do not yet know the composition of the top gases.

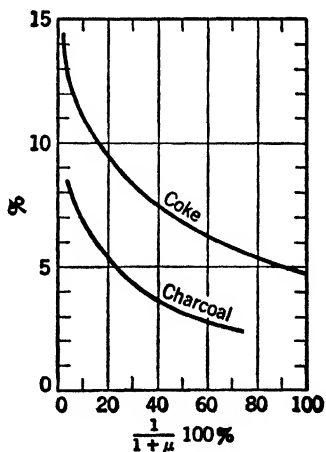
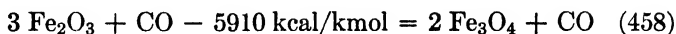


FIG. 53. External heat losses of blast furnaces as a function of the burden/fuel ratio.

In the preheating zone, Fe_2O_3 is reduced in accordance with the equation



According to equation 383, the following volume of CO disappears: $0.04677F_\mu\text{Fe}_2\text{O}_3$ SCM, and in its place $0.04647F_\mu\text{Fe}_2\text{O}_3$ SCM of CO_2 is formed. This slightly exothermic reaction releases the comparatively small amount of heat represented by

$$\frac{5910}{479.1} F_\mu\text{Fe}_2\text{O}_3 = 12.3F_\mu\text{Fe}_2\text{O}_3 \quad (\text{kcal per kg of burden}) \quad (459)$$

Furthermore, the heat required in the preheating zone consists of the enthalpy of the burden (including the amounts of gas already generated in the preheating zone), the enthalpy of the fuel (including the volatile constituents such as gas, tar, and the water of constitution), the heat content of the water of hydration (hydration enthalpy), and finally the proportional share of conduction and radiation losses. In order to find the temperature of the top gas, plot an H - t diagram, based either on 1 kg of fuel or on 1 SCM of gas (reaction zone), deducting the quantities of heat exchanged in the preheating zone from the initial point $t = t_R$. In so doing, it should be borne in mind that the volume of the gas is increased by the reactions in the preheating zone (especially by the amounts of steam), and that the quantities of heat required must be recomputed in terms of the reference quantities employed in the diagram. For example, if the fuel used has a moisture content of 10% and the basic unit is 1 SCM of reaction gas, the amount of water to be evaporated is

$$\frac{w}{1 - w} F^* \quad (\text{kg H}_2\text{O/SCM of gas})$$

In this case, too, the total quantity of fuel (i.e., the amount of fuel generating gas + the carburization carbon) must be used.

$$Q_{preh} = F^*(H_C)_{t_0}^R + F_\mu(H_\mu)_{t_0}^R + F^*H^*_{w_f} + F_\mu[Q_{hydr} + H^*_{w_\mu}] - Q_{red} \quad (460)$$

where F = quantity of fuel, gasified

F^* = quantity of fuel, including carbon of carburization

μ = ratio of burden to fuel; $F\mu$ = quantity of burden

$(H_C)_{t_0}^{t_R}$ = enthalpy of fuel between temperatures t_0 (temperature of fuel as charged) and t_R (reaction temperature)

$(H_\mu)_{t_0}^{t_R}$ = enthalpy of burden between temperature t_0 (of burden as charged) and t_R

$H^*_{w_f}$ = heat content of the moisture in the fuel (enthalpy and heat of vaporization), reduced to the fuel quantity F^* (indicated by the asterisk)

$H^*_{w_\mu}$ = heat content of the moisture in the burden (enthalpy and heat of vaporization), reduced to the fuel quantity F^*

Q_{hydr} = heat of hydration

Q_{red} = heat of reduction ($\text{Fe}_2\text{O}_3 \rightarrow \text{Fe}_3\text{O}_4$)

9

EXAMPLE OF COMPUTATION

Charcoal Blast Furnace Sandviken No. 3 (M. Wiberg ¹)

GIVEN ASSUMPTIONS

Composition of Burden

Ore Burden	Charcoal Ash	Burden + Coal Ash (0.01492 kg ash/kg burden)
58.12 % Fe ₂ O ₃	3.0 % Fe ₂ O ₃	57.31 % Fe ₂ O ₃
18.11 % Fe ₃ O ₄	3.0 % MnO	17.84 % Fe ₃ O ₄
1.29 % FeO	10.0 % MgO	1.27 % FeO
2.04 % MnO	15.0 % CaO	2.05 % MnO
3.52 % MgO	6.0 % Al ₂ O ₃	3.62 % MgO
3.92 % CaO	50.0 % SiO ₂	4.08 % CaO
1.41 % Al ₂ O ₃	0.8 % P ₂ O ₅	1.48 % Al ₂ O ₃
11.54 % SiO ₂	12.2 % alkalis	12.11 % SiO ₂
0.018 % P ₂ O ₅	—	0.03 % P ₂ O ₅
0.030 % SO ₃	100.0 %	0.03 % SO ₃
—	—	0.18 % alkalis
100.00 %	—	100.00 %

Charcoal

Entering Charge	Entrance to Reaction Zone (Coke, Ash and Moisture-Free)	Gas-Forming Coke, Ash and Moisture- Free (Deducting Carburizing C)
75.2 % C	98.45 % C	98.325 % C
2.4 % H ₂	1.55 % H ₂	1.675 % H ₂
6.4 % O ₂	—	—
3.1 % ash	100.00 %	100.000 %
12.9 % H ₂ O	—	—
—	—	—
100.0 %	—	—

¹ Martin Wiberg, Undersökningar, beträffande reduktionensförlopp samt försök med förreducerad sinter vid Sandvikens masugn nr 3, *Jernkont. Annaler*, Vol. 119 (1935), No. 12, pp. 499–548. Also Olika faktorerers inflytande på masugnens kolåtgång, *Jernkont. Annaler*, Vol. 121 (1937), No. 7, pp. 355–454.

GIVEN ASSUMPTIONS (*Continued*)

12.7% volatiles (assumed)	$H_i = 8380.7$ kcal/kg (according to equation 457)
$H_i = 6630$ kcal/kg	
Weight by volume, 16.48 kg/hl	

Pig Iron Produced

4.42 % C
1.35 % Si
1.51 % Mn
0.023 % P
0.006 % S

Temperatures

Pig iron	1311°C
Slag	1433°C
Top gases	213°C

Top Gas Generated

2731 SCM(dry)/ton of pig iron

Top Gas Analysis

24.7 % CO
13.4 % CO ₂
4.9 % H ₂
0.5 % CH ₄
56.5 % N ₂

100.0 %

Coal Consumption

49.8 hl/t of pig = 820.9 kg of moist coal/ton of pig iron
 = $820.9 \times 0.84 = 689.7$ kg net coal/ton of pig iron
 = $689.7 \times 0.8591 = 592.4$ kg net coke/ton of pig iron, after
 deducting 12.7% volatiles + 1.39% dust loss

Amount of net coke = $592.4 - 44.2 = 548.2$ kg/ton of pig iron
 carburizing carbon per ton of pig

Burden yield = 57.76%, referred to the burden weight per ton of pig (ore burden + fuel ash)

= 1705.9 kg + 820.9×0.031 kg of coal ash = 1731.3 kg/ton of pig iron

$$\mu = \frac{\text{Burden (+ ash)}}{\text{Net coke (+ carburizing C)}} = \frac{1731.3}{548.2} = 3.1582$$

and, reduced according to equation 385,

$$\mu_r = 0.9809 \times 3.1582 = 3.0979$$

Carbon and Oxygen Content of the Burden

$$\Sigma c_{\text{burden}} = 0 \quad c' = 0$$

$$\begin{aligned} O_2 \text{ burden} &= 0.26716 \times 0.5731 + 0.27640 \times 0.1784 + 0.22269 \\ &\quad \times 0.0127 + 0.56354 \times 0.0003 \\ &\quad \times 0.0127 + 0.56354 \times 0.0003 \\ &\quad \times 0.0127 + 0.56354 \times 0.0003 \\ &= 0.20542 \text{ (according to equation 441)} \end{aligned}$$

$$o' = \mu \Sigma O_2 \text{ burden} = 3.1582 \times 0.20542 = 0.64876 \text{ kg}$$

EXAMPLE OF COMPUTATION

GIVEN ASSUMPTIONS (*Continued*)*Composition of "Hypothetical Fuel"*

$$\begin{aligned}
 F_h &= 0.98325 \text{ kg} = 59.64 \% \text{ C} \\
 &0.01675 \text{ kg} = 1.02 \% \text{ H}_2 \\
 &0.64876 \text{ kg} = 39.34 \% \text{ O}_2 \\
 \hline
 &1.64876 \text{ kg} \quad 100.00 \%
 \end{aligned}$$

$$\begin{aligned}
 C_F &= 1.8664 \times 0.5964 = 1.11312 \\
 H_F &= 11.121 \times 0.0102 = 0.11343 \\
 O_F &= 0.7005 \times 0.3934 = 0.27558 \\
 N_F &= 0
 \end{aligned}$$

Composition of Blast

$$\begin{array}{ll}
 1.500 \% \text{ H}_2\text{O} & C_M = 0 \\
 20.685 \% \text{ O}_2 & H_M = 0.015 \\
 77.815 \% \text{ N}_2 & O_M = 0.20685 + 0.0075 = 0.21435 \\
 \hline
 100.000 \% & N_M = 0.77815
 \end{array}$$

$$M = \frac{C_F O_G - C_G O_F}{C_F O_M - C_M O_F} = 4.66527 O_G - 1.15500 C_G$$

$$F = \frac{C_G O_M - C_M O_G}{C_F O_M - C_M O_F} = 0.89838 C_G$$

$$v_{N_2} = M N_M = 0.77815 M$$

*Example of Computation * (Triangle Method).*

$$\begin{array}{ll}
 t = 650^\circ\text{C} \Delta = 0.001 & x(\text{CO}) \text{ estimated } 0.216 - 0.217 - 0.218 \\
 & y(\text{H}_2) \text{ estimated } 0.0354 - 0.0364
 \end{array}$$

$$K'_{pB} = 2.9332 \quad K'_{pW} = 1.4976 \quad 0.24 K_{pM} = 0.057581$$

CO	(CO) ²	CO ₂	H ₂	CO·H ₂	H ₂ O	(H ₂) ²	CH ₄	N ₂	Σ
0.21600	0.046656	0.13685	0.03540	0.0076464	0.01145	0.001253	0.00007	0.59248	0.99225
0.21700	0.047089	0.13812	0.03640	0.0078988	0.01183	0.001325	0.00008	0.59751	1.00094
0.21800	0.047524	0.13940	0.03540	0.0077172	0.01156	0.001253	0.00007	0.60146	1.00589
0.21702	0.047098	0.13812	0.03585	0.0077802	0.01165	0.001285	0.00007	0.59725	0.99996

* This is the second successive computation, and the estimated values are therefore fairly certain. It was preceded by a computation with $\Delta = 0.01$, $x = 0.206 - 0.216 - 0.226$, $y = 0.0307 - 0.0407$. The example is chiefly intended to indicate the order in which the computation is done.

GIVEN ASSUMPTIONS (*Continued*)

$C_G =$	0.21600	0.21700	0.21800	0.21702
	0.13685	0.13812	0.13940	0.13812
	0.00007	0.00008	0.00007	0.00007
	<hr/>	<hr/>	<hr/>	<hr/>
	0.35292	0.35520	0.35747	0.35521
$O_G =$	0.10800	0.10850	0.10900	0.10851
	0.13685	0.13812	0.13940	0.13812
	0.00573	0.00591	0.00578	0.00583
	<hr/>	<hr/>	<hr/>	<hr/>
	0.25058	0.25253	0.25418	0.25246
$H_G =$	0.03540	0.03640	0.03540	0.03585
	0.01145	0.01183	0.01156	0.01165
	0.00014	0.00015	0.00014	0.00015
	<hr/>	<hr/>	<hr/>	<hr/>
	0.04699	0.04838	0.04710	0.04765
$F = 0.89838 C_G =$	0.31706	0.31910	0.32114	0.31911
$4.66427 O_G =$	1.16902	1.17812	1.18582	1.17779
$-1.155 C_G =$	0.40762	0.41026	0.41288	0.41027
	<hr/>	<hr/>	<hr/>	<hr/>
$M =$	0.76140	0.76786	0.77294	0.76752
$-F \times 0.11343 =$	-0.03596	0.03620	0.03643	0.03620
$-M \times 0.015 =$	-0.01142	0.01152	0.01159	0.01151
	<hr/>	<hr/>	<hr/>	<hr/>
	-0.04738	0.04772	0.04786	0.04771
	+0.04699	0.04838	0.04710	0.04765
	<hr/>	<hr/>	<hr/>	<hr/>
$\psi =$	-0.00039	+0.00066	-0.00070	0.00006
$\varphi =$	-0.00775	+0.00094	+0.00589	
$A' = \frac{0.00775}{0.01364} =$	0.56818		$B' = \frac{0.00869}{0.01364} =$	0.63710
$C' = \frac{0.00070}{0.00031} =$	2.25806		$D' = \frac{0.00136}{0.00031} =$	4.38710
$A' + C' =$	2.82624		$B' + D' =$	5.02420
$y = 0.03540 + 0.001 \times \frac{1.82624}{4.02420} =$	0.03585			
$z =$	0.21600 + 0.001 \times 1.13636 + (1 - 1.27420) \times 0.00045381			
$x =$	0.21702			

Gas Composition at 650°C

21.70 % CO
 13.81 % CO₂
 3.59 % H₂
 1.17 % H₂O
 0.01 % CH₄
 59.72 % N₂

100.00 %

The final results of computations made for five temperatures are listed in the following table:

625	650	675	700	725	°C
17.16	21.70	26.46	31.13	35.40	% CO
16.10	13.81	11.40	9.04	6.88	% CO ₂
3.22	3.59	3.97	4.33	4.66	% H ₂
1.35	1.17	0.98	0.81	0.65	% H ₂ O
0.01	0.01	0.01	0.01	0.00	% CH ₄
62.16	59.72	57.18	54.68	52.41	% N ₂
100.00	100.00	100.00	100.00	100.00	%
0.29890	0.31911	0.34023	0.36095	0.37987	F_h
0.18129	0.19355	0.20636	0.21892	0.23040	F
0.19591	0.20916	0.22300	0.23657	0.24898	F^*
0.79879	0.76752	0.73478	0.70268	0.67355	M
601.7	748.1	901.7	1052.0	1189.1	$H_{i,G}$
220.1	227.0	233.5	239.8	246.0	H_G
821.8	975.1	1135.2	1291.8	1435.1	$H_{i,G} + H_G$

Here three different quantities of fuel are listed: the "hypothetical fuel" F_h (kg/SCM); the actual gas-generating fuel entering the reaction zone F (kg/SCM), which is found from the equation

$$F = \frac{F_h}{1 + c' + o'} = \frac{F_h}{1.64876} = 0.60652F_h \quad (\text{kg/SCM})$$

and, finally, the total fuel introduced into the reaction zone (= gas-forming fuel + carburizing fuel):

$$F^* = 1.08063F \quad (\text{kg/SCM})$$

The coefficient 1.08063 is found from the ratio of the carburizing carbon (44.2 kg/t of pig) to the quantity of gas-forming net coke (548.2 kg/t of pig). It is found that the carburizing C is 8.063% of the gas-forming net coke, and hence a quantity that cannot be ignored in the computation. Put into equation form, we have

$$F^* = F(1 + \mu \varepsilon C_{pig})$$

ε = burden yield (allowing for the ash content of the fuel)

C_{pig} = C content of the pig iron

Hence, in our example,

$$F^* = F(1 + 3.1582 \times 0.5776 \times 0.0442) = 1.08063F$$

The foregoing table then includes the quantity of gasifying agent (amount of blast), M (SCM/SCM); the heating value of the gas, $H_{i,G}$ (kcal/SCM); the enthalpy of the gas, H_G (kcal/SCM); and the sum of these last two quantities, the right side of our heat-balance equation 456, page 232. Thus the reference unit is 1 SCM of moist gas, all the quantities of water driven off in the preheating zone, such as fuel and burden moisture, water of formation, and water of hydration, not yet appearing here in our computation, of course.

The left side of the heat-balance equation 456 consists of the following quantities:

FH'_i	= 1447.9	1545.8	1648.2	1748.5	1840.2
F^*H_f	= 38.7	43.4	48.6	54.0	59.5
$F\mu_r H_\mu$	= 77.8	86.6	96.1	106.0	115.8
MH_M	= 95.8	92.0	88.1	84.3	80.8
$F\mu(Q\Sigma + \epsilon'H_{prod} + \epsilon''H_{sl})$	= 656.5	700.9	747.3	792.7	834.3
Left side	= 1003.7	1066.9	1133.7	1200.1	1262.0

The H - t diagram (see Figure 54) then provides as the point of intersection the desired reaction temperature $t_R = 675^\circ\text{C}$. The following comment applies to the various items. The heating value H'_i is the heating value of the actual gas-forming fuel entering the reaction zone, with a percentage reduction for Q_{ext} for the heat losses. Wiberg has demonstrated a loss of 0.232×10^6 kcal/t of pig iron = 4.1% through radiation, conduction, and cooling water, referred to the total heat supplied (fuel + hot blast) of 5.699×10^6 kcal/t of pig iron. The quan-

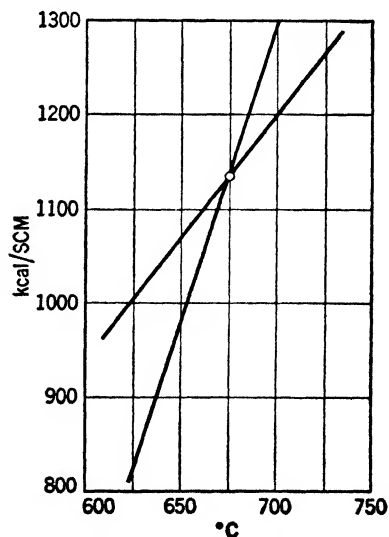


Fig. 54. H - t diagram of the blast furnace (sample calculation).

tity of fuel introduced into the reaction zone is 592.4 kg/t of pig, with a heating value of 8380.7 kcal/kg = 4965×10^6 kcal/t of pig, and thus the heat losses are

$$\frac{0.232}{4.965} \times 100 = 4.7\%$$

Then the reduced fuel heating value is

$$0.953 \times 8380.7 = 7986.8 \text{ kcal/kg}$$

The heat content of the fuel may be taken from Table VII in the appendix, page 306, since almost pure carbon is involved. The total fuel, including the carburizing C, should be entered here, thus, for 625°, say, $0.19591 \times 197.5 = 38.7$ kcal/SCM, etc.

By the time of entrance into the reaction zone, the quantity of burden per kilogram of fuel is only 3.0979 kg or

$$0.18129 \times 3.0979 = 0.56162 \text{ kg/Nm}^3$$

at 625°. The heat content of the burden (assumed equal to that of blast-furnace slag) should be taken from Table VII, page 306; consequently $H_\mu = 138.6$ kcal/kg (interpolated),

$$F_{\mu R} H_\mu = 0.56162 \times 138.6 = 77.8 \text{ kcal/SCM}$$

The quantities of heat required for the shaft and hearth reactions are in turn based on the total charge F_μ . They are:

For the reduction of Fe_2O_3

$$1152.7 \times 0.9666 \times 0.5731 = +638.5 \text{ kcal/kg of burden}$$

For the reduction of Fe_3O_4

$$1152.7 \times 0.1784 = +205.6 \text{ kcal/kg of burden}$$

For the reduction of FeO

$$894.9 \times 0.0127 = +11.4 \text{ kcal/kg of burden}$$

For the reduction of P_2O_5

$$2535.9 \times 0.0003 = +0.8 \text{ kcal/kg of burden}$$

Subtotal for the shaft reactions $Q_{shaft} = 856.3$ kcal/kg of burden

For the reduction of SiO_2

$$7245.2 \times 0.0135 \times 0.5776 = +56.5 \text{ kcal/kg of burden}$$

kcal \times kg Si \times burden yield

For the reduction of MnO

$$589.8 \times 0.0151 \times 0.5776 = +5.1 \text{ kcal/kg of burden} \\ \text{kcal} \times \text{kg Mn} \times \text{burden yield}$$

For the formation of FeSi

$$-686 \times 0.0135 \times 0.5776 = -5.4 \text{ kcal/kg of burden}$$

For the formation of Fe₃P

$$-1400 \times 0.00023 \times 0.5776 = -0.2 \text{ kcal/kg of burden}$$

For the formation of FeS

$$-720 \times 0.00006 \times 0.5776 = -0.0 \text{ kcal/kg of burden}$$

For slag formation

$$0.2167(-145) = \underline{-31.6 \text{ kcal/kg of burden}}$$

$$\text{Subtotal for the hearth reactions} = +24.6 \text{ kcal/kg of burden}$$

Heat content of the slag

$$0.2167 \times 480 = 104.0 \text{ kcal/kg of burden}$$

Heat content of the pig iron

$$0.5776 \times 280 = \underline{161.7 \text{ kcal/kg of burden}}$$

$$\text{Total heat required} = 1146.6 \text{ kcal/kg of burden}$$

$$Q_z + \epsilon' H_{prod} + \epsilon'' H_{sl}$$

The quantity of slag is computed as follows:

$$28.06 \text{ kg Si correspond to } 60.06 \text{ kg SiO}_2$$

$$1 \text{ kg Si correspond to } 2.1404 \text{ kg SiO}_2$$

$$\text{SiO}_2 \text{ yield } (\epsilon_{\text{SiO}_2}) = \frac{2.1404 \times 0.0135 \times 0.5776}{0.1211} \times 100 = 13.78\%$$

$$\epsilon'' \text{ from equation 437, page 222}$$

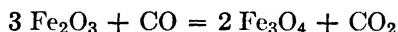
$$\epsilon'' = (1 - 0.1378) \times 0.1211$$

$$+ 0.0148 + 0.0404 + 0.0362 + 0.0205 = 0.2167$$

$$\text{Al}_2\text{O}_3 \quad \text{CaO} \quad \text{MgO} \quad \text{MnO}$$

or a slag yield of 21.67%.

The reaction temperature is 675°C, but the gas composition given above for this temperature is changed in the preheating and pre-reaction zone by the reduction of the Fe_2O_3 * and by the addition of the volatiles, as follows, from



Quantity of CO consumed: -0.0175 SCM

Quantity of CO_2 produced: $+0.0173 \text{ SCM}$

Additional volume of distillation gas: $0.085 \text{ SCM/kg of coal}$
 $= 0.22300 \times 0.085 = 0.0190 \text{ SCM/SCM of the following composition:}$

5 %	CO	=	0.0010	SCM	CO
15 %	CO_2	=	0.028	SCM	CO_2
52 %	H_2	=	0.0099	SCM	H_2
28 %	CH_4	=	0.0053	SCM	CH_4
<hr/>			<hr/>		
100 %			0.0190	SCM	

The gas analysis, in terms of dry gas, then exhibits very good, or at any rate adequate, agreement with the measured analysis of the stack gas.

Computed Gas Analysis		Measured Gas Analysis
Without Distillation Gas	With Distillation Gas (0.0190 SCM/SCM)	
24.97	24.60	24.7 % CO
13.25	13.28	13.4 % CO_2
4.01	4.91	4.9 % H_2
0.01	0.53	0.5 % CH_4
57.76	56.68	56.5 % N_2
<hr/>	<hr/>	<hr/>
100.00	100.00	100.0 %

* No other reactions occur in this example.

The volume of dry gas is found from the calculation to be $\frac{548.2}{0.20636} \times 0.9902 \times 1.0190 = 2680$ SCM/t of pig iron as against a measured volume of 2731 SCM (error of 1.87%). We still have to see whether the heat balance sheet of the preheating zones checks, i.e., whether, starting with a gas temperature of 675°C at the lower end of this zone, the measured top gas temperature of 213°C is attained after meeting the heat requirements set forth here. It is best to base all quantities on 1 SCM of reaction gas.

The following quantities enter the preheating zone:

- (1) The total amount of charcoal, i.e., $\frac{820.9}{592.4} = 1.3857$ kg/kg F^*

with a heat content of 2.3 kcal/kg at ambient temperature of 15°: *

$$Q_1 = 1.3857 \times 0.22300 \times 2.3 = 0.7 \text{ kcal/SCM}$$

- (2) The total amount of burden, i.e., $0.20636 \times 3.1582 = 0.65173$ kg of burden per SCM of gas, with a heat content of 2.6 kcal/kg:

$$Q_2 = 0.65173 \times 2.6 = 1.7 \text{ kcal/SCM}$$

- (3) The amount of heat generated in the exothermic reduction of the Fe_2O_3 to Fe_3O_4 :

$$Q_3 = 0.65173 \times 0.5731 \times 12.3 = 4.6 \text{ kcal/SCM}$$

- (4) The reaction gas at 675°C and enthalpy of:

$$Q_4 = 233.5 \text{ kcal/SCM}$$

The following quantities leave the preheating zone:

- (5) The dried, devolatilized, and dust-free charcoal, i.e., 0.22300 kg/SCM, with a heat content of 217.8 kcal/kg at $t = 675^\circ\text{C}$:

$$Q_5 = 0.22300 \times 217.8 = 48.6 \text{ kcal/SCM}$$

- (6) The previously reduced burden, less an assumed dust loss of 1%, i.e., $0.0809 \times 0.65173 \times 0.99 = 0.63289$ kg/SCM, with a heat content of 150 kcal/kg at $t = 675^\circ\text{C}$:

$$Q_6 = 0.63289 \times 150 = 94.9 \text{ kcal/SCM}$$

* We ignore the heating values of charcoal and gas, since no chemical exchanges occur, with the exception of the reduction of Fe_2O_3 .

(7) The top gases, with a heat content at 213°C of 70.1 kcal/SCM, plus 0.0190 SCM of gas resulting from the devolatilizing of the charcoal at 77.4 kcal/SCM = 1.5 kcal/SCM, or a total of:

$$Q_7 = 71.6 \text{ kcal/SCM}$$

(8) The moisture of the charcoal = 12.9% H₂O per kg. Raw charcoal = $0.129 \times 1.3857 \times 0.22300 = 0.0399 \text{ kg H}_2\text{O/SCM}$. Heat content of the steam = 99.0 kcal/kg = heat of evaporation of 583.2 kcal/kg, less the heat content of water at 15° = 667.2 kcal/kg:

$$Q_8 = 0.0399 \times 667.2 = 26.6 \text{ kcal/SCM}$$

No appreciable amounts of condensible constituents are to be present in the charcoal. The heat balance of the preheating zone is then as follows:

Heat Added	Heat Removed
$Q_1 = 0.7 \text{ kcal/SCM}$	$Q_5 = 48.6 \text{ kcal/SCM}$
$Q_2 = 1.7 \text{ kcal/SCM}$	$Q_6 = 94.9 \text{ kcal/SCM}$
$Q_3 = 4.6 \text{ kcal/SCM}$	$Q_7 = 71.6 \text{ kcal/SCM}$
$Q_4 = 233.5 \text{ kcal/SCM}$	$Q_8 = 26.6 \text{ kcal/SCM}$
<hr/>	<hr/>
240.5 kcal/SCM	241.7 kcal/SCM

Assuming a small amount of external heat losses within the preheating zone, e.g., 0.5% of the ingoing total heat = $0.005 \times 240.5 = 1.2 \text{ kcal/SCM}$, the balance sheet checks. The temperature of 675° at the end of the reaction zone agrees with the computation backwards from the stack-gas temperature of 213°C.

The blast-furnace curve

The presentation of the change of the gas composition in the blast furnace, the so-called blast-furnace curve, and the comparison of the CO contents, as measured, with values as expected from equilibrium considerations have frequently been the cause of misinterpretations. Considerations of the blast-furnace curve alone, as are found in the earlier literature,^{2,3} do not disclose much.

² Carl Brisker, *Berechnung und Untersuchung des Eisenhochofens*, Halle (Saale), 1909.

³ W. A. Schlesinger, Das Diagramm eines modernen Eisenhochofens, *Stahl u. Eisen*, Vol. 31 (1911), No. 29, pp. 1182-1183.

General considerations as to what reactions may take place in the blast furnace become possible by comparison with the Boudouard curve and the equilibrium curves for Fe_3O_4 and FeO reduction.⁴ Even there, errors have frequently occurred, e.g., the Boudouard curve for $P_{\text{CO}_2+\text{CO}} = 1$ Atm is used instead of approximately $\frac{1}{3}$ Atm.^{4,5} The mistakes made in nearly all investigations of the blast-furnace curve are to neglect the simultaneity of the reduction processes on the ore and on the coke, i.e., the coexistence of these two body materials, and to disregard actual gas conditions in the blast furnace. For example, the seemingly low moisture content of the wind should not simply be disregarded. If we examine the overall reaction in the blast furnace—no matter how often the partial reactions of ore reduction by CO and CO_2 reduction to CO on the carbon repeat themselves—we have to keep in mind that we are not dealing with carbon or iron oxides as pure body materials, but rather that solid carbon as a coexistent solid phase is added to Fe_3O_4 and FeO . Diepschlag⁶ noted this fact without, however, drawing the necessary conclusions. On the contrary, when discussing the experiments of Geimer⁷ he concluded⁸ that “from the measurements it does not appear as if equilibrium between iron and its oxides has been attained even approximately” and that “the difference between oxygen removal and the final conditions as given by the equilibrium is incalculable and apparently arbitrary.”

Eichenberg and Oberhoffer,⁹ in interpreting their results, express this in a similar way and with even less reservation: “Both curves show” [two different kinds of burdens were used] “that equilibrium in the blast furnace is apparently far from reached.” In their

⁴ M. Levin and H. Niedt, Untersuchungen über die Zusammensetzung des Gastromes im Hochofen, *Metallurgie*, Vol. 8 (1911), No. 17, pp. 515–539; No. 18, pp. 555–581.

⁵ Norbert Metz, Studien über die im Hochofen zwischen den Eisenerzen und Gasen obwaltenden Verhältnisse, *Stahl u. Eisen*, Vol. 33 (1913), No. 3, pp. 93–104.

⁶ E. Diepschlag, *Der Hochofen (Der Industrieofen in Einzeldarstellungen*, Vol. VI, L. Litinsky, editor), Leipzig, 1932, p. 196.

⁷ Paul Geimer, Über Veränderungen in der Gichtgaszusammensetzung beim An- und Ausblasen des Hochofens sowie beim Umsetzen verschiedener Möller, *Stahl u. Eisen*, Vol. 43 (1923), No. 21, pp. 681–686.

⁸ E. Diepschlag, *ibid.*, p. 233.

⁹ Georg Eichenberg und Paul Oberhoffer, Beiträge zur Kenntnis des Hochofenprozesses, *Arch. Eisenhüttenwes.*, Vol. 1 (1927–1928), No. 10, pp. 613–628.

attempt to explain the quite considerable difference by the influence of the gangue of the ore, they miss the obvious explanation. According to them, "the difference may only be apparent."¹⁰

A clarification of these disputed questions is provided in the blast-furnace curve of Wiberg and in the comparison of the above recalculation of his blast-furnace experiment in Sandviken * with the theoretical, i.e., calculated, values. Referring to Figure 55, the Boudouard curve for dry air and the equilibrium curves for Fe_3O_4 and FeO reduction are plotted in dotted lines, as is customary in similar presentations of the blast-furnace curve. It should be noted that they by no means represent actual conditions in the blast furnace as can be seen by comparing them with the fully drawn curves which are recalculated for these particular conditions. Actually, the Boudouard curve is shifted still further to the left, which is due to the CO content resulting from the decomposition of steam and primarily from the burden. The equilibrium curves of the ore reduction, however, are shifted considerably owing to the presence of hydrogen,[†] although, on a percentage basis, it seems to be unimportant. The measured points of Wiberg's blast-furnace curve may be connected in two groups of curves (for the measurements at the walls and in the center of the furnace), both of which intersect the gas curve at point $t = 675^\circ\text{C}$, i.e., the temperature which, from the calculation and the heat balance, resulted as the reaction temperature.

As to the frequently disputed question, which is almost always answered in the negative, whether or not in the blast furnace the equilibria of ore reduction and the gas equilibria are attained, the following can be said.

The calculated results, obtained under the assumption that all equilibria (with the exception of the methane equilibrium and that of a few hearth reactions) are reached, are in excellent agreement with Wiberg's measurement. Consequently, the equilibria in the blast furnace *are* complete. This was to be expected from the results in gas producers, and is reaffirmed by the investigation,

¹⁰ R. Durrer, *Die Metallurgie des Eisens*, 2nd ed., Berlin, 1942, p. 250.

* See footnote 1.

† The calculation was made according to equation 379, p. 379, using the value $n = \text{H}_2/\text{CO} = 0.03505$. It results from the ratio $\text{H}_2:\text{CO}$ in a reducing agent containing 35.09% CO, 1.23% H_2 , and 63.68% N_2 , which is the product of complete conversion of the oxygen of the wind to CO and H_2 .

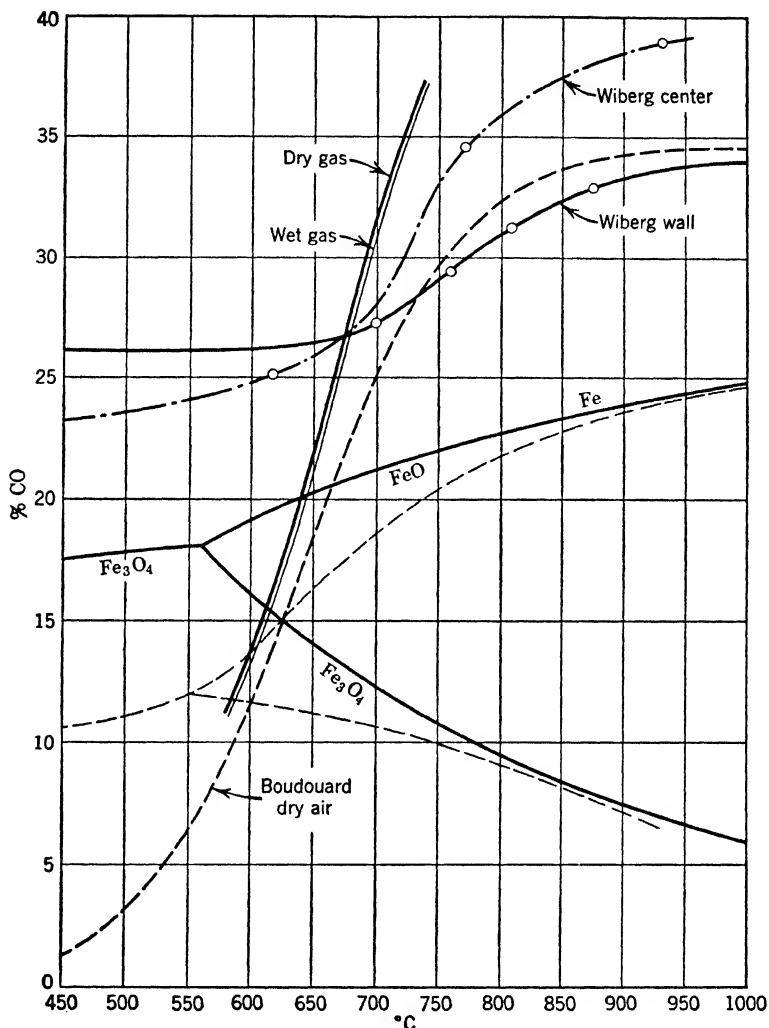


FIG. 55. Blast-furnace curve (experimental results by M. Wiberg).

so that the assumption that the equilibria are complete is now also justified for the shaft reactions. Of course this is true only for the reaction zone as a whole. Within this zone we are, of course, far from equilibrium at first, since a certain reaction volume (height of stock column) and a certain reaction time are required.

However, at the end of the reduction zone, i.e., in the intersection with the gas curve (in our example at 675°), there is equilibrium.

Only the following questions still require clarification: Why does the blast-furnace curve not coincide with the theoretical equilibrium curve of Figure 55, not even in the intersection with the gas curve, and why does the CO content continue to decrease after the point of intersection? The answer to the first question has already been briefly discussed above. The curves of iron ore reduction are for the pure solid phases of Fe_3O_4 or FeO , whereas the blast-furnace curve is for a body material consisting of Fe_3O_4 or FeO and C. That, under these conditions, the blast-furnace curve continually lies above the theoretical value has therefore no relation to the departure from equilibrium in the blast furnace, where the solid phase is changing practically all the time or where the two solid phases are present simultaneously. Consequently, the theoretical value expected is, on the FeO at 675° , a gas mixture containing 20.6% CO. It has the opportunity, however, to bring its CO_2 content to equilibrium on the carbon at 675° , whereby the CO content increases to 26.7%.

As this temperature is the reaction temperature at which equilibrium prevails, the CO content should extend horizontally toward the left from this point. The fact that the CO content continues to decrease after this temperature is entirely due to the reduction of Fe_2O_3 to Fe_3O_4 , taking place outside the main reaction zone, which is not considered here. In this reduction CO disappears, and CO_2 is formed—a reaction which, as we have seen, takes place at such low temperatures that the equilibrium curve of Figures 41, 42, or 43 would coincide with the x -axis. If the burden contained only Fe_3O_4 and FeO , there would, consequently, not be such a decrease.

Blast furnace under pressure

Blast pressures in usual blast-furnace operation are about 1 at gage, just enough to overcome the resistance of the stock column, the adjacent gas coolers, cleaners, and to deliver enough pressure to feed the blast-furnace pipe lines. The ideal furnace is the one that has highest hearth temperatures and lowest top temperatures ("warm feet and cold head," according to human comfort and health). Low shaft temperatures (equivalent to low reaction temperatures) mean lower CO and higher CO_2 content, lower

heating value of the top gases, and smaller heat losses or better fuel economy. As known from the high-pressure gasification, high pressure means a shifting of equilibria to higher CO_2 and H_2O content and higher temperatures. As the heating value of the top gases is the most deciding item in the heat balance, higher pressures—besides higher throughput—improve fuel economy considerably. Higher throughput, with nearly constant external heat losses, in its turn diminishes the percentage of heat loss and contributes to the fuel saving.

Two proposals have been made to increase operating pressures of blast furnaces:

(1) Arthur D. Little, Inc. (U. S. Patent 2,131,031) proposed and Republic Steel Corporation pioneered the first experiments in 1944 in their Cleveland and Youngstown Divisions at 10 psi (0.7 at) top pressure.¹¹ Only slight alterations are necessary; the hopper has to be tightened and built in one piece and a pressure equalizer valve has to be provided to remove pressure if the big bell is dumped. The experiments resulted in saving 220 lb (110 kg/t) of fuel per ton of pig iron in the Youngstown plant and 130 to 225 lb (65 to 112.5 kg/t) in the Cleveland furnace. Production increased 22 to 24%, and flue dust decreased 14% with improved pig iron quality (less sulfur charged by less coke consumption). The largest blast-furnace blowers ever built are capable of delivering 40 psi (2.8 at) pressure, allowing a top pressure of 20 to 25 psi (1.4 to 1.76 at). A rough calculation, given below, shows the influence of pressure within this range.

(2) At the same time the author proposed to operate a low-shaft blast furnace under pressures of about 20 at (285 psi), using an oxygen-steam mixture as blast, reducing the pressure to atmospheric during tapping-off. A second calculation will show the influence of both high pressure and oxygen-steam blast.

A calculation with variation of the pressure showed that the reaction temperature was exactly the same as at normal pressures. The following calculations, therefore, are made for a (constant) reaction temperature of 675°C (1247°F). The burden-coke ratio has been varied, and by a graphical method that ratio which fits with the heat balance of the whole blast furnace has been determined to be compared with the result at about atmospheric top

¹¹ F. S. Slater, Operation of the iron blast furnace at high pressure, *Am. Iron and Steel Inst.*, May 21-22, 1947.

pressure. The fuel economy in percentage of atmospheric top pressure operation is found by

$$\varepsilon_f = \mu \left(\frac{1}{\mu} - \frac{1}{\mu_p} \right) 100 \quad (\%) \quad (461)$$

The results, in comparison with the experiments of Wiberg reported on page 236, are shown in Table 53.

TABLE 53

INFLUENCE OF PRESSURE OPERATION ON BLAST-FURNACE PERFORMANCE
($t_R = 675^\circ\text{C}$)

$p = 1$	2.4	3.1	20.0 Atm
$\mu = 3.1582$	3.43	3.65	5.14
Gas Analysis			
26.46	19.86	18.20	8.73 % CO
11.40	15.37	16.72	24.81 % CO ₂
3.97	3.25	3.07	1.72 % H ₂
0.98	1.45	1.62	2.81 % H ₂ O
0.01	0.01	0.01	0.02 % CH ₄
57.18	60.06	60.38	61.91 % N ₂
100.00	100.00	100.00	100.00 %
CO/CO ₂ 2.32	1.29	1.09	0.35
$F_h = 0.34023$	0.32723	0.33305	0.37596 kg/SCM
$F = 0.20636$	0.19197	0.19034	0.18287 kg/SCM
$F^* = 0.22300$	0.20878	0.20808	0.20687 kg/SCM
$M = 0.73478$	0.77186	0.77589	0.79560 SCM/SCM
$(1/\mu)1000 = 316.64$	291.55	273.97	194.55 kg/t
$\varepsilon \dots$	25.09	42.67	122.09 kg/t
$\varepsilon\% \dots$	7.92	13.48	38.56 %

Fuel saving $\varepsilon\%$ increases rapidly at first and flattens at high pressure, but additional fuel savings result from operating conditions such as increased throughput, reduced heat losses, less flue dust, and smaller dimensions.

The calculation at 2.4 at pressure gives a fuel saving of 7.92%, but this comparison is not quite conclusive because, besides pressure, some other operation conditions have been changed. The burden is somewhat different, and the pig iron yield per weight unit of burden is higher at the pressure operation unit. Throughput was higher, thus reducing external and cooling water heat

TABLE 54

RESULTS OF PRESSURE OPERATION OF BLAST FURNACES (AFTER SLATER)

	Cleveland		Youngstown
	(a)	(b)	(c)
Top pressure		9.7 0.66 1.66	9.8 psi 0.67 at gage 1.67 at abs
Blast pressure	28.2 1.92 2.92	30.5 2.08 3.08
Pressure reaction zone		~2.4	28.2 psi 1.92 at gage 2.92 at abs 2.4 at abs
Fuel rate:			
Normal pressure		1746	1705 lb/t
Pressure operation	1494	1635	1482 lb/t
Fuel saved	252	111	223 lb/t
Fuel saved, %	14.4	6.4	13.1 %

losses, and flue dust losses were smaller. The sum of these differences, partly due to high pressure operation, raised the fuel saving above the calculated figure (assuming identical operation and yield conditions, except pressure).

Blast furnace with oxygen-enriched blast

The use of oxygen-enriched air for blast-furnace operation was proposed decades ago by C. H. von Linde and discussed by many metallurgists.¹² Experiments have been run in Belgium, Germany, and Russia. The most complete series of experiments has been

¹² Ernst Karwat, Technische Wirkungen, gegenwärtiger Stand und Ausichten der Sauerstoffverwendung, *Brennstoff-Chemie*, Vol. 17 (1936), No. 8, pp. 141-149.

published by W. Lennings.¹³ Test runs IIa, c, producing hematite pig iron with 2% Si from a burden of Spanish (Menas Rubio) and Swedish (Luossavaara Kiirunavaara) ores, are chosen for comparison of calculation and actual performance. Some missing details of information regarding the composition of the burden are obtained by calculation from the slag and pig iron composition. In spite of a slight difference in the burden of runs IIa and IIc, the same composition has been assumed as a basis of calculation. (See Table 55.)

The total heat requirement for the shaft and hearth reactions is calculated as follows:

Reduction of Fe_2O_3 (after pre-reduction to Fe_3O_4)

$$1152.7 \times 0.9666 \times 0.2561 = +285.4 \text{ kcal/kg}$$

Reduction of Fe_3O_4

$$1152.7 \times 0.3887 = +448.1 \text{ kcal/kg}$$

Decomposition of CaCO_3

$$433.1 \times 0.1839 = +79.6 \text{ kcal/kg}$$

Subtotal (shaft reactions, main reaction zone) = +813.1 kcal/kg

Reduction of SiO_2

$$7245.5 \times 0.019 \times 0.44967 = +61.9 \text{ kcal/kg}$$

Reduction of MnO

$$589.8 \times 0.013 \times 0.44967 = +3.4 \text{ kcal/kg}$$

Formation of FeSi

$$686 \times 0.019 \times 0.44967 = -5.9 \text{ kcal/kg}$$

Formation of FeS

$$720 \times 0.0002 \times 0.44967 = -0.1 \text{ kcal/kg}$$

Slag formation

$$0.22899 \times 145 = -33.2 \text{ kcal/kg}$$

Subtotal (hearth reactions) = +26.3 kcal/kg

¹³ Wilhelm Lennings, Die Verwendung von sauerstoffangereichertem Gebläsewind im Hochofenbetrieb, *Stahl u. Eisen*, Vol. 55 (1935), No. 20, pp. 533-544; No. 21, pp. 565-572. Also: Versuche mit sauerstoffangereichertem Wind bei eisenreichen und eisenarmen Erzmöhlern, *Stahl u. Eisen*, Vol. 63 (1943), No. 42, pp. 757-767. W. M. Pollitzer, Utilization of oxygen in smelting low-grade ores, *Steel*, Vol. 122 (1948), No. 7, pp. 98-104. Also Utilization of oxygen in the German iron and steel industry, *Fiat Final Report* 1203 (6/14/47).

TABLE 55

BLAST-FURNACE OPERATION WITH OXYGEN-ENRICHED AIR (W. LENNINGS)

Results and Basis of Calculation

Burden, 2070 kg/t pig iron

Composition

Burden	Pig Iron	
8.61 % SiO_2	4.16 % C	
18.39 % CaCO_3	1.9 % Si	
2.30 % MgCO_3	1.3 % Mn	
1.20 % MnO_2	0.02 % S	
25.61 % Fe_2O_3		
38.87 % Fe_3O_4		
0.63 % S		
3.25 % Al_2O_3		
1.14 % H_2O		
<hr/>		
100.00 %		
	% yield of iron	48.3%
	% yield of silicon	22.8%
Run:	IIa	IIc
Oxygen content of the blast	21.0 %	26.0 %
Pig iron production, t/day	43.1	52.6
Blast temperature, °C	742	726
Top gas temperature, °C	364	205
Pig iron temperature, °C	1375	1385
Top gas composition		
% CO	32.9	36.7
% CO_2	6.6	11.0
% H_2	1.4	1.62
% CH_4	0.05	0.05
% N_2	59.0	50.53
% O_2	0.05	0.1
	<hr/>	
	100.00	100.00
Coke consumption (dry, ash-free basis) kg/t pig iron	972.42	822.27
Coke analysis		
% C	97.9	
% H_2	0.5	
% O_2	0.6	
% N_2	1.0	
	<hr/>	
%	100.0	

Enthalpy of the slag ($\sim 1500^{\circ}\text{C}$)

$$0.22899 \times 429 = +98.2 \text{ kcal/kg}$$

Enthalpy of the pig iron (1375°C)

$$0.44967 \times 290 = +130.4 \text{ kcal/kg}$$

Total (kcal/kg burden)	1068.0
------------------------	--------

The heat requirement of the pre-reduction zone includes further:

Reduction of Fe_2O_3 to Fe_3O_4 (exothermic)

$$-12.3 \times 0.2561 = -3.2 \text{ kcal/kg}$$

Decomposition of MgCO_3

$$326 \times 0.023 = +7.5 \text{ kcal/kg}$$

Reduction of MnO_2 to MnO

$$-140.6 \times 0.012 = -1.7 \text{ kcal/kg}$$

$$\text{Dehydration } 965.8 \times 0.0114 = +11.0 \text{ kcal/kg}$$

Total (kcal/kg burden)	+13.6
------------------------	-------

The reaction gas analysis has been computed for 700, 725, and 750°C , resulting in a reaction temperature of 725°C by heat balance if the external heat loss amounts to 10%. The final top gas analysis has been corrected by the decrease of CO and increase of CO_2 due to the reactions in the pre-reduction zone (below 725°C). The result is given in Table 56.

The agreement is fairly good, considering the possibilities of practical deviation of measurements and the necessary assumptions to fill the gap of incomplete reporting of the test runs.

The same calculation has been repeated for run IIc with 26.0% O_2 in the blast. The result is given in Table 57. For this run, a fuel saving of 15.4% and an output increase of 22% were achieved. Accordingly, for the heat balance computation the external heat loss was lowered to 8.07%. Under otherwise equal conditions (and assuming the same burden), the reaction temperature was 713°C . The gas analyses are compared in the table.

The results of calculation and actual performance are in very close agreement. This enables us to enlarge the range of oxygen

TABLE 56
COMPARISON OF GAS ANALYSES
Lennings run IIa, 21.0% O₂
 $t_R = 725^\circ\text{C}$

Reaction Zone (Wet Basis)	Calculated Top Gas		Measured (Dry Basis)
	(Wet Basis)	(Dry Basis)	
33.90	32.93	33.2	32.9 % CO
6.31	7.25	7.3	6.6 % CO ₂
1.80	1.78	1.8	1.4 % H ₂
0.24	0.77 % H ₂ O
0.00	0.00	0.0	0.05 % CH ₄
57.75	57.27	57.7	59.0 % N ₂
			0.05 % O ₂
100.00	100.00	100.0	100.00 %

content in the blast beyond the range covered by experiments and to draw conclusions about the optimum percentage. Oxygen contents of the blast (dry basis) of 30, 35, and 40% are included

TABLE 57
COMPARISON OF GAS ANALYSES
Lennings run IIc, 26.0% O₂
 $t_R = 713^\circ\text{C}$

Reaction Zone (Wet Basis)	Calculated Top Gas		Measured (Dry Basis)
	(Wet Basis)	(Dry Basis)	
37.38	35.99	36.4	36.7 % CO
9.86	11.11	11.2	11.0 % CO ₂
1.84	1.82	1.84	1.62 % H ₂
0.33	1.06 % H ₂ O
0.00	0.00	0.00	30.05 % CH ₄
50.59	50.02	50.56	50.53 % N ₂
			0.10 % O ₂
100.00	100.00	100.00	100.00 %

in the following calculations. The calculation is somewhat time-consuming because of the unknown burden/fuel ratio; it is necessary to cover at least nine cases with three different μ values and

three different reaction temperatures. Thus a correlation of μ and t_R is possible, and, by a heat balance of the total furnace (not reaction zones only as used for the determination of the reaction

TABLE 58
CALCULATED RESULTS OF BLAST-FURNACE OPERATION AT 30 TO 40%
OXYGEN IN THE BLAST

O ₂ Content (Dry Blast)	30%	35%	40%
Analysis of Blast			
O ₂	29.65	34.59	39.53
N ₂	69.17	64.23	59.29
H ₂ O	1.18	1.18	1.18
t_R (°C)	715	770	850
Q_{ext} (%)	7.15	6.41	5.9
Reaction Zone Gas Analysis			
% CO	41.31	52.14	61.87
% CO ₂	11.54	6.15	2.14
% H ₂	1.91	2.19	2.44
% H ₂ O	0.37	0.22	0.10
% CH ₄	0.00	0.00	0.00
% N ₂	44.87	39.30	33.45
	<hr/>	<hr/>	<hr/>
	100.00	100.00	100.00
H_i kcal/SCM	1297	1580	1931
Top Gas Analysis (Dry Basis)			
% CO	40.1	51.0	60.8
% CO ₂	13.2	7.6	3.4
% H ₂	1.9	2.2	2.4
% CH ₄
% N ₂	44.8	39.2	33.4
	<hr/>	<hr/>	<hr/>
	100.0	100.0	100.0
Heating Value (Top Gas)			
H_i kcal/SCM	1259	1598	1898

temperature), the final burden/fuel ratio μ is ascertained. This value and the reaction temperature enable us to calculate the gas analysis to be expected and disclose the operating conditions and

performances of the blast furnace in every detail. Omitting all these intermediate calculations and based on the same burden as before, Table 58 summarizes the results obtained, and Table 59 gives a comparison of the different operations.

TABLE 59

OPERATION OF A BLAST FURNACE WITH OXYGEN-ENRICHED AIR

Oxygen Content, % (Dry Basis)	Fuel Consumption, kg/t pig iron (Dry Ash-Free Basis)	Fuel Consumption, %		% CO ₂ (Top Gas, Dry)
		Decrease	Increase	
21	972.42 *	7.3 (6.6)
26	822.27 *	15.44	...	11.2 (11.0)
30	758.02 †	22.05	...	13.2
35	985.48 †	...	1.34	7.6
40	1179.36 †	...	21.28	3.4

* Measured. † Calculated.

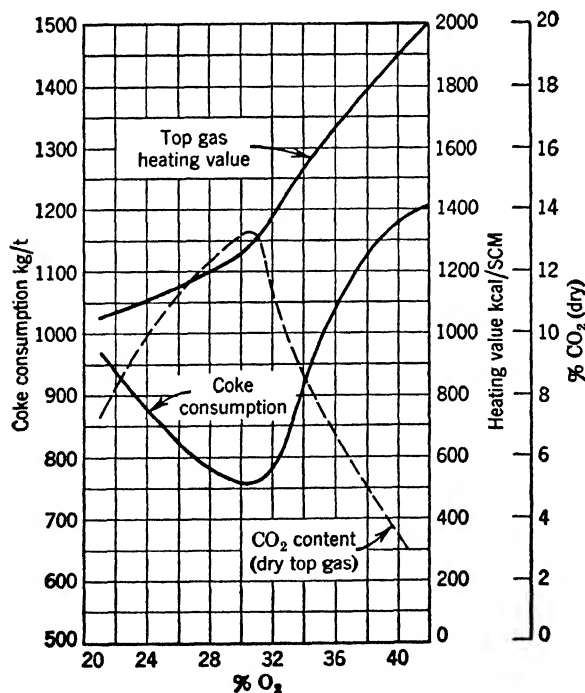


FIG. 56. Blast-furnace operation with oxygen-enriched blast.

EXAMPLE OF COMPUTATION

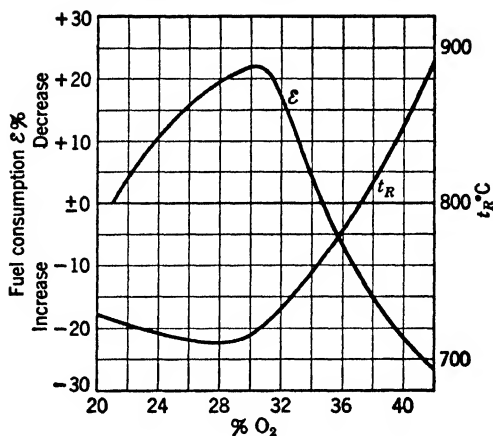


FIG. 57. Blast-furnace operation with oxygen-enriched blast. Reaction temperature and fuel consumption.

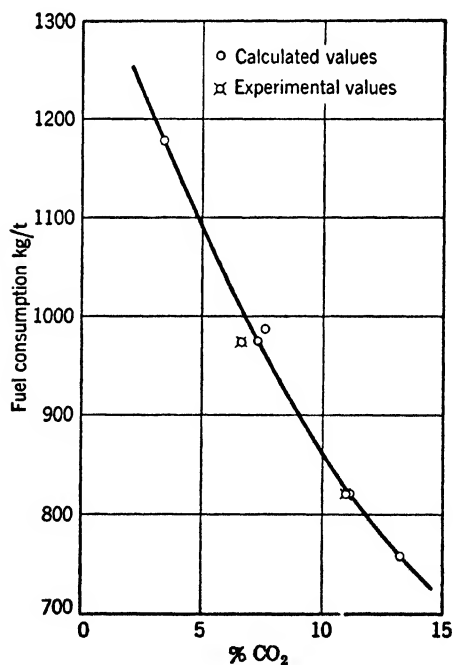


FIG. 58. Blast furnace. Fuel consumption as a function of the CO₂ content in the top gas.

These results as demonstrated in Figures 56 and 57 show a decrease of coke consumption or an increase of fuel savings, with oxygen contents increased up to about 30% O₂. Beyond this limit a sharp drop caused by increasing heating value of the top gas occurs (which may be an economic asset for the utilization of this gas but is a decisive amount of heat output in the heat balance of the furnace itself) and increases the fuel consumption. Except for higher capacity, an oxygen content of more than 30% is undesirable for this burden.

It is noteworthy that the fuel consumption is closely correlated with the CO₂ content of the top gas. This is shown in Table 59, but this result is limited to the burden on which these measurements and calculations are based. This indicates that the CO₂ content is a simple effective characteristic of the blast-furnace performance (see Figure 58).

Water-gas high-pressure low-shaft blast furnace

Increasing oxygen content (beyond 30%) increases fuel consumption again, but increasing pressure decreases it considerably. Both these measures adopted in blast-furnace operation result in a completely new and unusual technique of oxide reduction, using water gas as a strong reducing agent and increasing the capacity ten to twenty times. Other advantages are the low fuel consumption and the elimination of nearly all inerts in the reducing gases, as both components of water gas, carbon monoxide and hydrogen, are reducing agents. This increase in capacity and reaction velocity enables us to lower the height of the stock column to such an extent that small-size coke and even a much weaker fuel than standard metallurgical coke may be used. The savings would be reflected not only in a lower fuel consumption but also in a cheaper fuel. Capital cost would go down although the capital cost of an oxygen plant is included. Total production cost according to such a process is estimated to be 40 to 50% lower than standard practice.

The following operation conditions may be chosen as an example: $P = 20$ Atm; $t_R = 675^\circ\text{C}$. Unlike most of the preceding calculations, x_M is assumed to be 1.0 (instead of 0.24 as used before) because of the presence of large quantities of freshly reduced iron oxide, known as a very active catalyst for methane formation. Setting the reaction temperature at this lowest possible value

again requires a set of nine cases varying in μ and blast composition in order to meet the heat balance both of the reaction zone to give the temperature of 675° and of the whole furnace to ascertain the burden/fuel ratio. As a final result, μ equals 3.813, the fuel consumption is 584.88 kg/t pig iron, or the fuel savings are 39.85% compared with the standard blast-furnace practice (21% O₂; $P = 1$ Atm). The blast is composed of:

72.0 % H ₂ O
26.6 % O ₂
1.4 % N ₂
<hr/>
100.0 %

assuming an oxygen purity of 95%. Steam is superheated to 450°C, oxygen is admitted at room temperature. Gas analyses are shown in Table 60.

TABLE 60
HIGH-PRESSURE WATER-GAS BLAST FURNACE
($P = 20$ Atm; $t_R = 675^\circ\text{C}$)

Reaction Zone		Top Gases		
(Wet)		(Wet)	(Dry)	(Dry, CO ₂ -Free)
% CO	11.39	9.59	13.10	33.18
% CO ₂	42.21	44.32	60.52	...
% H ₂	12.62	12.54	17.12	43.36
% H ₂ O	26.95	26.77
% CH ₄	5.64	5.60	7.64	19.36
% N ₂	1.19	1.18	1.62	4.10
<hr/>		<hr/>		
%	100.00	100.00	100.00	100.00
Heating Value, H_i kcal/SCM		1091	1489	3772

The future trend in pig iron and steel production may lie in increased pressures and slightly oxygen-enriched blast as far as remodeling of existing equipment is concerned. New plants, however, would offer great advantages if the standard methods were dropped and processes resulting in high CO₂ content of the effluent gases were adopted. As far as lower-grade ores are concerned, the high-pressure operation has a favorable outlook, resulting not only in a marked fuel saving but also in a top gas which,

after condensing of its moisture and stripping of its CO_2 content, represents a valuable gas of more than 3500 kcal/SCM (with allowance for a small remainder of CO_2 after the scrubber) or 375 to 400 Btu/SCF.

High-grade ores may be worked off, preferably by reduction by gases to sponge iron yielding CO_2 only (such as in the Wiberg process, Edvin or Norsk Staal process, and similar processes), and slag and iron can be separated in the open hearth or electric furnace. Production of the reducing gases is affected by oxygen gasification of any carbonaceous material, or partial combustion of natural gas, thus making oxygen a common and versatile tool of future metallurgy.

Cupola furnace

The cupola furnace may be regarded as a gas producer charged with coke and the pig iron and scrap to be molten. The purpose is to melt down the charge, separate slag from iron, and overheat the molten iron to a certain extent to obtain a good viscosity. It is not the purpose of the furnace, however, to produce a combustible gas because gas production not only increases the coke consumption and affects the economy but also increases the sulfur pick-up and affects the quality of the product. The difference in the heat balance of a slagging-ash producer and a cupola furnace is only that in the latter the ratio of the charge (the burden) and the fuel, μ , is in the range of 6 to 12 in standard furnaces, and up to 20 in extraordinarily well-operated or hot-blast cupola furnaces.

To compare actual results of foundry practice and cupola research work with calculated data, we turn to an example of the influence of the coke charge. The following simplifications are made. The fuel is assumed to be coke with 8-kg ash content per 100 kg C, but the ratio μ is expressed as pure carbon % per 100 kg Fe. The heat of slag formation and slag enthalpy is 400 kcal/kg slag ($= 0.08 \times 400 = 32$ kcal/kg C); the enthalpy of the cast iron at tapping temperature is assumed to be 270 kcal/kg. Allowance is made for the burning of Fe, Mn, and Si by using a sliding scale of the external heat losses

$$Q_{ext} = 5 + 1.25 \times \gamma \% \quad (462)$$

γ = coke charge in %. The losses range from 10% at 4% coke charge to 25% at 16% coke charge. This does not necessarily

mean that at 4% coke ratio the loss is as low as 10% but that the heat delivered by burning part of the metal charge is relatively high (and relatively low at 16% coke charge), thus resulting in a lower external heat loss if Q_{ext} expresses both the actual heat loss by radiation and conduction and the gain by heat delivery from the metal charge.

The blast entering the cupola furnace is assumed to be dry air.

Figure 59 represents the enthalpy-temperature ($H-t$) diagram. Curve a illustrates the sum of enthalpy and (lower) heating value of the gas, and the curves marked by the coke ratio (4 to 16%) represent the remaining members of the heat balance, such as the heat input by the fuel, its heating value and its enthalpy, the enthalpy of the blast, minus the external heat loss according to equation 462, minus the heat losses by the enthalpy of the tapped slag and cast iron. The intersection points with curve a give the *reaction temperature*. As a characteristic of the gas analysis, the *combustion efficiency ratio*

$$\eta_c = \frac{\text{CO}_2}{\text{CO}_2 + \text{CO}} \times 100\% \quad (463)$$

is used, as proposed by Jungbluth and co-workers.^{14, 15, 16} Combustion is perfect or 100% if the cupola furnace releases only CO_2 and no combustible gases and decreases with increasing CO content of the top gases. The combustion efficiency ratio, therefore, is not identical with the thermal efficiency of the cupola furnace. The latter efficiency is always smaller because of the losses represented by the enthalpies of top gas, cast iron, and slag, the losses due to unburnt carbon, and the external heat losses. The combustion efficiency ratio indicates only the influence of the top gas composition upon the efficiency. Table 61 shows the details, but all items of the heat balance (Σ^*) are given together to save space. The resulting reaction temperatures and corresponding

¹⁴ H. Jungbluth and P. A. Heller, Windmenge, Kokssatz und Schmelzleistung bei Kupolöfen, *Techn. Mitt. Krupp*, Dec., 1933, No. 4, pp. 99-105; *Arch. Eisenhüttenwes.*, Vol. 7 (1933-1934), No. 3, pp. 153-155.

¹⁵ H. Jungbluth and E. Bruehl, Der Zusammenhang zwischen Kokssatz und Abgaszusammensetzung bei Kupolöfen verschiedener Durchmesser, *Techn. Mitt. Krupp-Forschungsberichte*, Feb., 1939, No. 1, pp. 1-4.

¹⁶ S. C. Massari and R. W. Lindsay, Melting in the cupola, *Trans. Am. Foundrymen's Assoc.*, Vol. 49 (1941), pp. 94-122.

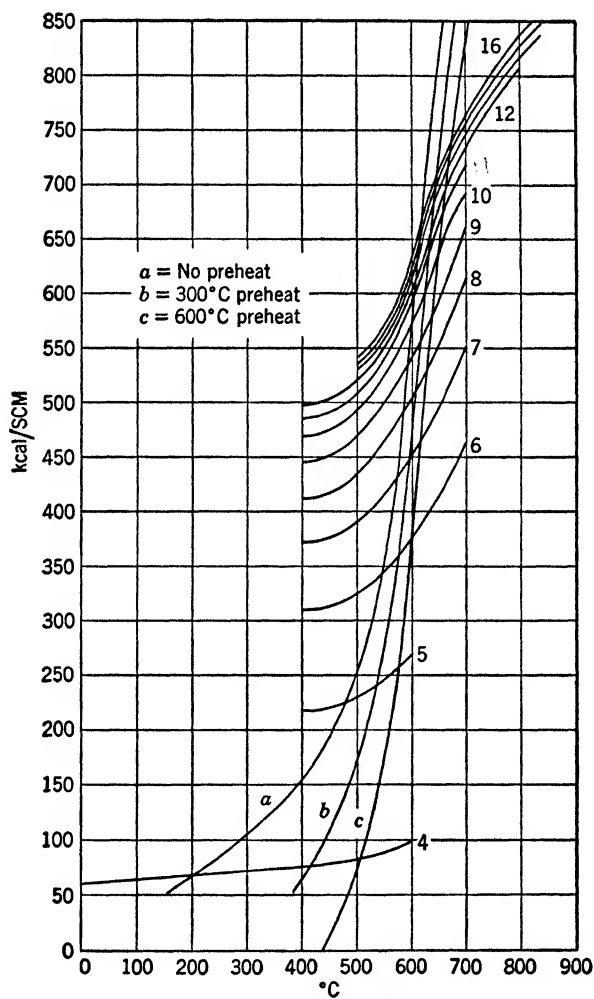
FIG. 59. H - t diagram of the cupola furnace.

TABLE 61

CUPOLA FURNACE

(Dry Blast; Fuel: Carbon; Q_{ext} , Equation 462)

$t_R =$	200	300	400	500	600	700	800	900°C
% CO	0	0.03	0.41	2.90	11.52	25.05	32.00	34.21
% CO ₂	21	20.98	20.75	19.24	14.03	5.84	1.64	0.30
% N ₂	79	78.99	78.84	77.86	74.45	69.11	66.36	65.49
	100	100.00	100.00	100.00	100.00	100.00	100.00	100.00
H_G kcal/SCM	67.7	103.1	139.3	175.5	208.0	235.4	265.8	299.8
H_1 kcal/SCM	0	0.9	12.4	87.6	347.9	756.5	966.4	1033.1
kcal/SCM	67.7	104.0	151.7	263.1	555.9	991.9	1232.2	1332.9
$\eta_c = \frac{\text{CO}_2}{\text{CO}_2 + \text{CO}} \%$	100	99.86	98.06	86.90	54.91	18.91	4.88	0.87
F	0.1125	0.1126	0.1134	0.1186	0.1369	0.1655	0.1802	0.1851
M	1.000	1.000	0.998	0.986	0.942	0.875	0.840	0.829
Σ^*								
$\gamma = 4\%$	66.9	70.4	74.6	81.9	98.6	124.3	142.3	...
$\gamma = 5\%$	216.2	230.1	269.6	331.0	367.4	...
$\gamma = 6\%$	306.8	324.9	379.0	463.3	511.4	...
$\gamma = 7\%$	368.2	389.2	453.2	553.0	616.1	...
$\gamma = 8\%$	411.4	434.4	505.4	616.0	677.8	...
$\gamma = 9\%$	442.5	466.9	542.9	661.4	727.2	...
$\gamma = 10\%$	465.1	490.5	570.1	694.3	763.0	...
$\gamma = 11\%$	481.4	507.6	589.8	718.2	789.0	...
$\gamma = 12\%$	493.2	519.9	604.1	735.4	807.7	...
$\gamma = 13\%$	501.3	528.5	613.9	747.3	820.7	...
$\gamma = 14\%$	506.7	534.0	620.4	755.1	829.2	...
$\gamma = 15\%$	509.9	537.4	624.2	759.7	834.2	...
$\gamma = 16\%$	511.2	538.7	625.7	761.5	836.2	...

γ	4%	5%	6%	7%	8%	9%	10%	11%
$t_R =$	200	475	542	575	589	595	602	606
$\eta_c =$	100	91.5	76.5	65	58.9	56.1	53.5	51.5

γ	12%	13%	14%	15%	16%
$t_R =$	610	614	616	617	618
$\eta_c =$	50	48.5	47.5	47.0	46.5

$$\Sigma^* = FH'_{i,C} + FH_C + MH_M - F32 - \frac{100}{\gamma} 270$$

$H_{i,C} = 8080 \text{ kcal} - Q_{ext} \text{ (equation 462); } \gamma = \text{coke ratio in } \%$

values of combustion efficiency ratio are presented at the bottom of this table.

Figure 60 illustrates these results (curve 1) in comparison with measured data of Jungbluth and Heller (curve 2) and Jungbluth and Bruehl (between curves 3). The calculated values are in

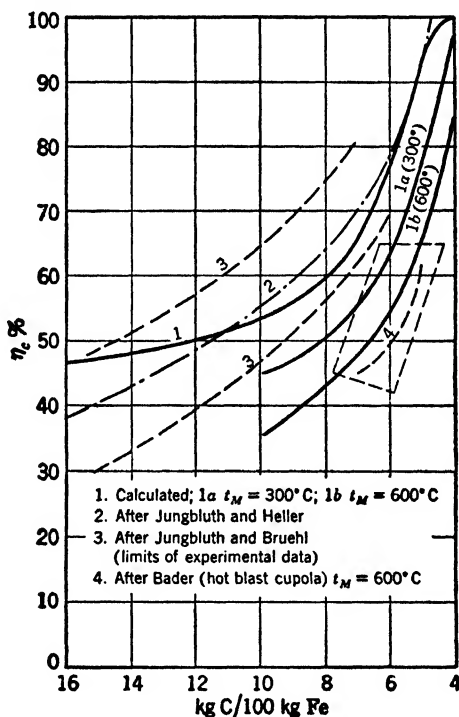


FIG. 60. Cupola furnace. Comparison of calculated and experimental results.

very good correlation with these experimental data, and considering the original location of the points as measured the shape of curve 1 is entirely justified. The point of inflection at the upper end of curve 1 has not been established by Jungbluth and Heller, who have worked down to about $\gamma = 8\%$ and extrapolated according to the general trend of their mean values.

Hot-Blast Cupola Furnace. Low coke ratios may be obtained by introducing part of the heat requirement as highly preheated air. Increasing temperatures are very favorable for the melting

zone but are detrimental to CO formation. Figure 59 shows in curves *b* and *c* the enthalpy of the blast at 300° and 600° and room temperature. This is simpler and gives the same results as the addition of this amount of heat to each of the curves from 4 to 16% coke ratio in Figure 59. The results, which appear in the following table, agree fairly well with the experimental results of M. Bader.^{17,18}

TABLE 62
HOT-BLAST CUPOLA FURNACE
(Dry Blast; Fuel: Carbon; Q_{ext} , Equation 462)

$\gamma =$	4%	5%	6%	7%	8%	9%	10%
$t_M = 300^\circ\text{C}$							
t_R	412	538	575	598	609	615	623
η_c	96	77.5	65	55.2	50.5	48	45
$t_M = 600^\circ\text{C}$							
t_R	508	576	600	616	629	638	650
η_c	85	64.8	54.9	47.8	42.5	39	35

A New Type of Hot-Blast Cupola Furnace. Although preheating of the blast results in decreasing fuel consumption, full credit is given to this device only if the necessary heat can be taken from the top gases. Utilization of the top gas seems to be essential because of the otherwise increasing losses due to combustible gases. Hot-blast furnaces making either part or full use of top gas in order to preheat the blast are used, for example, in the Griffin hot-blast process (U. S. Patent 1,627,536).^{19, 20, 21} Economically unfavorable, on the other hand, is the fact that all heat produced is made by burning foundry coke, or the gases thereof, which is an extremely expensive fuel. The calculation, however,

¹⁷ Marcel Bader, Betriebserfahrungen mit dem Heisswindkupolofen, *Die Giesserei*, Vol. 30 (1943), No. 23/24, pp. 241-246.

¹⁸ Eugen Piwowarsky, Der Aachener Heisswind-Kupolofen, *Die Giesserei*, Vol. 30 (1943), No. 20/22, pp. 221-225.

¹⁹ Eugen Piwowarsky, *Hochwertiges Gusseisen*, Berlin, 1942, pp. 877-894.

²⁰ F. K. Vial, Hot blast applied to the cupola, *Iron Age*, Vol. 120 (1927), No. 16, pp. 1071-1076.

²¹ Rogers A. Fiske, Hot blast cupola in Pullman Foundry, *Iron Age*, Vol. 123 (1929), No. 13, pp. 872-875.

gives some indications of how one may proceed so that there will be high temperatures in the melting zone, low coke consumption, and low reaction temperatures in the reaction zone, or, in other words, no excessive heat losses due to combustible gases. Figure 61 shows the solution of the problem. An independent air heater delivers a high-blast temperature of about 400 to 600°C, using

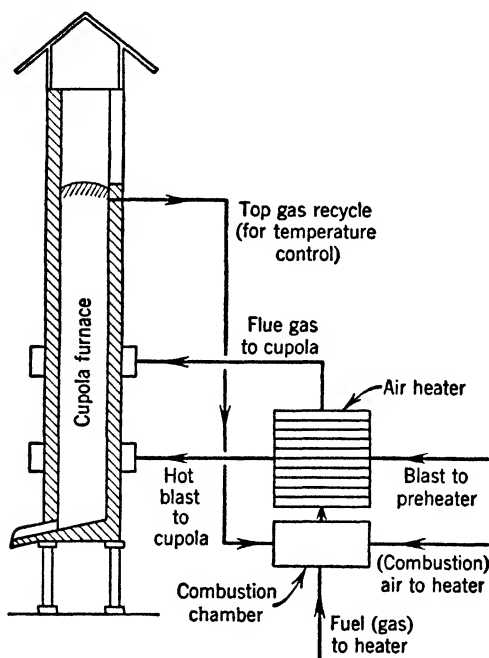


FIG. 61. Suggested hot-blast cupola furnace.

the cheapest fuel available (coal, oil, gas, or waste fuels). The flue gas of the heater is introduced above the melting zone into the reduction zone and mixes with the hotter gases passing up the shaft of the cupola furnace. Assuming the gas temperature at this point to be 600 to 700°C, it will be lowered by admixing the colder flue gas to about 400°C (practically no CO or less than ½%). The heat is dissipated but not lost, and even the enthalpy of the flue gases is utilized to preheat the downcoming charge. With proper height of the column, the exit gas temperature will be not more than 200°C in spite of hot-blast and high iron tem-

peratures. This trick of introducing more and colder gas into the cupola furnace permits operation with small-sized fuel without increases in CO losses. Under equal reaction temperature conditions a smaller size of the coke means a higher overall reaction rate (see p. 283) and a shorter reduction zone; or, with a given bed height or coke column, a higher CO content. The use of large-sized coke, therefore, is sometimes considered necessary in standard foundry practice even if the purchase price of such special coke is largely higher than ordinary grades. To avoid an intermediate rise in temperature by introducing excess air with the flue gas, the combustion in the preheater combustion chamber may be done without excess air by recycling top gases to control the combustion temperature.

In round figures and assuming blast-furnace gas as the fuel used for preheating, for every kilogram of C used in the cupola furnace ($t_R = 600^\circ$), 6.88 SCM of air are needed and will be preheated to 600°C . 7.3 SCM of gas pass upwards through the shaft from the melting zone. To deliver the necessary heat 1.62 SCM of blast-furnace gas are burnt, delivering 2.9 SCM of flue gas to which an equal amount of top gas is recycled to keep the temperature entering the preheater at 1000°C . Finally 5.8 SCM of gas (flue gas leaving the air heater) at about 200°C or less are fed back into the cupola furnace into the reducing zone, lowering its reaction temperature from 600° to 400 to 420°C . Total coke consumption will be reduced to $\gamma = 5$ kg of pure coke per 100 kg Fe plus $5 \times 1.62 = 8.1$ SCM blast-furnace gas (or an equivalent of 1.1 kg C). This performance represents a fuel saving of at least 50 to 60%. It also has many other economic and metallurgical advantages, such as high superheat of the cast iron, low viscosity, low sulfur pick-up, low blast pressures, high furnace capacity, and the possibility of using small-sized coke.

Influence of Weather Conditions. It is known that weather conditions affect the operation of shaft furnaces and that the cupola has a tendency to give a thick liquid cast iron in humid weather. To examine this question, we drop the assumption of a dry air blast and assume for a comparison a hot humid day with a temperature of 35°C (95°F), $\varphi = 90\%$ saturation. The composition of the blast will then be

20.30 % O₂
 76.39 % N₂
 3.31 % H₂O

100.00 %

Table 63 shows gas composition and heat balance under otherwise identical conditions as Table 61.

TABLE 63
 CUPOLA FURNACE (HUMID BLAST)

t_R °C	400	500	600	700	
% CO	0.41	2.90	11.58	25.39	
% CO ₂	20.32	19.11	14.17	6.01	
% H ₂	0.62	1.37	2.08	2.47	
% H ₂ O	2.64	1.85	1.00	0.38	
% CH ₄	0.01	0.01	
% N ₂	76.00	74.76	71.17	65.75	
	100.00	100.00	100.00	100.00	
H_G kcal/SCM	139.7	176.0	208.4	235.6	
H_i kcal/SCM	29.5	123.7	403.6	830.5	
Σ kcal/SCM	169.2	299.7	612.0	1066.1	
F kg/SCM	0.1111	0.1180	0.1380	0.1683	
Σ^*					
$\gamma = 9\%$	433.7	464.8	547.2	672.4	t_R °C 579
$\gamma = 10\%$	455.8	488.2	574.6	705.9	587
$\gamma = 11\%$	471.8	505.3	594.5	730.2	595

Figure 62 demonstrates the heat balance of both cases: dry air, $\gamma = 9\%$, resulting in 595°C reaction temperature, and humid air, $\gamma = 11\%$, resulting in the same reaction temperature. In order to achieve the same temperature level 11% or 22% more coke are necessary than at (completely) dry air, or under identical conditions of charge humid weather causes a decrease in temperature due to H₂ formation. This effect is small at high temperatures or already uneconomically operated furnaces, but high at low

temperatures or with cupola furnaces with a low coke charge. This effect, too, is eliminated by the proposed type of hot-blast furnace.

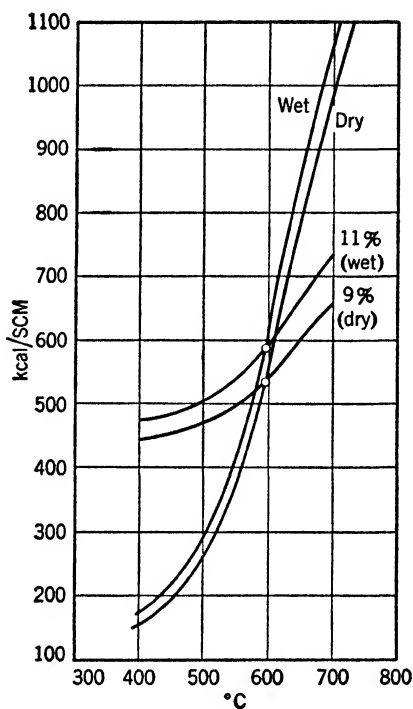


FIG. 62. *H-t* diagram of a cupola furnace under different weather conditions.

P A R T T H R E E

Reaction Kinetics

10

REACTION KINETICS

It might seem to be daring to write about the problems of gas producers and furnaces without attention to the reaction kinetics and without introducing appropriate terms into the calculations. Without question, reaction kinetics plays a definite part in the problems referred to. Fortunately, many practical questions can be answered without going deeply into this rather complicated, and more or less unknown, subject. Considering until now only the stoichiometry of the processes and assuming a full or a certain known approach to the equilibrium—later confirmed and justified by comparison of calculated and measured results—we must still render an account of the role of the reaction velocity, where it has to be taken into consideration and in what way it influences the practical results.

Generally speaking, every reaction can be divided into two basically different partial processes, according to the mechanism of the overall process, a physical and a chemical partial process. The physical process consists of the transport of one reactant to the other as the necessary condition of the second partial process, the chemical reaction proper spoken between these two (or more) reactants. In other words, the physical partial process is mass transfer (mixing) if homogeneous reactions are considered, or a carrying of the gaseous (or fluid) reaction agent to the surface of the solid reagent, if heterogeneous reactions are under consideration. In gas producers and furnaces we always have to deal with heterogeneous reactions with carbon (coke, char, etc.) or iron oxides as solid reagents and oxygen, carbon dioxide, steam hydrogen, carbon monoxide, or hydrocarbons as gaseous reagents. Oxidation and reduction are the processes involved.

The mass transfer of the gaseous reagents to the surface of the fixed reagents is done by diffusion and by convection. Convection can take place in laminar or turbulent flow. It, therefore, depends mainly upon these factors that are characteristics of the fluid

flow or mass exchange in fluid flow such as surface, particle size, bulk, hourly flow, linear velocity, pressure drop. The chemical reaction, on the other hand, will be influenced mainly by the concentration of the reagents, the temperature, and the pressure. Because the experimental study of each of these partial processes is an extremely difficult problem, such basically important processes as the combustion and gasification of carbon and the reduction of iron ores are not better understood and numerically known in spite of a great number of investigations.¹

Such processes like combustion or gasification, which depend upon two or more different factors, may be compared to a current passing through different resistances. We may differentiate between a *physical* and a *chemical reaction velocity*, which, on their part, are inversely proportional to a *physical* and a *chemical reaction resistance*. If we sum up all physical factors in one term, the physical reaction velocity, v_{phys} , and all chemical influences on the chemical reaction velocity (e.g., the carbon conversion in weight units per unit of surface and time), v_{chem} , we obtain as an expression of the total velocity, v ,

$$\frac{1}{v} = \frac{1}{v_{phys}} + \frac{1}{v_{chem}} \quad (464)$$

$$v = \frac{1}{\frac{1}{v_{phys}} + \frac{1}{v_{chem}}} \quad (465)$$

or by simply introducing the reciprocals, R = overall resistance, R_{phys} = physical reaction resistance, R_{chem} = chemical reaction resistance

$$R = R_{phys} + R_{chem} \quad (466)$$

Hence we have two resistances in series, and the greatest is consequently decisive. It so happens that in the range of high temperatures predominating in the combustion and oxidating zones of gas producers and blast furnaces, the chemical reaction resistance is so small and the reaction velocity so high that the influence of the chemical reaction resistance on the total velocity of the process

¹ Summarizing presentations of the subject are given in K. Fischbeck, Reaktionsgeschwindigkeit in heterogenen Systemen, in Eucken-Jakob, *Der Chemie-Ingenieur*, Vol. III, Part 1, pp. 242-359. Martin A. Mayers, The combustion of carbon, *Chem. Rev.*, Vol. 14 (1934), pp. 31-53.

disappears and the physical reaction resistance remains as the only decisive factor. Figure 63 or Table 64 indicates that, for example, at a temperature of 1200°C , $2.037 \times 10^{-2} \text{ g/cm}^2 \text{ sec} = 730 \text{ kg/m}^2 \text{ hr}$ could be burnt chemically, but practically only about $7.2 \text{ kg/m}^2 \text{ hr}^*$ or 100th of this rate are obtained. The

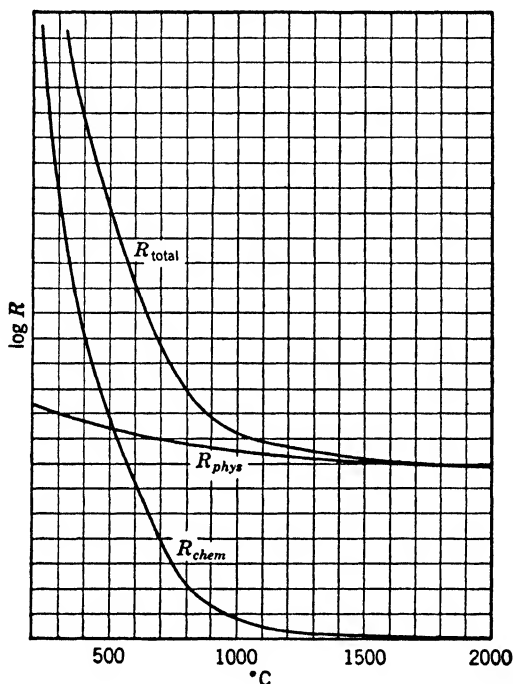


FIG. 63. Physical, chemical, and total reaction resistance (diagrammatic).

immensely high chemical reaction velocity cannot be effective because it is not possible for the relatively slow oxygen transport to keep pace, not even roughly.

Unfortunately we have not enough correct data at our disposal to illustrate these relations. The numerous investigations differ widely in procedure, in presentation of the results, and, above all, in the results themselves, which sometimes do not agree even in the order of magnitude. This lack of agreement may be ascribed to the fact that the complete elimination of physical influences

* These data refer to the surface of the particle not to the specific rate of combustion of a furnace per square meter grate or shaft area.

TABLE 64

CHEMICAL REACTION VELOCITY OF THE REACTION OF COMBUSTION OF
CARBON BY AIR *

(Equation 467)

t °C	log A	A	
		$\text{g/cm}^2 \text{ sec} \times 10^3$	$\text{kg/m}^2 \text{ hr}$
0	0.261 - 26	1.824×10^{-26}	6.6×10^{-26}
200	0.299 - 12	1.991×10^{-12}	7.2×10^{-11}
400	0.994 - 7	9.863×10^{-7}	3.5×10^{-6}
600	0.079 - 3	1.200×10^{-3}	4.3×10^{-2}
800	0.015 - 1	1.035×10^{-1}	3.7
1000	0.342	2.198	79
1200	1.309	2.037×10^1	730
1400	2.044	1.106×10^2	3,980
1600	2.623	4.198×10^2	15,100
1800	3.090	1.230×10^3	44,300
2000	3.474	2.989×10^3	108,000

* It is emphasized that this table does not reproduce correct measurements, but is based on estimations. It serves only to illustrate clearly and by means of figures the fundamentals of the process. Yet these results make it clear that even a shifting of one or two orders of magnitude does not basically change the character of the curve, but means a shifting of 200 to 400°C. A deviation of such a magnitude meanwhile seems to be unlikely.

(such as diffusion)—by working under vacuum or by extrapolating to operation conditions where physical factors disappear or can be kept constant—is not accomplished completely. As both the physical and the chemical reaction velocity may differ by several orders of magnitude, even small remaining perturbations play a considerable part. Under these conditions the data which can be derived by estimating from the experiments of Tu, Davis, and Hottel² on the combustion rate of carbon (in air) serve our purpose best. The left branch of the presented family of curves (see Figure 64) is controlled essentially by the chemical reaction

² C. M. Tu, H. Davis, and H. C. Hottel, Combustion rate of carbon, *Ind. Eng. Chem.*, Vol. 26 (1934), No. 7, pp. 749-757.

velocity, because obviously changes in the physical operating conditions (e.g., air flow) do not show up. In the range of highest temperatures the influence of chemical factors is insignificant, but the influence of flow velocities is well illustrated. Principally the same picture is disclosed by the experiments of other investigators, such as Choukhanova,^{3,4} although the experimental lay-out (a bore in a solid piece of coal) and other operating conditions

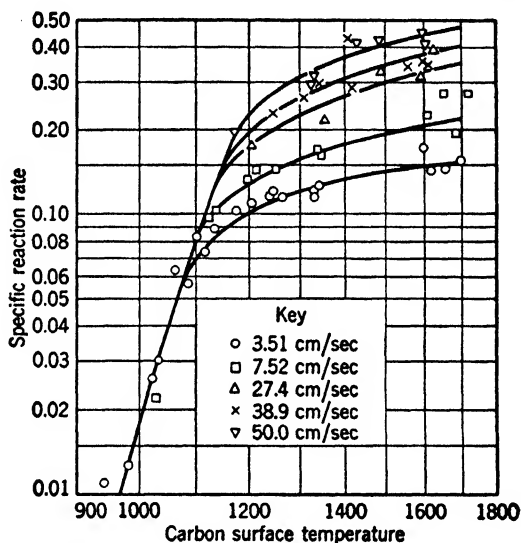


FIG. 64. Combustion rates of carbon after Tu, Davis, and Hottel.

(flow velocities 100 to 350 m per sec) were widely different. The chemical reaction velocity may be expressed in the best manner by an equation of the Arrhenius' type. We use the equation

$$\log A = 7.462 - \frac{9064}{T} \quad (467)$$

for the isolation of the chemical process from the total result. A is given as grams of carbon per $\text{cm}^3 \text{ sec} \times 10^3$, T° Kelvin

³ O. A. Choukhanova, *J. techn. phys.* (Leningrad), Vol. 9 (1939), No. 4, pp. 295-304. See also W. Gumz, *Kurzes Handbuch der Brennstoff und Feuerungstechnik*, Berlin, 1943, pp. 302-304.

⁴ A. S. Predvoditelev and O. A. Choukhanova, *J. techn. phys.* (Leningrad), Vol. 10 (1940), No. 13, pp. 1113-1120.

(absolute temperature). Table 64 presents the evaluation of this formula for a wide range of temperatures.

These data reflect the extraordinary influence of the temperature, making it easy to understand that the chemical reaction velocity (and so the reactivity of the carbon) is not decisive in the

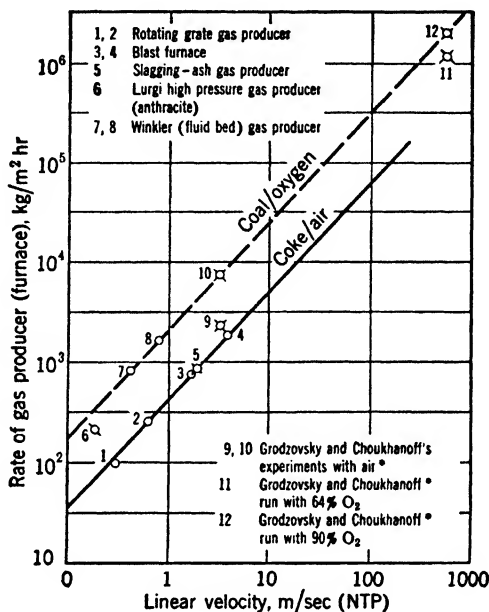


FIG. 65. Rates of gas producers and furnaces vs. linear gas velocity. (* M. K. Grodzovsky and Z. F. Choukhanoff, The primary reactions of the combustion of carbon, *Fuel Sci.*, Vol. 15 (1936), No. 11, pp. 321-328.)

zone of combustion in furnaces and gas producers. The rate of carbon conversion, consequently, is proportional to the amount of oxygen offered. In other words, it depends upon the velocity of air flow or the specific air rating of the shaft area. It is known that this principle holds true even with the extreme operating conditions, i.e., highest velocities, as might be illustrated by Figure 65. In this figure the rate of gasification refers to the shaft area of the producer, the hearth area of the blast furnace, or the nozzle area in Grodzovsky and Choukhanoff's experiments. The rate-controlling limits are the pressure available in the blast and the stability of the fuel bed, but no chemical factors whatsoever.

With blast furnaces and similar shaft furnaces in addition, high ratings influence the heat balance favorably by decreasing the external heat losses. Hence, the fuel/burden ratio goes down, the gas quantity decreases relative to the burden, the heat exchange between gas and charge improves, and the top gas temperatures consequently decline. A similar effect results from an increase of pressure. Besides, the bed remains stable in spite of higher ratings and losses due to carryover decrease.

With regard to rate limitations by carry-over losses, the arrangement of down-flow (countercurrent or batchwise) as effected in the Flesch-Winkler and similar gasification systems is very promising. They allow linear velocities which are prohibitive in up-flow systems, and rates of gasification which increase proportional to pressure in high-pressure gas producers.

The chemical reaction of iron oxide reduction has been investigated in numerous experiments. Of these, the work of Bone and co-workers,⁵ Hofmann,⁶ Kamura,⁷ Meyer,⁸ Olmer,⁹ Schenck,¹⁰ Specht and Zapffe,¹¹ Tennenbaum and Joseph,¹² Udy and Lorig,¹³

⁵ William A. Bone *et al.*, An experimental inquiry into the interactions of gases and ore in the blast furnace, *J. Iron Steel Inst.* (London), Vol. 115 (1927), No. 1, pp. 127-180; Vol. 121 (1930), No. 1, pp. 35-95; Vol. 129 (1934), No. 1, pp. 33-46; Vol. 129 (1934), No. 1, pp. 47-96; Vol. 137 (1938), No. 1, pp. 85-107.

⁶ Konrad Hofmann, Zum Reduktionsmechanismus der Eisenoxyde im strömenden Gas (II), *Z. anorg. Chem.*, Vol. 38 (1925), pp. 715-721.

⁷ Heihachi Kamura, Reduction of iron ores by carbon monoxide, *Trans. AIME*, Vol. 71 (1925), pp. 549-567.

⁸ Hans Heinz Meyer, Die Reduktionsgeschwindigkeit von Eisenerzen in strömenden Gasen, *Mitt. K. W. Inst. Eisenforsch.*, Vol. 10 (1928), pp. 107-116.

⁹ François Olmer, Sur la réduction des oxydes de fer en présence de substances étrangères, *Rev. métallurgie*, Vol. 38 (1941), No. 5, pp. 129-134. See also *J. phys. chem.*, Vol. 46 (1942), No. 3, pp. 405-414; Vol. 47 (1943), No. 4, pp. 313-325.

¹⁰ Rudolf Schenck, Systematik der metallurgischen Vorgänge mit besonderer Rücksichtnahme auf die Beteiligung von Gasen, *Z. f. Elektrochemie*, Vol. 43 (1937), No. 7, pp. 438-450.

¹¹ O. George Specht and Carl A. Zapffe, The low temperature gaseous reduction of magnetite ore to sponge iron, AIME Technical Paper 1960, *Metals Technology*, Vol. 13 (1946), No. 4.

¹² Michael Tennenbaum and T. H. Joseph, Reduction of iron ores under pressure, *Trans. AIME*, Vol. 135 (1939), pp. 59-72; Vol. 140 (1940), pp. 106-125.

¹³ M. C. Udy and C. H. Lorig, The low temperature gaseous reduction of magnetite, *Trans. AIME*, Vol. 154 (1943), pp. 162-180.

Wetherhill and Furnas,¹⁴ Wiberg,¹⁵ and the summarizing publication of Baukloh¹⁶ may be mentioned as examples.

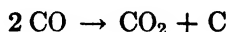
Some of the most important findings of this research work are the following. There is a very substantial difference between the reduction velocities of the three stages of oxidation: Fe_2O_3 (easy), Fe_3O_4 (difficult), and FeO (very slow, about eight times slower than Fe_3O_4). The gangue, especially those impurities with a tendency to combine with the iron oxides (SiO_2 , CaO , TiO_2 , Cr_2O_3 , Al_2O_3) or isomorphous oxides (MgO , MnO , ZnO), slows down the reduction process. The kind of reducing agent (CO , H_2 , hydrocarbons, or mixtures thereof) is reflected as well in the mass transfer considerations (diameter and velocity of the molecule, diffusivity) of the reagents and the products of reaction (see Table 65) as in

TABLE 65

MOLECULE DIAMETER, AVERAGE MOLECULE VELOCITY, AND DIFFUSIVITY OF SOME REDUCING AGENTS AND THEIR REACTION PRODUCTS

Substance	Molecule Diameter (cm)	Average Molecule Velocity (m/sec)	Diffusivity $\left(D = \frac{k_0}{\rho_0 c_v} [\text{m}^2 \text{hr}^{-1}]\right)$
CO	3.22×10^{-8}	493	0.0881
CO_2	3.39×10^{-8}	394	0.0417
H_2	2.39×10^{-8}	1838	0.6850
H_2O	1.13×10^{-8}	615	0.0516

the secondary reactions, the most important of which is the carbon formation according to reaction



With reference to the equilibrium conditions of this reaction carbon formation is ample at low temperatures and decreases with increasing temperatures. Inversely, the reaction velocity is

¹⁴ W. H. Wetherhill and C. C. Furnas, The rate of reduction of iron ores with carbon monoxide, *Ind. Eng. Chem.*, Vol. 26 (1934), No. 9, pp. 983-991.

¹⁵ Martin Wiberg, Om reduktion av järnmalm med koloxid, väte och metan, *Jernkont Annaler*, Vol. 124 (1940), No. 5, pp. 179-212.

¹⁶ W. Baukloh, Die Roheisengewinnung durch den Hochofenprozess, in A. Eucken and M. Jakob, *Der Chemie-Ingenieur*, Vol. III, Part 5, pp. 388-449, Leipzig, 1940.

low at low temperatures and great at high temperatures. Hence a maximum of carbon formation results in the medium temperature range (at about 600°C). Increased pressure favors carbon formation, vacuum opposes it. While formerly carbon formation was regarded as a *conditio sine qua non* to enable the so-called direct reduction, the main effect of the carbon formation, inasmuch as it takes place inside the ore lumps, is the rupture of the ore by the products of further reaction. On the other hand, the covering of the external surface with carbon is detrimental to the proceeding of the reaction and partly accountable for the fact that carbon monoxide at first reacts more slowly than hydrogen. At high temperatures, however, it reacts faster, because the reaction products of hydrogen are less easily removed. (See Table 65.) According to Wiberg, CO-H_2 mixtures (e.g., 75% $\text{CO} + 25\% \text{H}_2$) proved to be specially active reducing agents.

The physical reaction velocity depends basically upon the type of mass transfer realized, the fixed bed operation aerated by the gaseous reaction agents, or the fluidized bed with the solid particles in suspension. In both cases, there are two main characteristics of the process: particle size (particle diameter, surface, and shape factor) and the velocity of the gas relative to the particles. In a fixed bed we generally deal with lumps of relatively small surfaces, but we are able to force the gaseous reagent through the bed at very high linear velocities, and thus effect a lively mass and heat transfer. The torn and tortuous shape of the void space helps to increase the turbulence of the flow, to change the direction of flow frequently, and to cause effective contact of the gas and solid. The slowness of the chemical process caused by the limited surface of the reagent is compensated for by a very long residence time of the solids in the reaction space and by the adopted height of the fuel layer. The direct relationship between particle size and height of the fuel bed or the furnace is obvious. The blast furnace is high because a coarse coke is used. With small-size coke and ore, the reduction could be completed to the same degree in a low-shaft furnace; and if we proceed to powder fineness, the reduction could be accomplished, in principle, in a layer of a few centimeters (e.g., on a sintering grate). In such cases, the advisability of lowering the particle sizes depends upon other factors, like crushing cost, production of super fines, pressure drop, limitation of the linear velocity by the stability of the bed, etc.

TABLE 66

TERMINAL VELOCITY (M/SEC) OF COAL, CHAR, IRON, IRON ORE,
AND SPONGE IRON

d (mm)	0.001	0.01	0.1	1	10	100
Equation	Stokes'		(1)	(2)	(3)	(3)
Coal/air $\rho_s = 1200 \text{ kg/m}^3$		0.00152				
750°C	0.0000152	0.00132	0.147	6.795	39.26	127.4
1000°C	0.0000132	0.00117	0.129	6.730	43.50	142.1
1250°C	0.0000117		0.115	6.590	47.17	155.2
1500°C	0.0000109	0.00109	0.108	6.536	50.62	167.6
Char/air $t = 1000^\circ\text{C}$ $\rho_s = 900 \text{ kg/m}^3$	0.00000989	0.000989	0.0971	5.402	37.48	123.0
700 kg/m ³	0.00000769	0.000769	0.0757	4.439	32.91	108.5
500 kg/m ³	0.00000549	0.000549	0.0542	3.392	27.58	91.66
$t = 500^\circ\text{C}$		d (mm) = 0.1	0.5	1.0	5.0	
Equation		(1)	(2)	(2)	(3)	
Metallic iron/H ₂ $\rho_s = 7850$		2.39	34.19	73.91	231.5	
Metallic iron/sy-gas		1.31	16.88	34.38	97.6	
Iron ore/H ₂ $\rho_s = 5200$		1.61	24.76	56.37	186.9	
Iron ore/sy-gas						
Sponge iron/H ₂ $\rho_s = 2000$		0.63	11.30	29.04	113.0	
Sponge iron/sy-gas		0.35	5.81	14.02	50.0	

$$(1) \frac{1}{v} = 1.835 \frac{\rho}{\rho_s - \rho} \nu \frac{1}{d^2} + 0.1349 \sqrt[5]{\left(\frac{\rho}{\rho_s - \rho}\right)^2 \frac{1}{\nu d}}$$

Range of validity $\text{Re} < 8$

$$(2) \frac{1}{v} = 1.835 \frac{\rho}{\rho_s - \rho} \nu \frac{1}{d^2} + 0.1514 \sqrt{\frac{\rho}{\rho_s - \rho} \frac{1}{d}}$$

Range of validity $8 < \text{Re} < 300$

$$(3) \frac{1}{v} = 1.835 \frac{\rho}{\rho_s - \rho} \nu \frac{1}{d^2} + 0.1463 \sqrt{\frac{\rho}{\rho_s - \rho} \frac{1}{d}}$$

Range of validity $300 < \text{Re} < 2500$

$$\text{Stokes' equation: } \frac{1}{v} = 1.835 \frac{\rho}{\rho_s - \rho} \nu \frac{1}{d^2}$$

If we pass on to a suspended-fuel gasification, the process characteristics are changed completely. The reacting surfaces increase rapidly with decreasing particle size (increasing fineness), but at the same time the relative velocity between the particle and the

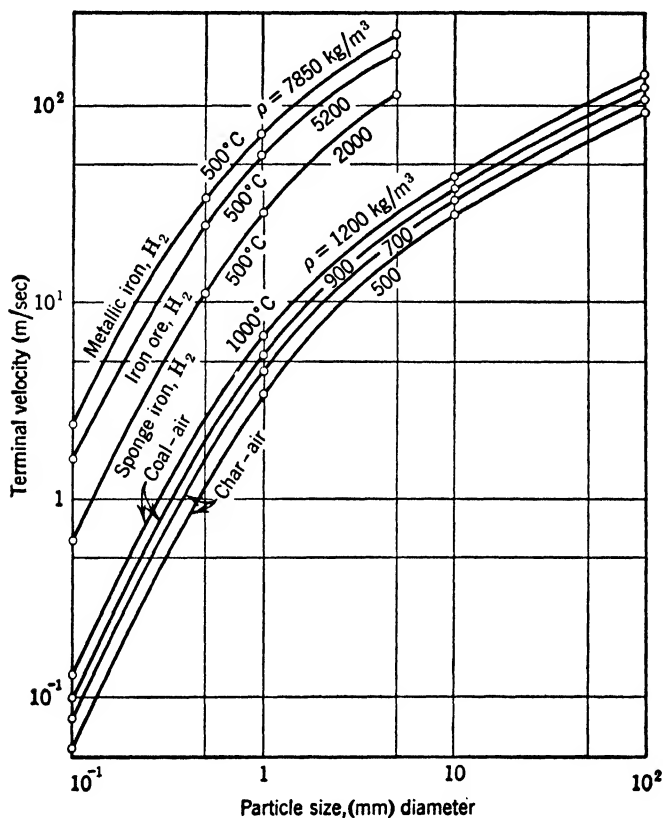


FIG. 66. Terminal velocities of iron, iron ore, sponge iron, coal, and char in different fluidizing agents.

carrier gas, which controls the mass transfer, is more and more limited. The maximum relative velocity of a particle in suspension is equal to its terminal velocity, if we disregard the influence of additional forces in nonhomogeneous velocity fields.¹⁷ Table 66 and Figure 66 show some terminal velocities of coal, char, and ore

¹⁷ Wilhelm Gumz, *Theorie und Berechnung der Kohlenstaubfeuerungen*, Berlin, 1939.

particles under different conditions of operation, indicating the influence of particle diameter and density. A superfine char particle (e.g., $1\ \mu$) has practically no velocity relative to its surroundings and consequently follows any movement of its carrier gas. As mass transfer is confined within the possibilities of diffusion, the enormous increase in surface is not effective. Sometimes processes involving powdered materials are overestimated because of their large surface area, and a corresponding increase in rate is expected, but the counteracting influence of the limited terminal velocity is overlooked. In some such cases, other factors such as heat transfer play an even greater part, e.g., in catalytic processes where the initiating or directing of a reaction or the heat distribution and dispersion or uniformity of temperature is more important than the accomplishment of the reaction itself.

The overall resistance of the reaction is obtained as the sum of the physical and the chemical resistance, and upon it depend the time and space required for the reaction. In a fixed bed, the solid reactant can be moved very slowly through the reaction space; the gaseous reactant, meanwhile, sometimes travels through in seconds or fractions thereof. Fortunately, an increase in heat and mass transfer of the same order of magnitude is associated with the decrease of residence time (or increase of gas velocity), so that the effects nearly balance. The space that is needed is nearly the same at low velocities (low rating) as at high velocities (high rating). Reaction space in a fixed bed is expressed and characterized by the height of the bed. Hence this height is essentially a function of the absolute value of the overall velocity of the reaction. In the range of high temperatures, the physical transport of gaseous material predominates as a speed-controlling factor; consequently, the necessary height of the fuel bed depends mainly upon the particle size. As this height designates the space within which the reaction has to come to the equilibrium (in general), and as the necessary heat and mass transfer has to be completed, the final state of equilibrium can be expected only at the end of this distance, not at intermediate points. Within the fuel bed of a gas producer or shaft furnace no equilibrium (gas temperature as well as mass concentration) can be expected because the time elapsed is not sufficient. From practical observations of temperatures and gas analyses within the fuel bed of gas producers, erroneous conclusions have sometimes been drawn regarding the

possibilities of approaching the equilibrium. That there cannot be equilibrium at any place within the reaction space follows logically from the finiteness of the overall reaction velocity. The argument that even at high temperatures, when high reaction velocities prevail, big discrepancies are found results from a misconception of chemical and overall reaction velocity, which, as has been shown, is controlled by physical factors, mainly at high temperatures. The great difference in concentrations of reagents which control the mass transfer is advantageous in countercurrent systems. The approach is quick but slows down considerably so that most of the space is required for the adjustment of the last percentage.

In contradistinction to these systems, the gaseous phase in a fluidized bed is subject to a far-reaching equalization in temperature as well as in mass concentration. Thus the first part of the reaction is slowed down and the second accelerated. In general, however, this equalization works towards a certain degree of retarding the reaction itself, which practically may be balanced or even overbalanced by larger surface and long residence time in the reactor. The maintenance of the fluidized bed presupposes an adequate particle size distribution and a linear gas velocity within the limits of 5 to 20% of the terminal velocity of the average-size particle. As a powder consists of a mixture of small, medium, and coarse particles with a big ratio of finest to coarsest material, a long residence time means an increasing loss of finest material (which is an essential component for maintaining a hindered flow of the solids). This elutriation causes a change in fluidization properties for the worse. On the other hand, agglomeration of particles as well as swelling of individual particles cause deterioration by formation of too heavy or too light material no longer adapted for the chosen linear velocity. Fluidization properties, therefore, are limited in both directions (with regard to particle size), and changes in size and size distribution may cause troubles (e.g., with high swelling index of the coal or high friability of the solids).

If velocities beyond the terminal velocity of the coarsest material are used (sweep type), all particles are carried straight through the reaction chamber. Their residence time in the reaction space is very limited and sufficient only if fine grinding is applied. The difficulties of such a process, as stated before, lie in the maintenance

of sufficiently high temperatures, i.e., in the mastering of the heat balance of the individual particle. High preheating, high oxygen content, or high pressure, therefore, besides fine grinding, is a necessary condition for successful operation.

The simultaneous influence of physical and chemical factors has different effects in various particle size ranges with regard to the variability of the dominant laws of mass transfer and reaction (including secondary influences favoring or retarding the reactions). The process of iron ore reduction is widely different with regard to particle size, which varies from the lumps of some 100 mm diameter used in the standard blast-furnace process down to finest grains of 0 to 0.1 mm used in the reduction of iron oxide catalysts in fluid beds. In the coarse end of this range, mass and heat transfer (velocity) and the physical structure of the solid reactants, such as purity, density, and porosity, predominate, while all chemical factors even including temperature are less important (as far as temperatures are kept above 600°C). At the other end, when finest powders are reduced, all physical influences recede rather completely and all chemical factors including temperature are outstanding. The temperature, in fact, not only accelerates the reaction velocity but also provokes sintering and melting, and thus largely influences the physical structure and surface of the solid reagent. In catalyst preparation, this is not wanted, and therefore limits the application of higher temperatures. It can be seen that physical and chemical proceedings sometimes are so intimately related that a complete separation is difficult.

The practical effect of the kinetics, as sketched, is smaller than usually realized. In fixed beds, as in gas producers, blast furnaces, cupola furnaces, and similar shaft furnaces, enough residence time for the gases to approach equilibrium is easily provided. This, as has been demonstrated, is not so much a problem of the gas velocity, as of sufficient height of the fuel bed, which depends mainly upon the average particle diameter or size. Sufficient bed height given, reaction kinetics has only small influence.

With gasification or reduction in suspension or fluidized beds, the choice of the linear velocity is a main factor. Regarding the predominant influence of particle size and size distribution to the linear velocity to be chosen, most attention has to be paid to preparing a proper mixture of particle sizes. Because of this

necessity, part of the frequently mentioned universal applicability of the fluidized technique is lost.

In this connection, it might be advisable to look once more at the "reactivity" of the fuels and the "reducibility" of the ores, which often are misinterpreted. The difference in reactivity of two kinds of coke (the notion of reactivity—reaction with the carbon—is applicable only to coke or to the coke formed by devolatilizing coals) is very large in the range of low temperatures, e.g., between charcoal and overheated metallurgical coke. But these differences disappear in the range of high temperature (above 1000°C). In any process (such as a gas producer using lump coke or a blast furnace) where within the practical range of temperatures the physical mass transfer is responsible for the reaction time necessary, but chemical reaction velocity is not, the reactivity, speeding up the chemical reaction velocity only, cannot exert any influence on the overall rate of reaction. Even an increase in the chemical reaction velocity (e.g., by catalysts) to ten times or a hundred times its value would make no visible change. This is in agreement with practical experience; by switching to a more reactive fuel (e.g., from metallurgical coke to charcoal) no higher rates or yields result. Statements of lower consumption of gasifying agents (including oxygen) are erroneous. Using coal (not coke), we may establish a considerable drop in weight by devolatilization, but this has nothing to do with the "reaction," properly speaking, and this loss in weight should not be ascribed to the high reactivity of this high-volatile fuel. The coke obtained might be somewhat more reactive because of its porous structure and enlarged surface. This difference is usually only small and less significant.

In a similar position is the reducibility of the ores. With all the wide varieties in density, porosity, amount of gangue, and kind of oxide practically any ore can be completely reduced in a blast furnace * and equilibria are approached. Incidentally, this would not hold in a shaft furnace with limited temperatures (as a Wiberg sponge iron shaft furnace). Here, also, the provision of a sufficient bed height, adapted gas velocities, particle sizes, etc., are necessary conditions. Only such statements as "direct reduction is necessary when working off very dense and coarse magnetite" are erroneous. If the physical properties and the size of a

* As far as the FeO content of the slag is concerned, see p. 208.

piece of ore make it travel down into lower layers of the furnace, it will stay in temperatures where CO_2 is unstable and will be readily reduced to CO if coke is present. This does not mean that this is a property (the "reducibility") of this ore, and reduction is done by carbon directly.

The part played by the surface temperature of the reacting solids has frequently been mentioned. It will be really decisive if we try to compare experiments made in a different scale. As the conductivity adjustment of temperatures is a dynamic process and a slow one in bulk material, difficulties are encountered in running and interpreting small-scale experiments. Many standard errors * in gasification and reduction processes are derived from and strengthened by such laboratory-scale experiments so that this point has to be stressed somewhat.

Pilot-plant experiments (semicommercial scale) have been run mostly with small gas producers of equal type and equal rate (in $\text{kg per m}^2 \text{ hr}$) as full-size producers. But in order to achieve similarity in the model, the fuel size should also be adapted to the small shaft diameter (and usually smaller bed height). Fulda and Gehlhoff,† e.g., operated an experimental gas producer of 492 mm diameter. To compare with a commercial size of 3000 mm using crushed coke of an average diameter of 60 mm, the fuel should be crushed down to about 10 mm. Actually their experiments were made with crushed coke of 60/40 mm. Similar conditions have been used by Neumann‡ in his frequently discussed experiments. The gas producer had 470 mm diameter. No size of coke used is given, emphasizing the fact that no attention was paid to the problem of adequate particle size.

Let us pick out run No. 13 from Neumann's experiments, operated with dry air ($v'_{\text{H}_2\text{O}} = 0.0132$). Calculated back from the gas analysis, the external heat losses, if the final gas is considered, are 27.5% of the heating value of the coke charged; and if the

* As "standard errors," widely spread in the technical literature, we refer to the following statements:

"... that equilibria in gas producers and shaft furnaces are (by far) not approached. . . ."

"... that the residence time is (by far) not sufficient for it . . ." and "that the reactivity (and reducibility) exerts a substantial influence upon the rate, yield, and gas composition. . . ."

† See footnote 7, p. 109.

‡ See footnote 4, p. 109.

gas consumption in the uppermost layer is considered, 17.8%. The final gas ¹⁸ is a mixture of two different kinds of gas: the gas penetrating the core of the fuel gas (central gas) and the gas flowing through the peripheral section, strongly affected by the heat losses of the wall, and partially channeling between the fuel bed and the wall (peripheral gas). The specific rate in this run was 54 kg/m² hr, which is quite low. The external heat loss, therefore, was at least two to three times as much as the loss of a commercial-size gas producer. It is obvious that conclusions drawn from such small-scale experiments are of limited value. The same holds true for reduction. Experiments on a laboratory scale to measure "reducibility" or even to find the gas composition to be expected, the ratio of "direct" to "indirect reduction," which often have been made and discussed, are of no value. Their results never can match the results of a full-size blast furnace.

If the pilot plant is considered as a "cut-out" cylinder of the fuel bed of the full-size plant, there will be a considerable influence due to the flow along the wall if the particle size is unaltered.* Besides, in the commercial plant this cylinder is surrounded by incandescent fuel of equal temperature. To imitate this temperature field in the small-scale model, the small gas producer should have an isothermal heating jacket of different capacity at every height to be adapted for the course of temperatures.

If a considerable dissipation of heat and a marked influence on the heat balance, the reaction temperature, and the gas composition in pilot plants exist, the problem of measuring reaction temperatures which no longer are constant throughout the cross-section turns out to be rather precarious. Conclusions about the approach to the equilibrium, therefore, based on measurements of temperatures and correlated gas analyses, have to be handled critically and with discretion. It is hardly possible to overcome the difficulty of a correct measurement of the reaction temperatures because it is the temperature of the solid surface or the boundary layer that matters, not the temperature of the gas phase most commonly indicated by thermocouples or aspiration pyrometers.

¹⁸ Kurt Neumann, *Die Veränderlichkeit der Gasphase im Gasgenerator*, Z. VDI., Vol. 58 (1914), No. 42, pp. 1481-1484; No. 43, pp. 1501-1504.

* According to Horak (see footnote 7, p. 30) no such wall effect is experienced with commercial-size 3 m diameter gas producers.

The gas analysis—if a full approach to the equilibrium is assumed—is a more convenient and better method of reaction temperature determination, and in many cases calculation is even easier and more reliable than measurement!

To fulfill the requirements of the theory of similarity, the ratio of lengths (bed height, particle diameters) meanwhile is not the only condition. According to Traustel,¹⁹ comparing the reactivity of two different fuels, the similarity of the temperature field requires a diameter ratio of

$$\frac{(D)}{D} = \frac{(d)}{d} \sqrt{\frac{(\alpha)}{\alpha}} \quad (468)$$

where D is the gas producer diameter, (D) the diameter of the small-scale model, d and (d) are corresponding particle diameters, and α and (α) mean the thermal diffusivity ($\alpha = \frac{k}{\rho_0 c_p}$ m²/hr).

Since these similarity conditions have always been disregarded, the results obtained do not correspond to the behavior of the fuels in full-size equipment.* This fact, in another way, is shown by the multitude of experimental methods used or proposed to measure reactivity. Durrer²⁰ uses five pages to list the most important publications; M. A. Mayers²¹ quotes more than one hundred papers—an indication of the uncertainty of and the dissatisfaction with all these methods.

The reservations and objections made against pilot plant experiments are even more necessary against laboratory scale apparatus in which the diameters are only a few centimeters. Among the most frequently discussed experiments is the work done by Clem-

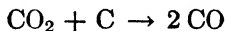
¹⁹ Sergei Traustel, Ein Modellgesetz zur vergleichenden Prüfung der Reaktionsfähigkeit fester Brennstoffe, *Feuerungstechn.*, Vol. 31 (1943), No. 1, pp. 1-8.

* A more detailed discussion of the model laws of gasification and shaft furnace processes has been published by Traustel during the preparation of this book: Sergei Traustel, Model laws of gasification and smelting, *Iron and Coal Trades Rev.*, Vol. 158 (1949), No. 4237, pp. 1167-1172; No. 4238, pp. 1225-1231; Sergei Traustel, Modellgesetze der Vergasung und Verhüttung (*Scientia Chimica*, Vol. 4), Berlin, 1949.

²⁰ Robert Durrer, *Die Metallurgie des Eisens*, 2nd ed., Berlin, 1942.

²¹ Martin A. Mayers, The physical properties and reactivity of coke, in National Research Council, *Chemistry of Coal Utilization* (H. H. Lowry, Editor), New York, 1945, Vol. I, pp. 863-920, especially pp. 895-904.

ent, Adams, and Haskins.²² They used a porcelain tube of 15 mm diameter and 600 mm length, half of which was filled with the fuel examined, heated at the full length. The fuel (charcoal and coke) had particle sizes of 5 mm, equally sized. Compared with commercial-size gas producers, this is an extremely coarse material. According to the law of similarity, it should not have more than 0.3 mm in diameter. The authors, pointing to the fact that Boudouard²³ in his study of the producer equilibrium (named after him) needed as much as 30 sec to approach equilibrium in the reaction



suspected a strong influence of residence or contact time, which they also found in the results of their own experiments. At medium temperatures, considerable time was needed for the curves to come to an equilibrium, i.e., run horizontally without further change. At 800°C, it took 1½ min; at 700°C, no equilibrium at all could be expected. As the contact time of the gas in a commercial gas producer is about ¼ sec, many authors jumped to the premature conclusion that with respect to these experiments this time is absolutely insufficient and an approach to equilibrium could not be expected anyhow. Hence any attempt to calculate gas producer performances would be futile.

These conflicts of opinion or interpretation are based on an uncritical application of laboratory tests to commercial-scale gas producers. In fact, these experiments have been run isothermally, i.e., the gasifying agent was preheated to 800°C, for example, and the tube heating coil was controlled to maintain 800°C inside the tube. But as the reaction consumes heat, it is necessary to deliver heat and to have a temperature difference to do so. The higher the capacity or rate of gasification of the tube, the greater this temperature difference has to be. The thermocouple indicates the temperature of the gas phase, hence a higher temperature than the surface temperature. Owing to

²² T. K. Clement, L. H. Adams, and C. N. Haskins, Essential factors in the formation of producer gas, *Bur. Mines Bull.* 7 (Washington, 1911), pp. 5–38. T. K. Clement and L. H. Adams, Effective temperatures for water-gas generation, *loc. cit.*, pp. 39–57.

²³ O. Boudouard, *C. R. Acad. Sci.*, Paris, Vol. 128 (1899), pp. 824, 1524; Vol. 130 (1900), p. 132; Vol. 131 (1900), p. 1204. *Ann. chim. phys.*, Series 7, Vol. 24 (1901), p. 354.

the poor heat conductivity of beds of coarse material—which moreover depends upon the nature of the gas filling the void space more than upon the solid material itself—the heat transfer is definitely obstructed. Therefore, there will be an equilibrium between heat delivery and heat consumption (equal to progress of reaction) which is substantially influenced by physical characteristics. Traustel²⁴ estimated roughly the ratio of contact time necessary between laboratory and commercial scale (in a typical case) as 140:1. This unexpected result reflects the misconceptions possible if those experimental data are applied to practical operations. The gas producer and shaft furnace with countercurrent flow are not operated isothermally but with high initial temperatures and high initial concentrations of the reducing agents. Laboratory experiments unable to produce true similarity, especially that of temperature fields, indicate no conclusive results and cannot be applied to the operating conditions of commercial-size plants. Calculation in this field has shown promising results and sometimes an amazing agreement of calculating prediction with reality.

²⁴ Traustel, Thesis, Berlin, see footnote 1, p. 49.

Appendix

APPENDIX

TABLE I
PROPERTIES OF GASES

Matter	Symbol	Mol. Weight, m	Specific Weight, kg/SCM	Specific Volume, SCM/kg	Mol. Vol., SCM/kmol	Heating Value, kcal/SCM	
						Gross	Net
Oxygen	O ₂	32.000	1.42895	0.699815	22.39
Nitrogen	N ₂	28.016	1.2505	0.79968	22.40
Argon	Ar	39.944	1.7839	0.56057	22.39
Air	...	28.960	1.2928	0.77351	22.40
Carbon dioxide	CO ₂	44.010	1.9768	0.50587	22.26
Carbon monoxide	CO	28.010	1.2500	0.80000	22.41	3,020	3,020
Sulfur dioxide	SO ₂	64.060	2.9263	0.34173	21.89
Hydrogen sulfide	H ₂ S	34.076	1.5392	0.64969	22.14	6,140 *	3,660 *
						7,200 †	6,720 †
Hydrogen	H ₂	2.016	0.08987	11.12718	22.43	3,050	2,570
Water vapor	H ₂ O	18.016	(0.804)	1.24378	(22.4)
Ammonia	NH ₃	17.031	0.771	1.297	22.09

Saturated Hydrocarbons

Methane	CH ₄	16.042	0.7168	1.39509	22.38	9,520	8,550
Ethane	C ₂ H ₆	30.068	1.356	0.73746	22.17	16,820	15,370
Propane	C ₃ H ₈	44.094	2.0037	0.49908	22.01	24,320	22,350
n-Butane	C ₄ H ₁₀	58.120	2.703	0.36996	21.50	32,010	29,510
Benzene	C ₆ H ₆	78.108	(3.48)	(0.2874)	(22.4)	34,960	33,520

Unsaturated Hydrocarbons

Acetylene	C ₂ H ₂	26.036	1.1709	0.85404	22.24	14,090	13,600
Ethylene	C ₂ H ₄	28.052	1.2605	0.79334	22.25	15,290	14,320
Propylene	C ₃ H ₆	42.078	1.915	0.52219	21.97	22,540	21,070
Butylene	C ₄ H ₈	56.104	(2.50)	(0.4000)	(22.4)	29,110	27,190

* If burnt to SO₂.

† If burnt to SO₂.

Values in parentheses () assumed being an ideal state at standard temperature and pressure.

TABLE II
 PROPERTIES OF STEAM-AIR OR GAS MIXTURES

t °C	P Physical Atm	g H ₂ O/SCM (dry)
-20	0.0010162	0.8181
-19	0.0011188	0.9008
-18	0.0012301	0.9905
-17	0.0013511	1.0880
-16	0.0014837	1.198
-15	0.0016279	1.311
-14	0.0017847	1.438
-13	0.0019541	1.575
-12	0.0021409	1.725
-11	0.0023422	1.888
-10	0.0025609	2.065
-9	0.0027961	2.255
-8	0.0030545	2.464
-7	0.0033323	2.689
-6	0.0036333	2.933
-5	0.0039585	3.196
-4	0.0043108	3.482
-3	0.0046921	3.791
-2	0.0051044	4.126
-1	0.0055477	4.486
±0	0.0060280	4.877
1	0.0064787	5.244
2	0.0069620	5.638
3	0.0074746	6.057
4	0.008022	6.504
5	0.008604	6.980
6	0.009224	7.487
7	0.0098816	8.026
8	0.010580	8.599
9	0.011323	9.211
10	0.012111	9.859
11	0.012946	10.55
12	0.013831	11.28
13	0.014770	12.06
14	0.015765	12.88
15	0.016817	13.76

TABLE II (*Continued*)

PROPERTIES OF STEAM-AIR OR GAS MIXTURES

t °C	P Physical Atm	g H ₂ O/SCM (dry)
16	0.017931	14.68
17	0.019110	15.67
18	0.02035	16.71
19	0.02167	17.81
20	0.02306	18.98
21	0.024525	20.22
22	0.02607	21.53
23	0.027709	22.92
24	0.02943	24.38
25	0.031252	25.94
26	0.03316	27.58
27	0.035171	29.32
28	0.03729	31.15
29	0.039517	33.09
30	0.04186	35.13
31	0.044327	37.30
32	0.04691	39.58
33	0.049631	42.00
34	0.052486	44.55
35	0.05549	47.25
36	0.05862	50.08
37	0.061922	53.09
38	0.06538	56.25
39	0.068997	59.60
40	0.07278	63.12
41	0.076750	66.86
42	0.08091	70.79
43	0.08557	74.96
44	0.08981	79.35
45	0.09457	84.00
46	0.09953	88.89
47	0.10473	94.08
48	0.11016	99.56
49	0.11582	105.34
50	0.12173	111.46

TABLE II (Continued)
 PROPERTIES OF STEAM-AIR OR GAS MIXTURES

t °C	P Physical Atm	g H ₂ O/SCM (dry)
51	0.12791	117.96
52	0.13435	124.8
53	0.14106	132.1
54	0.14806	139.8
55	0.15535	147.9
56	0.16294	156.5
57	0.17085	165.7
58	0.17909	175.4
59	0.18766	185.8
60	0.19657	196.8
61	0.20586	208.5
62	0.21554	221.0
63	0.22551	234.2
64	0.23596	248.4
65	0.2468	263.5
66	0.25803	279.7
67	0.26974	297.1
68	0.28183	315.6
69	0.29442	335.6
70	0.3075	357.1
71	0.32103	380.3
72	0.33516	405.4
73	0.34968	432.4
74	0.36478	461.8
75	0.3805	493.9
76	0.39662	528.6
77	0.41346	566.9
78	0.43079	608.6
79	0.44879	654.8
80	0.4674	705.8
81	0.48663	762.3
82	0.50657	825.6
83	0.52718	896.7
84	0.54847	976.9
85	0.5704	1067.7

TABLE II (*Continued*)
 PROPERTIES OF STEAM-AIR OR GAS MIXTURES

t °C	P Physical Atm	g H ₂ O/SCM (dry)
86	0.59319	1172.6
87	0.61671	1287.5
88	0.64100	1435.9
89	0.66607	1604.1
90	0.6919	1806.0
91	0.71862	2053.9
92	0.74620	2364.4
93	0.77466	2764.7
94	0.80398	3298.4
95	0.8342	4046.3
96	0.86544	5172.3
97	0.89757	7047.3
98	0.93067	10795.5
99	0.96484	22069
100	1.00000	

TABLE III
ENTHALPY OF GASES (KCAL/SCM)

t °C	CO	CO ₂	H ₂	H ₂ O	CH ₄	N ₂	O ₂
0	0	0	0	0	0	0	0
100	31.2	41.5	30.9	37.1	38.8	31.2	31.5
200	62.6	87.1	62.0	74.2	84.2	62.5	63.4
300	94.6	136.1	93.4	112.1	135.6	94.4	97.3
400	127.3	187.4	124.5	151.0	192.8	126.7	131.9
500	160.3	242.2	156.0	191.2	255.3	159.6	167.5
525	168.9	256.1	163.9	201.5	272.2	167.9	176.5
550	177.6	270.0	171.8	211.8	289.1	176.3	185.5
575	186.2	283.9	179.7	222.1	306.0	184.7	194.5
600	194.9	297.9	187.6	232.5	322.9	193.1	203.5
625	203.5	312.2	195.6	243.2	340.9	201.6	212.7
650	212.2	326.6	203.6	253.9	359.0	210.2	221.9
675	220.9	341.0	211.6	264.6	377.1	218.8	231.1
700	229.6	355.4	219.6	275.3	395.2	227.4	240.3
725	238.5	369.9	227.6	286.3	414.2	236.1	249.6
750	247.4	384.5	235.6	297.4	433.2	244.9	259.0
775	256.3	399.1	243.6	308.5	452.2	253.6	268.4
800	265.3	413.7	251.7	319.6	471.2	262.4	277.8
825	274.3	428.7	259.8	331.0	491.0	270.3	287.2
850	283.3	443.7	268.0	342.4	510.9	280.2	296.7
875	292.3	458.7	276.1	353.8	530.7	289.1	306.2
900	301.4	473.8	284.3	365.3	550.6	298.1	315.7
925	310.5	488.8	292.5	376.9	571.3	307.1	325.2
950	319.6	503.8	300.8	388.5	592.1	316.2	334.7
975	328.7	518.8	309.0	400.1	612.9	325.3	344.2
1000	337.8	533.9	317.3	411.8	633.7	334.4	353.8
1050	356.6	565.2	334.1	436.7	...	353.0	373.3
1100	375.4	596.5	351.0	461.6	...	371.6	392.8
1150	394.2	627.8	367.8	486.5	...	390.2	412.4
1200	413.0	659.1	384.7	511.4	...	408.8	431.9
1250	431.9	690.4	401.5	536.2	...	427.3	451.4
1300	450.7	721.7	418.3	561.1	...	445.9	470.9
1350	469.5	753.0	435.2	586.0	...	464.5	490.4
1400	488.4	784.3	452.0	610.9	...	483.1	510.0
1450	507.2	815.6	468.9	635.8	...	501.7	529.5
1500	526.0	846.9	485.7	660.7	...	520.3	549.0

TABLE IV

ENTHALPY OF FORMATION (KCAL/KMOL) *

C (diamond)	(s)	0
C (α -graphite)	(s)	-490
C (β -graphite)	(s)	-220
CO	(g)	-26,840
CO ₂	(g)	-94,450
H ₂	(g)	0
H ₂ O	(g)	-68,350
O ₂	(g)	0
N ₂	(g)	0
NH ₃	(g)	-11,000
Al ₂ O ₃	(s)	-380,000
CaO	(s)	-151,700
CaCO ₃	(s)	-289,500
MgO	(s)	-146,100
MgCO ₃	(s)	-268,000
MnO	(s)	-96,700
Mn ₂ O ₃	(s)	-233,000
Mn ₃ O ₄	(s)	-345,000
Fe	(s)	0
FeO	(s)	-64,300
Fe ₃ O ₄	(s)	-266,900
Fe ₂ O ₃	(s)	-198,500
FeS	(s)	-23,100
FeS ₂	(s)	-35,500
FeCO ₃	(s)	-172,800
P ₂ O ₅	(s)	-360,000
S (rhombic)	(s)	0
S (monoclinic)	(s)	-75
S	(g)	66,300
S ₂	(g)	29,200
H ₂ O	(g)	-5,300

* Data from P. Russel Bichowsky and Frederik D. Rossini, *The Thermochemistry of the Chemical Substances*, Reinhold Publishing Corp., New York, 1936.

TABLE V
EQUILIBRIUM CONSTANTS

$t, ^\circ\text{C}$	Producer Gas Reaction (equation 46)		Heterogeneous Water-Gas Reaction (equation 47)		Methane Formation (equation 49)
	$K_{PB} = \frac{p^2\text{CO}}{p\text{CO}_2}$	$K'_{PB} = \frac{p\text{CO}_2}{p^2\text{CO}}$	$K_{PW} = \frac{p\text{CO}p\text{H}_2}{p\text{H}_2\text{O}}$	$K'_{PW} = \frac{p\text{H}_2\text{O}}{p\text{CO}p\text{H}_2}$	$K_{PM} = \frac{p\text{CH}_4}{p^2\text{H}_2}$
350	0.0000067644	147.833	0.00014038	7123.5	55.511
400	0.000081025	12.342	0.00095380	1048.4	16.393
450	0.00068667	1,456.3	0.0050255	198.99	5.5944
500	0.0044016	227.19	0.021512	46.487	2.2019
550	0.022448	44.547	0.077520	12.900	0.96592
600	0.094715	10.558	0.24179	4.1358	0.46357
650	0.340925	2.9332	0.66776	1.4976	0.23992
700	1.07266	0.93226	1.6618	0.60176	0.13237
750	3.00907	0.33233	3.7830	0.26434	0.077154
800	7.64633	0.13078	7.9688	0.92549	0.047156
850	17.8366	0.056064	15.698	0.063702	0.030336
900	38.6164	0.025896	29.166	0.034286	0.019845
950	78.3033	0.012771	51.477	0.019426	0.013540
1000	149.886	0.0066717	86.826	0.011517	0.0095072
1050	272.62	0.0036681	140.73	0.0071060	0.0068505
1100	473.83	0.0021105	220.18	0.0045412	0.0050527
1150	790.78	0.0012646	333.86	0.0029953	0.0038005
1200	1272.7	0.00078573	492.50	0.0020305	0.0029237
1250	1982.4	0.00050444	708.85	0.0014107	0.0022859
1300	2998.7	0.00033348	998.14	0.0010019	0.0018168
1350	4415.1	0.00022650	1378.2	0.00072558	0.0014660
1400	6346.3	0.00015757	1870.7	0.00053456	0.0011998
1450	8923.8	0.00011206	2500.4	0.00039994	0.00099504
1500	12299	0.000081307	3296.2	0.00030338	0.00083542

TABLE VI
EQUILIBRIUM CONSTANTS (HOMOGENEOUS REACTIONS)

$t^{\circ}\text{C}$	Homogeneous Water-Gas Reaction		Homogeneous Methane Formation		
	$K_W = \frac{p_{\text{CO}_2} p_{\text{H}_2\text{O}}}{p_{\text{CO}_2} p_{\text{H}_2}}$	$K'_W = \frac{p_{\text{CO}_2} p_{\text{H}_2}}{p_{\text{CO}_2} p_{\text{H}_2\text{O}}}$	$K_{\text{F}_3} = \frac{p_{\text{CH}_4} p_{\text{H}_2\text{O}}}{p_{\text{CO}} p_{\text{H}_2}}$	$K_{\text{F}_8} = \frac{p_{\text{CH}_4} p_{\text{H}_2\text{O}}}{p_{\text{CO}_2} p_{\text{H}_2}}$	$K_{\text{F}_7} = \frac{p_{\text{CH}_4} p_{\text{CO}_2}}{p_{\text{H}_2} p_{\text{CO}}}$
350	0.048186	20.753	3.95430×10^5	1.9054×10^4	8.2064×10^6
400	0.084947	11.772	1.7188×10^4	1.4601×10^3	2.0232×10^4
450	0.13664	7.3185	1.113×10^3	1.5208×10^2	8.1471×10^3
500	0.20462	4.8871	1.0236×10^2	2.0945×10^1	5.0025×10^2
550	0.28958	3.45381	1.2460×10^1	3.6082×10^1	4.3029×10^1
600	0.39172	2.55284	1.9172×10^{-1}	7.5101×10^{-1}	4.8944×10^{-1}
650	0.51057	1.95859	3.5930×10^{-1}	1.8345×10^{-1}	7.0373×10^{-1}
700	0.64548	1.54923	7.9655×10^{-2}	5.142×10^{-2}	1.2340×10^{-1}
750	0.79542	1.25719	2.0395×10^{-2}	1.6222×10^{-2}	2.5641×10^{-2}
800	0.95954	1.04217	5.9176×10^{-3}	5.6782×10^{-3}	6.1671×10^{-3}
850	1.13623	.88010	1.9325×10^{-3}	2.1958×10^{-3}	1.7008×10^{-3}
900	1.32400	.75529	6.8041×10^{-4}	9.0086×10^{-4}	5.1391×10^{-4}
950	1.52112	.65741	2.6303×10^{-4}	4.0010×10^{-4}	1.7292×10^{-4}
1000	1.72624	.57929	1.0949×10^{-5}	1.890×10^{-5}	6.3429×10^{-5}
1050	1.93724	.51620	4.8680×10^{-6}	9.4305×10^{-6}	2.5128×10^{-5}
1100	2.15199	.46469	2.2948×10^{-6}	4.9384×10^{-6}	1.0664×10^{-5}
1150	2.36862	.42219	1.1402×10^{-6}	2.7007×10^{-6}	4.8137×10^{-6}
1200	2.58422	.38696	5.9366×10^{-7}	1.53415×10^{-6}	2.2972×10^{-6}
1250	2.79657	.35758	3.2247×10^{-7}	9.0181×10^{-7}	1.1531×10^{-6}
1300	3.00440	.33285	1.8203×10^{-7}	5.4689×10^{-7}	6.0587×10^{-7}
1350	3.20351	.31216	1.0637×10^{-7}	3.4076×10^{-7}	3.3205×10^{-7}
1400	3.39248	.29477	6.4137×10^{-8}	2.1758×10^{-7}	1.8905×10^{-7}
1450	3.56898	.28019	3.9796×10^{-8}	1.4203×10^{-7}	1.1150×10^{-7}
1500	3.73127	.26801	2.5345×10^{-8}	9.457×10^{-8}	6.7925×10^{-8}

TABLE VII

ENTHALPY OF CARBON (COKE), BLAST-FURNACE SLAG (BURDEN) AND
PIG IRON (KCAL/KG)

t °C	Blast		
	Carbon *	Furnace Slag	Pig Iron
0	0	0	0
100	22.9	18.4	...
200	49.6	39.6	...
300	79.6	62.3	...
400	112.9	85.7	...
500	148.9	109.3	...
550	167.9	121.0	...
600	187.5	132.8	...
625	197.5	141.3	...
650	207.6	144.5	...
675	217.8	150.4	...
700	228.2	156.3	...
725	238.8	162.2	...
750	249.4	168.2	...
800	270.9	180.3	...
850	292.9	192.7	...
900	315.2	205.5	...
950	337.9	218.9	...
1000	360.8	233.0	168.6
1100	407.4	264.3	183.8
1200	454.7	301.0	264.0 †
1300	502.3	371.8 †	279.2 ‡
1400	550.0	400.4 †	294.5 ‡
1500	597.5	429.0 †	313.9 ‡
1600	644.5	457.6 †	...
1700	690.6	486.2 †	...
1800	735.5	514.8 †	...

* Enthalpy of carbon (coke): $H_C = 0.209333t + 0.2024 \times 10^{-3}t^2 - 50.9333 \times 10^{-6}t^3$ kcal/kg, representing $H_{C\ 500^\circ} = 148.9$, after W. Fritz and H. Kneese, *Feuerungstechn.*, Vol. 30 (1942), No. 12, p. 275. $H_{C\ 1000^\circ} = 360.8$ and $H_{C\ 1500^\circ} = 597.5$ kcal/kg, after Landolt-Börnstein, *Chem.-Phys. Tabellen*.

† Including (240 kcal/kg) melting heat.

‡ Including (65 kcal/kg) melting heat, after C. Schwarz, *Arch. Eisenhüttenwes.*, Vol. 7 (1933), No. 5, pp. 281-292.

TABLE VIII
CONVERSION TABLE—METRIC TO ENGLISH SYSTEM

	<i>n</i>	1/ <i>n</i>
1 m (meter)	3.2808 ft	0.30480
1 cm (centimeter)	0.3937 in.	2.540
1 mm (millimeter)	0.03937 in.	25.40
1 μ (micron = $\frac{1}{1000}$ mm)	0.00003937 in.	24,400
1 m ² (square meter)	1,550 sq in.	0.00064516
1 m ² (square meter)	10.7639 sq ft	0.092903
1 cm ² (square centimeter)	0.1550 sq in.	6.4516
1 m ³ (cubic meter)	61,023 cu in.	0.000016387
1 m ³ (cubic meter)	35.3145 cu ft	0.028317
1 dm ³ (cubic decimeter)	61.023 cu in.	0.0163872
1 l (liter)	61.025 cu in.	0.0163867
1 l (liter)	1.0567 qt (U.S. liquid measure)	0.94633
1 hl (hectoliter = 100 l)	2.8378 (U.S.) bu (U.S. dry measure)	0.35238
1 hl	21.9975 Imperial gal	0.0454596
1 hl	26.418 (U.S.) gal (liquid measure)	0.037853
1 cm ³ (cubic centimeter)	0.061024 cu in.	16.38716
1 SCM (standard cubic meter, 0°C, 760 mm Hg)	37.2281 SCF (60°F, 30 in. Hg, dry)	0.0268614
1 SCM (0°C, 760 mm Hg, wet)	37.6622 SCF	0.0265518
1 kg (kilogram)	2.204622 lb (avoirdupois)	0.4535924
1 kmol (kilogram-mole)	2.204622 lb-mole	0.4535924
1 t (ton = 1000 kg)	1.10231 short tons	0.907184
1 t	0.984206 long tons	1.0160471
1 g (gram)	0.035274 oz. (avoirdupois)	28.3495
1 g	15.43253 grains	0.064798
1 at (kg/cm ² = 10,000 kg/m ² = 735.5 mm Hg technical atmosphere, absolute)	14.2234 psi	0.070307
1 Atm (10,332.3 kg/m ² = 760 mm Hg physical atmosphere, absolute)	14.69604 psi	0.068046

TABLE VIII (Continued)
CONVERSION TABLE—METRIC TO ENGLISH SYSTEM

	<i>n</i>	1/ <i>n</i>
1 mm Hg (mercury column = 0.00135951 kg/cm ² = 0.00131579 Atm)	0.03937 in. Hg	25.4
1 SCM/kg (dry)	16.8864 SCF/lb	0.059219
1 SCM/kg (wet)	17.0833 SCF/lb	0.058537
1 SCM/kmol (dry)	16.8864 SCF/lb-mole	0.059219
1 SCM/kmol (wet)	17.0833 SCF/lb-mole	0.058537
1 kg/SCM (dry)	0.059219 lb/SCF	16.8864
1 kg/SCM (wet)	0.058537 lb/SCF	17.08329
1 kg/m ²	0.20482 ft/sq ft	4.88241
1 kg/m ³	0.062428 lb/cu ft	16.0184
1 kg/hl	0.77687 lb/(U.S.) bu	1.2872
1 kg/t	2 lb/short ton	0.5
1 g/SCM (dry)	0.41454 grain/SCF	2.41231
1 g/SCM (wet)	0.40976 grain/SCF	2.44044
1 g/cm ²	99.565 grains/sq in.	0.010044
1 kcal	3.96832 Btu	0.2520
1 kcal/m ²	0.36867 Btu/sq ft	2.71245
1 kcal/m ² °C	0.20482 Btu/sq ft °F	4.8824
1 kcal/m ³	0.11237 Btu/cu ft	8.8991
1 kcal/SCM (dry)	0.106595 Btu/SCF	9.38132
1 kcal/SCM (wet)	0.105366 Btu/SCF	9.49071
1 kcal/kg	1.80 Btu/lb	0.5555...
1 kcal/kg °C	1 Btu/lb °F	1
1 kcal/m hr °C	0.67197 Btu/ft hr °F	1.48816
1 kcal/kmol	1.80 Btu/lb-mole	0.5555...
<i>T</i> °K (degree Kelvin)	1.8°F abs	0.5555...
<i>t</i> °C (degree centigrade)	$\frac{5}{9} (t\text{ °F} - 32)$	$\frac{9}{5} t\text{ °C} + 32$
<i>t</i> °C (°K) temperature difference	1.8 <i>t</i> °F	0.5555...
1 mkg (kilogram-meter)	7.233 ft-lb	0.1383
1 PS (horsepower = 0.736 kw = 632.5 kcal)	0.98632 hp	1.01387
1 kw (= 1.36 PS)	1.34102 hp	0.7457

NAME INDEX

- Adams, L. H., 293
 Allcut, E. A., 109
 Améen, E., 96
 D'Ans, J., 176
 Arthur D. Little, Inc., 251
 Atwell, H. V., 127, 128
 Axelson, S., 102

 Bachmann, H., 70
 Bader, M., 268
 Barclay, K. M., 149
 Baukloh, W., 190, 282
 Bichowsky, P. R., 303
 Bone, W. A., 109, 117, 281
 Boudouard, O., 293
 Brinkley, Jr., R., 63, 103
 Brisker, C., 246
 Bruehl, E., 264

 Cerasoli, T., 49
 Choukhanoff, Z. F., 280
 Choukhanova, O. A., 279
 Clement, T. K., 293
 Consolidated Mining and Smelting
 Company of Canada, Ltd., 149
 Cruse, K., 218

 Damköhler, G., 50
 Danulat, F., 49, 82, 168
 Davis, H., 278, 279
 Denis, F., 103
 Deschamps, J., 136, 160
 Diepschlag, E., 247
 Dodge, B. F., 22
 Dolch, P., 5, 157, 158
 Drawe, R., 168
 Durrer, R., 190, 248, 292

 Edse, R., 50
 Eichenberg, G., 247
 Eucken, A., 22, 27, 190, 276

 Fischbeck, K., 276
 Fischer, F., 131
 Fiske, R. A., 268
 Foster, J. F., 158
 Fritz, W., 71, 306
 Fuchs, O., 22
 Fulda, M., 109, 117, 290
 Furnas, C. C., 282

 Gehlhoff, G., 109, 117, 118, 290
 Geimer, P., 247
 Gibson, A. H., 109, 117
 Glaser, O., 222
 Grodzovsky, M. K., 280
 Gumz, W., 76, 129, 227, 285
 Gwyther, R. D., 109

 Haskins, C. N., 293
 Haslam, R. T., 109
 Hecker, E., 72
 Heller, P. A., 264
 Henselmann, J., 137
 Hofmann, K., 281
 Hole, I., 159
 Horak, W., 30, 291
 Hottel, H. C., 278, 279
 Hougen, O. A., 22
 Hubendick, E., 102
 Hubmann, O., 160
 Hydrocarbon Research, Inc., 129

 Jakob, M., 22, 190, 276
 Joseph, T. H., 281
 Jungbluth, H., 264

 Kamura, H., 281
 Kandiner, H. T., 103
 Karwat, E., 253
 Kilpatrick, J. E., 22
 Kinney, S. P., 206
 Kneese, H., 71, 306

- Körber, F., 208, 214, 218
 Kühl, H., 50, 217
- Lamort, J., 136
 Lane, J. C., 96
 Lax, E., 176
 Lennings, W., 254
 Levin, M., 247
 Lindsay, R. W., 264
 Litinsky, L., 247
 Löfroth, K. A., 102
 Lorig, C. H., 281
 Lowry, H. H., 292
 Lundström, T. B., 102
 Lurgi Gesellschaft für Wärmetechnik,
 160
 Lutz, H., 122
- Mackie, R. F., 109
 Magat, M., 103
 Massari, S. C., 264
 Mathesius, W., 224
 Mayers, M. A., 103, 276, 292
 Metz, N., 247
 Meyer, H. H., 281
 Mitchell, R. F., 149
 Musil, L., 166
- National Research Council Commit-
 tee, 292
 Neumann, K., 109, 116, 290, 291
 Newitt, D. M., 162
 Newman, L. L., 127, 149, 168
 Niedt, H., 247
 Nusselt, W., 27
- Oberhoffer, P., 247
 Oelsen, W., 218
 Olmer, F., 281
 Olsson, S., 102
 Osann, B., 205
- Philipon, H., 136, 143
 Pitzer, K. S., 22
 Piwowarsky, E., 268
 Plenz, F., 79
 Pollitzer, W. M., 254
 Predvoditelev, A. S., 279
 Prettre, M., 103
- Rambush, N. E., 117, 136
 Rankine, A., 222
 Reiser, H., 49
 Republic Steel Corporation, 251
 Reuter, A., 78
 Richter, H., 218
 Rinn, K., 22
 Rossini, F. D., 22, 303
 Roth, W. A., 218
 Royster, P. H., 206
 Rozinek, A., 129
- Sartori, G., 162
 Sauerwald, F., 206
 Schenck, H., 193, 199, 208, 209, 210,
 215
 Schenck, R., 281
 Schlapfer, P., 102
 Schlesinger, W. A., 246
 Schwarz, C., 22, 218, 306
 Senfter, E., 174, 232
 Slater, F. S., 251
 Smith, C. D., 136
 Société de la Vieille Montagne, 136
 Specht, O. G., 281
 Szikla, G., 129
- Taylor, W. J., 22
 Tennenbaum, M., 281
 Thyssen'sche Gas- u. Wasserwerke,
 G.m.b.H., 152
 Tobler, T., 102
 Traustel, S., 26, 49, 76, 78, 292, 294
 Tu, C. M., 278, 279
- Udy, M. C., 281
 Ulich, H., 22, 218
- Vial, F. K., 268
 Voellmecke, H., 137
 Voogd, G., 117
 Vorum, D. A., 158
- Wagman, D. D., 22
 Walker, W. J., 120
 Ward, I. T., 109
 Watson, K. M., 22

- | | |
|------------------------------------|-----------------------|
| Weil, B. H., 96 | Wohlschläger, H., 109 |
| Weir, H. M., 168 | Wright, C. C., 149 |
| Wesemann, F., 174 | Wright, E., 222 |
| Wetherhill, W. H., 282 | |
| Wheeler, R. V., 109, 117 | Zapffe, C. A., 281 |
| Wiberg, M., 96, 202, 236, 249, 282 | Zeise, H., 63 |

SUBJECT INDEX

- Air-gas composition, 38, 39
- Ammonia formation, 42
 - synthesis gas, 96, 101
- Anthracite, oxygen-steam gasification, 149
 - pressure gasification, 80-86
- Approach (to the equilibrium), degree of, 77, 78, 86
- Blast furnace, 173
 - calculation, 225
 - gas composition, 173
 - localization of shaft reactions, 192
 - under pressure, 250
 - with O₂-enriched blast, 253
- Blast-furnace curves, 246
- Blast-furnace slag, enthalpy, 306
- Boudouard reaction, 3, 9, 32
 - equilibrium constant, 10, 22, 304
- Brinkley method of calculation, 103
- Burden, enthalpy, 306
- Burden/fuel ratio, 226
- Burden yield (pig iron yield), 224
- Calculation, general rules, 91
- Calculation methods, blast furnace, 225
 - slagging-ash producers, 136
 - summary of starting equations, 48
- Calculation scheme, degree of reduction method, 63
 - Newtonian method, 58, 92
 - triangle method, 50, 86
- Calculations based on the gas analysis, 96
- CaO reduction, 207
- Carbonates, decomposition, 176, 177
- Carbon balance, 43
- Carbon enthalpy, 306
- Carbon formation, influence on reduction of oxides, 283
- Carbon gasification, with dry air, 38
 - with oxygen, 32
 - with steam, 33
- Carbon monoxide as ore-reducing agent, 178, 188, 193
- Carbon monoxide/hydrogen mixtures as ore-reducing agents, 201
- Charcoal blast furnace (Sandviken), 236
- Le Châtelier-Braun's principle, 15
- Chemical reaction velocity, 276
- Combustion of carbon, mechanism, 25
 - rate of reaction, 279
 - temperature, 26
- Combustion under pressure, 167
- Concurrent gasification, 123
- Conversion table (metric to English system), 307
- Cupola furnace, 263
- Degree of approach (equilibrium), 77
- Degree of dissociation, 35
- Dehydration of clay (kaolin), 175
- Desulfurization, with limestone, 214
 - with manganese, 217
 - with soda, 217
- Diffusivity, 71
- Direction of a reaction, 15
- Direct reduction, 178, 190
- Dissociation, degree of, 35
- Dolomite, decomposition, 176
- Down-draft gasification, 123
 - of wood, 129
- Edvin process, 263
- Electro water gas, 159
- Enthalpy of formation, 6, 303
- Equilibrium, incomplete, 76
 - of a reaction, 8
- Equilibrium constant, 20, 304, 305
- External heat losses, 75

- External heat losses, effect of, 121
of furnaces, 232, 233
- Ferric oxide reduction, 179
- Ferro alloys, production in slagging-ash producers, 136
- Ferroferric oxide reduction, 181
- Ferrous carbonate, decomposition, 176
- Ferrous oxide reduction, 182
- Fischer-Tropsch synthesis gas, 96
- Fluidized bed gasification, 129
- Fouchet gas producer (wood), 132
- Fuel consumption, from carbon balance, 44
- Fuel velocity in a gas producer, 70
- Gardie gas producer, 160
- Gas, enthalpy, 302
properties of, 297
- Gas analysis, calculation based on, 96
- Gas composition at equilibrium, 32
general case, 41
- Gas composition in blast furnaces, 173
- Gasification, concurrent, 123
in suspension, 124
of carbon with dry air, 38
at 20 Atm, 81
degree of conversion method, 35, 63
with oxygen, 145
of wastes, 141
- Gasification calculations, degree of reduction method (semigraphical), 63
Newtonian method, 58
triangle method, 50
- Gasification mechanism, 25
- Gasification reactions, 3
- Gasification theory of Denis, 103
- Gasification theory of Prettre and Magat, 103
- Gasifying agent, from material balances, 47
- Graphical method (degree of reduction), 63
- Graphical solution of the heat balance, 74
- Hearth reactions, 207
- Heat balance, 68
blast furnace, 241
preheating zone, 245
- Heat (enthalpy) of formation, 6, 303
- Heterogeneous reactions, equilibrium constant, 304
- High-pressure blast furnace, 245
- Hole electro water-gas producer, 159
- Homogeneous reactions, equilibrium constant, 305
- Hot-blast cupola furnace, 267
Griffin process, 268
Gumz process, 268
- H-t* diagram, 74
- Hubendick method of calculation, 102
- Hydrogen as reducing agent, 197
- Hydrogen balance, 44
- Hypothetical fuel (blast furnace calculations), 229
- Imbert gas producer, 132
- Incomplete equilibrium, 76
- Indirect reduction, 178, 190
- Iron carbide formation, 214
- Iron phosphate formation, 214
- Iron silicide formation, 214
- Iron sulfide formation, 214
- Kaolin dehydration, 175
- Koppers pulverized coal gasification process, 125
- Laboratory-scale experiments, 292
- Lime, decomposition, 176
- Low-shaft blast furnace, 261
- Lurgi high-pressure gas producer, 160, 167
- Magnesite decomposition, 176
- Manganese carbonate decomposition, 176
- Manganese dioxide reduction, 183
- Manganomanganic oxide reduction, 184
- Manganous oxide reduction, 185, 199
by iron, 200, 208
- Mass action, law of, 77

- Material balances, 43
- Mathematical treatment of gas producer performance, 109
- Maximum work, 21
- Mechanism of blast furnace reactions, 189
- Mechanism of gasification, 25
- Methane formation, 4, 7, 11
 - degree of formation method, 37
 - heterogeneous, equilibrium constants, 304
 - homogeneous reactions, 11
- Methane reforming, 107
- Model laws, 292
- Moisture content of the blast, influence, 109
- Moisture content of wood, effect on gasification, 130
- Molecular velocity, 282
- Molecule diameter, 282

- Newtonian approximation method (Traustel), 58
 - for carbon, 58
 - general case, 61
- Nitrogen balance, 46
- Norsk Staal process, 263

- Oxidation zone of a gas producer, 25
- Oxygen balance, 45
- Oxygen-enriched blast furnace, 253
- Oxygen gasification, 145
- Oxygen-steam gasification of anthracite, 149

- Pattenhausen gas producer, 158
- Performance of gas producers, 109
- Philipon gas producer, 143
- Phosphoric acid reduction, 186
- Physical reaction velocity, 276
- Pig iron enthalpy, 306
- Pig iron yield (burden yield), 224
- Pilot plant experiments, 290
- Plenz' experimental results (gasification of coke), 85
- Preheat of the blast (Philipon), 143
- Preheating of the blast, effect, 118
- Preheating (pre-reaction) zone of a blast furnace, reactions, 234
- Pressure, blast furnace under, 250
 - combustion under, 167
 - effect on equilibrium constant, 15
 - effect on gasification, 160
 - producer gas under, 163
- Pressure gasification of anthracite, 81
- Pressure gasification with oxygen, 167
- Pressure operation of blast furnaces, 250
- Principle of least resistance (Le Châtelier-Braun), 15
- Producer gas under pressure, 163

- Quotient of mass action, 77

- Rate of a gas producer, influence on reaction temperatures, 72
- Rates of gas producers, 280
- Reaction kinetics, 275
- Reaction resistance, 276
- Reaction temperature, 28
- Reaction velocity, 275
- Reactions in blast furnaces, 173
- Reactivity of fuels, 280
- Recycling off-gas, 120
- Reducibility of iron ores, 289
- Reduction of iron ores, 178
 - rate of, 282
- Reduction zone in a gas producer, 27, 31
- Reforming of methane, 107
- Residence time (fuel) in a gas producer, 70

- Sample calculations, 86
- Schlaepfer-Tobler method of calculation, 102
- Semigraphical method (degree of reduction), 63
- Signs in thermochemical data, 4
- Silicon dioxide reduction, 211
 - by iron, 212
 - by manganese, 212
- Similarity, law of, 292
- Slag formation, heat of, 218
- Slag yield, 221

- Slagging-ash producer, 136
Steam, gasification of carbon with, 33
Steam-air (-gas) mixtures, properties, 298
Steam decomposition, 116
Sulfur, 42
Surface temperature of heated particles, 71
Suspension, gasification in, 124
Sweep-type gas producer, 127
Synthesis gas, ammonia, 96, 101
 Fischer-Tropsch, 96
Szikla-Rozinek furnace, slag removal, 129

Temperatures, in gas producers, 28
 in water-gas producers, 157
Terminal velocity, 284
 effect on reaction rates, 285
Thermal efficiency, 166
Thyssen-Gálocsy gas producer, 151
Triangle method (Traustel), 50
 for carbon, 50
 general case, 56
Two-zone slagging-ash producer (Gumz), 144, 145

Vacuum, gasification in, 162

Velocity, relative, effect on reaction rates, 280, 285
 terminal, 284

Wastes, gasification of, 141
Water gas, at high pressure, 160
 from carbon, 154
Water-gas high-pressure low-shaft blast furnace, 261
Water-gas production, 154
Water-gas reaction, equilibrium constants, 10, 22, 304, 305
 heterogeneous, 4, 7, 36
 degree of reduction method, 37
 homogeneous, 4, 7, 8
Water-gas shift reaction, 4, 7, 8
 equilibrium constant, 8, 24, 305
Water of hydration, 175
Weather conditions, effect on cupola furnace operation, 270
Wellmann-Galuska gas producer, 149
Wiberg process, 263
 reduction gas for, 96, 98
Wood, down-draft gasification of, 129
Wood gas producers, improvements, 134

Yields of a blast furnace, 219

